NSWC MP 89-242

SBIR REPORTS ON THE CHEMISTRY OF LITHIUM BATTERY TECHNOLOGY

EDITOR: W. P. KILROY

RESEARCH AND TECHNOLOGY DEPARTMENT

NOVEMBER 1989

NAVAL SURFACE WARFARE CENTER

Dahlgren, Virginia 22448-5000 • Silver Spring, Maryland 20903-5000

NSWC MP 89-242

SBIR REPORTS ON THE CHEMISTRY OF LITHIUM BATTERY TECHNOLOGY

W. P. KILROY, EDITOR
RESEARCH AND TECHNOLOGY DEPARTMENT

NOVEMBER 1989

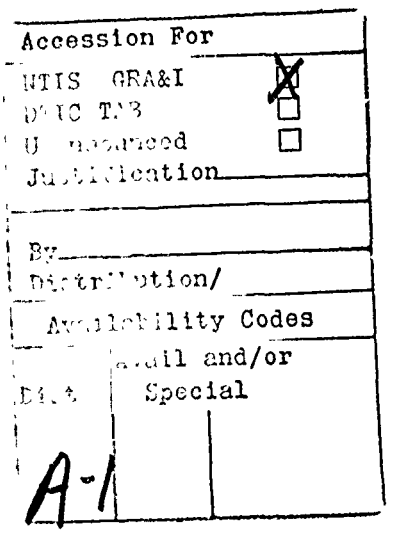

NAVAL SURFACE WARFARE CENTER
Dahlgren, Virginia 22448-5000 • Silver Spring, Maryland 20903-5000

FOREWORD

This report is a composite collection of four Phase I Small Business Innovative Research final reports. This work was conducted under contracts N60921-86-C-A457, N60921-88-C-0058, N60921-86-C-0274, and N60921-88-C-0057.

Approved by:

C. E. Mueller

C. E. MUELLER, Head
Materials Division

CONTENTS

INTRODUCTION

This report is a composite collection of four Phase I Small Business Innovative Research (SBIR) final reports on the development of lithium battery technologies. Although these studies were not fortunate to transition to a Phase II program, the work is unique and worthy of acknowledgment by the scientific community. An outline of the reports follow:

Appendix	Title	Authors	Project Manager
A	Identification of an Improved Mixed Solvent Electrolyte for a Li Secondary Battery	F. Walsh	F. Rucky
B	Catalyzed Cathodes for Li-$SOCl_2$ Batteries	P. Kane	W. Kilroy
C	Improved Li-$SOCl_2$ Cells Using New Electrolyte Salts	C. Schlaikjer	W. Kilroy
D	Development of Calcium Primary Cells with Improved Anode Stability and Energy Sensitivity	C. Schlaikjer	W. Kilroy

The authors and this Center are indebted to the Navy SBIR program for financial support of the research and special thanks to Don Wilson for his assistance in publishing this report.

APPENDIX A

IDENTIFICATION OF AN IMPROVED MIXED SOLVENT ELECTROLYTE FOR A LITHIUM SECONDARY BATTERY

FINAL REPORT - PHASE I
December 1987 - May 1988

Prepared for:

Naval Surface Warfare Center
Silver Spring, MD 20903-5000

Under Contract No. N60921-86-C -A457

Energy Conversion Corporation
20 Assembly Square Drive
Somerville, MA 02145

Fraser Walsh
Principal Investigator

F. Rucky
Project Manager

TABLE OF CONTENTS

LIST OF FIGURES

LIST OF TABLES

1.0 IDENTIFICATION AND SIGNIFICANCE OF THE OPPORTUNITY

1.1 Problem Addressed

Much attention has been given to the development of a rechargeable lithium battery for military applications because of its high expected energy density. Despite the attention, a practical rechargeable battery capable of operation over the full military temperature range (-40°C to +71°C) has not been developed. One of the practical problems encountered has been maintenance of good cycle life and/or energy density of the cell especially at reduced temperatures.

The cycle life of the lithium anode in electrolytes based on $LiClO_4$/1,3-dioxolane or 2-methyl-tetrahydrofuran (2-Me-THF) has been reported as high (1) but these two preferred electrolytes are of limited utility either because of safety (cell detonation with $LiClO_4$/1,3-dioxolane) or because of poor rate capability at low temperatures. Improved electrolytes have been developed which are blends of 2-Me-THF and THF with low levels of 2-methyl furan; this blend has been reported to provide cells with improved cycle life and only 50% loss in capacity on discharge at 2 mA/cm² at -20°C (2). However, this blend does not provide significant (less than 2% of RT) cell discharge capacity at -40°C even at 0.5 mA/cm², and thus is not a satisfactory electrolyte for multipurpose cells.

In previous work, ECO studied the performance of secondary lithium cells with an electrolyte blend of a cyclic ether (e.g., 2-Me-THF or 1,3-dioxolane) and an alkyl urea. Laboratory cells which use these electrolyte blends with cathodes prepared with Vulcan XC-72 and PTFE were shown capable of providing a factor of ten increase in discharge capacity at 0.2 mA/cm² and -40°C compared to cells with the 2-Me-THF/THF/2-Me-F blend (3). Based on the data reported herein obtained in a Phase I SBIR program, ECO has identified a new cathode composition/mixed solvent electrolyte combination which provides a lithium secondary cell with good cycle life, excellent high rate performance, and significant discharge capacity at -40°C even at rates of 2 mA/cm². In addition to the work planned for Phase I, ECO developed and implemented a design for a spirally wound electrode for a AA-size cell; data on hermetic AA-size cell performance with this spirally wound electrode were obtained at rates of 1 - 8 mA/cm² (50 to 400 mA) at temperatures of -40° to 71°C. While this design is still unoptimized, the results obtained in this Phase I program indicate the technical feasibility of incorporating the program results in a lithium secondary cell to provide an energy-dense, multipurpose secondary cell capable of high rate performance over a broad temperature range. In its final design, this cell type will be of interest in both military and non-military applications; it will have commercial potential as a viable product as desired under the SBIR program.

1.2 Phase I Research Goals

The goal of this Phase I program was to evaluate selected electrolytes containing solvent mixtures for Li/TiS_2 cells and to demonstrate that these mixed-solvent electrolytes support improved high-rate low-

temperature (-40°C) cell performance and cycle life. The electrolyte mixtures to be studied contain a cyclic ether and a co-solvent such as an alkyl urea or a straight-chain ether. The function of the co-solvent is to interact both with the cyclic ether to enhance its resistance to carbon-oxygen bond cleavage, and with the solvated lithium species to prevent it from further reacting with the charge-activated carbon-oxygen bond.

In this Phase I study, emphasis was placed on characterization of electrolyte chemical stability and of anode surface layer parameters in order to understand why an electrolyte containing a mixture of a cyclic ether and a co-solvent provides an improved electrolyte. In addition, during the Phase I program ECO evaluated the performance of hermetic AA-size lithium secondary cells which contain a mixed-solvent electrolyte, and demonstrated that the operational temperature range, rate capability and cycle life of such cells is increased.

The rechargeable lithium battery has been considered as the desired alternative to a number of primary and secondary batteries in a number of peacetime applications (i.e., portable communication devices, undersea instrumentation packages, radio control devices for robots, etc.). However, the minimum practical cathode energy density goal for commercial or military market penetration by a lithium secondary battery has been described by Brummer (1) as 165 W-hr/kg (75 W-hr/lb) at C/3 or 200 W-hr/kg (90 W-hr/lb) at C/10, and this level has not as yet been reached in a practical cell after many years of research. An objective of the Phase I program was to demonstrate the technical feasibility of reaching this cathode energy density in a practical cell through proper combination of cathode materials and electrolyte components.

In Phase I, the specific technical objective is to demonstrate the utility of an electrolyte composed of a mixture of a cyclic ether and a co-solvent such as an alkyl urea. As listed in the Phase I proposal, the Phase I research program attempted to answer the following questions:

1. What is the temperature range of performance at 2 mA/cm^2 of lithium secondary cells with a cyclic ether-alkyl urea based electrolyte?

2. How do anode surface characteristics vary as a function of cycle life in the mixed solvent electrolyte?

3. Is the mixed solvent electrolyte chemically stable on extended cycling over a broad temperature range and in deep discharge?

4. Do cell performance levels observed justify continued work on cells with the mixed solvent electrolyte?

Provided in the following sections is a description of the methods used and the results obtained in the Phase I program, and specific answers to the questions listed above are provided in Section 5. In general, the results obtained were all positive in that an electro-

lyte/cathode material combination was identified which is chemically stable on extended cycling, and which supports high-rate cell performance over a broad temperature range. In addition to achieving the planned goals of Phase I, a spirally wound electrode design was developed and its use demonstrated in hermetic AA-size cells. The technical feasibility of the application of this electrode design with the program-developed electrolyte/cathode material combination was demonstrated and, based upon the results obtained, the feasibility of developing a useful high-rate secondary cell with broad temperature capability verified.

2.0 PREVIOUS WORK

2.1 Electrolyte Degradation Reactions

Electrolytes which have been considered the electrolytes of choice for lithium secondary batteries are based on the use of $LiClO_4$/1,3-dioxolane or of $LiAsF_6$/2-Me-THF. Ether-based polar organic solvents are, in general, preferred because they have enhanced lithium solute solvation properties. However, the resulting electrolytes suffer due to chemical degradation reactions on standing or in cell cycling. An extreme example is the reported detonation of cycled cells with $LiClO_4$/1,3-dioxolane electrolytes.

In a recently published study of the chemical and electrochemical degradation reactions of 2-Me-THF on lithium, Kerr (4) identified two degradation mechanisms. Chemical degradation of the cyclic ether apparently proceeds, after homolytic cleavage of the lithium-polarized carbon/oxygen bond, by further reaction of the secondary radical with lithium (e.g., 2-pentanol formation after hydrolysis). The secondary radical is apparently more stable than the primary radical, which apparently is in equilibrium with the polarized cyclic ether. However, when a solvated lithium atom is present, as would be the case at the anode surface on charging, the rate of reaction of this atom with the primary radical is apparently fast, and thus the major degradation product after hydrolysis is 1-pentanol. This report demonstrated the importance of considering the electrolyte degradation reactions in a lithium secondary cell as being electrochemically mediated; studies of electrolyte stability must thus be carried out in practical cells.

Abraham *et al.*, described an electrolyte blend based on $LiAsF_6$/2-Me-THF which contains a furan (2-Me-F); the advantage of the addition of the furan was a significant increase in cell cycle life (2). The level of addition of this furan is somewhat critical given that Kerr observed that a 4 v/o (4 mmoles/A-hr Li) addition in a half-cell test significantly reduced cycle life; Abraham *et al.*, claimed that the optimal use of the additive was related to lithium capacity (0.4 mmoles/A-hr Li). Thus, apparently a factor of 10 increase in ratio decreases benefit. Kerr further reported that in the absence of Li, thermal polymerization of the furan occurs perhaps initiated by AsF_6; the rate of this polymerization is significantly reduced in the presence of lithium as indicated by the measured levels of 2-Me-F (4) and by the reported enhanced cycle life of 2-Me-F containing cells (2).

The importance of reactions of $LiAsF_6$ in electrolyte degradation has also been identified by Yen et al., (5). This work has indicated that re-plated lithium reacts with the electrolyte to yield as a final product arsenic. Initial steps in this reaction sequence apparently involve reactions of the ether ring-cleaved products with the $LiAsF_6$ to form an oxyfluoride which leads to formation of an As-O polymer. These products form the lithium anode passivating layer and must be partially responsible for loss in lithium capacity on cycling, either by reacting irreversibly with lithium or by isolating lithium particles from the lithium metal substrate. It is important to notice that at the basis for these reactions of the solute is the degradation of the solvent: application of methods to improve solvent stability or to prevent reaction of solvent cleavage radicals with the solvent will result in an increased cycle life lithium secondary cell.

2.2 Mixed-Solvent Electrolyte Conductance

There have been a number of recent reports on the benefits of the use of mixed solvent electrolytes [i.e., Hunger (6), Matsuda and Sataka (7), Margalet and Canning (8), Tobishima and Yamagi (9), Takata et al. (10), Matsuda et al. (11)]. These reports have documented the increases in electrolyte conductance available through the use of mixed solvents. The cause of this electrolyte conductance increase can be partially explained by the formation of solvent-separated ion pairs, but solvent-solvent interactions have also been suspected as being of importance (12,13).

In a recently completed study (3), ECO measured the conductance of a number of solvents and solvent pairs with $LiAsF_6$, LiSCN, LiBr, $LiCF_3SO_3$ or $LiB(C_6H_5)_4$ as solute. Electrolytes with $LiAsF_6$ as solute were identified as having the highest specific conductance at 25°C; the highest specific conductance (13,400 uMHO/cm) was obtained for a 1.5 M $LiAsF_6$ solution of 1,3-dioxolane (23 v/o)/1,2-DME (77 v/o). However, this mixture did not have high specific conductance at -40°C (e.g., 280 uMHO/cm). However, the addition of 10 v/o of 1,1,3,3-tetramethyl urea to the mixture provided an electrolyte with a specific conductance of 4000 uMHO/cm. ECO also observed that the peak in conductance which occurs as a function of volume ratio of the solvents in the mixture could be closely correlated with a peak in change in ^{13}C-chemical shift determined by NMR. These data provide evidence indicating that conductance in mixed solvents is related to the formation of solvent-solvent pairs in which there is sufficient electron charge overlap to induce a change in the concentration of active solvated species. The obvious effect of this interaction is a change in electrolyte conductance as a function of temperature. A second, perhaps not so obvious effect, is that this concentration can affect the chemical stability of the electrolyte. Indeed, ECO showed that electrolytes with solvent mixtures, with volume ratios defined as those providing a maximum in ^{13}C-NMR chemical shift, are significantly more chemically stable on reflux over Li(Hg) than electrolytes prepared with the individual solvents (3). This NMR-based technique was used in the Phase I program to determine solvent ratios for testing.

2.3 Low Temperature Performance

Previous work with lithium secondary cells with 2-Me-THF-based electrolytes has indicated that the low-temperature performance of these cells is limited. Abraham et al. (14) described the use of a $LiAsF_6$/(THF/2-Me-THF/2-Me-F) electrolyte in cells discharged at -20°C. Despite this being their best electrolyte with cell performance significantly improved, performance still was extremely limited (e.g., only 20% capacity utilization at 2.6 mA/cm^2). Performance at -40°C was not reported.

ECO reported (3) that, based on data from unoptimized laboratory cells, low temperature (-40°C) discharge capacity of a cell containing a 2-Me-THF/THF electrolyte can be increased by a factor of ten (from 2 to 29% of RT capacity) through replacement of the THF in the mixed solvent electrolyte with an alkyl urea.

2.4 Use of Alkyl Ureas

The alkyl ureas have been routinely used for solvating alkali metals in organic chemical reactions to form metastable solutions (16). Specific alkyl ureas have been used to facilitate lithium enolate chemistry (17). These reported interactions led ECO to consider the alkyl ureas as co-solvents in mixed solvent electrolytes for secondary lithium cells.

ECO demonstrated that there is considerable electronic interaction between the alkyl ureas and cyclic ether solvents based on changes in ^{13}C-NMR chemical shifts as a function of volume ratio and based on the observed increase in low temperature conductance of mixed solvent electrolytes containing an alkyl urea (3). These initial data suggested that cell performance with an alkyl urea-containing electrolyte at reduced temperature should be improved, and, as described in the previous section, data were obtained supporting this supposition.

In the Phase I program, ECO evaluated the extent of increased solvent stability, and thus cycle life, obtained through addition of an alkyl urea to the electrolyte of a lithium secondary cell. As described in Section 2.1, Kerr (4) reported data indicating that electrochemical degradation of a cyclic ether proceeds via a mechanism on which a primary radical is formed by oxygen-carbon bond cleavage; this radical is in equilibrium with the charge polarized ether. The equilibrium is driven toward radical formation by reaction of the radical with a solvated lithium atom formed electrochemically at the anode during charge. Given that the alkyl ureas are highly effective at solvating alkali metal ions, it is likely that such solvation will result in a reduced rate of reaction between free lithium atoms and the polarized carbon-oxygen bond in the cyclic ether. This supposition was tested in the Phase I program by measurement of the rate of degradation of the electrolyte on cycle-testing of secondary lithium cells.

5 Anode Surface Layer Characterization

The layer which forms on the anode surface during cycling is the result of chemical reaction between the lithium (metal or solvated atoms) and the electrolyte. This reaction can be modeled as a corrosion reaction, and the layer formed thus acts as a protective layer. It also acts as a solid electrolyte through which ionic migration must occur. In a recent study of the characteristics of surface layers on lithium anodes in aprotic media, Garrean et al. reported (18) that the solid-electrolyte interphase (SEI) model presented by Peled (19) could be used as a basis for analysis of the change of characteristics in the anode surface layers.

In this model of the SEI, Peled divided the layer into at least two zones: a thin compact layer and a porous secondary layer. The behavior of the anode with compact layer can be represented by a RC parallel network. Using this RC network model, values for the layer resistance, R, and capacitance, C, are determined by measuring the change in cell potential, V, as a function of time, t, after application of a current pulse, I, because, for a parallel RC network,

$$V = IR\,(1 - e^{-t/CR})$$

and thus,

$$\frac{dV}{dt} = \frac{I}{C} e^{-t/CR}$$

A plot of log dV/dt vs. t gives as its slope a value for 1/2.3 CR and, at the t=0 intercept, a value for log I/C. Film resistivity can be obtained from the slope of the plot of 1/C vs. R obtained as the film grows with time.

The apparent film thickness (D) of the compact layer can be determined based on the use of the parallel-plate-capacitor equation:

$$D = 8.85 \times 10^{-8}\ E\ k\ 1/C\ (=)\ cm$$
$$= K\ 1/C\ (=)\ Å$$

where E is the dielectric constant of the layer, k is the layer roughness factor, and C is the layer capacity (uF/cm^2). The value of K is 93.9 assuming a roughness factor of 1 and a dielectric constant value of 10.62.

This approach toward characterizing the surface layer which affects anode behavior is thus subject to real time analysis with the values of various parameters characterizing the layer (R, C, D) being determined based on the measurement of certain readily-available experimental values (V vs. t, I). Such values can be related to cell discharge parameters or electrolyte chemistries; changes in the values as they correlate to changes in cell parameters or chemistries can be used to create a better understanding of the factors affecting anode performance, and thus cell cycle life.

In the Phase I program, ECO used this method of surface layer analysis to aid in developing an increased understanding of the changes obtained in lithium secondary cells through the use of electrolytes containing mixtures of cyclic ethers and co-solvents.

2.6 Spirally Wound Electrode Design

In a recent report Anderman and Lundquist (21) described the performance of both rectangular planar and spirally-wound TiS_2 cathodes in 1 M $LiAsF_6$/2-MeTHF electrolyte. Results obtained using a 20 cm^2, 80 mA-hr spirally wound cell included initial capacity utilization of ove: 90% falling to 70% after 400 cycles at 0.75/1.5 mA/cm^2 with a lithium turnover number of 43. Based on these results and upon some assumptions on the thickness of the anode and cathode, they forecasted that the capacity of an AA-size spirally-wound electrode cell will be approximately 1 A-hr at a rate of 200-300 mA.

In the preparation of the spirally wound cathode, Anderman and Lundquist used commercially available TiS_2 (Degussa) and a nonfluorinated polymer binder. Previously Yen *et al.* (22) reported on the use of ethylene-propylene-diene-terpolymer (EPDM) as a cathode material binder to provide a flexible cathode. In the Phase I program, ECO developed a spirally-wound cathode design based on the use of EPDM, TiS_2 from Degussa and a high surface area carbon black (Ketjenblack 300J). AA-size cells with 50 cm^2 surface area cathodes were discharged at rates as high as 400 mA and at temperatures over the range of -40° to 71°C. The results of these tests will be described in later sections, but they indicate that the performance forecast of Anderman and Lundquist may indeed be feasible, and that a lithium secondary cell with spirally-wound electrodes can be a commercially-viable alternative power supply.

3.0 METHODS

3.1 Materials

The electrolyte solvents used included 2-Me-THF, THF, 2-methylfuran (2-Me-F), 1,3-dioxolane, 1,2-dimethoxyethane (1,2-DME), 1,1,3,3-tetramethyl urea (TMU) and 1,3-dimethyl-1,3-trimethylene urea (DMTU). These solvents were obtained from Aldrich Chemical at a minimum of 99% chemical purity; anhydrous solvents were obtained when available and were used as received. Solvents containing an inhibitor or not anhydrous were purified by distillation from a solution in which a sodium-benzophenone ketyl had been formed. The purified solvents were stored in amber bottles in a dry room (<0.5% R.H.).

The solutes used were lithium hexafluoroarsenate ($LiAsF_6$) and lithium tetrafluoroborate ($LiBF_4$). They were obtained as electrochemical grade materials from Lithco and Alfa/Ventron respectively. They were dried under vacuum (1 torr) at 100°C for 2 hours prior to use.

Electrolytes were prepared in the dry room just prior to use as 1 M solutions by addition of the solute to the solvent mixture after the mixture had been chilled to approx. 0°C. After the addition of the

solute, the electrolyte was warmed to room temperature and then added to the cell. Electrolytes with 2-methyl-furan were prepared with the furan added at a content of 0.4 mmoles/A-hr capacity just prior to electrolyte addition to the cell.

Anodes for laboratory cells were prepared by pressing 18 mil lithium foil (Lithco) onto 4 cm^2 SA stainless steel or nickel screens to which was spot welded a metal foil (1 mil) lead. Reference electrodes were prepared similarly except their surface area was only 0.1 cm^2. Anodes for the spirally wound AA-size cells were prepared as 4 mil lithium foil (3.8 cm x 14.0 cm); a stainless steel (316) 1 mil foil tab welded to the glass-to-metal seal was spot welded to a thin (3.8 cm x 0.3 cm) piece of screen which was pressed into one end of the foil and was the center insert in the mandrel used in winding the electrode.

Cathodes were prepared from TiS_2 (Degussa), carbon black (Ketjenblack 300J or 600; Akzo Chemicals), and a binder. Three binders tested were Vistalon (Exxon Chem.), a chlorinated ethylene-propylene copolymer, Polysar (Exxon Chem.), a ethylene-propylene-diene terpolymer, and a similar product sold by Aldrich Chemicals. The binder was dissolved as a 3 w/o solution in cyclohexane. The cathode material was prepared as a thick slurry in cyclohexane and applied to the stainless steel current collector; after solvent removal, the cathodes were pressed at 3000 psi and then dried under vacuum (1 torr) at 100°C for 1 hour. Cathode size for the laboratory cells was 4 cm^2; for the spirally wound cells, cathode dimensions were 3.8 cm x 12.7 cm. Cathode loading was 20 - 25 mg/cm^2 and was determined by a weight difference ($\pm$ 1%) prior to cell assembly. The thickness of the cathode used in the spirally wound cells was approx. 20 mil; this thickness could be reduced significantly is thinner stainless steel screen has been used (e.g., 4 mil rather than 12 mil).

The cell separator used was a 2 mil microporous polypropylene film (Celgard 2400).

3.2 Cell Types Tested

3.2.1 Lithium Cycle Life Testing - Cell Type 1

The laboratory cells used to evaluate electrolyte stability on lithium cycle consisted of a two-piece circular glass cell (5.0 cm dia.) with the top and bottom piece held together on a Viton O-ring gasket with a pinch clamp. The cell top-piece (3 cm high) had three feed-throughs (sealed with 0.6 cm dia. rubber septa) through which passed the electrode (anode, cathode, reference) leads; a fourth septa-sealed feed-through was used to fill the cell. In the bottom piece of the cell, the electrode stack (anode, separator, reference, separator, cathode) was held in compression (approx. 10 g/cm^2) using a glass weight. The cathode in these tests consisted of a 4 cm^2 nickel or stainless steel foil (1 mil). Two ml. of electrolyte were added to the cell just prior to initiation of the lithium cycle test. Cell assembly was carried out in a dry room; continuous cell cycling was done on the bench using an Amel Model 545 Electrometer. Cell voltage and cathode

vs. reference voltage were monitored and recorded using an IBM-compatible PC equipped with a MetraByte DASH-8 data logger and EXP-16 multiplexer. Software developed in-house was used in data acquisition and analysis. This software allowed for variable time-period data acquisition during cell cycle and automatic data acquisition on change in polarity of the electrometer.

3.2.2 Li/TiS_2 Cell Performance - Cell Type 2

The laboratory cells used to test electrolyte chemical stability and Li/TiS_2 cell performance demonstration were almost identical to those used in evaluation of lithium cycle life as described in the previous section. Only the cathode was changed from a metal foil to a stainless steel screen containing the TiS_2/carbon black/binder matrix. On cell cycle, the computer-based datalogging and analysis system was again used with the Amel Model 545 Electrometer.

3.2.3 AA-Size Spirally Wound Cells

AA-size hermetic Li/TiS_2 cells with spirally wound electrodes were made to test the performance of such cells using the electrolytes and cathode matrix composition identified as improved under this Phase I program. The AA-size cells were 1.36 cm in diameter and 5.33 cm long; when filled they weighed approx. 20 g. A glass-to-metal terminal (Fusite) was used which was welded to the cell top; the cell top and bottom were welded in-house to the can using an Nd:YAG laser welder (Raytheon SS 501). The cell was filled through a circular port on the bottom of the can which was then covered and welded shut. Cell assembly and filling was carried out in a dry room.

The spirally wound electrode was prepared using a 4 mil lithium foil (3.8 x 14.0 cm) and a 20 mil cathode (3.8 x 12.7 cm). The lithium foil was placed between two pieces of Celgard 2400 and the end with the strip of stainless steel screen as tab was inserted in the slot of a mandrel. The mandrel was mounted on a platform and connected to a rotating wheel. The mandrel was rotated slightly, the cathode placed on the inner side of the separator-isolated anode, and then the electrode was wound with tension being applied to maintain a tight spiral. After the electrode was wound, it was slid off of the mandrel and inserted into the cell can (prior to top and bottom piece insertion and welding). Electrode tabs were spot welded (anode to glass-to-metal pole and cathode to can wall), and then the top and bottom cell pieces were pushed in place for laser welding. The resulting spirally wound electrode structure had a theoretical capacity of approx. 250 mA-hrs (TiS_2-limited); this theoretical capacity could have been increased if a thinner cathode was used as would have been obtained if a thinner stainless steel screen current collector had been used because a reduction in cathode thickness would have permitted a significant increase in the length of the cathode in the spirally-wound electrode.

3.3 Test Procedures Used

3.3.1 ^{13}C-NMR Shift Measurement

^{13}C-NMR spectra were obtained in-house using an FT-NMR (IBM NR80) on 2 ml samples using a tube-in-tube technique where the exterior wide-bore (10 mm dia.) NMR tube contained the sample and a sealed narrow-bore (5 mm) NMR tube containing the internal standards of CD_3COCD_3 (for NMR signal lock) and TMS (for shift position reference). Resident NMR computer routines were used to identify the shift position of each ^{13}C-bond signal in the sample; the ratio of cyclic ether to co-solvent in the presence and absence of 1 M solute was varied in the samples. The effect of these variations in sample composition on bond shift position was determined by normalizing the measured bond shift position to the TMS reference position and to the shift position of the ^{13}C-bond in the neat solvent. In-house developed software was used to calculate the change in ^{13}C shift as a function of change in sample composition.

3.3.2 GC/MS Chemical Analyses

A GC/MS with HP 5970 MS detector was used to analyze samples of cell electrolyte before and after cell cycle. 0.5 ul of electrolyte were injected directly on the column. Microbore capillary (0.53 mm dia.) column (BP-5; 11 ft. glass; SGE) conditions used in evaluating 2-Me-THF based electrolytes were 150°C with a helium flow rate of 77 cm/sec and splitter ratio of 7/1. Interface temperature was 240°C. The MS was scanned over the range of 10 to 300 amu. Similar conditions were used in analysis of 1,3-dioxolane-based electrolytes except that the GC temperature was reduced to 100°C (42 cm/sec He).

3.3.3 Lithium Surface Layer Characterization

The capacitance and the resistance of the compact layer portion of the lithium surface layer was determined following the galvanostatic transient methods described by Issacs and Leach (23) who modified the RC-network model analysis for a constant current load (19) to permit the use of a square wave current step on a steady-state condition. Under this method, when 4T is the period of the square wave oscillation, and I is the current applied, then:

$$\log \frac{dV}{dt} = \log \frac{I}{C} \left(1 + \tanh \frac{T}{CR}\right) - \frac{t}{2.3CR}$$

Thus, in a plot of log (dV/dt · 1/I) vs. t, the slope equals -1/2.3 CR and the intercept at t = 0 equals log 1/C (1 + tanh T/CR). Values for R and C can thus be determined based on a plot of experimentally derived values for log dV/dt · 1/I vs. t. The apparent film thickness, D, was estimated from the parallel-plate-capacitor equation which relates D to 1/C as described in Section 2.5.

Using a function generator (Global Model 2001) and a dual trace storage oscilloscope (Leader LBO-5825), values of dV/dt vs. t were obtained, along with T and I, for each lithium cell cycle experiment.

In these determinations, a square wave pulse current (100 uA, 15 kHz) was superimposed on the cell driving current (5 - 10 mA). The resulting voltage transient (working electrode vs. lithium reference) was recorded simultaneously with the square wave pulse using a dual-channel storage oscilloscope. The voltage vs. time data obtained were analyzed and fitted to a mono-exponential decay equation of the form:

$$V = P_1 - P_2 e^{-P_3 t}$$

This equation form comes from an RC model in which the load voltage decays exponentially with time. The derivative of the fitted curve was determined as a function of time, and values for C, R and D determined following the graphical method described in the previous paragraph. Analyses of the data were carried using IBM-compatible hardware and in-house developed software.

3.3.4 Lithium Cycle Tests

Initial screen of electrolytes was carried out in laboratory cells (Cell Type 1) with lithium cycled between a lithium foil and a lithium-plated metal (nickel or stainless steel) foil electrode. In cell test, lithium was first plated onto the metal foil electrode in the electrolyte of interest at constant current (10 mA; 2.5 mA/cm^2). The cell was then cycle tested at 10 mA discharge/charge cycles of 10 min. duration each with the discharge consisting of partially stripping the lithium off of the metal foil electrode. Electrode failure was judged based on a cut-off voltage (working vs. reference) of 1.0 V; this voltage was monitored and recorded using an IBM-compatible PC equipped with a MetraByte DASH-8 data logger and EXP-16 multiplexer; voltage data were stored to disk on one minute intervals during the charge/discharge cycle. Four cells were tested for every electrolyte parameter tested.

3.3.5 Laboratory Cell Cycle Tests

Laboratory cells with lithium anode and TiS_2-containing cathode were used to initially characterize the performance of such cells with the program-identified electrolytes and cathode matrix compositions. In these laboratory cell tests (Cell Type 2), planar 4 cm^2 electrodes were used with Celgard 2400 as separator material. An Amel Model 545 Electrometer was used to cycle the cells at rates from 2 to 8 mA (0.5 to 2 mA/cm^2). Cells were cycled at room temperature, at -40°C (Puffer Hubbard Model ICF3506 Freezer), and at 71°C (heated sand bath).

The laboratory cells were cycled over the voltage range of 2.7 to 1.7 V at the set current: all cells were cycled for at least 10 cycles with improved cells cycled for 50 cycles. During cycle testing, cell voltage was recorded at minimum at 30 min. intervals and when the polarity of the electrometer changed (marking change from cell charge to discharge or discharge to charge). Cell voltage was monitored and recorded using an IBM-compatible PC equipped with a MetraByte DASH-8 data logger and EXP-16 multiplexer; all cell tests were run in duplicate. Samples of cell electrolyte were analyzed by GC/MS before and after the cycle test.

3.3.6 AA-Size Hermetic Cell Tests

AA-size hermetic Li/TiS_2 cells with spirally wound electrodes were prepared and cycled. These cells were cycled at -40°, RT, and 71°C at rates of 50 to 400 mA (1 to 8 mA/cm^2). The cells were cycled over the voltage range of 2.7 to 1.7 V; all cells were cycled for a minimum of ten cycles with improved cells cycled continuously for periods of up to 10 days. During cycle testing, cell voltage was recorded at minimum at 30 min. intervals and when the polarity of the electrometer changed (marking change from cell charge to discharge or discharge to charge). Cell voltage was monitored and recorded using an IBM-compatible PC equipped with a MetraByte DASH-8 data logger and EXP-16 multiplexer; all cell tests were run in duplicate.

4.0 RESULTS

4.1 Initial Electrolyte Mixture Selection

4.1.1 1,3-Dioxolane-Based Electrolyte

Initial screening of solvent mixtures was carried out using a NMR technique previously developed by ECO (3): this previous work showed a strong correlation between electrolyte chemical stability and conductance and change in ^{13}C-shift for mixed-solvent non-aqueous electrolytes. In this screening, a series of evaluations were carried out using an FT-NMR (IBM NR80) to determine the change in ^{13}C shift of the carbon atoms in two cyclic ethers [2-methyl tetrahydrofuran (2-MeTHF) or 1,3-dioxolane (DIOX)] as a function of extent of addition of an alkyl urea [1,1,2,2-tetramethyl urea (TMU) or 1,3-dimethyl-1,3-trimethylene urea (DTMU)] or of a alkyl ether [1,2-dimethoxyethane (DME)] in the presence of 1 M $LiAsF_6$.

Provided in Figures 1 and 2 are the data obtained on change in ^{13}C shift as a function of 1,3-dioxolane content in a mixed electrolyte containing 5 v/o DTMU and 1 M $LiAsF_6$, with Figure 1 showing the change in carbon shifts of DME and DTMU and Figure 2 showing the change in shifts of 1,3-dioxolane and DTMU over the same 1,3-dioxolane concentration range In both figures, abrupt or significant changes are shown for electrolytes containing over 70 v/o 1,3-dioxolane. The greatest change occurs with the carbons of DME. The addition of greater amounts of DTMU (10 and 20 v/o) decreases the magnitude of the change, but significant changes are still observed for electrolytes containing over 70 v/o 1,3-dioxolane (Figures 3 - 6); as the DTMU content increases, the magnitude of the shift of the carbons in DME decreases while those of 1,3-dioxolane and DTMU remain relatively constant. Omitting the solute ($LiAsF_6$) from the electrolyte causes significant change in the observed results: all of the changes in carbon shifts remain small although there still is a significant change as the 1,3-dioxolane content rises above 70 v/o (Figures 7 - 8). Increasing the DTMU content in the absence of the solute does not have a pronounced affect on the magnitude of the observed changes in shifts (Figures 9 -10).

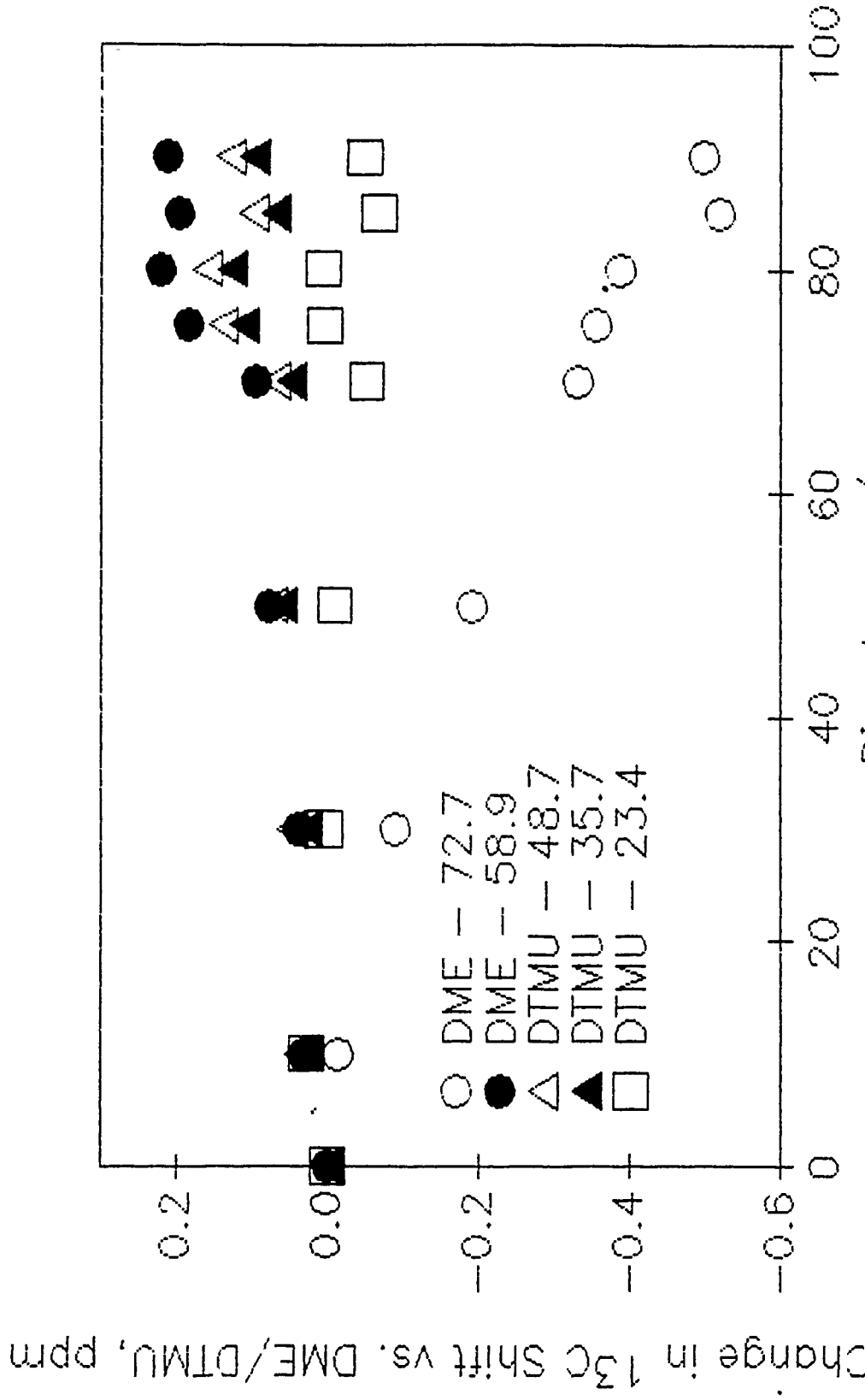

FIGURE 1. DIOXOLANE/DME WITH 5% DTMU AND 1 M $LiAsF_6$

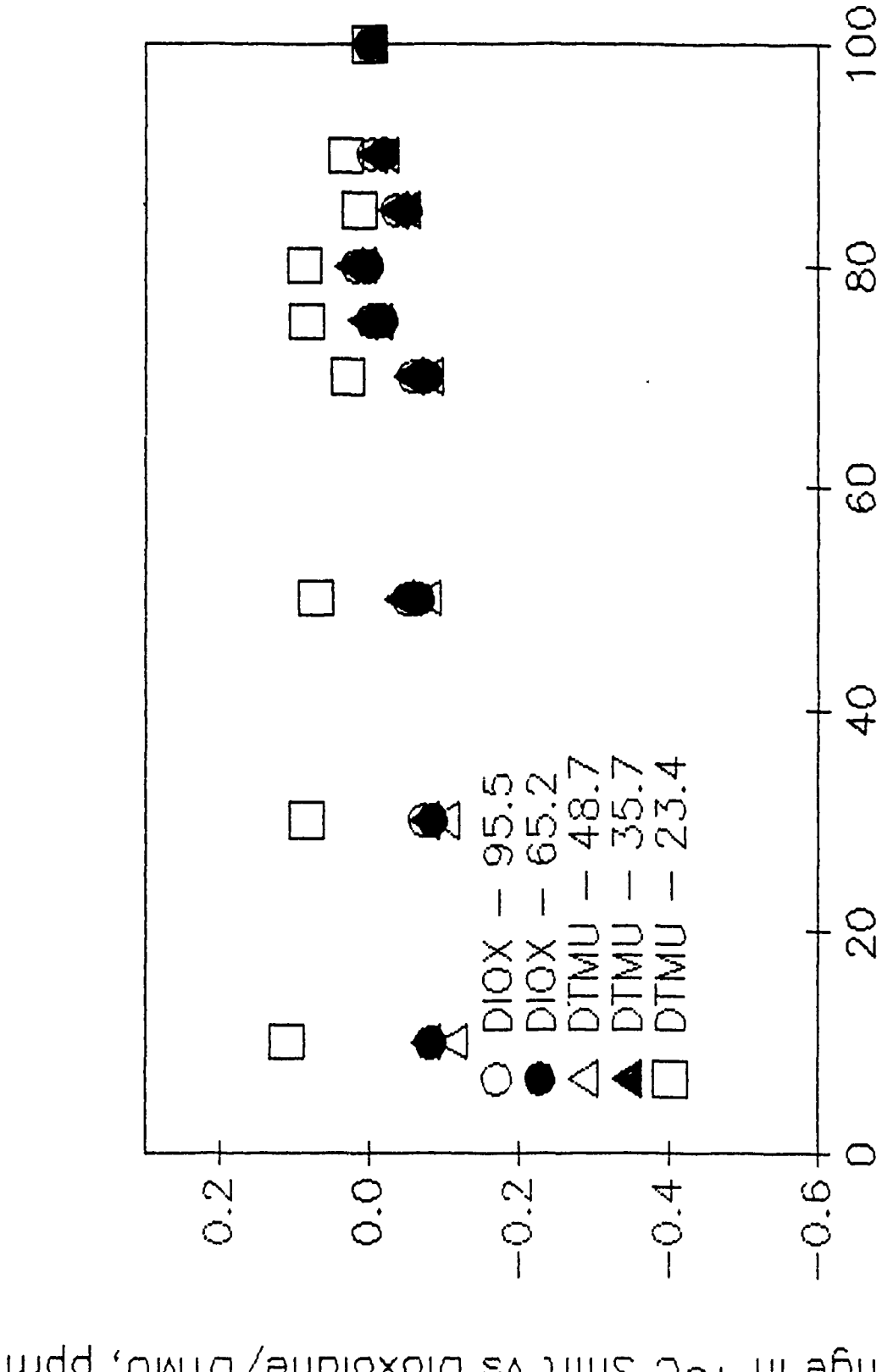

FIGURE 2. DIOXOLANE/DME WITH 5% DTMU AND 1 M $LiAsF_6$

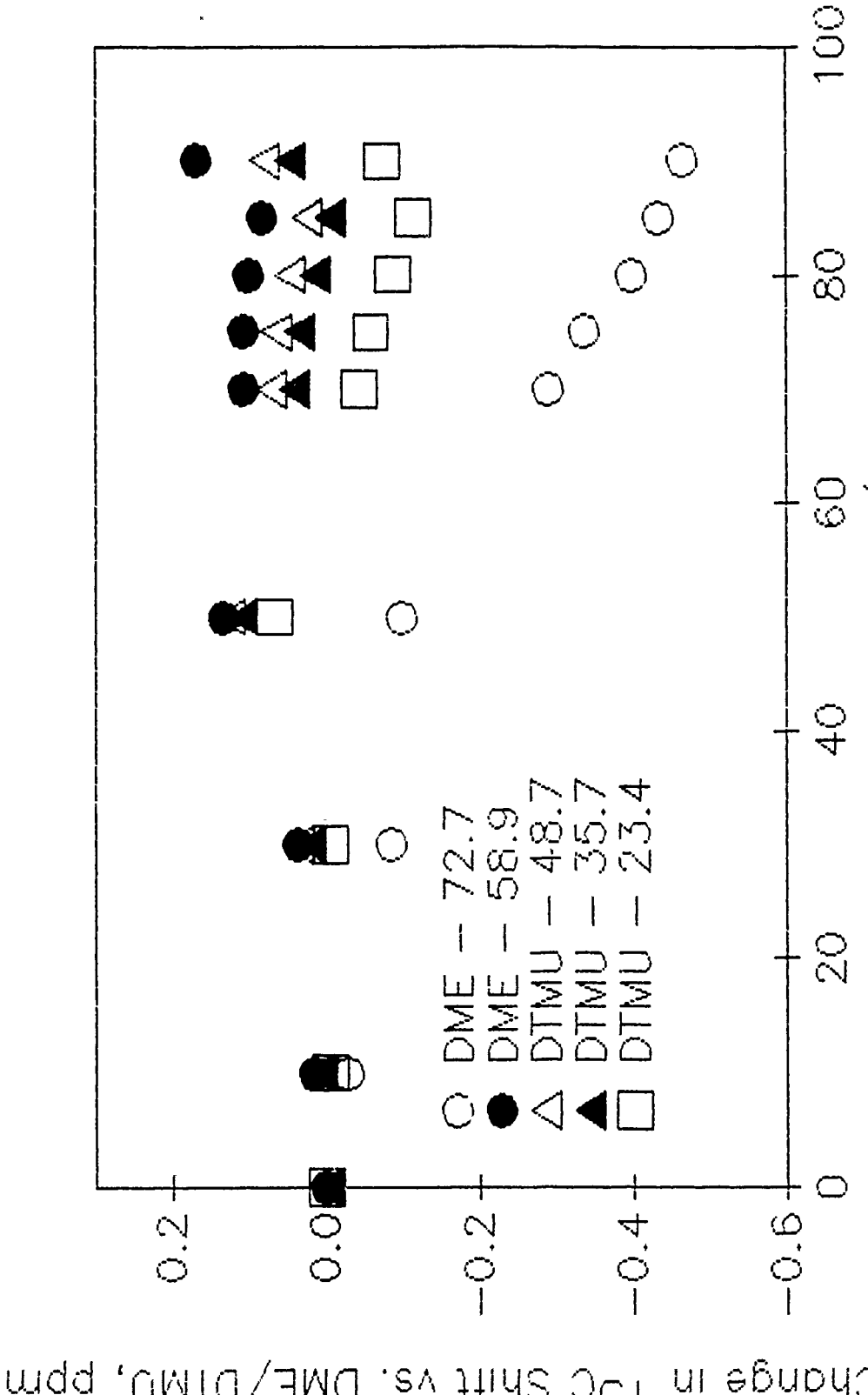

FIGURE 3. DIOXOLANE/DME WITH 10% DTMU AND 1 M $LiAsF_6$

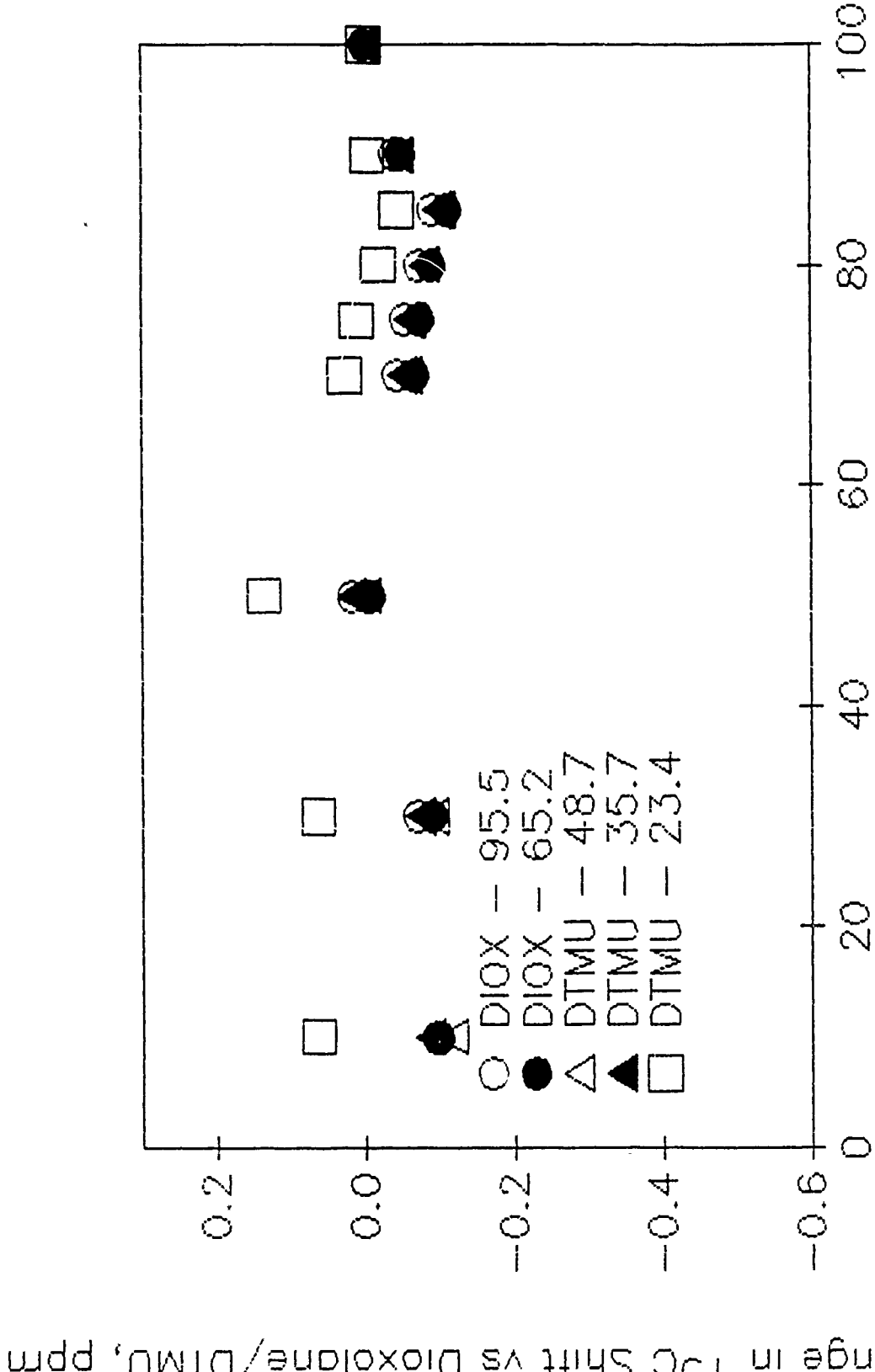

FIGURE 4. DIOXOLANE/DME WITH 10% DTMU AND 1 M $LiAsF_6$

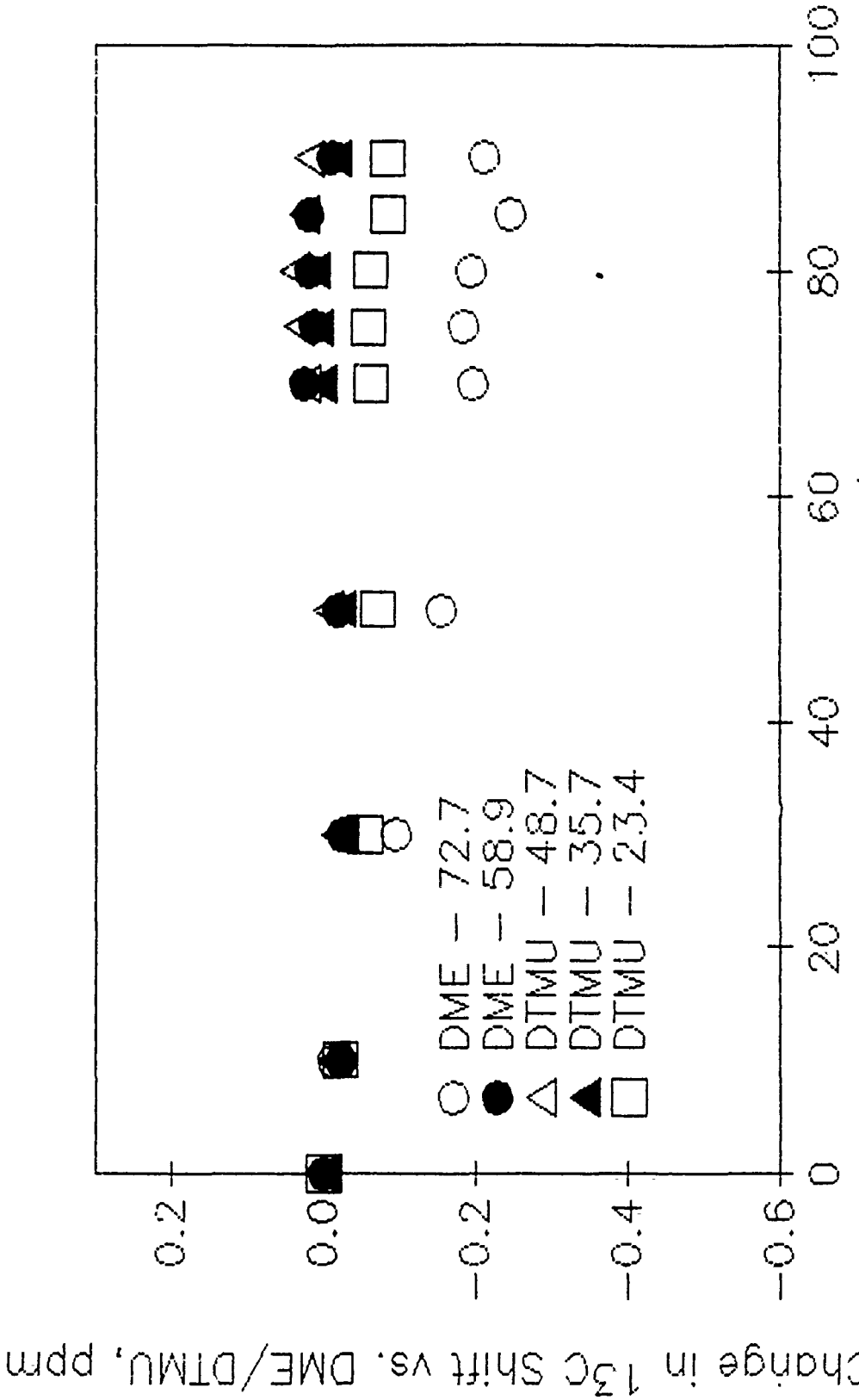

FIGURE 5. DIOXOLANE/DME WITH 20% DTMU AND 1 M $LiAsF_6$

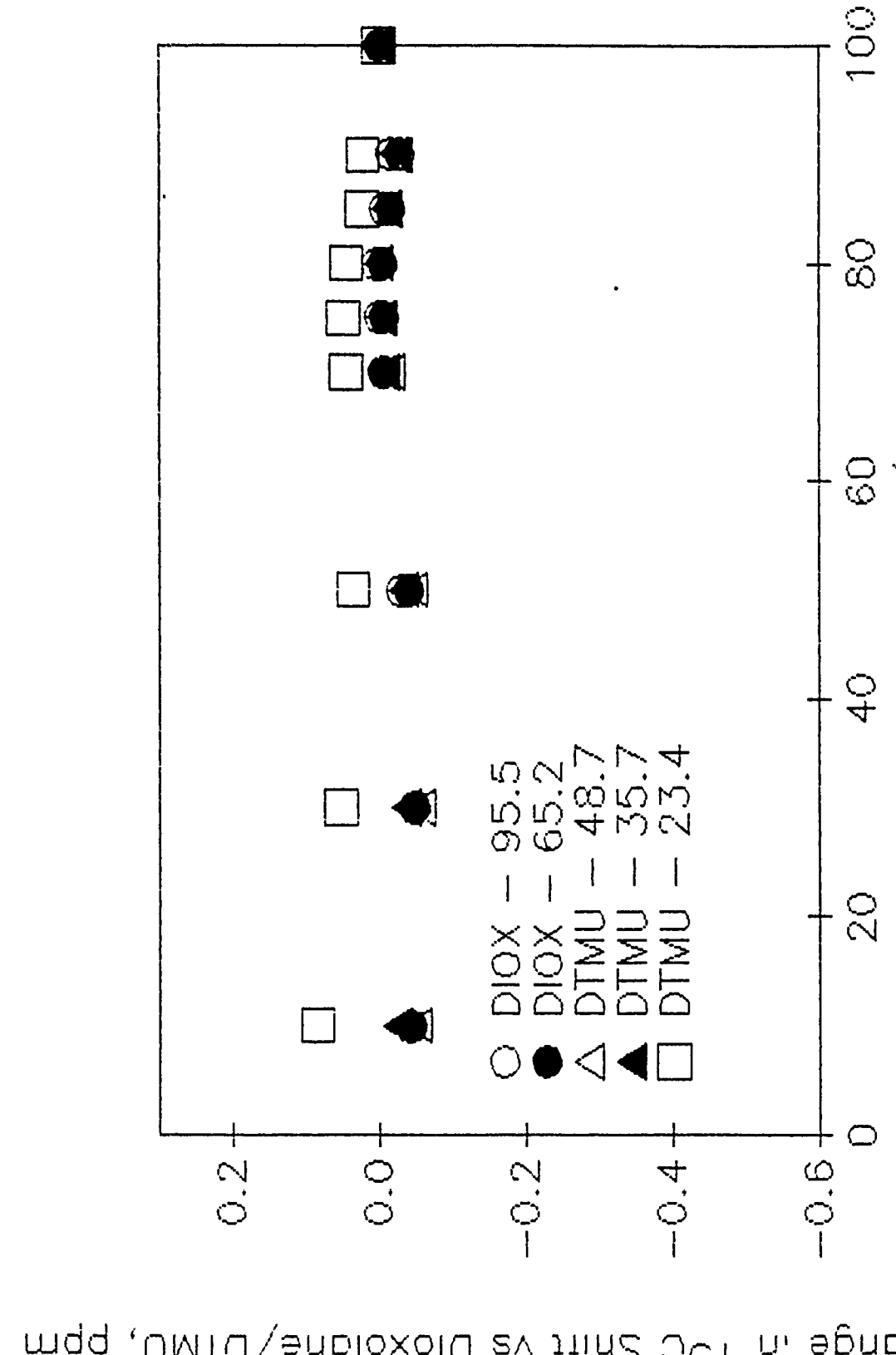

FIGURE 6. DIOXOLANE/DME WITH 20% DTMU AND 1 M $LiAsF_6$

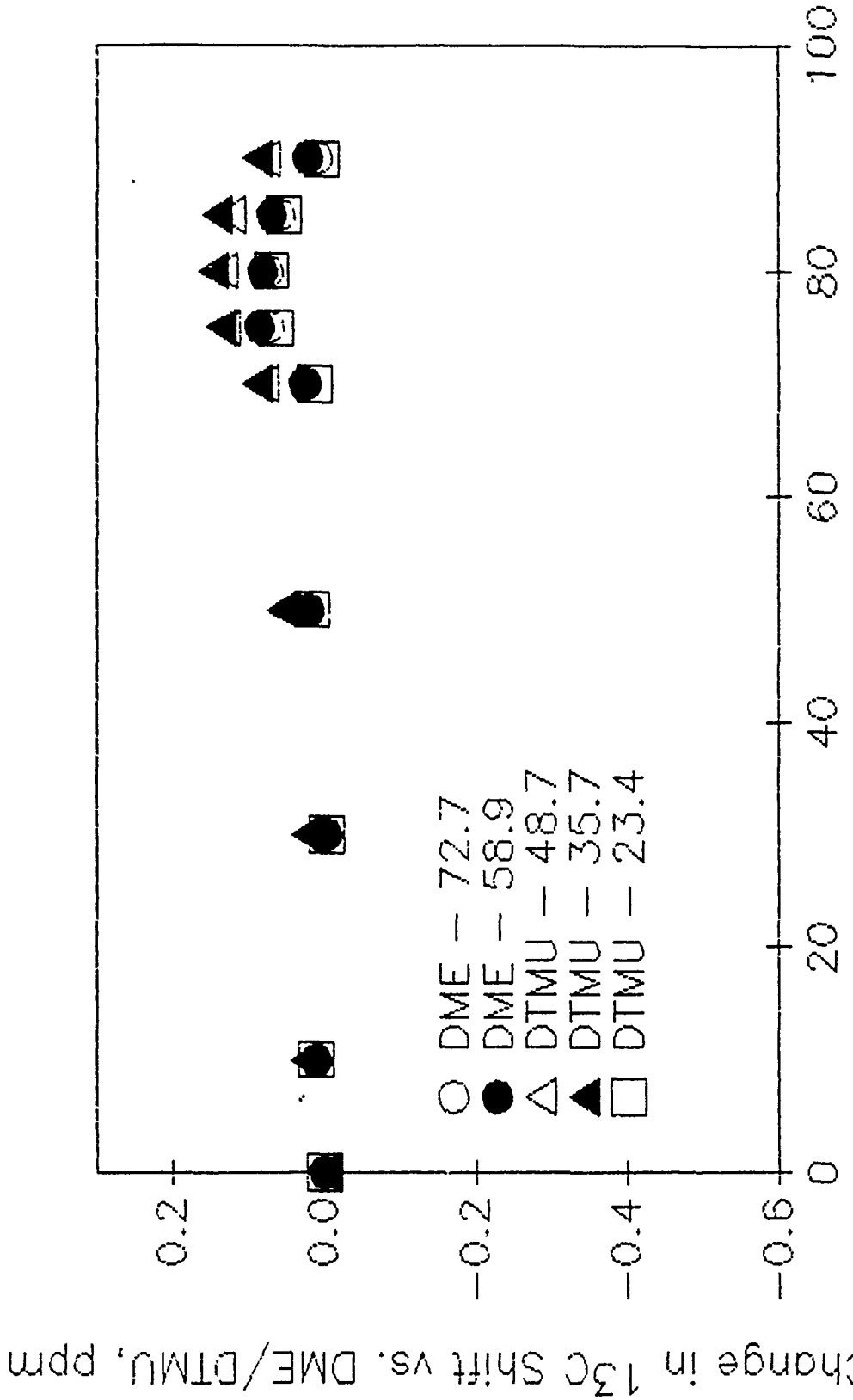

FIGURE 7. DIOXOLANE/DME WITH 5% DTMU

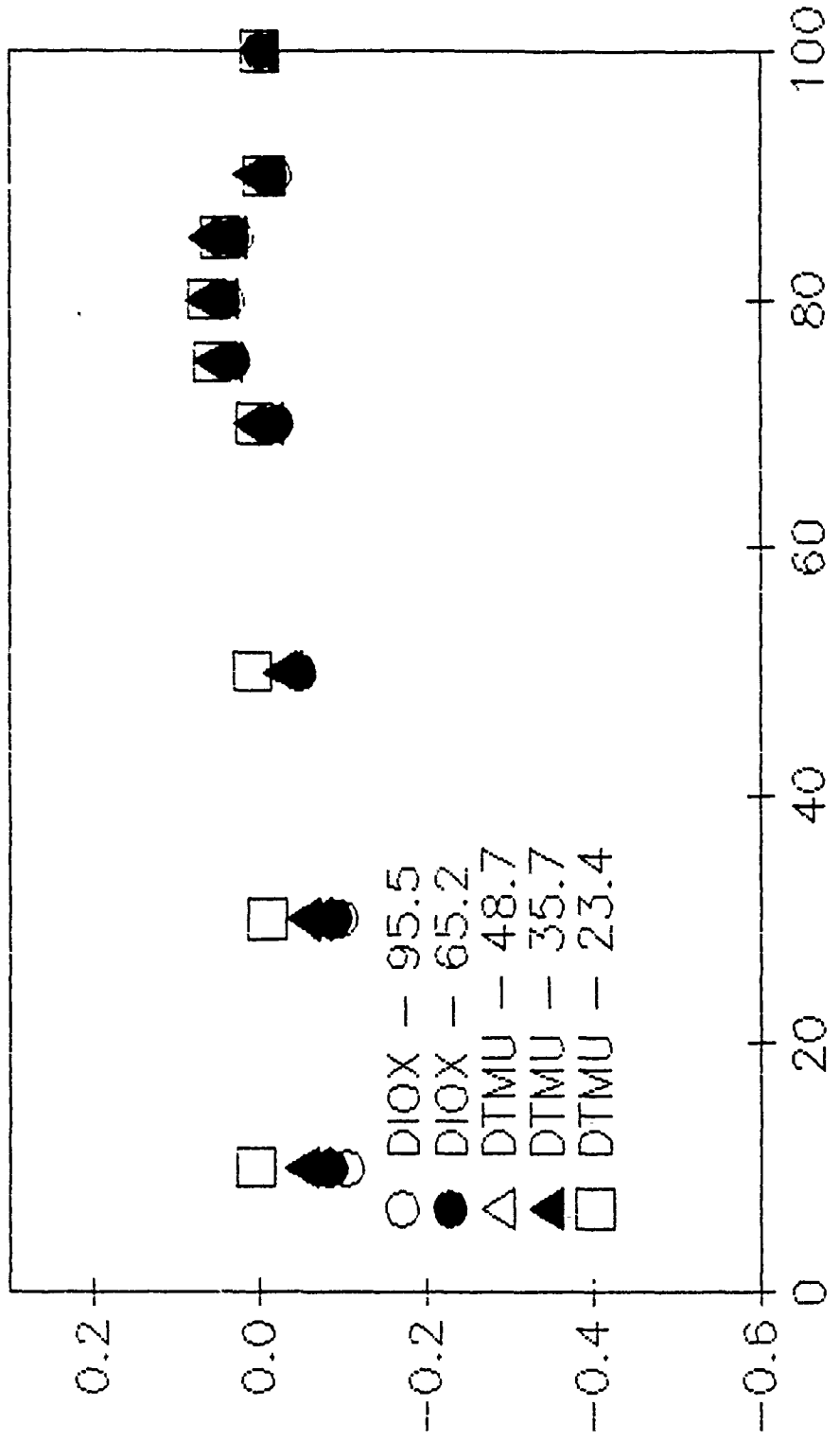

FIGURE 8. DIOXOLANE/DME WITH 5% DTMU

From the data provided in Figures 1 - 10, it is apparent that the 2,3-methylene carbons (72.7 ppm) of DME undergo the largest change in electron cloud density in the presence of the solute ($LiAsF_6$) and that this change is a function of 1,3-dioxolane concentration. In the absence of the solute a solvent-solvent interaction is still observed at a electrolyte 1,3-dioxolane content of approximately 80 v/o which represents a 1:4 ratio of DME:DIOX on a molecular basis. This 1:4 ratio suggests the presence of hydrogen bonding between the protons of the methylene carbons and the oxygens of the dioxolane: such bonding would result in increased shielding of the carbon due to increased electron cloud density from the oxygen as it associates with the hydrogen on the carbon. Increased electron shielding on the carbon is indicated by the increased positive value of the ^{13}C shift shown in Figures 7 - 10.

The addition of the solute to the electrolyte results in apparent deshielding of the methylene carbons of DME as the 1,3-dioxolane content of the electrolyte increases as shown by the increased negative value of the ^{13}C shift (Figures 1 - 6). This deshielding of the methylene carbons would result from the association of the lithium atom in the solute with the oxygen atom alpha to the methylene carbons; apparently such association is enhanced when the DME:DIOX ratio is 1:4 or greater on a molecular basis. This apparent requirement of a combined interaction of DME and 1,3-dioxolane to cause enhanced electron cloud interaction with lithium parallels the facility of various crown ethers to form tight complexes with lithium ions when the molecular structure (oxygen- and carbon-containing ring) of the crown ether is suitably tailored to cause extensive electron sharing in linear-bonding hybrid orbitals (24). Based on the observed enhanced deshielding of the methylene carbons of DME compared to that of either of the 1,3-dioxolane carbons, it is apparent that the extent of electron sharing with lithium is greater between the oxygens alpha to the methylene carbons. That this lithium:oxygen association affects the proton:oxygen association observed in the absence of the solute is unlikely given that the observed discontinuity in change in shift observed as the 1,3-dioxolane content exceeds 70% remains unaffected.

The net affect of the association of the oxygens in DME to form a electron-sharing cage for lithium ions with the oxygens of 1,3-dioxolane or of the proton-oxygen interaction of the two solvents should be enhanced stability of the electrolyte solution to chemical degradation by lithium radicals formed in electrochemical cycling of lithium. The increased overlap of electron clouds in the mixed solvent should prevent adventitious interaction with the lithium radical. The addition of DTMU, an alkyl urea, does not detrimentally affect this potentially protective association until the electrolyte content of DTMU rises above 10 v/o (Fig. 5 vs. Fig. 3). Based on these ^{13}C-NMR results, two mixed-solvent electrolytes chosen for further study were DME:1,3-dioxolane in a 1:4 by volume ratio and the same mixture containing 5 v/o DTMU.

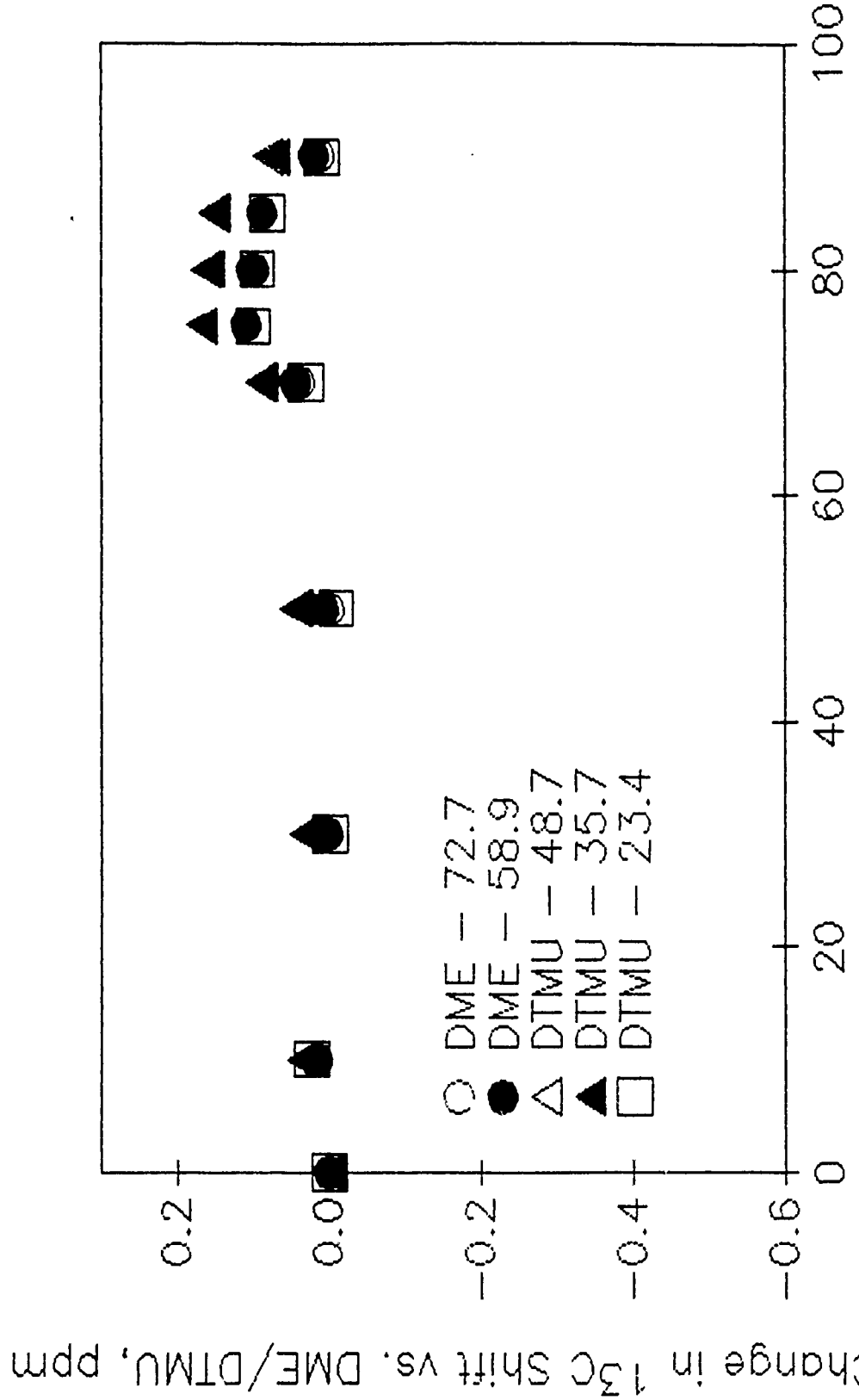

FIGURE 9. DIOXOLANE/DME WITH 10% DTMU

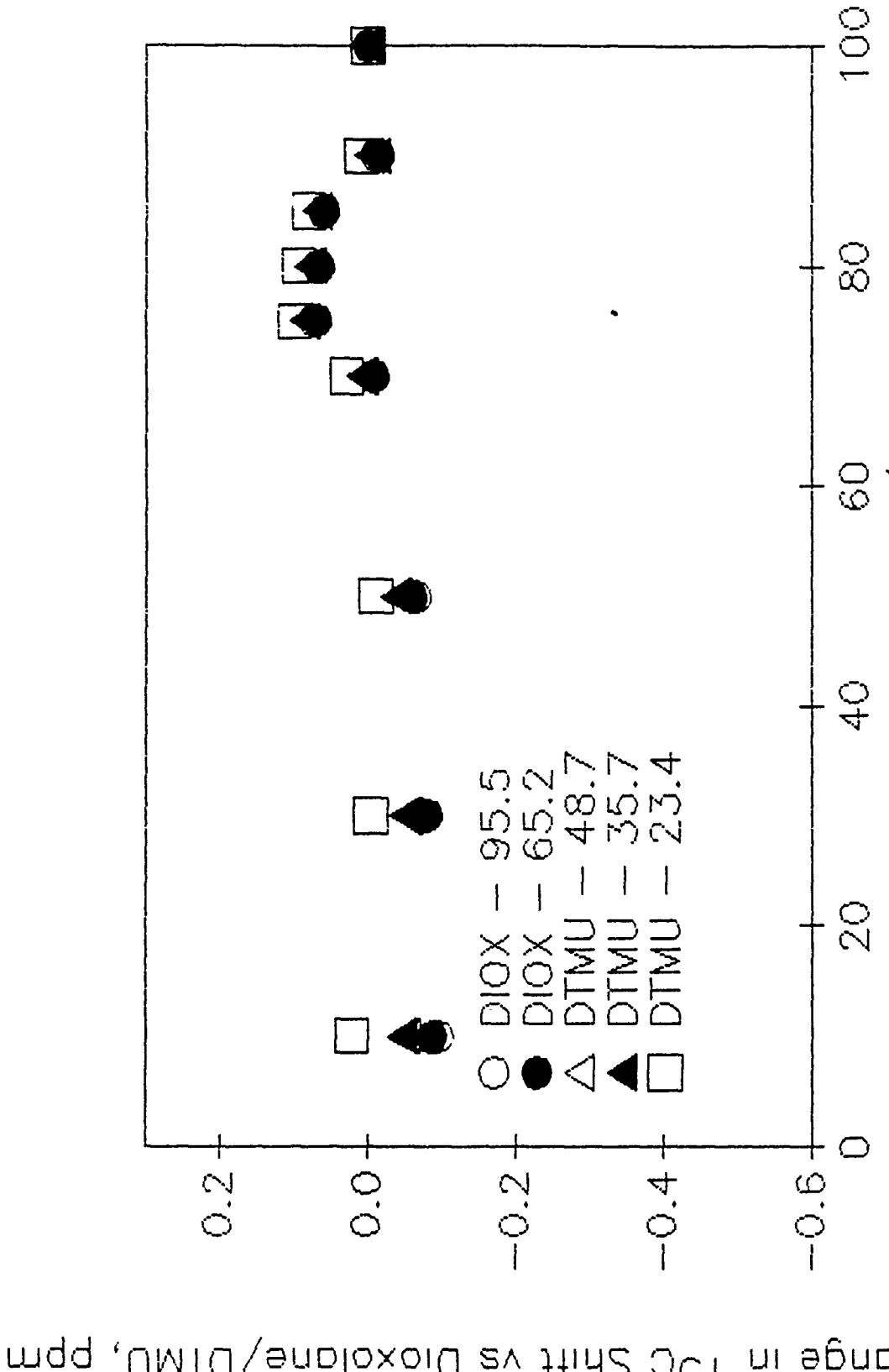

FIGURE 10. DIOXOLANE/DME WITH 10% DTMU

4.1.2 2-MeTHF-Based Electrolyte

^{13}C-shift data were also obtained for and mixed solvent electrolyte based on 2-MeTHF with 1 M $LiAsF_6$. Provided in Figures 11 - 14 is a presentation of the data obtained. The extent of deshielding shift (reduction in electron density) of the carbons alpha to the oxygen in 2-MeTHF and increased shielding of the other three carbons is shown to be a function of volume ratio of 2-MeTHF (Figure 11) although the relationship is not as obvious as with the 1,3-dioxolane-based electrolyte. For the 2-MeTHF-based electrolyte an apparent discontinuity in shift of the carbons alpha to the oxygen occurs at a 2-MeTHF content of approximately 80 v/o. At a similar concentration a significant change in shift also occurs for the carbon alpha to the oxygen in TMU (Figure 12). In the absence of the solute, no significant trends or changes in shifts are observed for either solvent as a function of solvent ratio (Figures 13 and 14).

The results provided in Figures 12 - 14 indicate electron cloud sharing between the oxygen of 2-MeTHF and lithium from the solute; the extent of sharing is apparently altered by the presence of an alkyl urea. However, the extent of solvent-solvent interaction in this solvent mixture is decreased compared to that observed for the 1,3-dioxolane-based electrolyte. Based on these results, two additional electrolytes chosen for further study were 2-MeTHF (with 2-MeF) and a mixture of 2-MeTHF and TMU (80 v/o 2-MeTHF) both with 1 M $LiAsF_6$.

4.1.3 Effect of Change in Solute

An additional NMR-based study was made of 1,3-dioxolane-based electrolytes containing $LiBF_4$ as solute. Provided in Figure 15 is a display of data on the change in ^{13}C-shifts as a function of 1,3-dioxolane concentration by volume for a DME-1,3-dioxolane mixture. Some electron cloud sharing is indicated which is deshielding of the carbons in 1,3-dioxolane for lower 1,2-dioxolane contents. Addition of 1 M $LiBF_4$ to the mixed solvent system again results in a significant deshielding of the methylene carbons in DME (Figure 16). However even more increased deshielding is observed on the addition of 1 M $LiAsF_6$ (Figure 17). A comparison of Fig. 1 with Fig. 17 shows that the presence of 5 v/o DTMU apparently enhances the proton:oxygen interaction but does not affect the lithium:oxygen association. Based on these results, a fifth electrolyte chosen for additional study was DME/1,3-dioxolane (1:4 by volume) with 1 M $LiBF_4$; this electrolyte was chosen because it permits evaluation of the effect of a different solute and of the extent of chemical stability as related to the observed extent of ^{13}C-shift.

4.2 Lithium Cycle Life

4.2.1 Laboratory Cell Data

Lithium cycle life was tested in laboratory cells with stacked electrode configuration so as to more closely model the electrode/separator surface contact effects of a practical Li/TiS_2 cell.

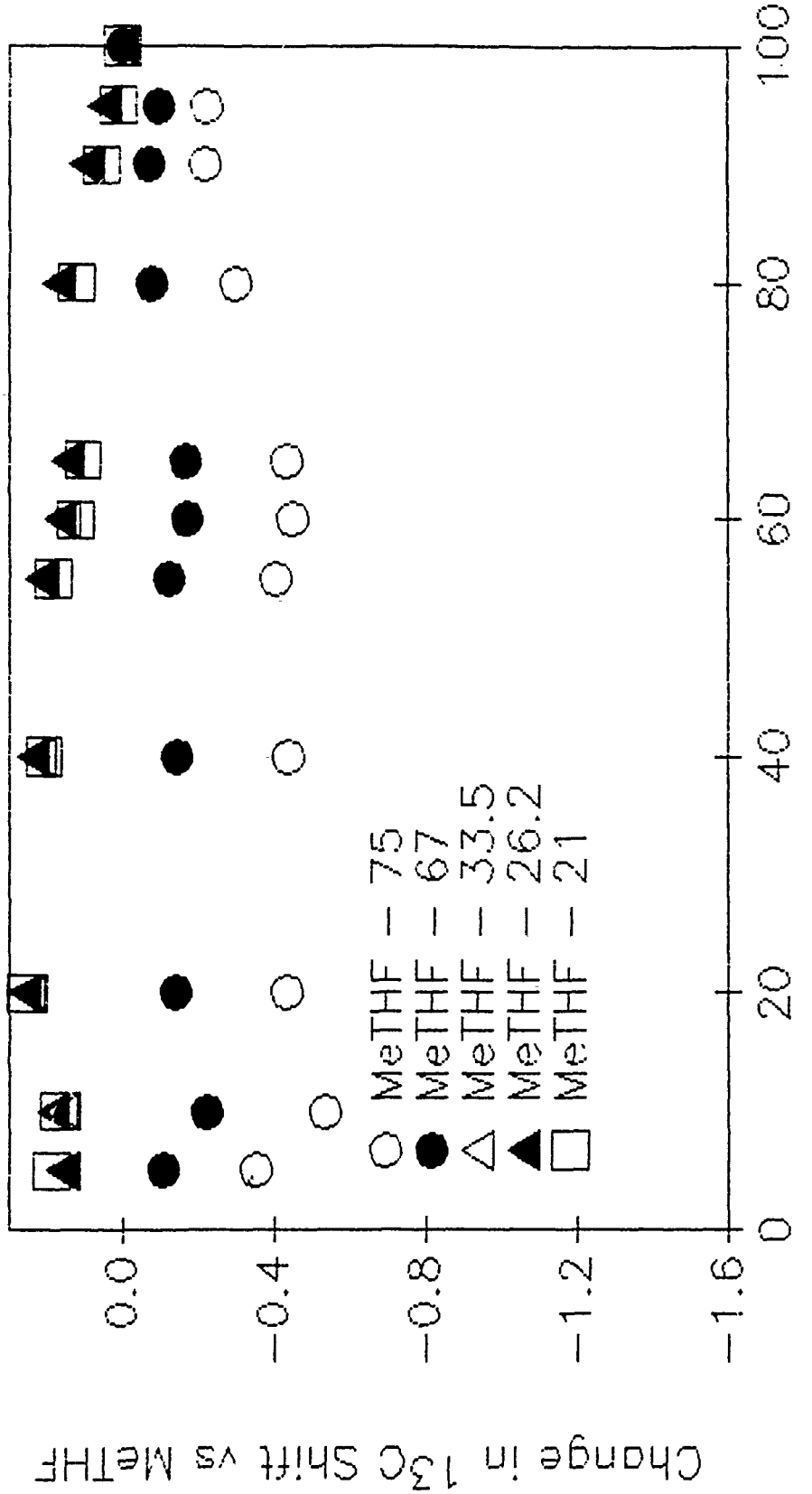

FIGURE 11. MeTHF WITH TMU AND 1 M $LiAsF_6$

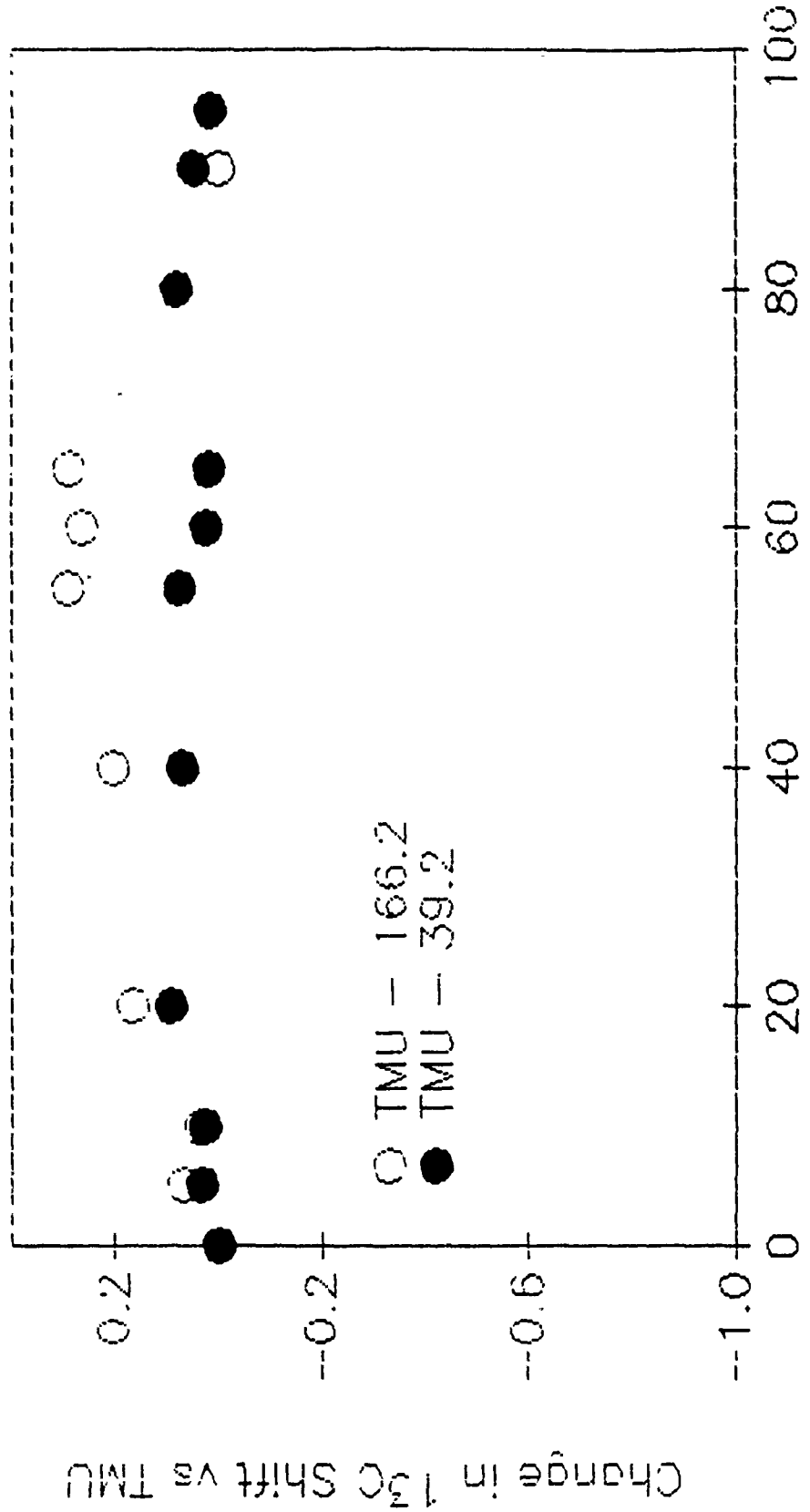

FIGURE 12. MeTHF WITH TMU AND 1 M $LiAsF_6$

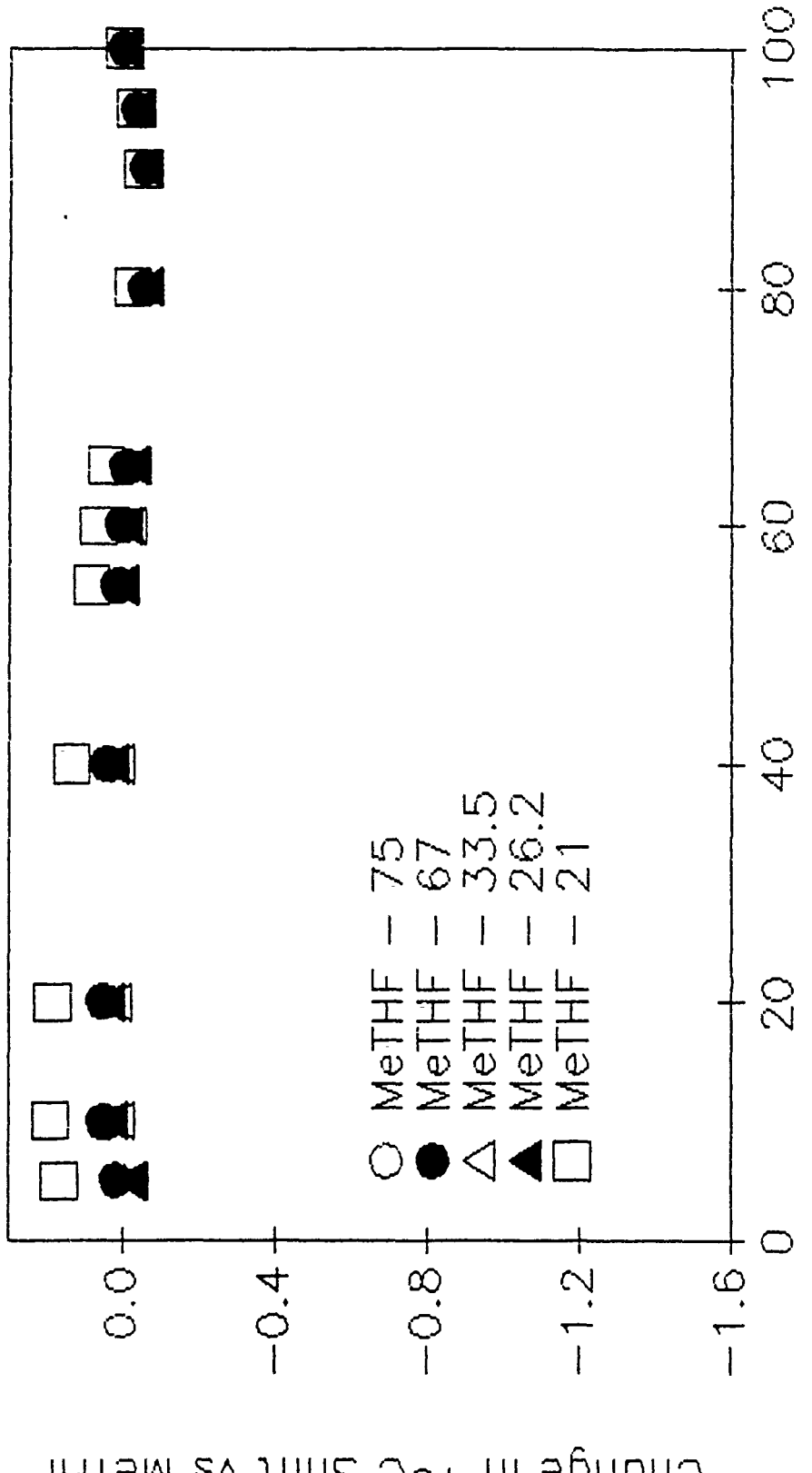

FIGURE 13. MeTHF WITH TMU

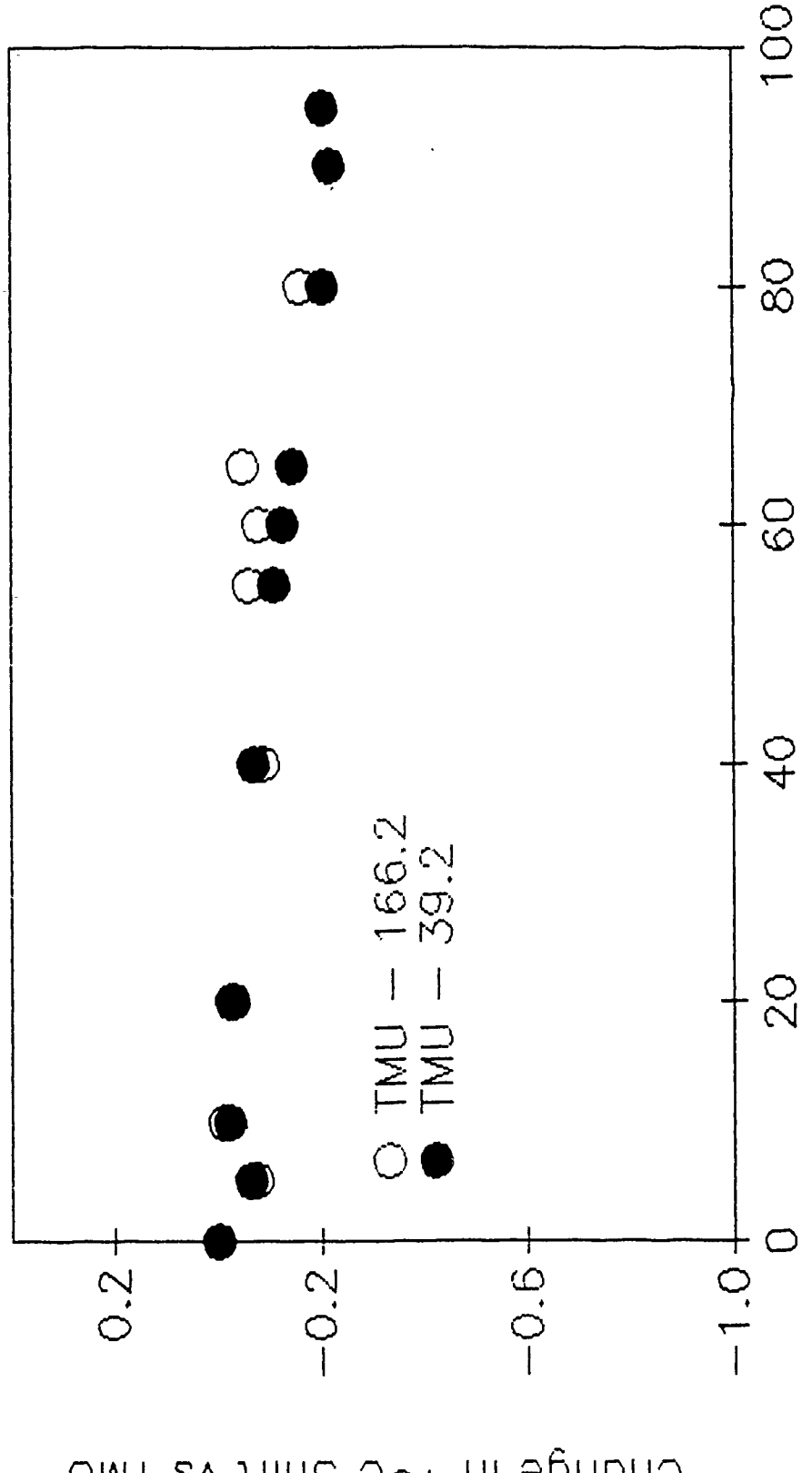

FIGURE 14. MeTHF WITH TMU

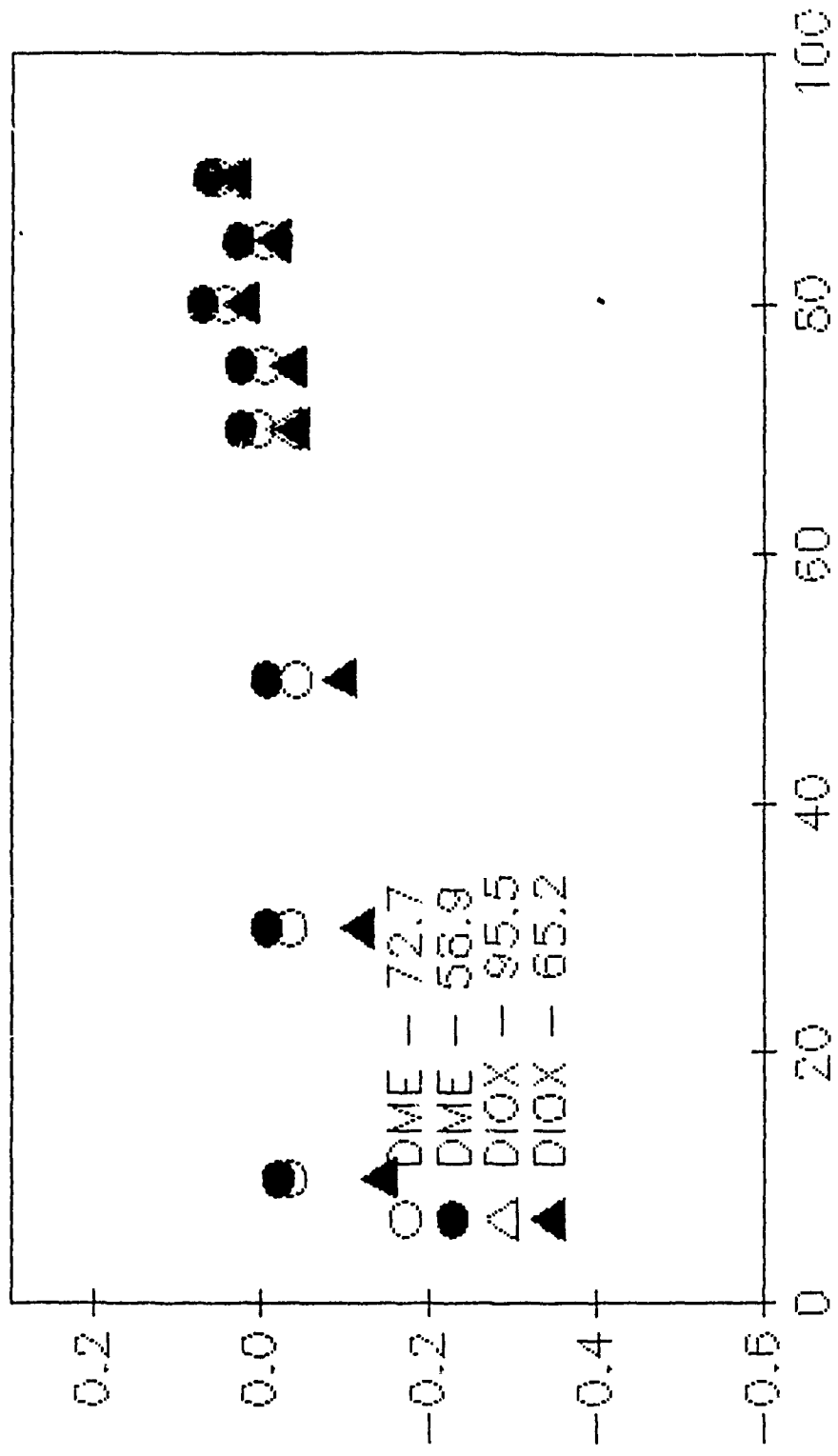

FIGURE 15. DIOXALANE/DME WITH NO ELECTROLYTE

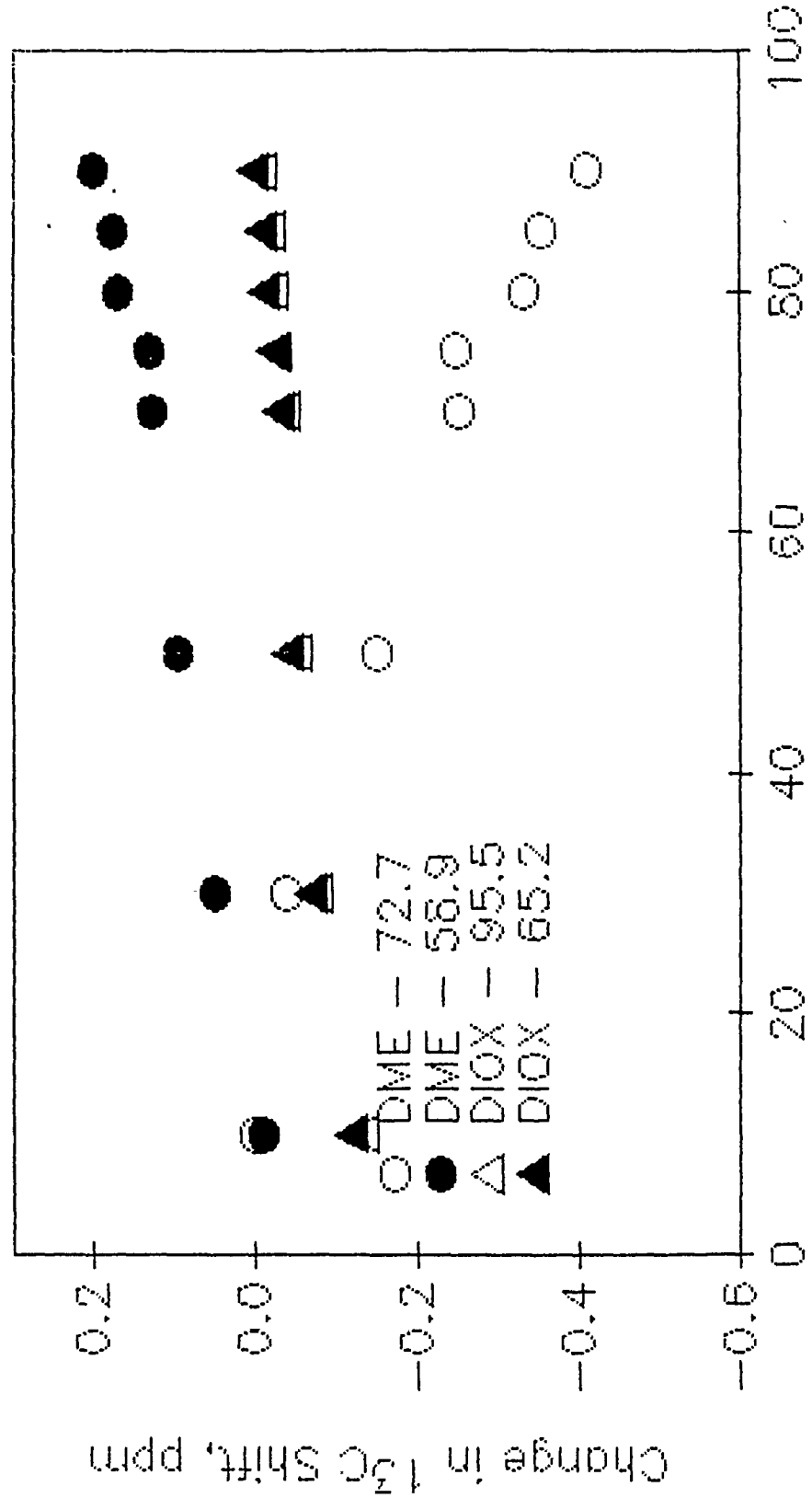

FIGURE 16. DIOXALANE/DME WITH 1 M $LiBF_4$

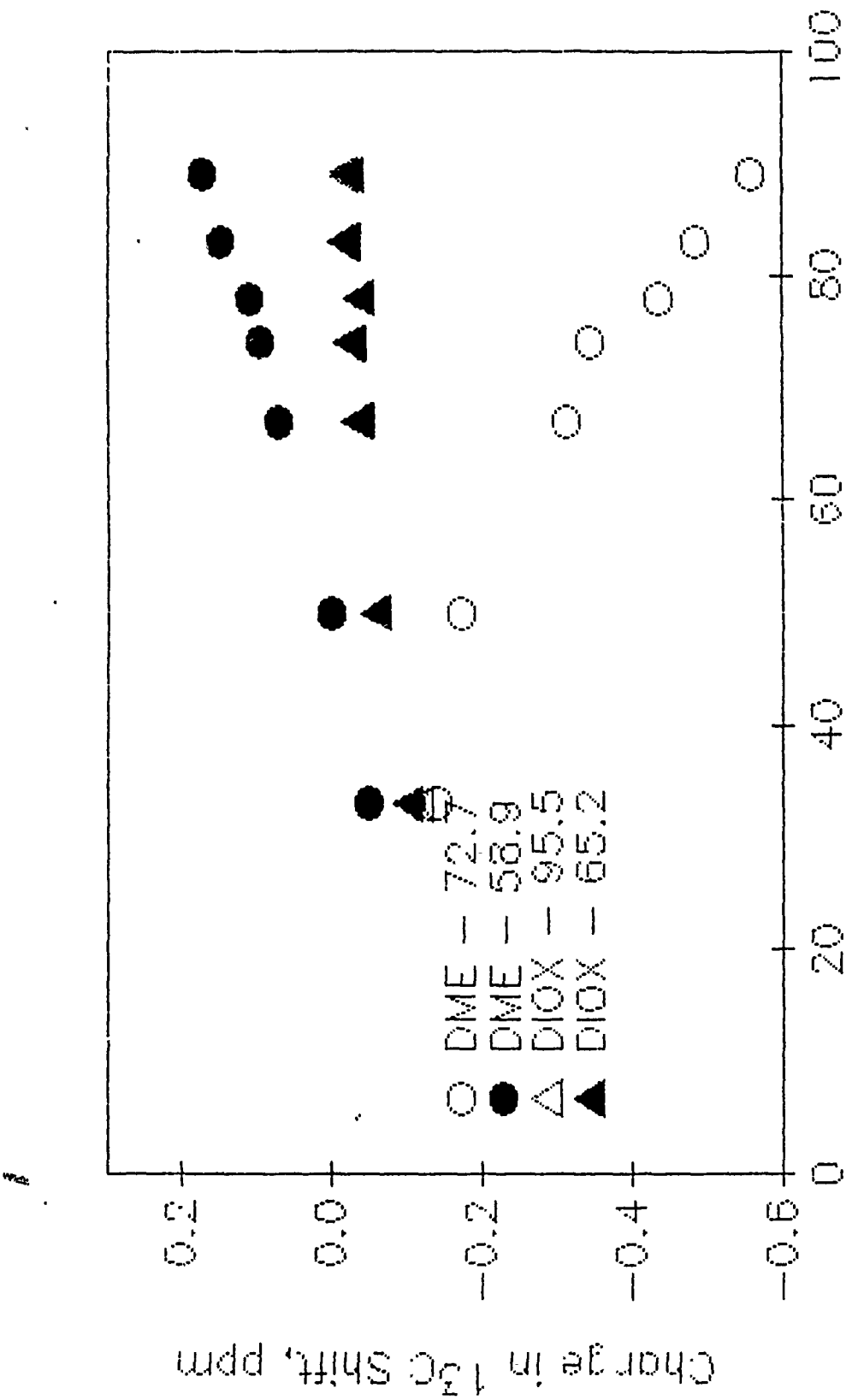

FIGURE 17. DIOXALANE/DME WITH 1 M $LiAsF_6$

The laboratory cells (Cell Type 1) were prepared to contain an electrode stack consisting of a lithium foil electrode (4 cm^2 SA), a lithium foil reference electrode (0.1 cm^2 SA), and a 4 cm^2 nickel or stainless steel foil electrode. Cells tested varied both in separator material (located on either side of the reference electrode between the two working electrodes) and in electrolyte.

The initial series of laboratory cells prepared varied in separator material; the electrolyte used was 1 M $LiAsF_6$/2-MeTHF. In previous work Kerr (4) examined the stability on lithium cycle of this electrolyte in a test cell which used a wide electrolyte gap rather than a physical separator barrier between electrodes; the study by Kerr thus did not include aspects of soft shorting of the cell due to localized dendrite penetration of the separator. In the lithium cycle tests using the Cell Type 1, lithium was first plated onto the metal foil electrode at constant current (10 mA; 2.5 mA/cm^2) for 20 min; the lithium was then cycled at 10 mA on 10 min. cycles. This cycle regime is a strenuous test condition given literature reports that lithium plating (Li/TiS_2-cell re-charge) should be carried out at rates of less than 0.5 mA/cm^2 to increase lithium cycle life. If, however, an electrolyte provides improved lithium cycle performance under these strenuous conditions (e.g., high rate charge and electrode-separator physical contact), this improved performance will only be magnified under less strenuous conditions.

In this initial series of laboratory cell tests, a study was made of the effect of three separator types on lithium electrode cycle life. The three separators tested were Celgard 2400, Rayperm 2-2065 and Craneglas 7-200. The Celgard and Rayperm separator materials are porous organic films approximately 1 mil thick with a void volume in excess of 70%. Rayperm is prepared from a halogenated (chlorofluoro) polypro-polyethylene co-polymer; Celgard is a microporous polypropylene film. Craneglas is fiberglass (7 mil) mat with up to 90% void volume; this material is conventionally used in primary lithium cells. Each separator was tested in four different cell cycle tests. Cells with Celgard 2400 as separator were observed to have approximately twice the cycle life of those containing Craneglas and 50% more than those with Rayperm. Based on these results, all additional cell tests were carried out using only the Celgard separator.

A second series of laboratory cells were tested which varied in electrolyte solvent ratio. Those cells with 2-MeTHF-based electrolyte contained either no TMU or a 1:4 by volume TMU:2-MeTHF ratio with 1 M $LiAsF_6$; those with 1,3-dioxolane-based electrolyte contained a 1:4 by volume DME:1,3-dioxolane ratio with or without 5 v/o DTMU. Provided in Table 1 is a listing of the observed cycle life (to a 1 V vs. reference cut-off) of these cell types based on duplicate cell test results; also provided is a listing of a parameter, F.O.M. (Figure Of Merit), which is calculated based on the number of cell cycles times the ratio of lithium cycled to the initially plated lithium. This parameter thus provides an estimate of the extent of available turn-over of the initially plated lithium (e.g., a value of 1 would imply no replating of lithium).

TABLE 1

Cycle Life of Selected Cells

with Me-THF-based electrolyte

	Cell 1	Cell 2	Cell 3	Cell 4
No. cycles to failure	6	6	9	11
F.O.M.	3	3	4.5	5.5
Contained TMU	No	No	Yes	Yes

with 1,3-dioxolane/DME-based electrolyte

	Cell 1	Cell 2	Cell 3	Cell 4
No. cycles to failure	12	12	6	7
F.O.M.	6	6	3	3.5
Contained DTMU	Yes	Yes	No	No

The data provided in Table 1 show that the addition of an alkyl urea co-solvent to the electrolyte results in an approximate doubling of the cycle life of the lithium electrode. Factors limiting cell cycle life are not identified by these data, but they may include cell shorting due to dendrite growth, lithium radical reaction with the electrolyte to form a surface passivating layer, and formation of electrochemically-unavailable lithium zones. The latter limitation is unlikely given the observation that the metal foil electrodes did not show hydrogen gas generation upon insertion into cold water after cycle test.

An additional series of laboratory cells were prepared and tested which contained 2-MeTHF-based electrolytes with 1.2 v/o 2-Me-F, an additive concentration reported by Abraham et al. to improve lithium cycle life (2). In the cells tested, a combination of this additive in an electrolyte containing a TMU:2-MeTHF volume ratio of 1:4 increased the FOM to 16.5 or an additional increase in cycle life of a factor of three. In the absence of the TMU, a FOM of 8.5 was observed. Thus, the addition of both the alkyl urea and the 2-methyl furan appears beneficial in enhancing lithium cycle life.

4.2.2 Electrolyte Chemical Stability on Lithium Cycle

Aliquots of electrolyte from the laboratory cells used to test lithium cycle life were withdrawn prior to and during the lithium cycle test; these samples were analyzed by GC/MS. The mass range examined was 50 to 300 amu; a capillary column held at 120° to 230°C was used in analysis. Provided in Figure 18 are exemplar total ion chromatograms of the electrolyte from selected cells. These data show that, in the absence of TMU, some chemical degradation of the 2-MeTHF-based electrolyte occurs; in the presence of TMU no additional compounds are detected. Similarly some additional peaks are observed for the 1,3-dioxolane-based electrolyte in the absence of DTMU, albeit at an intensity level at least a factor of five less than for the 2-MeTHF-based electrolyte. In the presence of 5 v/o DTMU even these minor peaks are not present.

The initial Cell Type 1 cells prepared used a nickel foil electrode and a lithium foil on nickel screen electrode; these cell components were observed to be suitable for both of the electrolyte types in the absence of addition an alkyl urea. However, upon addition of an alkyl urea to these electrolytes, a light blue-green color was observed to rapidly develop in the electrolytes suggesting the dissolution of the nickel in a solvation reaction enhanced by the presence of the urea. The lithium cycle life of the cells with nickel components and an alkyl urea in the electrolyte was significantly lower (less than 4 cycles). Upon replacement of the nickel components with 314 stainless steel screen and foil, the discoloration of the electrolyte was not observed. The data provided in Figure 18 and Table 1 are from cells with stainless steel components.

The data obtained in these GC/MS studies show that the addition of an alkyl urea co-solvent to a 2-MeTHF- or 1,3-dioxolane-based electrolyte is beneficial in reducing the rate of chemical degradation of the

MeTHF electrolyte pre-cycle

MeTHF electrolyte post cycle

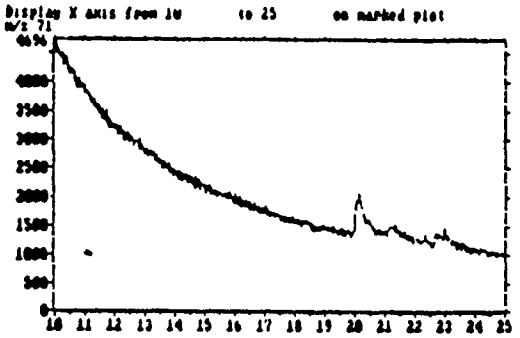

MeTHF/TMU electrolyte pre-cycle

MeTHF/TMU electrolyte post cycle

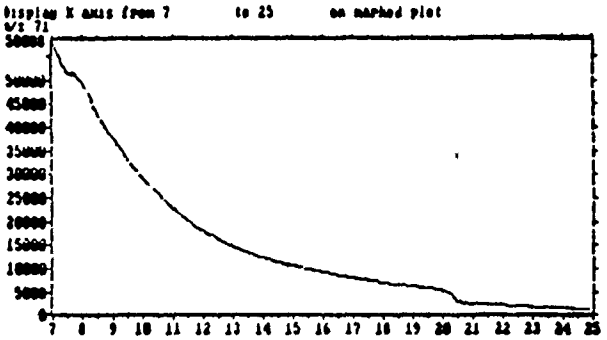

1,3-dioxolane/DME electrolyte pre-cycle

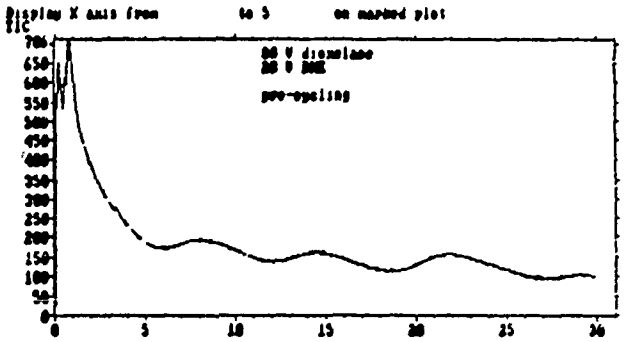

1,3-dioxolane/DME electrolyte post cycle

FIGURE 18. SELECTED GC/MS DATA

electrolyte on lithium cycle; the data also indicate that the 1,3-dioxolane-based electrolyte has increased chemical stability compared to the 2-MeTHF-based electrolyte.

4.2.3 Lithium Surface Layer Characterization

As selected intervals during lithium cycle life testing using the laboratory cells, selected characteristics of the lithium surface layer were determined. These determinations were based on the use of a galvanostatic transient method with a square wave current (100 uA) pulse (15 kHz) superimposed on the cell cycle current (10 mA). The resulting voltage transient (working vs. reference electrode) was recorded simultaneously with the applied square wave (to determine $I_{applied}$ based on the voltage drop observed across a resistor in series with the pulse generator) using a dual-channel digital storage oscilloscope. The voltage vs. time data of the electrode recovery portion of the voltage transient were transferred to disk and analyzed by fitting to a mono-exponential decay equation of the form:

$$V = P_1 - P_2 e^{-P_3 t}$$

This equation form was used to model the expected time-dependent response of a lithium electrode with the surface layer acting as an RC network (19). Based on the values of the parameters obtained on curve fit, a plot was made of log (dV/dt · 1/I) vs. t; the slope of this plot equals 1/2.3 CR, where C and R are the capacitance and resistance of the surface film. For a square wave pulse load, the intercept of this plot equals log [1/C·(1 + tanh T/CR)] where 4T is the period of pulse load application (23). Surface film thickness, D, was estimated from the parallel-plate-capacitor equation ($D \propto 1/C$).

Provided in Tables 2 and 3 are values for the surface film parameters C, R and D obtained in analysis of data obtained on laboratory cells with various electrolytes. Cells 1 and 2 of Table 2 were prepared with a DME/1,3-dioxolane (1:4 by volume ratio) based electrolyte with 5 v/o DTMU; cells 3 and 4 were prepared with an electrolyte lacking the DTMU. These data show that during cell cycle, lithium layer thickness becomes less on cycle in DTMU-containing cells than in the absence of DTMU; this result correlates with the decreased cycle life of the DTMU-free cells suggesting that the presence of this layer may be passivating to the lithium electrode. There is considerable noise in the data as evidenced by the range of values observed for C, R and D in the cell test replicates so precise correlation between cycle life and layer thickness, capacitance or resistance is not appropriate. In general, however, the surface layer on the lithium formed in cells with electrolyte containing DTMU appears to have greater increase in capacitance (especially compared with the capacitance of the oxide layer on the stainless steel foil) suggesting that the surface layer in DTMU-containing cells may have increased porosity.

Provided in Table 3 are corresponding data for cells containing electrolytes based on 2-MeTHF: cells 3 and 4 contained 20 v/o TMU. Again there is considerable noise in the calculated parameter values, but the general trends observed with the 1,3-dioxolane-based electro-

Table 2
Electrolyte based on 80 v/o 1,3-Dioxolane, 20 v/o DME

After 1.5 hrs on 10 min cycles (discharge cycle)

	Cell 1	Cell 2	Cell 3	Cell 4
Slope	-130400	-210200	-195400	-369500
Intercept	7.959	8.118	8.065	8.868
CR	.00000333	.00000207	.00000223	.00000118
1+tanh(T/CR)	1.9999090	1.9999998	1.9999994	2
C, uF	.02197912	.01524158	.01721987	.00271038
R, ohms	151.69957	135.70927	129.21643	434.13792
D, cm	.00004276	.00006166	.00005458	.00034677

After 1.5 hrs on 10 min cycles (charge cycle)

	Cell 1	Cell 2	Cell 3	Cell 4
Slope	-185400	-234100	-326000	-240900
Intercept	8.214	8.17	8.311	8.789
CR	.00000235	.00000186	.00000133	.00000180
1+tanh(T/CR)	1.9999987	2.0000000	2.0000000	2.0000000
C, uF	.01221883	.01052160	.00977305	.00325110
R, ohms	191.92552	137.35383	136.46603	555.14364
D, cm	.00007092	.00006951	.00009617	.00028909

After lithium charge for 40 min

	Cell 1	Cell 2	Cell 3	Cell 4
Slope	-207200	-352900	-389400	-289400
Intercept	8.271	8.304	8.297	8.886
CR	.00000210	.00000123	.00000112	.00000150
1+tanh(T/CR)	1.9999997	2	2	2.0000000
C, uF	.01071593	.00993185	.01009323	.00260034
R, ohms	195.81794	124.04821	110.62320	577.75491
D, cm	.00008771	.00009463	.00009312	.00036144

Before lithium charge

	Cell 1	Cell 2	Cell 3	Cell 4
Slope	-203400	-350200	-338200	-329400
Intercept	8.28	8.308	8.296	8.917
CR	.00000214	.00000124	.00000129	.00000132
1+tanh(T/CR)	1.9999997	2	2.0000000	2.0000000
C, uF	.01049615	.00984079	.01011649	.00242120
R, ohms	203.65323	126.16126	127.07747	545.15321

Table 3
Electrolyte based on Me-THF w/o TMU

After 2.0 hrs on 10 min cycles (discharge cycle)

	Cell 1	Cell 2	Cell 3	Cell 4
Slope	-360700	-371600	-250500	-403300
Intercept	8.776	8.911	8.262	8.929
CR	.00000121	.00000117	.00000174	.00000168
1+tanh(T/CR)	2	2	2.0000000	2
C, uF	.00334989	.00245488	.01094032	.00235521
R, ohms	359.82889	476.61364	158.64794	457.73482
D, cm	.00028030	.00038250	.00008583	.00039868

After 2.0 hrs on 10 min cycles (charge cycle)

	Cell 1	Cell 2	Cell 3	Cell 4
Slope	-617800	-324700	-293500	-453300
Intercept	8.936	8.875	8.473	8.493
CR	.00000070	.00000134	.00000148	.00000096
1+tanh(T/CR)	2	2.0000000	2.0000000	2
C, uF	.00231755	.00266704	.00673023	.00642732
R, ohms	303.66467	502.06492	220.10711	149.23011
D, cm	.00040516	.00035207	.00013952	.00014609

After lithium charge for 20 min at 10 mA

	Cell 1	Cell 2	Cell 3	Cell 4
Slope	-461000	-361700	-281100	-218200
Intercept	8.80	8.821	8.487	8.293
CR	.00000094	.00000120	.00000155	.00000199
1+tanh(T/CR)	2	2	2.0000000	1.9999999
C, uF	.00276077	.00302016	.00651673	.01018662
R, ohms	341.61839	398.00970	237.34568	195.60838
D, cm	.00034012	.00031091	.00014409	.00009218

Before lithium charge

	Cell 1	Cell 2	Cell 3	Cell 4
Slope	-455500	-433200	-260500	-238100
Intercept	8.718	8.786	8.374	8.317
CR	.00000095	.00000100	.00000167	.00000183
1+tanh(T/CR)	2	2	2.0000000	2.0000000
C, uF	.00382851	.00327363	.00845337	.00963896
R, ohms	249.31809	306.58699	197.43968	189.44484

lytes are again observed such as increased capacitance of the surface layer in the presence of the alkyl urea.

The data obtained in this study of lithium surface layer characteristics indicate a change in the parameters studied as a function of electrolyte composition. Further physical and chemical analyses of the layers formed will be necessary to provide a more complete understanding of the changes which were observed.

4.3 Li/TiS_2 Laboratory Cell Performance

4.3.1 Cathode Composition

The effect of material composition on TiS_2 cathode capacity was studied in a series of laboratory cells (Cell Type 2). In this study the capacity on the first discharge cycle was used as an indicant in ranking a cathode matrix; this testing was done in an iterative fashion to develop an improved cathode matrix. Cathodes were tested in complete cells with a cell stack (anode, separator, cathode) held under compression. Variables in this study were the type of carbon used to increase cathode matrix conductance and thus rate capability, cathode binder material, and electrolyte solution composition. Provided in Table 4 is a listing of the data obtained with each result being the average of duplicate cells.

The data provided in Table 4 show the benefit of the use of an EPDM binder (5 w/o) and Ketjenblack 300J (20 w/o) with TiS_2 as the cathode matrix; this cathode composition provides increased cathode discharge capability with 1,3-dioxolane-based electrolytes independent of electrolyte solute. This cathode matrix composition was used in all the additional cell tests including the hermetic AA-size cells with spirally-wound electrodes.

4.3.2 Effect of Electrolyte on Li/TiS_2 Cell Performance

Following determination of the components of an improved cathode matrix, a series of laboratory cells (Cell Type 2) were prepared and cycled at a discharge/charge rate of 1.0 mA/cm^2. These cells were prepared with a electrode stack (anode, separator, cathode) held under compression. The tests carried out permitted determination of the effect on cathode (and cell) cycle performance of changes in electrolyte composition: the electrolytes tested were those identified as being of interest based on the ^{13}C-NMR study described in Section 4.1. Provided in Tables 5 and 6 is a summary of the data obtained in these room temperature tests with the data presented based on the average performance of duplicate cells.

Provided in Table 5 are data on cathode cycle efficiency (coulombs in/out), average discharge capacity over third through seventh cycle (expressed as a percentage of first discharge cycle), extent of TiS_2 utilization (based on the measured cathode weight), and observed cathode material energy density. The data presented in this Table show that the use of the DME/1,3-dioxolane electrolyte provides cells with high cycle efficiency and maintenance of discharge capacity on cycle

Table 4

Effect of Cathode Components
on Li/TiS_2 Cell Discharge Capacity

Carbon Type	Binder Type	Electrolyte Type	First Cycle Discharge, mA-hrs
----	Vistalon	1	< 0.5
----	Vistalon	2	< 0.5
----	Polysar EPDM	1	4
Crystalline graphite	Polysar EPDM	1	1
Amorphous graphite	Polysar EPDM	1	7
Ketjenblack 300J	Polysar EPDM	3	15
Ketjenblack 300J	Polysar EPDM (10 w/o)	3	14
Ketjenblack 300J w/fibers	Polysar EPDM (10 w/o)	3	13
Ketjenblack 300J	Aldrich EPDM	3	18
Ketjenblack 600	Aldrich EPDM	1	14
Ketjenblack 300J	Aldrich EPDM	1	18

Notes:

1. Electrolyte Type 1 was 16:4:1::DIOX:DME:DTMU with 1 M $LiAsF_6$.
2. Electrolyte Type 2 was 32:8:1::MeTHF:TMU:MeF with 1 M $LiAsF_6$.
3. Electrolyte Type 3 was 16:4:1::DIOX:DME:DTMU with 1 M $LiBF_4$.
4. Binder at 5 w/o of solids and carbon as 20 w/o of solids for solids load of approximately 25 mg/cm^2.

Table 5

Effect of Solvent System on Secondary Cathode Performance

Electrolyte System:	MeTHF	MeTHF TMU	DIOX/DME	DIOX/DME DTMU
Cycle Efficiency, %	99	92	100	97
Disc. Capacity, % of 1st cycle	79	57	106	79
TiS_2 Utilization, %	70	40	78	57
Cathode Energy Density, A-hr/kg	130	75	145	105

Notes:

1. All values calculated as averages of two cells over five (third through seventh) charge/discharge cycles.
2. All electrolytes contain 1 M $LiAsF_6$; 4 cm^2 cathode prepared to contain 78 w/o TiS_2, 17 w/o Ketjenblack 300J, 5 w/o EPDM (Aldrich) at 25 mg/cm^2 load.

Table 6

Effect of Use of $LiBF_4$ as Electrolyte Solute

	MeTHF	MeTHF TMU	DIOX/DME	DIOX/DME DTMU
Cycle Efficiency, %	0	126	140	126
Disc. Capacity, % of 1st cycle	0	60	85	65
TiS_2 Utilization, %	0	2	32	34

Notes:

1. All values calculated as averages of two cells over five (second through seventh) charge/discharge cycles.
2. All electrolytes contain 1 M $LiBF_4$; 4 cm^2 cathode prepared to contain 78 w/o TiS_2, 17 w/o Ketjenblack 300J, 5 w/o EPDM (Aldrich) at 25 mg/cm^2 load.

(approx. 100%); cathode energy density is over 145 A-hr/kg or over 300 W-hr/kg (based on average discharge voltage of 2.1 V). The addition of the alkyl urea does not improve cathode performance in either the 2-MeTHF- or 1,3-dioxolane-based electrolytes.

Provided in Table 6 are parallel data obtained with cells where the electrolyte contains $LiBF_4$ rather than $LiAsF_6$ as electrolyte solute. The use of this solute is shown to significantly alter the performance of the TiS_2 cathode in the four electrolytes tested. The statistically higher than 100% cycle efficiency observed for three of the electrolyte systems suggests that the electrolytes are undergoing electrochemical reduction; the lower TiS_2 utilization, especially for the 2-MeTHF-based electrolytes, suggests that the intercalation reaction at the cathode is impeded in this electrolyte. The decreased electrochemical stability of the $LiBF_4$-based electrolytes indicated by a comparison of the data presented in Tables 5 and 6 correlates with the decrease in change in ^{13}C-shift with this solute described in Section 4.1.3.

4.3.3 Electrolyte Stability on Full Cell Cycle

Electrolyte samples were taken before and after discharge from the cell types identified in Table 5. These samples were again analyzed by GC/MS following the procedures outlined in Section 4.2.2 in which a 0.5 ul aliquot was injected on a capillary column held at 120° to 230°C and the mass range of 50 to 300 amu monitored for the presence of electrolyte breakdown products. As shown by the total ion chromatograms provided in Figure 19, no significant electrolyte degradation was observed after fifty cycles for the 1,3-dioxolane-based electrolytes.

4.3.4 Effect of Temperature on Laboratory Cell Performance

Additional Li/TiS_2 laboratory cells were prepared and discharged at elevated and reduced temperature. Provided in Table 7 is a listing of parameter values based on average values for replicate cells. The cells tested contained the DME/1,3-dioxolane (1:4 by volume ratio) electrolyte with 5 v/o DTMU; the cells were discharged/charged at 1 mA/cm^2. Cell cycle at elevated temperature is shown not to affect cathode performance with little change observed in cell cycle efficiency, maintenance of average discharge capacity, or TiS_2 utilization.

Cell performance at reduced temperature (-40°C) is shown by the data presented in Table 7 to suffer only in TiS_2 utilization: performance parameters of cycle efficiency and maintenance of discharge capacity are not significantly affected. Provided in Figure 20 is a graphical display of a cell cycled at -40°C; voltaic performance is shown to suffer at this reduced temperature with a reduction in average discharge voltage of 200 mV (from 2.1 to 1.9 V).

The data presented in Table 7 and Figure 20 show that the use of the 1,3-dioxolane-based electrolyte and the program-identified cathode

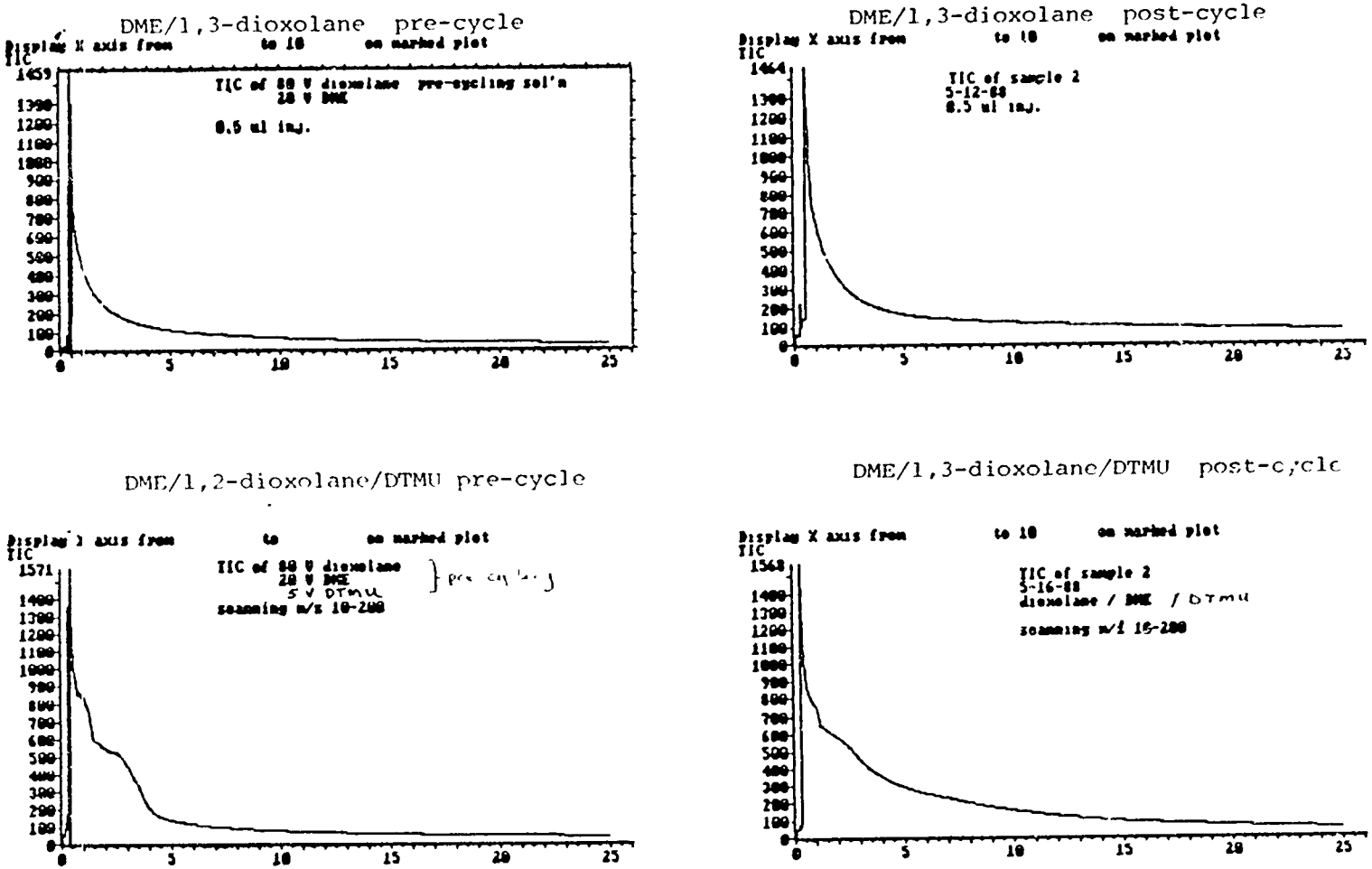

FIGURE 19 GC/MS TOTAL ION CHROMATOGRAMS OF PROGRAM SELECTED ELECTROLYTES

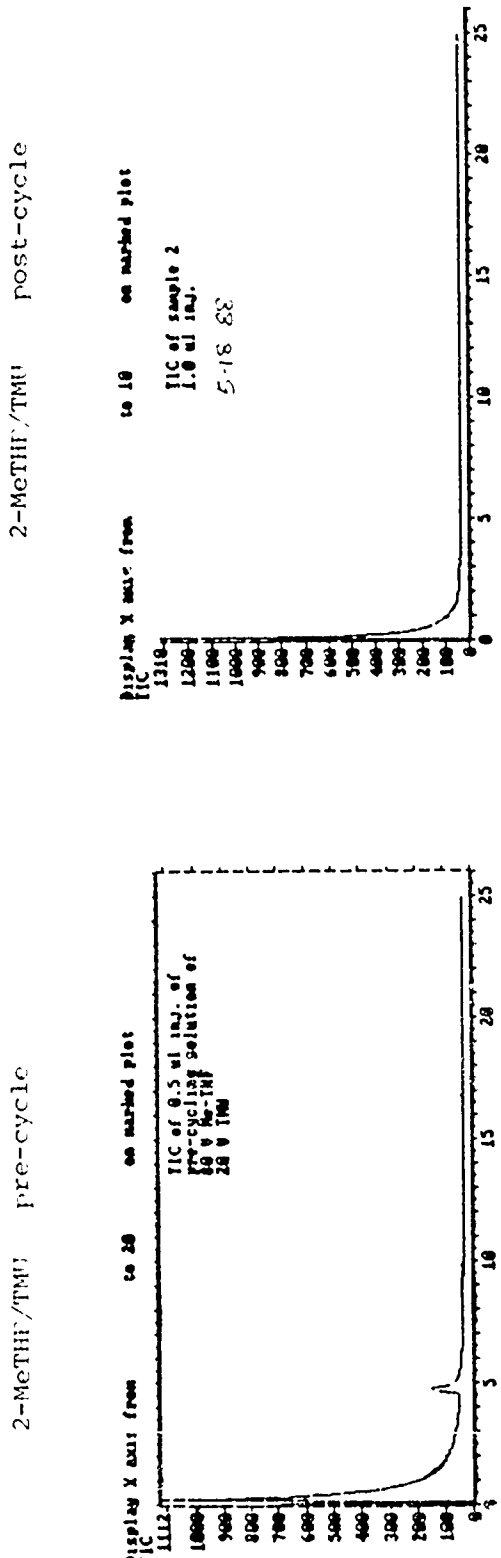

FIGURE 19. (CONTINUED)

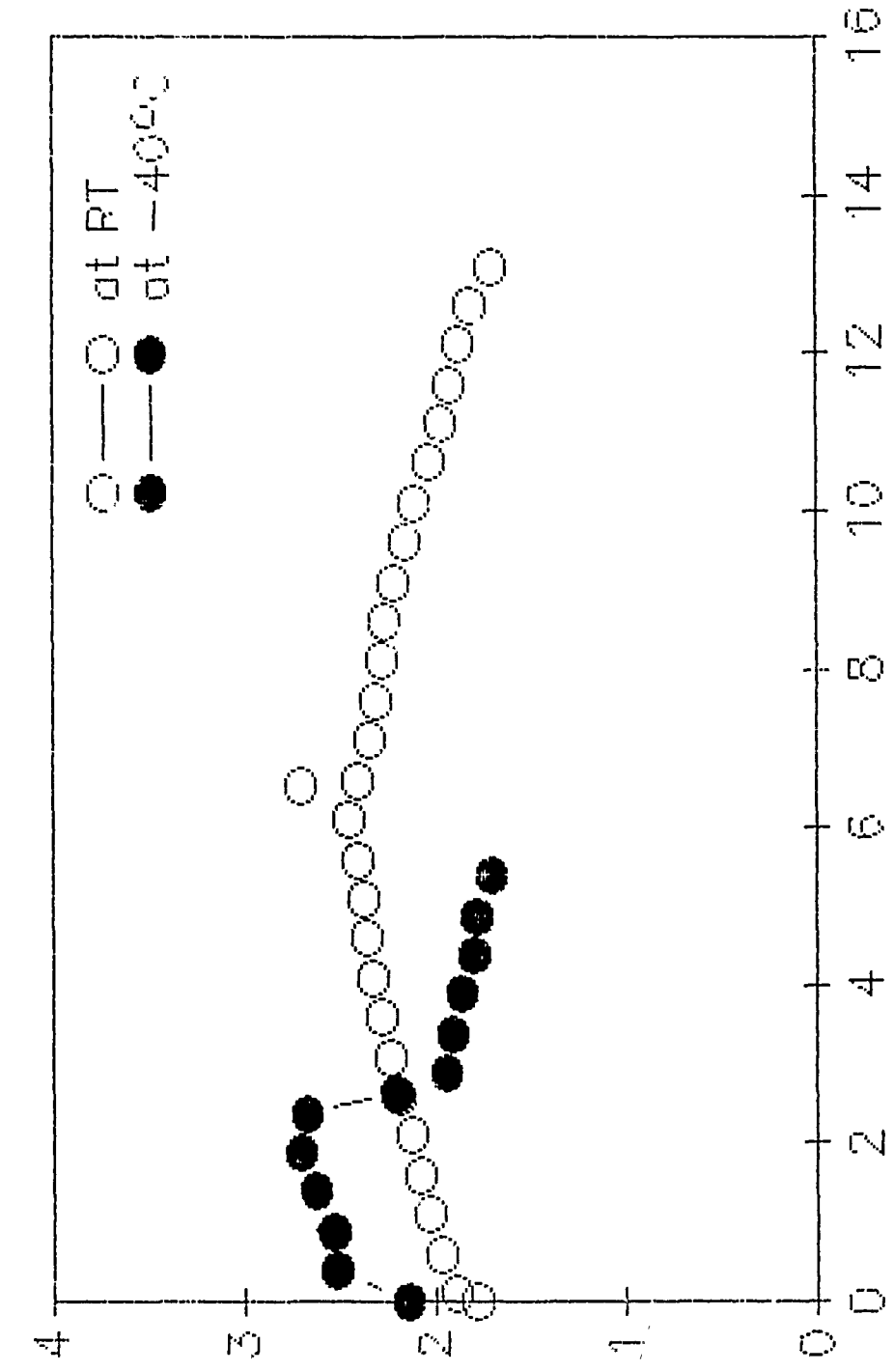

FIGURE 20. LABORATORY CELL PERFORMANCE DATA (AFTER 10 CYCLES)

Table 7

Effect of Temperature on Laboratory Cell Performance

Temperature, xC	-40	RT	+71
Cycle Efficiency, %	105	97	97
Disc. Capacity, % of 1st cycle	105	79	81
TiS_2 Utilization, %	26	57	58

Notes:

1. All values calculated as averages of two cells over five (third through seventh) charge/discharge cycles.
2. Electrolytes contain DME/DIOX/DTMU with 1 M $LiAsF_6$; 4 cm^2 cathodes prepared to contain 78 w/o TiS_2, 17 w/o Ketjenblack 300J, 5 w/o EPDM (Aldrich) at 25 mg/cm^2 load.

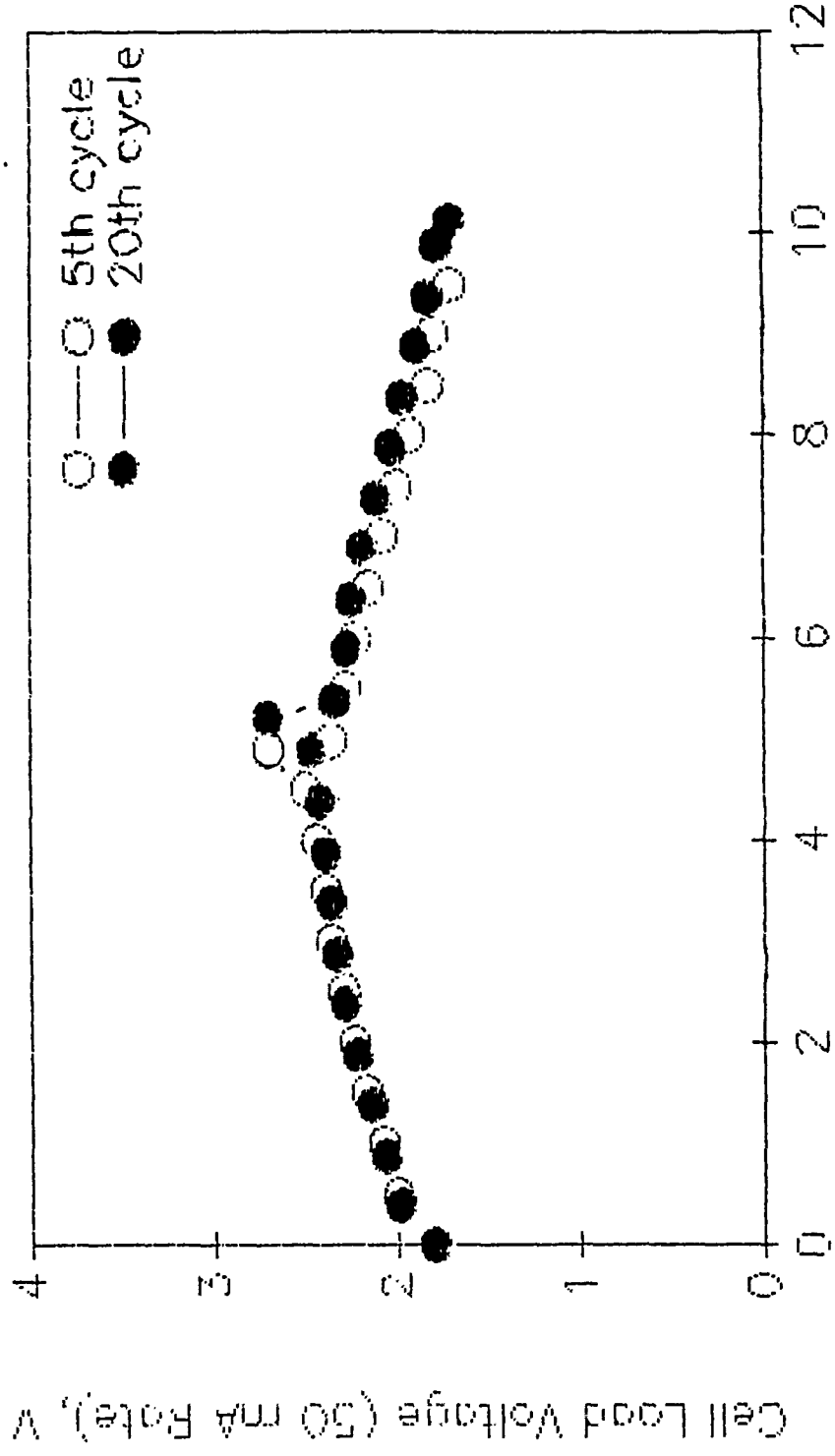

FIGURE 21. AA-SIZE CELL CYCLE VOLTAGE PROFILE @ RT

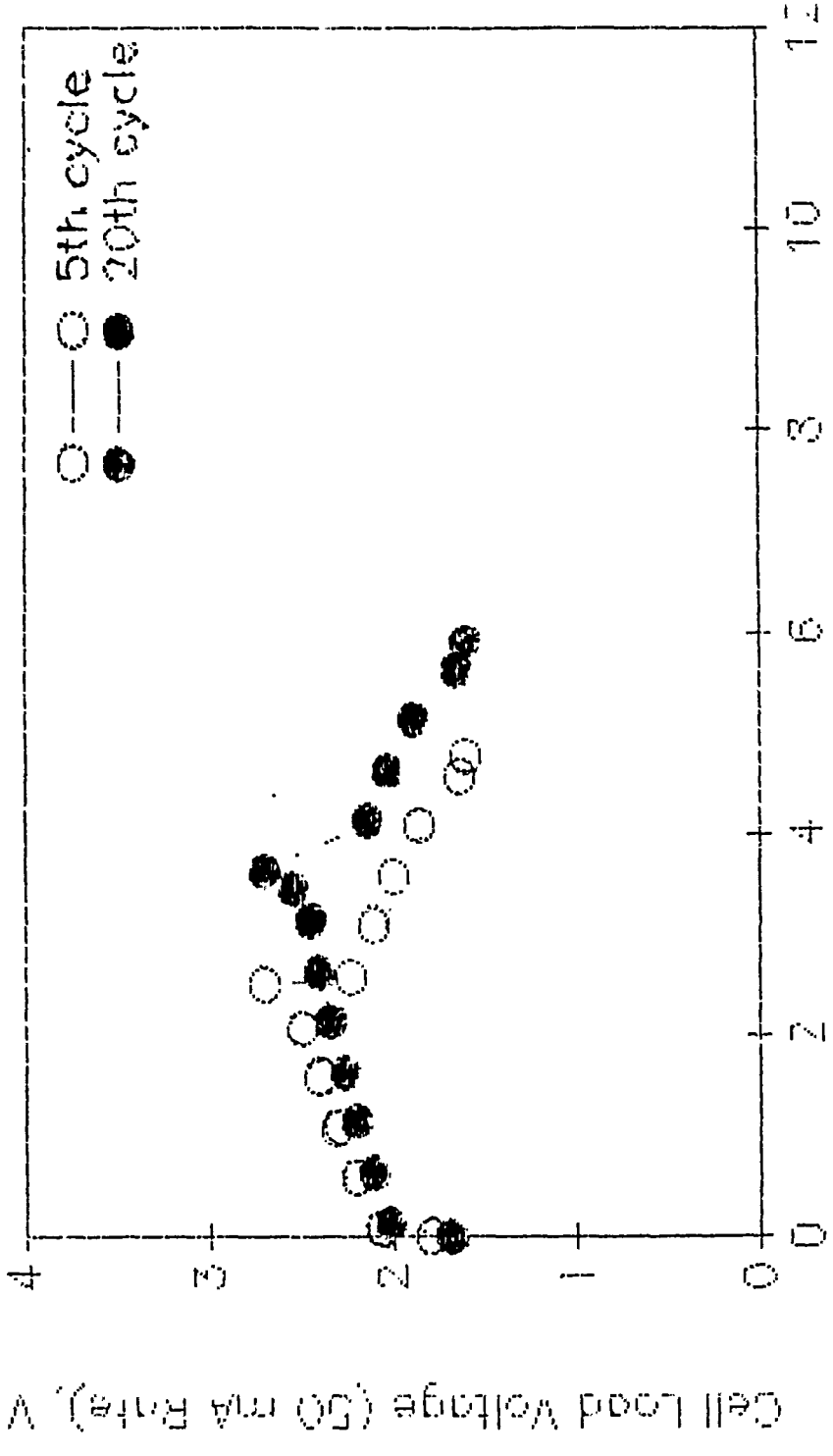

FIGURE 22. AA-SIZE CELL CYCLE VOLTAGE PROFILE @ –40°C

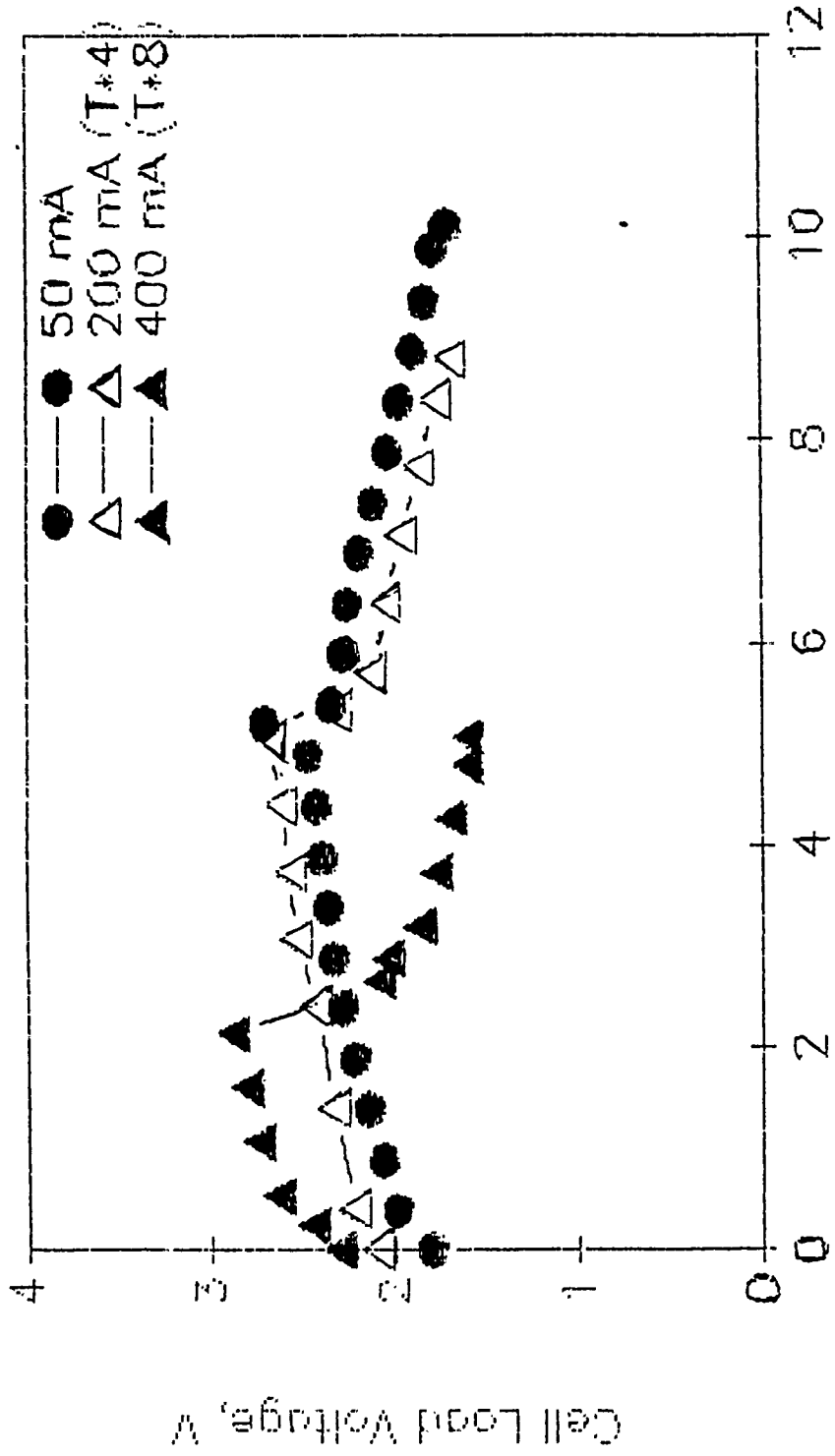

FIGURE 23. AA-SIZE CELL CYCLE VOLTAGE PROFILE @ RT

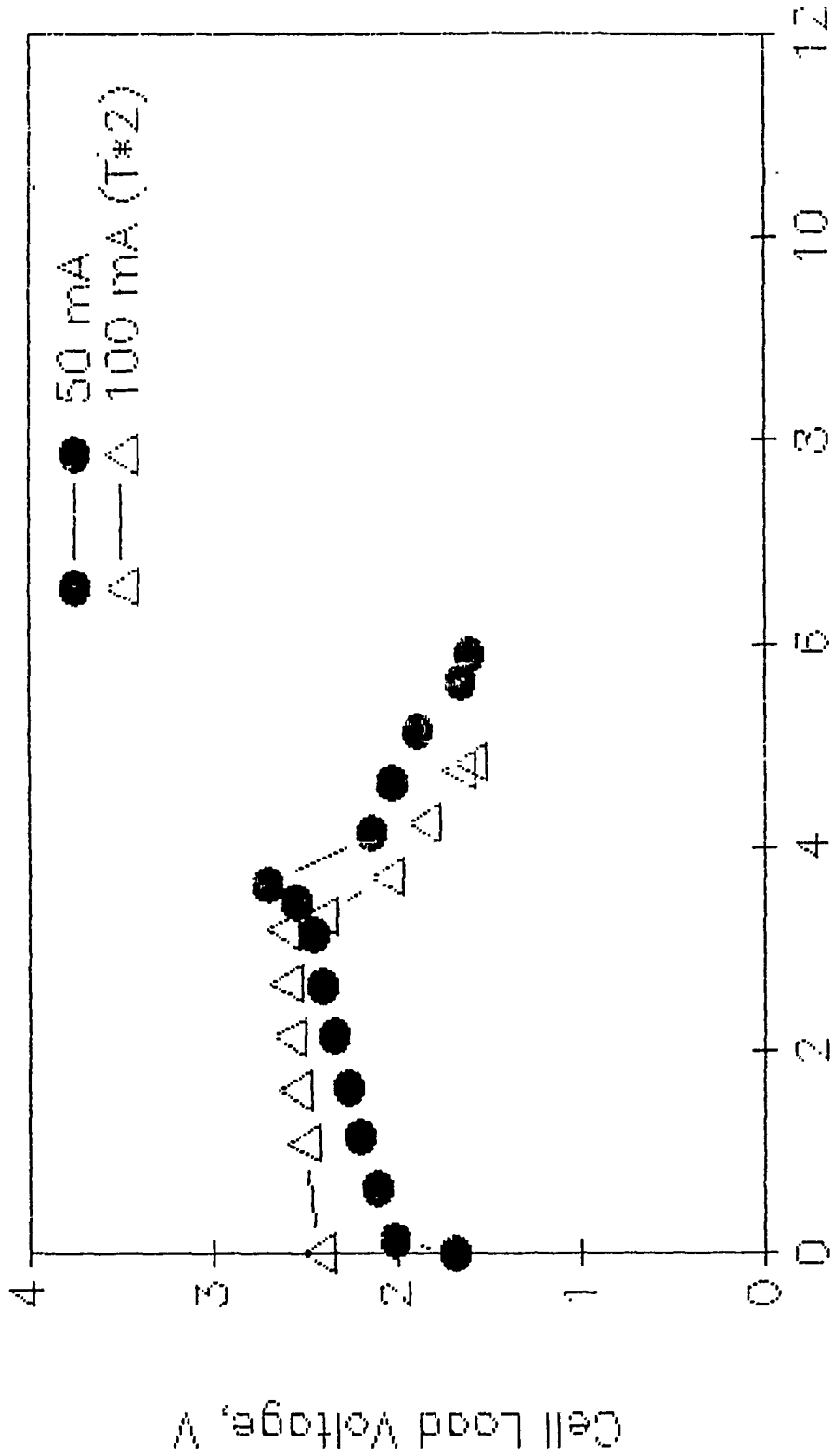

FIGURE 24. AA-SIZE CELL CYCLE VOLTAGE PROFILE @ -40°C

matrix composition provide a cell which is capable of high rate performance at -40°C.

4.4 AA-Size Li/TiS_2 Cell Performance

4.4.1 Performance over a Broad Temperature Range

Hermetic AA-size cells (Cell Type 3) with spirally wound electrodes were made and tested to demonstrate that the technology developed in the Phase I program can provide a practical lithium secondary cell with wide temperature performance range and high rate capability. The cells prepared had cathode surface area of 50 cm^2; the cells were filled with the 1,3-dioxolane-based electrolyte and were laser-weld sealed. The performance of this practical cell design was tested over the temperature range of -40° to +71°C at a 1 mA/cm^2 rate. Provided in Table 8 is a summary of the data obtained with cycle efficiency, maintenance of discharge capacity and extent of TiS_2 utilization listed. Again cell performance at elevated temperature is shown not to be significantly different from performance at room temperature.

The performance of the hermetic AA-size cells at -40°C is shown by the data presented in Table 8 to suffer mainly in TiS_2 utilization compared to performance at room temperature; the extent of loss of cathode capacity is small, however, compared to cells with conventional electrolytes and cathode compositions. With the program developed cathode composition and electrolyte, cathode utilization is over 50% at -40°C. Provided in Figures 21 and 22 is a graphical comparison of the cycle voltage profile of the AA-size cells at room temperature and at -40°C: at both room temperature and -40°C there is little change in cell performance over 20 cycles, although there is some loss in voltaic efficiency at the lower temperature as would be expected due to reduced electrolyte conductance. These results demonstrate that the technology developed under this Phase I program provide a practical cell capable of operation over a wide temperature range.

4.4.2 Performance at High Rate

An additional series of hermetic AA-size cells were constructed which were tested over a range of loads to demonstrate the high rate capability of this cell. The cells utilized spirally wound electrodes with the DME/1,3-dioxolane/1 M $LiAsF_6$ electrolyte. Provided in Figure 23 is a graphical display of the data obtained on the tenth discharge/charge cycle at room temperature; the data presented are average values of duplicate cells. Charge/discharge was carried out at 50, 200 or 400 mA (1, 4 or 8 mA/cm^2) over the voltage range of 1.7 to 2.7 V for the 1 and 4 mA/cm^2 rates and 1.6 to 2.9 V for the 8 mA/cm^2 rate. The data presented in Figure 23 are normalized for rate by multiplying the observed time by the rate factor (1, 4 or 8). Based on the data presented, the AA-size cell does not suffer at room temperature in performance or capacity at rates as high as 4 mA/cm^2; this cell type provides significant capacity at 8 mA/cm^2 although the available capacity is reduced to approximately 50% of the lower rate value over the cut-off voltage range used.

Table 8

Effect of Temperature on AA-Size Sealed Cell Performance

Temperature, xC	-40	RT	+71
Cycle Efficiency, %	66	89	100
Disc. Capacity, % of 1st cycle	108	108	112
TiS_2 Utilization, %	52	86	89

Notes:

1. All values calculated based on averages of five cells over cycles 11 -15 at 50 mA (1 mA/cm^2).
2. All electrolytes contain 20 v/o DME/80 v/o DIOX with 1 M $LiAsF_6$; 50 cm^2 cathode prepared to contain 78 w/o TiS_2, 17 w/o Ketjenblack 300J, 5 w/o EPDM (Aldrich) at 24 mg/cm^2.

High rate performance at reduced temperature was also tested. Provided in Figure 24 is a presentation of the average performance data obtained after ten cycles from replicate cells on discharge at 1 and 2 mA/cm^2 at -40°C. These data demonstrate that the technology developed under this Phase I program provides a practical lithium secondary cell capable of meeting the program goal of providing significant capacity on discharge at 2 mA/cm^2 at -40°C.

The recent report by Anderman and Lundquist (21) described the performance of laboratory Li/TiS_2 cells with spirally wound electrode. The electrode structure described was 20 cm^2 with a theoretical capacity of 80 mA-hr. The hermetic AA-size cells designed and tested under this Phase I program had an electrode structure of 50 cm^2 with an measured capacity on extended cycle of almost 250 mA-hr. These discharge data demonstrate that the cells made under the Phase I program are the next generation of cells moving forward from the cells made by Anderman and Lundquist toward the goal they forecast as achievable of a spirally-wound AA-size lithium secondary cell with energy density of over 100 W-hr/kg. The additional data described above on high rate and low temperature capability further demonstrate that this cell type will be of practical value once its design is optimized and validated.

4.5 Summary of Results

A technique based on ^{13}C-NMR was used to identify mixed-solvent electrolytes which have enhanced electron overlap between solution components; such overlap was proposed as providing increased chemical stability of the selected electrolytes to degradation by lithium radicals formed electrochemically in lithium cell cycle. Enhanced lithium cycle life in and chemical stability of the selected electrolytes was demonstrated in laboratory cell tests. The values of selected parameters characterizing the surface layer formed on the lithium on cell cycle were determined using a transient voltage method and a RC model; the values obtained were shown to be consistent with the observed enhanced electrolyte stability and cycle life of the selected electrolytes.

The composition of the cathode of Li/TiS_2 laboratory cells which utilized the selected electrolytes was varied in an iterative fashion and a cathode composition was identified which provided enhanced first cycle discharge capacity. The optimized composition included the use of Ketjenblack and an EPDM binder. Laboratory cells which utilized this optimized cathode composition were cycled at rates of 0.5 to 2 mA/cm^2 over the temperature range of -40° to 71°C. Chemical stability of the selected electrolytes tested was demonstrated using GC/MS. An electrolyte based on the use of DME/1,3-dioxolane (1:4 by volume ratio) with 1 M $LiAsF_6$ as solute was identified as providing a cell with high rate performance over the temperature range tested. Cycle life in excess of 50 cycles was demonstrated.

The design of a hermetic AA-size Li/TiS_2 cells with a spirally wound electrode was developed and the design implemented. The cells made were tested at rates of 1 to 8 mA/cm^2 over the temperature range of -40° to 71°C. The cell performance obtained demonstrated the

technical feasibility of using the program-developed technology to provide a lithium secondary cell with high rate capability over a broad temperature range.

5.0 TECHNICAL FEASIBILITY

5.1 Program Accomplishments

The Phase I program provided the following answers to the research questions identified in the original proposal and repeated in Section 1.2 above:

1. Lithium secondary cells with mixed solvent electrolytes chosen based on the techniques developed in the Phase I program are capable of providing significant (over 50% of theoretical) cell cycle capacity at 2 mA/cm^2 over the temperature range of -40° to +71°C.

2. Lithium surface characteristics were measured using a voltage transient technique; they were demonstrated to be affected by the electrolyte used and to change as a function of cycle life of the lithium electrode.

3. Electrolytes selected based on the program-verified ^{13}C-NMR technique were demonstrated to be chemically stable in Li/TiS_2 cells on extended cycle (50 cycles) over a broad temperature range and on deep discharge (to over 70% theoretical TiS_2 capacity).

4. The performance of hermetic AA-size cells demonstrated in the Phase I program indicates that the cathode composition and the electrolyte selected in Phase I are suitable to provide a lithium secondary cell with high rate capability over a broad temperature range; based on these results continued work to develop a practical cell using the program-identified components and cell design appears warranted.

In addition to successfully meeting the planned technical goals of Phase I, a design for a lithium secondary cell with spirally wound electrode was developed and the design was implemented. Cells with this design were tested at high rate over a broad temperature range and found to perform at the levels required at this stage in the design development process to meet the long term goal of developing a multipurpose lithium cell suitable for use by the modern Navy.

5.2 Future Direction

The Phase I program objective was accomplished of identifying the components of a lithium secondary cell which improve cell high rate performance over a broad temperature range. These components were tested in a Li/TiS_2 cell with a spirally wound electrode design; the observed performance capabilities of this cell indicate the technical feasibility of the use of this cell as a multipurpose cell for the Navy. However, further work will be required to extend this initial feasibility demonstration to a development level where this cell type is commercially available in a practical configuration. Such addi-

tional work, to be done under the SBIR program in a Phase II effort, would have the following objectives:

1. Complete a re-design of the spirally wound electrode to provide a secondary cell with higher practical capacity (i.e., 1 A-hr for an AA-size cell, etc.); such a re-design will include a review of electrode materials and physical dimensions as well as mechanisms for charge/overcharge control.

2. Characterize the effect on cell performance of changing the active cathode material from TiS_2 to an alternative intercalation material which may have higher theoretical energy density or demonstrated rate capability; incorporate such materials in the cell design if warranted by performance or capacity improvements.

3. Demonstrate the performance and discharge capacity of the re-designed cell in a practical configuration at high rate over a broad temperature range; verify cell cycle life under these conditions.

4. Develop plans for commercial manufacture of the program-demonstrated multipurpose lithium cell and provide a cost estimate for production on scale.

A Phase II program which accomplishes these objectives would provide the technical bases for the development of a business whose goal is the commercial production of a multipurpose secondary lithium cell. Achievement of commercialization would mark the successful completion of a SBIR-supported program.

6.0 ACKNOWLEDGEMENT

The author wishes to thank Ms. D. Barinelli, Mr. R. Fuksa and Mr. K. Yip for their technical support.

7.0 REFERENCES

1. Abraham, K.M. and S.B. Brummer, Chapt. 14 in Lithium Batteries, J.-P. Gabano, Ed., pp. 371-406, Academic Press, NY (1983).
2. Abraham, K.M., et al., J. Electrochem. Soc., 131:2197 (1984).
3. Walsh, F., DELET-TR-83-0384-F (1984).
4. Kerr, J.B., J. Electrochem. Soc., 132:2839 (1985).
5. Yen, S.P.S., et al., 31st Power Sources Symp., pp. 114-9 (1984).
6. Hunger, H.F., Report No. DELET-TR-81-17, NTISADA-A105 30 (Sept., 1981).
7. Matsuda, Y. and H. Satake, J. Electrochem. Soc., 127:877 (1980).
8. Margalit, N. and H.J. Canning, Paper #40, 158th Meeting of the Electrochem. Soc., Hollywood, FL, (Oct., 1980).
9. Tobishima, S. and Yamaji, A., Electrochim. Acta., 28:1067 (1983).
10. Takata, K., et al., J. Electrochem. Soc., 132:126 (1985).
11. Matsuda, Y., et al., ibid., 2538 (1985).
12. Salomon, M. and E. Plichta, Electrochim. Acta., 28:1681 (1983).
13. Salomon, M. in The Role of Data in Scientific Progress, 9th International CODATA Conf., Jerusalem, Israel, Elsevier, p. 327 (1984).

14. Abraham, K.M., et al., 31st Power Sources Symp., pp. 98-103 (1984).
15. Private communication by Dr. H. Hunger, 1985.
16. Young, C.A. and Dewald, R.R., J.C.S. Chem. Comm., 188 (1977).
17. Mukhopadhyay, T. and D. Easbach, Helvetica Chimica Acta., 65:364 (1982).
18. Garreau, M., et al., Paper No. 89, Fall Meeting of the Electrochemical Soc., Las Vegas, NV (1985).
19. Peled, E., Chapt. 3 in Lithium Batteries, J.-P. Gabano, Ed., Academic Press, NY, p. 45-72 (1983).
20. Brummer, S.B., Tech. Report No. 10 under ONR Contract No. N00014-17-C-0155 (1982).
21. Anderman, M., and J.T. Lundquist, J. Electrochem. Soc., 135:1167 (1988).
22. Yen, S.P.S., et al., ibid, 130:1107 (1983).
23. Issacs, H.S., and J.S. Leach, ibid, 110:680 (1963).
24. Czech, B.P., et al., J. Org. Chem., 49:4805 (1984).

APPENDIX B

CATALYZED CATHODES FOR LITHIUM-THIONYL CHLORIDE BATTERIES

FINAL REPORT
26 September 1986 - 31 March 1987

Prepared for:

Naval Surface Warfare Center
Silver Spring, MD 20903-5000

Under Contract No. N60921-86-C-0274

Battery Engineeering, Inc.
1636 Hyde Park Avenue
Hyde Park, MA 02136

Philip F. Kane
Principal Investigator

W. Kilroy
Project Manager

CATALYST FINAL REPORT

1.0 SUMMARY

Phase one of this program consisted of the preparation and preliminary evaluation of mixed oxide-catalyzed teflon-bonded acetylene black cathodes for the Li-$SOCl_2$ battery system. The mixed oxides were of spinel or perovskite morphology, and were both prepared by thermal decomposition of the respective nitrates in the proper molar amounts on the carbon substrate in a Nitrogen atmosphere. Specifics of the techniques used were derived directly from the literature, and are rendered in Section 2.0 of this report.

The performance of potential catalyst candidates was electrochemically tested through the use of two vehicles. The first type of test vehicle used was the demountable glass cell. This cell was used for rapid preliminary evaluation of the discharge potential of different catalysts at different rates. Stepped voltammetry was applied using potentiostatic methods and IR compensation. For these evaluations, 1 cm^2 pieces were selected from flat cathodes manufactured by both dry and wet processing methods. The potential of the working electrode (cathode) was lowered from its OCV ($\approx$ 3.6V)to the operating potential of 2.7 V vs the lithium reference electrode in 50 mV steps, then raised back to OCV by steps of the same voltage interval. Those cathodes manifesting the highest operating potentials were selected for further evaluation.

The second type of electrochemical evaluation vessel employed was the BEI Type 14-24 (1/2 AA size) cell. This cell employed a can positive carbon-limited bobbin-type design with spring-loaded anodes for increased rates of discharge. The cells were discharged through resistive loads and recorded using a digital voltage datalogger. Rate capability and capacity of the cathode types could thus be measured.

Chemical stability data of catalyzed cathodes in thionyl chloride-based electrolyte was generated by storing cathodes in electrolyte and subsequently analyzing the electrolyte for nickel and cobalt ions by titrating against an indicator.

In general, the performance levels achieved with most of the spinel-catalyzed cathodes surpassed those of uncatalyzed cathodes by a significant degree. The Ni-Co spinels were particularly good in this respect. Conversely, the perovskites that were screened did not improve cathode performance.

Hermetic cell testing of the more promising candidates verified that the performance improvements realized through the use of catalyzed cathodes in preliminary testing were applicable to actual production-type cells. In general, 311 catalyst types which improved the operating voltages of flooded demountable glass-housed test cells did likewise both in short-term polarization testing and in long-term discharge testing. In that only a small sample size was possible under the conditions of a Phase 1 program, the results of these hermetic cell tests are not altogether conclusive. Chemical stability testing indicated that, within the limitations imposed by our testing methodology, that the catalyst types tested were chemically stable in $SOCl_2$-based electrolyte.

2.0 BACKGROUND

The lithium-thionyl chloride battery system emerged during the mid-1970's as one of the highest energy dense battery systems known. Increasing demands have been made of this battery system with respect to energy, power, and safety, particularly by the military. The need for overall improvement of all of the referenced factors necessitates research in two major areas: cathodes and electrolyte. The cathode is recognized as the limiting factor within the system with respect to rate capability and capacity. Moreover, improvements in both safety and capacity as well as rate capability have been achieved within the Li-$SOCl_2$ system through the use of cathode catalysts (34). The cited improvements provided the impetus for continuing research and development of potential catalyst candidates for use in the $LiSOCl_2$ system.

Since all of the catalyst types cited above manifested actual or potential drawbacks, an entirely new approach to the problem was taken. The ideal catalyst material obviously must catalyze the reduction of thionyl chloride while maintaining chemical stability in its presence. Beyond that, the catalyst should be inexpensive and readily prepared from materials which are not considered strategic in nature. Both the spinels and the perovskites, for the most part, meet the last 3 qualifications. With respect to electrochemical performance and chemical stability in the $LiSOCl_2$ system, no published data wad known to be available prior to this work.

Most of the recent catalyst work wit[the Li-$SOCl_2$ system has centered about the use of inorganic catalysts (2, 3) . Althougn the catalytic activity of these compounds remains undisputed, their chemical stability in $SOCl_2$-based electrolytes has been questionable at best. Furthermore, $SOCl_2$ is known to attack most organic compounds, as it is a highly effective chlorinating agent. On the other hand, many inorganic compounds of transitional metals, such as Type 52 alloy and many of the stainless steels, tend to be chemically stable in $SOCl_2$-based electrolytes, while exhibiting little or no catalytic activity.

Mixed oxides or the transitional metals, such as the spinels and perovskites, have been known to be effective oxygen reduction catalysts in H2/O2 fuel cells, just as the pthalocyanines and tetraazaannulenes. Furthermore, since they are inorganic compounds, they are potentially more resistant to attack by $SOCl_2$ than the organometallics. Accordingly, this new group of compounds, the mixed transitional meta. oxides, represents, potentially, a highly effective new group cathode catalysts for the Li-$SOCl_2$ battery system.

3.0 CATALYST PREPARATION

3.1. SPINELS

Spinels are oxides of one or more transitional metals which assume a definite crystalline structure. The empirical formulae of spinels is usually M2O3 or MNO4 where M = transitional metal 1 and N = transitional metal 2, although MNO3 is also a possibility.. The catalytic activity of various spinels for oxygen reduction in fuel cells has been well documented (4-25). Many of the catalysts commonly used for $SOCl_2$ reduction in the Li-$SOCl_2$ system had a previously demonstrated effectiveness as oxygen catalysts in various fuel cell applications. This list of catalysts includes the noble metal platinum (26), transitional metal pthalocyanines (2), and transitional metal tetraazaannulenes (3). In that the spinels represented a large group of

candidates with a documented effectiveness as oxygen catalysts, just as the noble metals and transitional metal pthalocyanines and tetraazaannulenes, which had no previously documented use as catalysts in the Li-'$SOCl_2$ system, Battery Engineering Inc. proposed their use as $SOCl_2$-reduction catalysts. An extensive literature search revealed a number of methods which have been successfully employed in the manufacture of spinels (27-37). Some of the methods were deemed undesirable because they necessitated a number of complicated procedures requiring sophisticated and expensive equipment such as freeze-drying equipment, or because they were developed specifically for the growth of large crystals (30-37). The method practiced throughout the execution was derived from references 27-29, using Lang (38) as a physical reference for establishing the manufacturing temperatures.

Solutions of the nitrates of the respective transitional metals were prepared. Shawinigan Acetylene Black, 50% compressed, was slowly added to the nitrate solution until the weight of the transitional metal (5) in solution reached 5% of the total weight of the carbon and metal mixture. The basic mixture consisted of 19 g SAB, 1 g mixed metals, and 150 ml of water, and when properly prepared, attained a paste-like consistency. Portions of the mixture were transferred into 304 SS combustion boats and the nitrates were thermally decomposed to their respective oxides and calcined at 450 degrees C for 1 hr in a nitrogen atmosphere. In Practice, the thermal decomposition process was carried out in a Lindberg tube furnace fitted with a one inch OD 304 stainless steel tube. The tube was fitted with machined stainless steel end caps drilled and tapped to accept fittings for through-flow of N2 gas, as well as K-Type jacketed thermocouples, which monitored temperatures at both sides of the payload. An Omega temperature controller was used to carefully control the temperature. Since the gaseous thermal decomposition products of metal nitrates are oxides of nitrogen, all work was performed in a fume hood.

The resultant powders were seemingly low in density and flaky in consistency, and their surface was noticeably shinier than acetylene black, which had undergone similar treatment. The catalyzed powders were also characterized as having small particle sizes. No further treatment was necessary prior to their use in cathode fabrication.

3.2 PEROVSKITES

Perovskites are somewhat similar in formula and structure to the spinels. Perovskite-type compounds are defined as those having the empirical formula Ln1-x Mx M1 O3, where Ln is a lanthoid element such as lanthanum, M is an alkaline earth element such as strontium, and M1 is a transition metal (39). The catalytic properties of perovskites for oxygen reduction in various fuel cell systems is well documented (42-46), however, just as was the case with spinels, their use as reduction catalysts in the $LiSOCl_2$ system was undocumented prior to this work.

Perovskite-type compounds can be prepared by a number of methods (39-41). Again, as for spinels, many methods of perovskite preparation involve sophisticated and expensive equipment, as well as difficult and time-consuming techniques. A simplified method was chosen based upon that of Onbayashi et al. (39). Since nitrates of many different metals were purchased for the preparation of spinel-type catalysts, including lanthanum and strontium, these were used as the precursor for perovskite production.

The formation temperature for perovskites by thermal decomposition of the nitrates is considerably higher than for spinels (circa 1100 degree C vs 450 degree C for the spinels). Since strontium nitrate decomposes into the oxide at 1100 degree C (Lange), this temperature must be attained in order to produce the perovskite. Furthermore, the referenced techniques (39, 42) specify formation times in the range of 6-30 hours.

In practice, perovskite catalyzed carbons were prepared using the same apparatus used for the preparation of spinel-catalyzed carbon. The same method was used to prepare pastes of candidate materials, which were heated in 304 SS combustion boats in the Lindberg tube furnace to 1100 degree C for 6 hours. Again, a nitrogen atmosphere was used. This prevented the carbon from oxidizing during the process. The two candidate perovskite-based materials were of lower density than the spinel-catalyzed materials; otherwise, their physical morphology was similar. Again, no further treatment of the materials was necessary in order to fabricate cathodes.

4.0 CATHODE FABRICATION

Generally speaking,two different methods were used to fabricate candidate electrodes for initial performance evaluation. The first technique, henceforth referred to as the "dry" technique, began by wetting the catalyzed carbon prepared by the method of Section 3 with dilute isopropanol to produce a thick slurry of paste-like consistency. To this slurry, TFE emulsion (DuPont TFE 30) was added dropwise until the weight of the teflon solids reached 10% of the total weight of solids in the slurry. The mixture was then ultrasonically agitated to assure homogenuity and air dried to remove the excess solvent.

Subsequent to air drying, the mixture was dried at 100 degrees C °and cured at 280 - 320 degrees C in an Argon atmosphere. The cured mixture was ground into fine powder in a chopping mill and sieved through 100 mesh nickel screen to assure uniformity. Proprietary techniques were then used to uniformly coat both °sides of a 5 Ni 10 125 expanded nickel screen with the active material. The cathode was then pressed at 500-1000 psi to integrate the structure. The cathode was subsequently dried under vacuum and cut to size before testing ensued.

The dry manufacturing technique is successfully used to manufacture uncatalyzed TFE-bonded acetylene black electrodes and is suitable for use with some types of catalyzed carbon. Unfortunately, this technique did not readily adapt to use with many of the catalyzed carbons, thereby necessitating the use of another manufacturing technique.

The "wet" technique was used to prepare cathodes from catalyzed carbons that did not readily adapt to the dry technique. Since this category included the majority of the spinels, wet technique cathodes were manufactured from nearly all of this group. The method is based upon that of Breault et al (47), and began with the preparation of a dilute slurry of catalyst in water and adding DuPont TFE 30 emulsion dropwise to the slurry until the weight ratio of TFE solids to total solids in the slurry reached 1:10. The pH of the solution was then adjusted to between 1.5 and 4.0 with the dropwise addition of sulphuric acid. The slurry, at that point, became a colloidal suspension. This suspension was subsequently filtered and transferred to an expanded Ni substrate. The subassembly was then pressed at 500-1000 psi before air drying ensued. Cathodes prepared by the wet technique were oven dried, cured, and prepared for testing in an identical manner to those prepared using the dry technique.

Since the two referenced methods were utilized to fabricate flat cathode sheets, whereas formed bobbin-type cathodes were required for use in hermetically sealed 1/2 AA size cells, a variation of one of the techniques was employed. A proprietary dry-type method was used to form the cathodes in situ. This facilitated the handling of the cathodes.

5.0 TEST CELL DESIGN

5.1 DEMOUNTABLE CELL

The demountable cell used for initial performance screening of the various types of catalyzed cathodes is schematically represented in Figure 1. The cell and cover were off-the-shelf -items purchased from IBM Corporation. A quick-change system for mounting both working and counter electrodes was designed and implemented at Battery Engineering Inc. TFE gasketing and "O" rings were used to maintain tight sealing throughout the system. The reference electrode consisted of a small piece of lithium metal attached to a Ni 200 current collector and inserted into an isolated glass chamber containing electrolyte and having a Luggin capillary tube which could be positioned in close proximity to the working electrode to minimize the IR drop within the cell. The cell, of course, was electrolyte flooded.

The top of the glass body of the cell is threaded about its perimeter, as is the inner circumference of the thermoplastic cover. Five tapered holes in the cover provide access for the working and counter electrode holders, as well as the reference electrode chamber with Luggin capillary. The remaining two holes were fitted with tapered plugs, and were used for filling the test. cell with 1.8 M $LiAlCl_4$ in $SOCl_2$ electrolyte subsequent to assembly. An inner FEP liner protected the plastic cover from chemical attack by the electrolyte. During discharge, the electrolyte was stirred magnetically to aid diffusion.

In practice, the demountable glass test cell functioned precisely as required. No problems were experienced with this cell at any point throughout the program. The cell sealed tightly so that tests could be performed on the bench outside the dry room. The total time required to test one sample was approximately 1.5 -2 hr. During the course of one day, four to five electrodes could be tested in this cell.

5.2 HERMETIC 1/2 AA CELLS

Initially, Battery Engineering Inc. proposed to comprehensively evaluate promising candidates in a demountable flat cell with a stoichiometric volume of electrolyte and perform some full cell testing in fully instrumented 11C" size cells if time permitted. In that time would not allow for the manufacture and testing of "C" size cells, but full cell testing was, nonetheless, deemed highly desirable, a compromise was arranged to perform comprehensive testing with hermetically sealed bobbin-type 1/2 AA size cells. These cells required lesser amounts of catalyzed carbon and were more readily manufactured than wound "C" size cells, but still provided a hermetically enclosed environment for performance evaluation.

Standard Battery Engineering Inc. 304 SS hardware was used to house the test cells. The outer dimensions of these cells are 14 mm O.D. by 24 mm OAL. The cells are all can positive, i.e. the can assumes the cathode potential. This design provides a

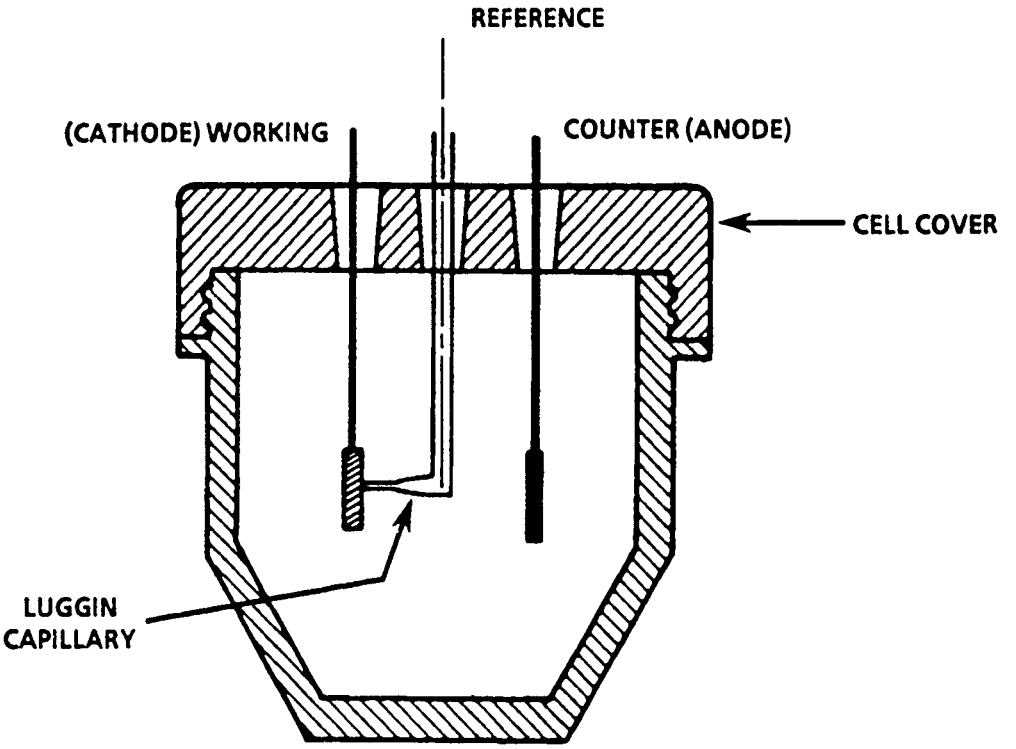

FIGURE 1. TEST CELL SCHEMATIC

distinct advantage in the manufacture of test cells, as the cathode was formed in situ, as the first step in the assembly process, thus eliminating the need to handle cathodes which could be highly delicate in nature. This design also provides the cathode with an integral current collector, i.e. the can.

Non-woven glass fiber material was used as the electrical separator. The anode, consisting of high purity lithium foil pressure bonded to .003" thick Hi metal foil, comprised the inner concentric cylinder of the design. The anode consisted of two separate halves and the inner active layer was spring loaded to maintain constant IR levels throughout the entire discharge as per Epstein et al. (49). The cover and can were joined using the TIG welding technique. The cells were evacuated and backfilled with 1.8 M $LiAlCl_4$ in $SOCl_2$ electrolyte. The stoichiometry of the test cells was carbon limited by a slight margin, at least with uncatalyzed cathodes.

6.0 PERFORMANCE TESTING

6.1 SCREENING

6.1.1 TEST EQUIPMENT

The demountable cell used to conduct initial performance screening is described in the previous section. Electrical test equipment was required to discharge the individual test cells in a controlled manner while monitoring the parameters of both current and voltage. In order to assure internal uniformity of the test cells, equipment was also required to perform impedance measurements on individual cells prior to testing. The method of W. J. Hamer (48) was used to determine the IR of test cells. This.s method required a minimum of equipment including a function generator, two digital voltmeters, and a simple electrical circuit. A schematic representation of the equipment used in IR determination is depicted in Figure 2. A Simpson 420 Function Generator was used to generate a signal, while two Fluke 8062A Digital Multimeters monitored voltages. System accuracy was verified through the measurement of resistors with known values.

Electrical performance was determined potentiostatically using an Electrosynthesis Corporation Model 410 Potentiostatic Controller coupled with a Sorenson Model QSA10-1.4 Power Supply. Both current and voltage were monitored with Fluke Model 8062A Digital -Multimeters.

6.1.2 CELL ASSEMBLY

All demountable cell hardware was thoroughly dried at elevated temperatures prior to use. Stainless steel electrode holders were cleaned via abrasive techniques to assure good mechanical and electrical contact to the electrodes. All cells were cleaned via abrasive techniques to assure good mechanical and electrical contact to the electrodes. All cells were assembled and activated with electrolyte inside the dry room.

The assembly process commenced with the bonding of lithium metal to the backing plate of the electrode holder. This anode subassembly was then attached to the anodic structural support via the support's integral spring clips.

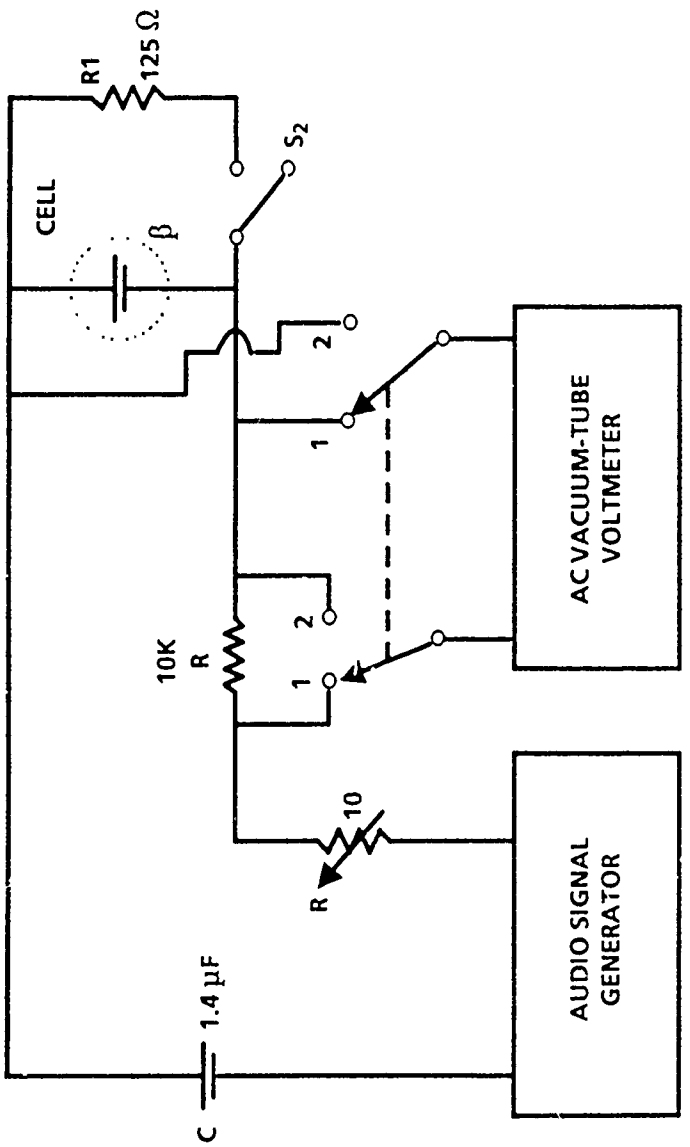

FIGURE 2. BLOCK DIAGRAM OF AC METHOD OF MEASURING IMPEDANCE OF PRIMARY CELLS.
B. CELL UNDER TEST, C. BLOCKING CAPACITOR; R. LOAD RESISTOR FOR CELL;
R. VARIABLE RESISTOR TO ADJUST THE LEVEL OF AC CURRENT; S2. SWITCH TO PLACE
LOAD ON CELL. NOTE; WHEN CELL IS UNDER LOAD, AN INDICATOR SHOULD BE
INSERTED IN THE DC CIRCUIT

Test cathodes were prepared by cutting 1 cm x 2 cm sections from the respective cathode sheet. A section measuring 1 cm x 1 cm was isolated in the center of the test cathode; the active material from the remainder of the cathode was removed, thus exposing the expanded nickel current collector. The exposed current collector of the test cathode was resistance welded to the cathode backing plate, which was attached to the cathodic structural support via integral spring clips.

A small piece of lithium metal was pressure bonded to a Ni wire current collector and inserted into the blown glass reference electrode chamber complete with Luggin capillary. All three electrode subassemblies were then inserted into the plastic tapered fittings and secured with threaded covers and TFE "O" rings.

The thermoplastic cell cover was fitted with a protective FEP gasket and inserted onto the glass body of the cells and secured by tightening the threads. The three electrode holder/tapered fitting subassemblies were then inserted into the empty cell and visually aligned. After verifying the absence of short circuiting across any two of the three electrodes, the test cell was filled with electrolyte from a small volumetric container through one of the two open ports in the cell cover. The filling and vent ports were subsequently plugged with the tapered stoppers and cell assembly was complete.

6.1.3 TEST PROCEDURE

Before the performance testing procedure commenced, the IR of each test cell was determined in order to assure the validity of comparative performance data. The IA was adjusted as required by the repositioning of the working and reference electrodes in order to reduce the internal impedance variations within test cells to an insignificant level. The method and its execution provided a high confidence level in the data generated. Sometimes the IA reading was excessively high and could not be sufficiently reduced by electrode repositioning. The cause of this phenomenon was nearly always the same: one or both of the active layers was delaminating from the current collector of the°working electrode.

Cathode test potentials ranged from approximately 3.6 V to 2.7 V vs lithium. The test procedure began invariably by allowing the system to establish an open circuit voltage, always near 3.6 V. The operating potential of the working electrode was changed stepwise in 50 mV increments from OCV to 2.7 volts, and back to OCV again. The timing of the process was carefully controlled in order that no cathode should experience increased polarization at some point during the test cycle due to capacity limitations. The 2.7 volt cutoff was selected as it is well below the potential at which the Li-$SOCl_2$ system can efficiently operate. Current densities of catalyzed electrodes ranged from approximately 34 to 75 mA/cm2. Uncatalyzed electrodes operated at 45.50 mA/cm2 at this potential, well in excess of what can be reasonably expected during extended periods of discharge with active Li-$SOCl_2$ cells.

The entire screening process, including setup and breakdown, took approximately 1.5 - 2 hr per cell. Accordingly, four or five electrodes could be tested per day. The process was quick, efficient, and effective.

6.2 COMPREHENSIVE TESTING

6.2.1 TEST EQUIPMENT

Comprehensive cathode testing was performed using hermetically sealed standard 1/2 AA size hardware. Two types of tests were performed. Polarization curves were run potentiostatically using the equipment of Section 6.1.1. Since the 1/2 AA test cells were not fitted with provision for reference electrodes, the reference electrode terminal of the potentiostat was connected to the anodic cell terminal to prevent overloading.

Capacity testing was performed on the 1/2 AA cells by the application of 160 Ohm resistive loads while monitoring cell voltage at 1 hour intervals with a Digitek Model 1000 Data Logger. This represents the preferred method of performing capacity testing on finished cells at Battery Engineering Inc.

6.2.2 CELL ASSEMBLY

Can-positive 1/2 AA cells were assembled from both standard uncatalyzed and catalyzed test cathodes using Battery Engineering Inc. standard assembly techniques. As per Section 4.0, cathodes were formed inside the cell containers. Into the can/cathode subassembly were inserted the separator, anodes, and internal - spring assembly. The cover assembly with integral glass-to-metal seal and fill port was inserted and the subassembly edge-welded using the TIG technique. Test cells were then evacuated and backfilled with electrolyte before closing via TIG.

6.2.3 TEST PROCEDURE

Polarization curves were run with the 1/2 AA size cells using the same technique described in Section 6.1.3. Whenever possible, two cells were tested using this technique; material limitations prevented this in some cases.

Capacity testing was executed simply by attaching resistive loads in parallel to the test cells after they were electrically connected to the data logger. Measurements were automatically taken at hourly intervals.

7.0 CHEMICAL STABILITY TESTING

The chemical stability of the more promising catalyst candidates was evaluated by storing sections of finished cathodes in glass ampules with 1.8 M $LiAlCl_4$ in $SOCl_2$ electrolyte and subsequent chemical analysis.

The analytical method used for the determination of Hi and Co ions in solution was a modified version of that of Harris and Sweet (50). According to this method, nickel and cobalt present as a mixture in an aqueous solution to be measured are reacted with an excess of a standard solution of ethylene diamine tetraacetic acid (EDTA) in an ammonium hydroxide-ammopium chloride buffer, then the excess is back titrated with standard zinc, using eriochrome black T as the indicator. A second aliquot of the solution to be measured is treated in an acetate buffer with a solution of alpha-nitroso-beta-napthol in glacial acetic acid, which selectively complexes the cobalt. The complex is extracted with chloroform, and the nickel remaining in the aqueous

phase is determined as before. The first measurement then represents the sum of the nickel and cobalt, while the second represents just the nickel.

The first difficulty with this approach is that the aluminum present in the aqueous test solution as the result of the hydrolysis of the electrolyte sample would interfere with the analysis, since it too forms a complex with EDTA. The second is that both the precision and the time required to perform the analyses are adversely affected by using an excess of the EDTA plus the standard zinc, since extra uncertainties are introduced during the preparation of the standard zinc and the titration of the sample with the zinc. Both nickel and cobalt can be directly titrated with EDTA at pH 5 in an acetate buffer using xylenol orange as the indicator, which removes the second objection. The problem remaining is that the cobalt and nickel must be separated front the aqueous matrix containing the aluminum. We hoped to accomplish each separation in turn by extracting the cobalt as the alpha-nitroso-beta-napthol complex, then the nickel as the dintethyl glyoxime complex, both from an acetate buffer into chloroform. The metals will extract back into aqueous phase containing HCl, leaving the ligands in the chloroform. The aqueous solutions could then be buffered with sodium acetate and titrated with EDTA, using xylenol orange as the indicator.

8.0 TEST RESULTS

8.1 DEMOUNTABLE CELL

The following spinels were prepared at a level of 5% on Shawinigan black, as described in section 3.1, in order to compare their performance versus a carbon-only control. This first group was made using the wet press technique:

Ni(l/2)Co(3/2)O(3)	Ni(3/2)Co(1/2)O(3)
Ni (5/6) Co (7/6)0(3)	Ni (1/3) Co (5/3)0(3)
Ni (7/6) Co (5/6)0(3)	Ni (5/3) Co (1/3)0(3)
NiCo0(3)	Ni(4/3)Co(2/3)0(3)
Ni (2/3) Co (4/3)0(3)	Ni (2/3) Al (4/3)0(3)
Mg(2/3)Al(4/3)O(3)	MnCr(2)0(4)
	MgFe(2)0(4)

This second group was prepared using the dry press technique:

Co (2)0(3)	NiCoO(3)
Ni(4/3)Co(2/3)O(3)	Ni(2/3)Co(4/3)0(3)
MnCoO(3)	Mn(2)0(3)
MnFeO(3)	Fe (2)0(3)

Tile following two perovskites were also prepared at a level of 5% on Shawinigan black:

La(6)Sr(4)CoO(3) La(4)Sr(6)CoO(3)

The current in milliamps versus the potential in volts for these test samples is shown in Figures 3 through 8, at the same time comparing each with the reference carbon electrode. The best of all of these samples was the wet pressed Ni (2/3)Co(4/3)O(3) which more than doubled the current density at low current, and at currents nigher than 20 mA nearly doubled the current, relative to uncatalyzed Shawinigan black. All of the nickel-cobalt spinels showed at least a moderate decree of catalytic activity, particularly those richer in cobalt. Co(2)0(3) , however, showed no catalytic activity at all relative to the Shawinigan black control.

8.2 HERMETIC 1/2 AA CELLS

Due to the rather small sample size resultant from time constraints and limited catalyst amounts, the data obtained from limited testing of the 1/2 AA cells is most suitable for the indication of performance trends and tendencies as opposed to the generation of precise numerical data. Furthermore, maintaining the internal uniformity of a small number of cells constructed from a wide variety of cathode materials by hand assembly methods is difficult at best. In general, the data is much in accordance with that generated with the flooded test cell configuration.

8.2.1 POLARIZATION TESTS

Polarization test data appear in Figure 9. The MnCo spinel clearly outperformed all other spinel catalysts and SAB throughout the range test potentials by a significant degree. This is in contrast to the results of the demountable cell polarization tests, where the MnCo showed good potential as a catalyst, performing as well as most of the NiCo spinels, but not as well as the $NiCo_2$ formulation. The most surprising aspect of this test is the degree by which the MnCo spinel outperformed the other catalysts. NiCo exhibited the next best levels of performance, falling well short of the MnCo performance levels, Particularly at high current densities, but performing better than the other NiCo formulation, as well as the control cells throughout the range of test potentials.

Ni_5Co, Ni_2Co, $NiCo_3$, and $NiCo_5$ all outperformed the control cells throughout the range of test Potentials, albeit by a lesser margin, particularly at the lower current densities. This data is not inconsistent with that of the flooded demountable cell tests.

$NiCo_2$ and Ni_3Co did not outperform the control cells at currents below 15 mA, although at higher currents they exhibited markedly less polarization. This is in contrast with demountable cell test data, at least with respect to $NiCo_2$, which demonstrated the best performance characteristics of the group when tested in the demountable cell.

Overall, polarization testing of hermetic 1/2 AA cells resulted in a few surprises when compared to analagous demountable cell test results, although most of the

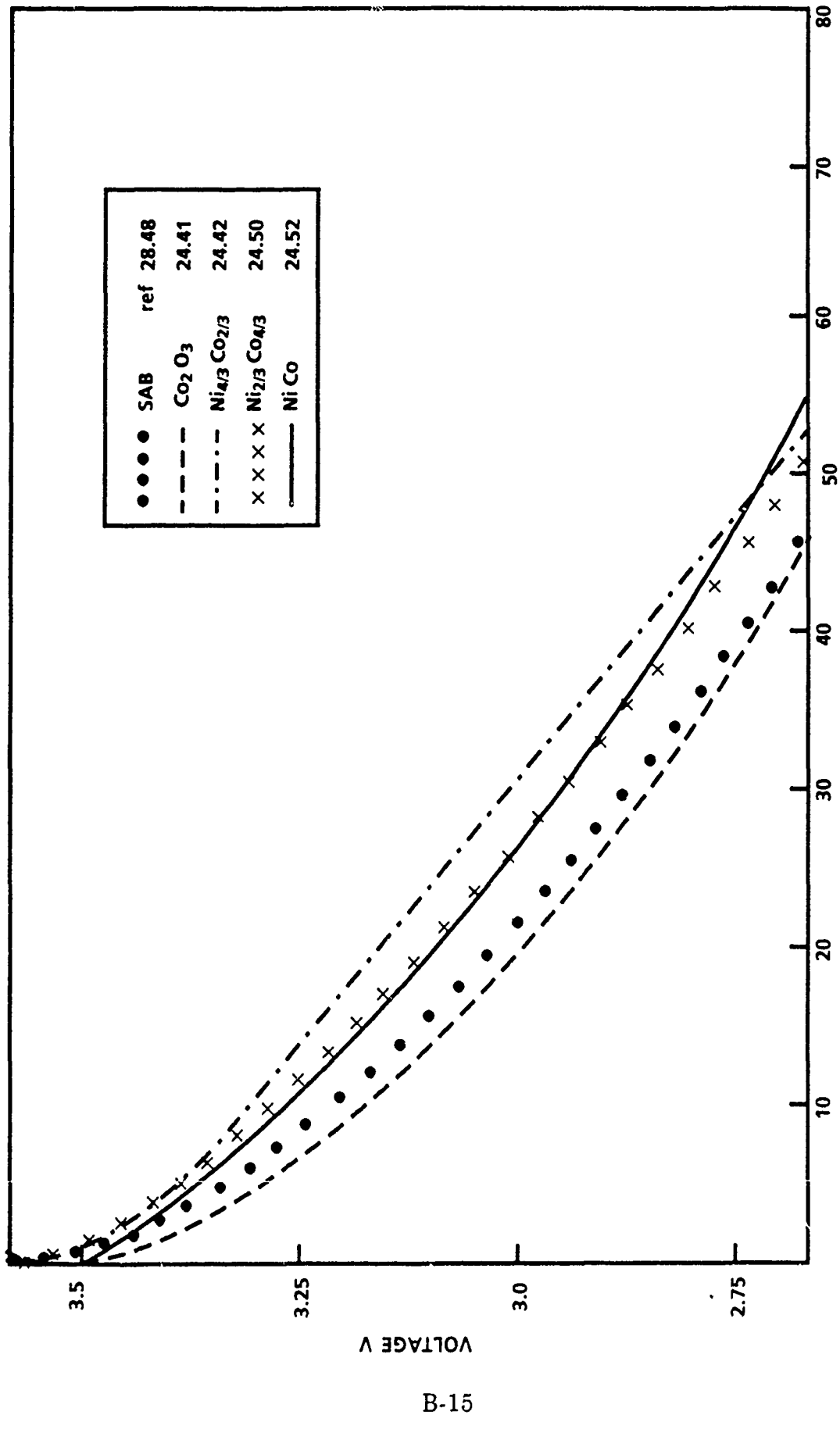
SAB ref 28.48
Co_2O_3 24.41
$Ni_{4/3}Co_{2/3}$ 24.42
$Ni_{2/3}Co_{4/3}$ 24.50
Ni Co 24.52
VOLTAGE V
3.5
3.25
3.0
2.75
CURRENT, mA
10
20
30
40
50
60
70
80

FIGURE 3

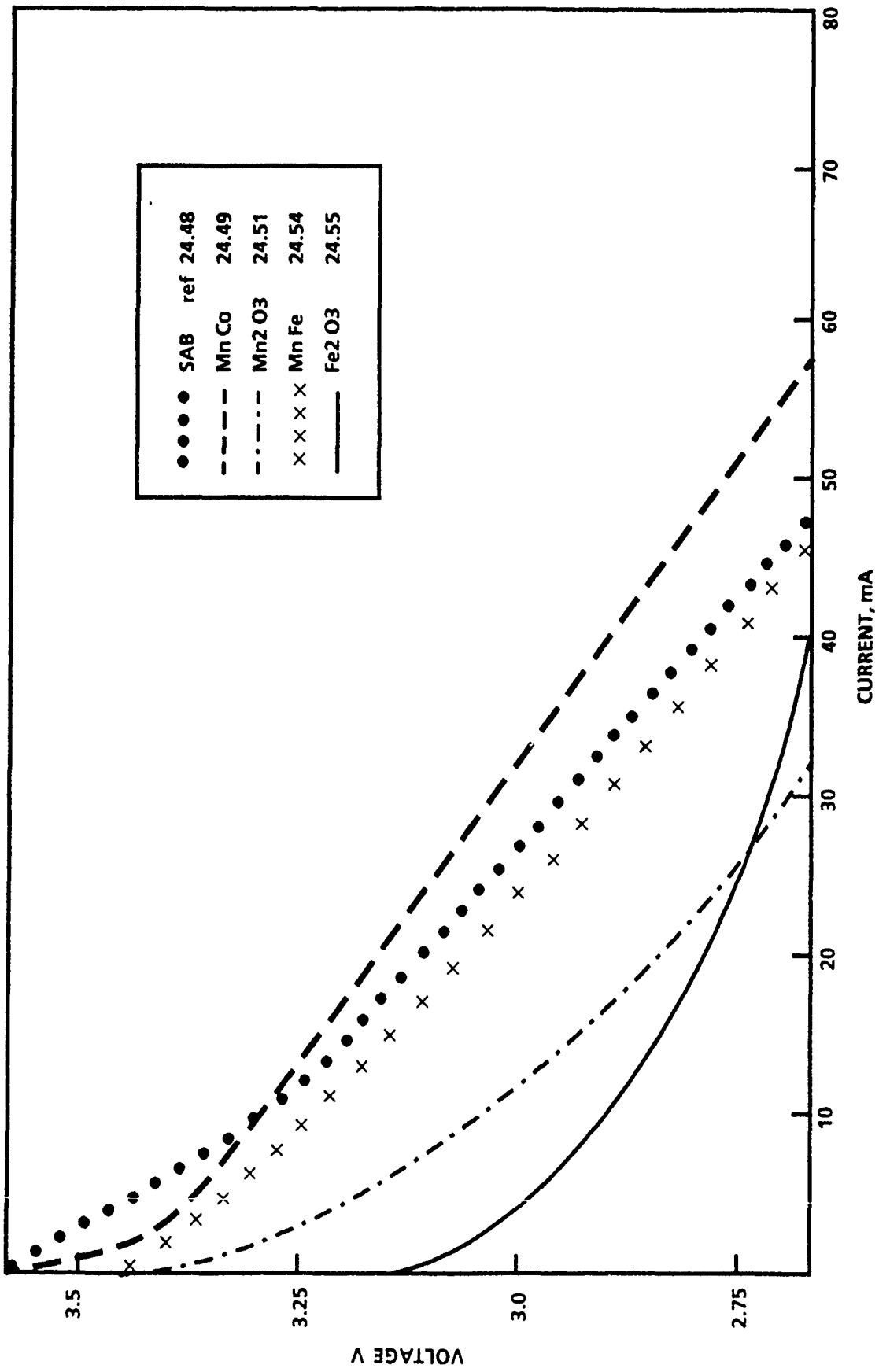
SAB ref 24.48
Mn Co 24.49
Mn2 O3 24.51
Mn Fe 24.54
Fe2 O3 24.55
VOLTAGE V
3.5
3.25
3.0
2.75
CURRENT, mA
10
20
30
40
50
60
70
80

FIGURE 4

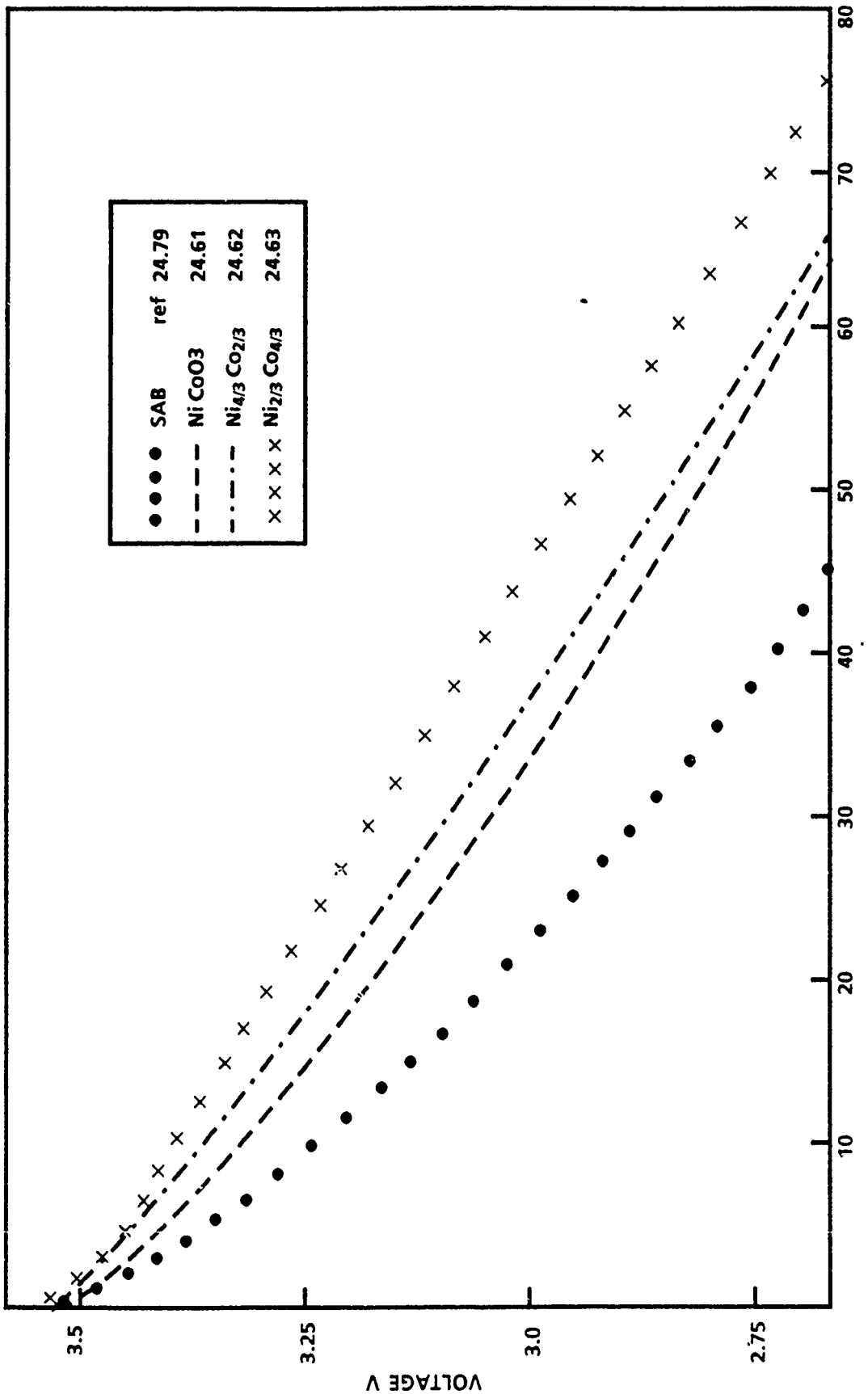
SAB ref 24.79
Ni CoO3 24.61
Ni4/3 Co2/3 24.62
Ni2/3 Co4/3 24.63
VOLTAGE V
3.5
3.25
3.0
2.75
CURRENT, mA
10
20
30
40
50
60
70
80

FIGURE 5

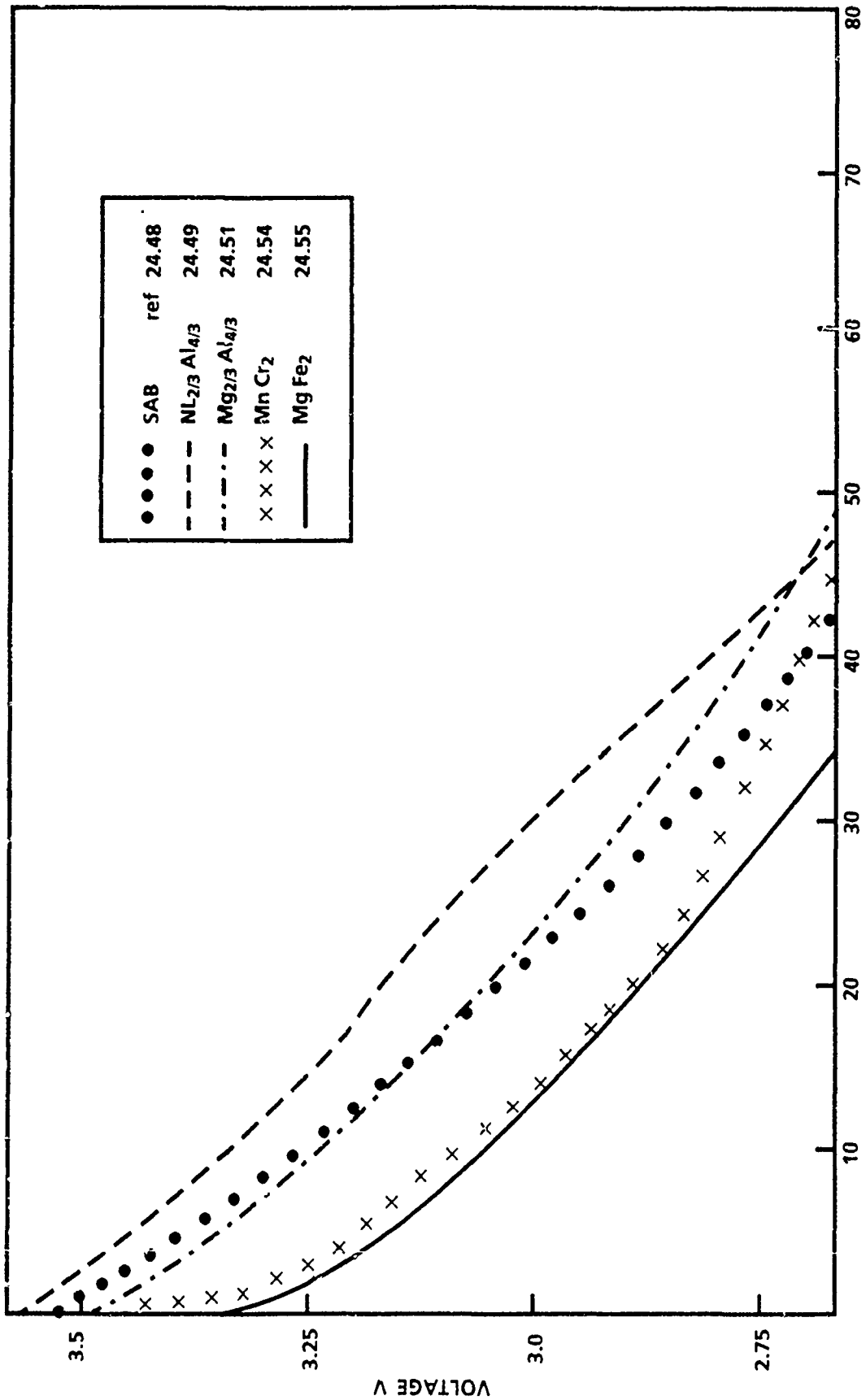
SAB ref 24.48
NL2/3 Al4/3 24.49
Mg2/3 Al4/3 24.51
Mn Cr2 24.54
Mg Fe2 24.55
VOLTAGE V
3.5
3.25
3.0
2.75
CURRENT, mA
10
20
30
40
50
60
70
80

FIGURE 6

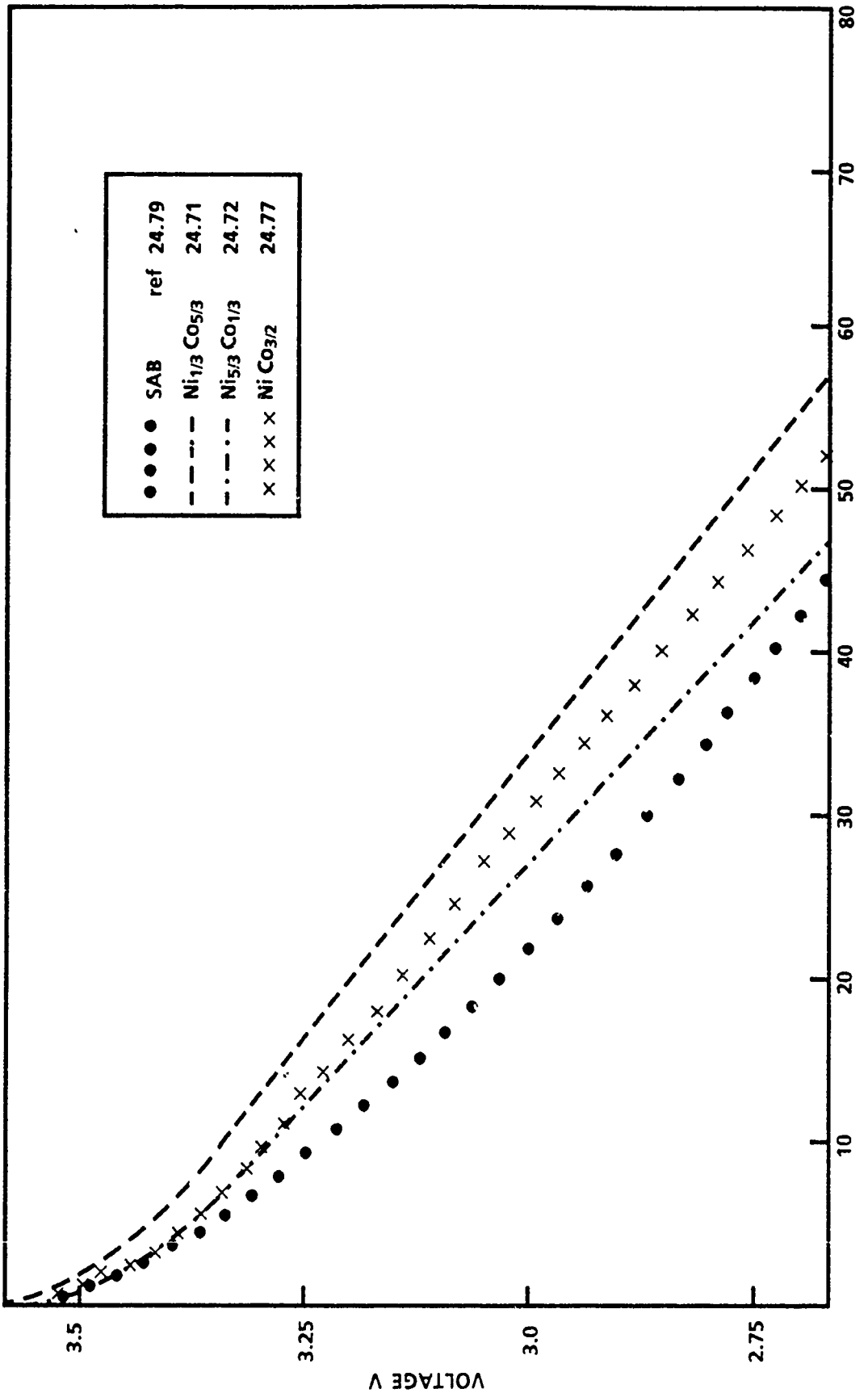
SAB ref 24.79
$Ni_{1/3}Co_{5/3}$ 24.71
$Ni_{5/3}Co_{1/3}$ 24.72
Ni $Co_{3/2}$ 24.77
VOLTAGE V
3.5
3.25
3.0
2.75
CURRENT, mA
10
20
30
40
50
60
70
80

FIGURE 7.

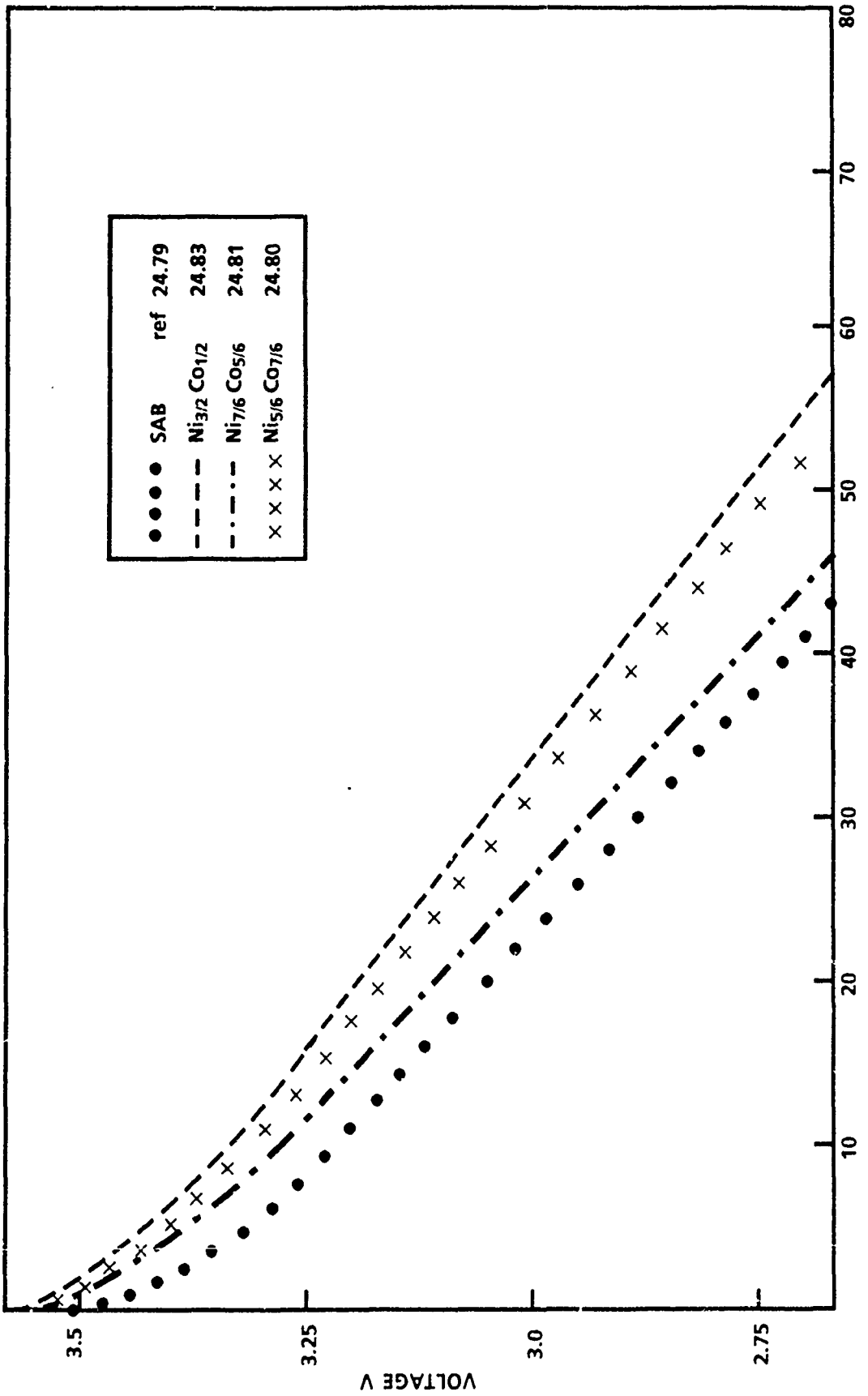
SAB ref 24.79
Ni3/2 Co1/2 24.83
Ni7/6 Co5/6 24.81
Ni5/6 Co7/6 24.80
VOLTAGE V
3.5
3.25
3.0
2.75
CURRENT, mA
10
20
30
40
50
60
70
80

FIGURE 8

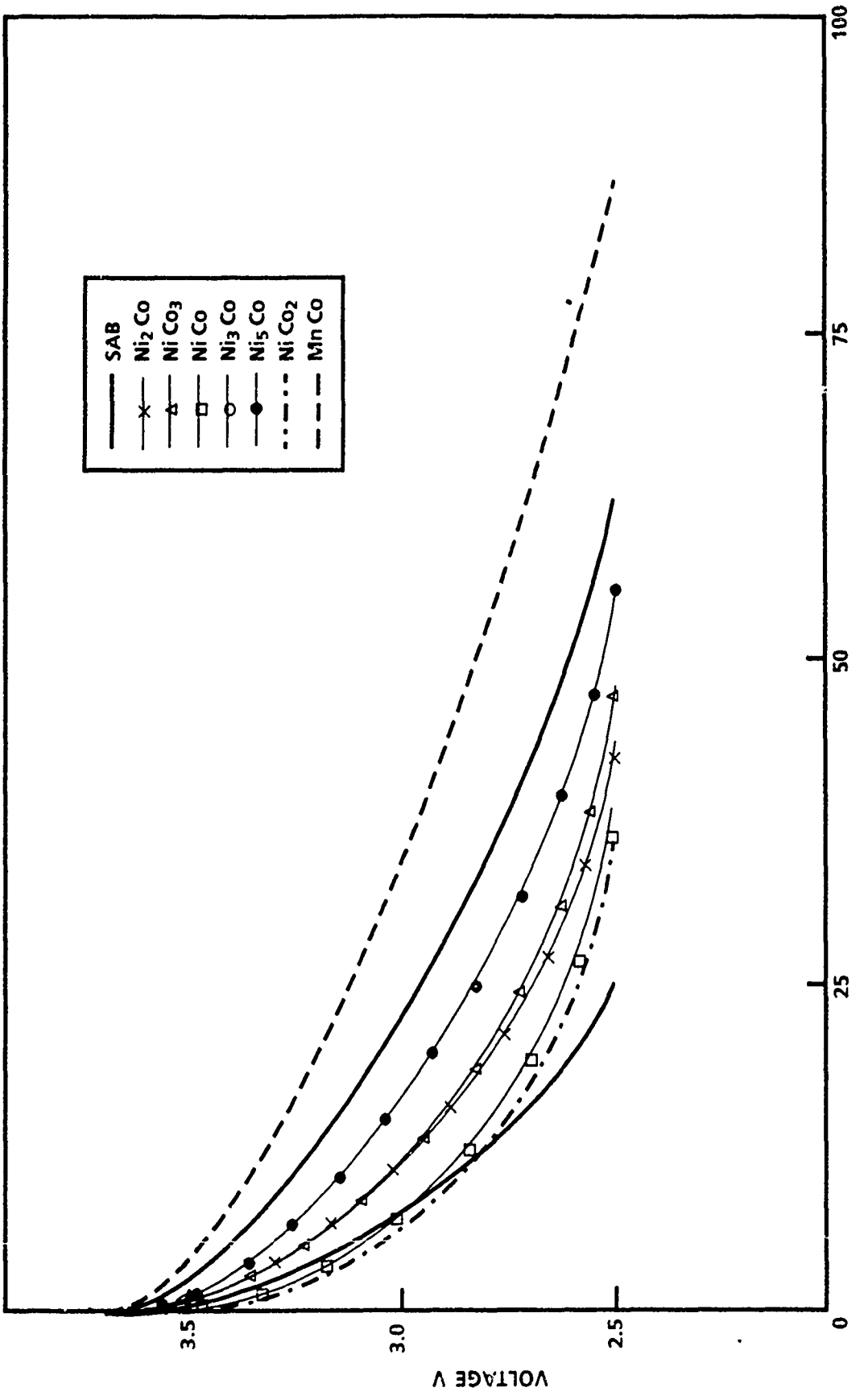
SAB
Ni_2 Co
Ni Co_3
Ni Co
Ni_3 Co
Ni_5 Co
Ni Co_2
Mn Co
VOLTAGE V
3.5
3.0
2.5
0
25
50
75
100
CURRENT, mA

FIGURE 9

data substantiates the -previous results, at least to a certain extent. When interpreting the data, one must consider a number of factors, including sample size, variability in manufacture surface phenomena, and the different manufacturing methods, i.e. wet and dry, for demountable cell cathodes. The objective of Phase I of the program was to manufacture and quickly evaluate a number of potential catalyst candidates. The purpose of full cell testing, basically, was to validate the results of the flooded cell tests. High current densities were achieved with cells of low-rate bobbin-type design because of the time constraints of the program. In order to fully evaluate these catalysts, a matrix of at least 20 with each type of catalyst would have to be discharged fully at different rates at each test temperature. The full cell polarization testing served as a vehicle to compare E vs i characteristics of cells featuring a number of different cathode catalysts vs control cells.

In the final analysis, it can be said that all eight catalysts, which showed good potential when screened initially in the demountable test cell, also showed good potential when integrated into actual production-type cells, at least with respect to polarization testing. Although the test results are not necessarily definitive, they are indicative that most Ni/Co combinations and the one Mn/Co combination-based catalysts manufactured under the program can enhance the operating voltage of a standard Li-$SOCl_2$ cell to greater and lesser degrees. These results are, in turn, indicative of the success of the Phase I program.

8.2.2 CONSTANT LOAD DISCHARGE TESTS

Control cells, as well as those with catalyzed cathodes of each type as tested in Section 8.2.1, were selected at random from the group for discharge testing. In that time permitted only the testing of two cells of each type, the results of this testing are far from being conclusive. The 1/2 AA cell design has 3.77 cm2 of electrode surface area. The purpose of this particular test was to verify the operating voltage improvements observed in the tests of Sections 8.1 and 8.2.1, as well as determine the effect, if any, these catalysts would have upon cathode utilization. Since the purpose of cathode catalysts is to improve cathodic efficiency at high rates of discharge, this group of cells was discharged at a rate approximately twice that for which these cells were designed. Accordingly, 160 Ohm resistors were used. Current densities at operating potentials are as follows:

E(V)	i(mA)	I(mA/cm2)
3.4	21.3	5.6
3.2	20	5.3
2.9	18.1	4.8

Although these current densities are considerably less than the upper limits of those of the floating cell polarization tests (40-75 mA/cm2) or the 1/2 AA polarization tests (6.4-22.9 mA/cm2), they are near the upper limit of those that can be realistically achieved with this particular cell design. The data of this test,which appears in Figure 10, should be compared to data for the corresponding current densities of the two types of a-polarization tests.

All of the catalysts employed were successful in significantly increasing the operating voltage of test cells. Control cells operated at approximately 2.92 volts, whereas catalyzed cells operated in the range from 3.26 to 3.40 volts. This data is more impressive when one considers that, since the test cells were discharged

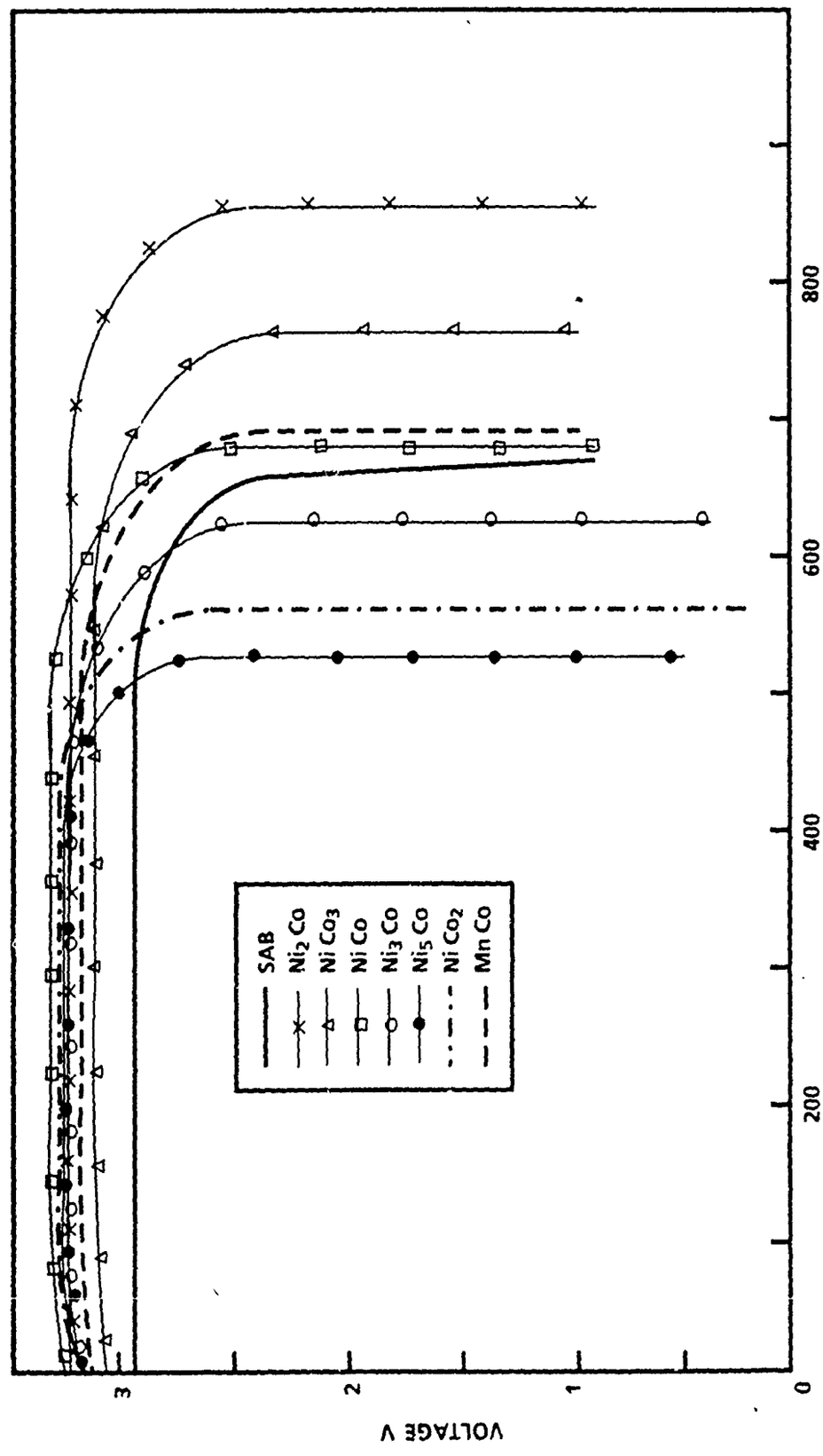
SAB
Ni_2 Co
Ni Co_3
Ni Co
Ni_3 Co
Ni_5 Co
Ni Co_2
Mn Co
VOLTAGE V
3
2
1
0
CURRENT, mAH
200
400
600
800

FIGURE 10

through resistive loads of equal value, the catalyzed cells were being discharged at currents 10-15% in excess of that of control cells.

Five of the different experimental cell types manifested operating voltages between 3.35 and 3.4 V : Ni_2Co, NiCo, Ni_3Co, $NiCo_2$, and Ni_5Co. The remaining two types, $NiCo_3$ and MnCo, operated at approximately 3.25 V. The MnCo exhibited the best performance in the polarization tests of 1/2 AA cells but was not a standout in the course of the discharge testing. This could have been due to some internal cell problems, such as partial short circuiting, or it could be that the catalyst is not suitable for long term discharge. The latter premise is supported by the fact that gradual deterioration of the operating voltage occurs throughout discharge.

Three catalyst types did not achieve the capacity of the SAB: -Ni_5Co, $NiCo_2$, and Ni_3Co. Two catalyst types achieved approximately equal discharge capacities: NiCo and MnCo. Two catalyst types generated higher discharge capacities than SAB: $NiCo_3$ and Ni_2Co.

The one aspect of this test that clearly stands out is that higher operating voltages can definitely be achieved through the use of spinel-type cathode catalysts. Whether or not their use improves cathode utilization has not been clearly demonstrated. Due to the excessively high rates of discharge, no test result approached the theoretical cell capacity of approximately 1.0 Ahr.

8.3 CHEMICAL STABILITY TESTS

A total of 5 samples were analyzed for the presence of nickel and cobalt ions in solution via titration according to the method of Harris and Sweet (50) with modifications necessitated by the presence of aluminum ions in the electrolyte. Of the 5 samples, one was a blank and one a standard containing 1.0 mg of both Ni and Co ions. The remaining 3 were unknowns prepared by storing Ni:Co ratios 5:1, 1:1, and 1:5, in 5 ml. aliquots of 1.8 M $LiAlCl_4$ in $SOCl_2$ electrolyte for two months.

Alpha-nitroso-betanapthol was added to the buffered solutions containing the samples prior to extracting the Ni and Co-containing samples from the aluminum-rich phase. The production of a case of the standard solution indicated red-orange color in the ions in the standard solution but not in the presence of cobalt the case of the electrolyte samples.

After the extraction of the Co-1nitroso-2-napthol and Ni-dimethyl-gloxine into chloroform, an attempt was made to break the -complex with 2M HCl in order to obtain aqueous solutions of Ni and Co without Al contamination. In none of the 5 solutions was either Ni or Co detected. Thus, the EDTA titrations were not necessary.

The limits of detection were determined by titration of aluminum-free standard solutions to be 0.7 mg for nickel and 1.5 mg for cobalt. We can therefore say at this point that if either the cobalt or the nickel did leach from the cathode samples, the amounts present were less than these stated minimum values. Atomic absorption would be better suited for this analysis.

9.0 CONCLUSIONS

As stated in the original proposal, the goal of the work conducted under the terms of this program was the improvement of current state-of-the-art $Li/SOCl_2$ battery technology through the use of carbon-based cathodes containing advanced non-noble catalysts. Initial electrochemical performance and chemical stability testing was performed in order to verify and quantify improvements made to the basic $Li/SOCl_2$ system through the use of spinel and/or perovskite based cathode catalysts.

Ultimately the use of seven different catalyst types resulted in performance improvements when applied to the $Li/SOCl_2$ system. These improvements were indicated in the polarization testing of glass-bodied flooded electrolyte test °cells, and substantiated in both polarization and long-term discharge testing of hermetically sealed production-type 1/2 AA cells. Whereas all seven of the successful catalyst types (oxides of MnCo, $NiCo_5$, $NiCo_3$, $NiCo_2$, NiCo, Ni_2Co, Ni_3Co, and Ni_5Co) demonstrated improved operating voltages in the $Li/SOCl_2$ system, the use of the $NiCo_3$ and Ni_2Co based catalyst types clearly demonstrated improved cathode utilization at high discharge rates. It is possible that improved cathode utilization could be realized with all seven of these catalyst types; however, more comprehensive testing would be required to demonstrate this.

Chemical stability testing indicated that at least the nickel / cobalt oxide-based combinations were stable in $SOCl_2$-based electrolyte for at least two months. Due to the limitations of our test methodology and the time limitations of a Phase 1 program to perform such testing, these results are not conclusive. Had the catalysts been even moderately unstable in $SOCl_2$-based electrolyte, however, the testing would have indicated so.

Based upon the results of this program, one can conclude that the spinel-based cathode catalysts tested herein showed great promise for application to the $Li/SO6I_2$ system. A number of different catalysts improved the discharge performance of $Li/SOCl_2$ cells while remaining chemically stable in $SOCI_2$-based electrolyte solutions for two month perions at ambient temperature. A number of questions still remain with regard to these spinel-based catalysts. These could be answered during the course of a Phase 2 program devoted to the study of spinel-based catalysts for $L/SOCl_2$ batteries.

Among the remaining questions, chemical stability is, perhaps, the most acute. A definitive answer could be given this question through long term storage and performance evaluation of $Li/SOCl_2$ cells containing spinel-based catalysts and/or electrolyte analysis via atomic absorption. Nearly as acute a question is how each of the seven catalyst types would perform in high-rate hermetically sealed cells, such as the C size cells used by Abraham et al. (1).

10.0 REFERENCES

1. K.M. Abraham, L. Pitts, and W.P. Kilroy, Journal of the Electrochemical Society, Vol. 132, No. 10, Oct. 1985.

2. N. Doddapenini, D.L. Chua, and R.F. Bis, Electrochemical Society Fall Meeting, Denver, Co., 1981.

3. F. Walsh, R.S. Morris, U.S. Patent No. 4,469,763, September 4, 1984.

4. M. Jose Yacaman and E. Pedrero Nieto; Journal of Crystal Growth; 7 (259-261) 1970.

5. D. Hesse and H. Bethge; Journal of Crystal Growth; 65 (69-76) 198:3.

6. J.M. Robertson, M. Jansen, B. Hoezstra, and P.F. Bongers; J. Crystal Growth; 41 (29-35) 1977.

7. A.C.C. Tseung, B.S. Hobbs, and A.D.S. Tantram; Electrochimica Acta; Vol. 15 (473-481) 1970.

8. L.G.J. deHaart and G. Blasse; J. Electrochem. Soc.; Vol. 132, No. 12 (2933-2938) Dec. 1985.

9. Y. Matsumoto, H. Manabe, and E. Soto; J. Electrochem. Soc.; Vol° 127, No. 4 (811-814) Apr. 1980.

10. A.C.C. Tseung and S. Jasem; Electrochimica Acta; Vol. 22 (31-34) 1977.

11. P.H. Robinson and D.J. Dumin; J. Electrochem. Soc.; Vol. 115, No. 1 (75-78) Jan. 1968.

12. C.C. Wang; Journal of Applied Physics; Vol. 40, No. 9 (3433-344˙) Aug. 1969.

13. J.M. Kowalski, K.H. Johnson and H.L. Tuller; J. Electrochem. Soc., Vol. 127, No. 9 (1969-1973) Sept. 1980.

14. R. Kanno, Y. Tazeda, K. Takada, and O. Yamamoto; Journal of the Electrochemical Society; Vol. 131, No. 3 (469-474) March 1984.

15. T. Ohachi and B.R. Pamplin; Journal of Crystal Growth; 42 (598-601) 1977.

16. V.A.M. Brabers, T.E. Whall, and P.S.A. Knapen; Journal of Crystal Growth; 69 (101-107) 1984.

17. G.W. Cullen and J.F. Corlsoy; J. Electro Chem. Soc.; Vol. 121 No. 10 (1345-1350) Oct. 1974.

18. G. Katz and R. Roy; Journal of Crystal Growth; 6 (221-227) 1970.

19. F. Emmenegger; Journal of Crystal Growth 3, 4 (135-140) 1968.

20. R.A.Piscitelli, S.K.Rhee, and F. N. Bradley; J. Electrochem. Soc.; Solid-State Science & Technology; Vol. 123, -No. 6 (929-933) June 1976.

21. M. Ehman; J. Electrochem. Soc.; Solid-State Science & -Technology; Vol. 121, No. 9 (1240-1243) Sept. 1974.

22. C.H. Kuhl, H. Schloherer, and F. Schwidefsky; J. Electrochem. Soc;Solid-State Science & Technology; Vol. 123, No. 1 (97-100) Jan. 1976.

23. T. Matsui and J.B. Wagner Jr.; J. Electrochem. Soc.; Solid State Science & Technology; Vol. 124, No. 7 (1141-1143) July 1977.

24. C.C. Wang, F.C. Dougherty, P.J. Zanzucchi, and S.H. McFarlane III; J. Electrochem. Soc.; Solid-State Science & Technology, Vol. 121, No. 4 (571-582) April 1974.

25. B. Wanklyn; J. of Crystal Growth, 7 (368-370) 1970.

26. N. Marincic; Catalyzed Electrodes for ALWT Applications, Internal Report to Sylvania from BEI, 1980.

27. A.C.C. Tseung and K.L.K. Yeung; J. Electrochem. Soc.; Vol. 125, No. 6 (1003-1005) June 1978.

28. V.S.Bagotzky, N.A. Shumilova, E.L.Khrushchicua; Electrochimica Acta; Vol. 21 (919-924) 1976.

29. S.M. Jasem and A.C.C. Tseung; J. Electrochemical Science and Technology; Vol. 126, No. 8 (1353-1360) Aug. 1979.

30. R. Falckenberg; J. Electrochem. Soc.; Solid-State Science & Technology; Vol. 123, No. 1 (63-65) Jan. 1976.

31. E. Cockayne and M. Chesswas; Journal of Materials Science 2 Lehers; (498-500) 1967.

32. T. Ocana 2, M. Guillen, C. and M. Jose Yacaman; Journal of Crystal Growth, 34 (103-10) 1976.

33. A. Landsberg and T.T. Campbell; Journal of Metals; (856-860) Aug. 1965.

34. W.J. King and A.C.C. Tseung; Electrochimica Acta; Vol. 19 (49:3-498) 1974.

35. T.B. Reed and E.R. Pollard; Journal of Crystal Growth 2 (243-247) 1968.

36. W.J.King and A.C.C. Tseung; Electrochimica Acta; (485-491) 1974.

37. C.C. Wang and S.H. McFarlane III; Journal of Crystal Growth; Vol. 3, 4 (485-489) 1968.

38. Lang's Handbook of Chemistry, McGraw-Hill Co., Editor John A. Dean, 15th Edition, 1973.

39. H. Ohbayshi, T. Kudo,, and T. Geto; Japanese Journal of Applied Physics; Vol. 13, No. 1 (1-6) Jan. 1974.

40. F.H. Mischgofsky and G.K. Richter-Van Leeween; Journal of Crystal Growth, 43 (213-223) 1978.

41. R.R. Neurgaonkar, E. Cross, and W.B. White; J. Electrochem. Soc.; Vol. 125, No. 7 (1130-1133) July 1978.

42. N.H. Chan, R.K. Shaima, and D.M. Smyth; J. Electrochem. Soc.; Vol. 128, No. 8 (1762-1769) Aug. 1981.

42. A.K.L.K.Yeung and A.C.C. Tseung; J. Electrochem. Soc.; Vol. 125, No. 6 (878-882) June 1978.

43. Y. Matsumoto, H. Manabe, and E. Sato; J. Electrochem. Soc.; Vol. 127, No. 4 (811-814) April 1980.

44. T. Kudo, H. Obayashi, and M. Yoshida; J. Electrochem. Soc.; Vol. 124, No. 3 (321-325) March 1977.

45. K. Scott, M.P. Kang, and J. Winnick; J. Electrochem. Soc.; Vol. 130, No. 2 (527-529) Feb. 1983.

46. J.O.N. Bockris and T. Otagewa; J. Electrochem. Soc.; Vol. 131, No. 2 (290-302) Feb. 1984.

47. R. Breault, R. Harding, F. Kemp; U.S. Patent 4,043,933, Aug. 1977.

48. W.J. Hamer, "Internal Resistance of Primary Batteries," from N.C. Cahoon and G.W. Heise, The Primary Battery, Wiley & Sons, NY, 1976.

49. Epstein, et al, U.S. Patent Application 865,570.

50. William Harris and Thomas Sweet; Analytical Chemistry; Vol. 26, No. 10 (1648-1651) Oct. 1954.

APPENDIX C

IMPROVED LITHIUM/THIONYL CHLORIDE CELLS USING NEW ELECTROLYTE SALTS

FINAL REPORT
December 1987 - May 1988

Prepared for:

Naval Surface Warfare Center
Silver Spring, MD 20903-5000

Under Contract No. N60921-88-C-0057

Battery Engineering, Inc.
1636 Hyde Park Avenue
Hyde Park, MA 02136

C. R. Schlaikjer
Principal Investigator

W. Kilroy
Project Manager

TABLE OF CONTENTS

LIST OF TABLES

LIST OF FIGURES

CHAPTER 1

INTRODUCTION

Lithium/ thionyl chloride cells have long been recognized for their high energy density, moderately high power density with appropriate electrode area, nearly constant potential discharge characteristic, ease of construction from relatively inexpensive and readily available components, and amenability to hermetic construction. The closest competitor in this field has been the lithium/ sulfur dioxide primary system with organic solvents, but the energy density is inferior to that possible with lithium/ thionyl chloride cells.

Because of the significant advantages which the lithium/ thionyl chloride electrochemical system offers, interest has abided in attempting to improve its startup or voltage delay characteristic and tolerance to discharge at higher current densities, both at ambient and at reduced temperatures. During this present study, we have addressed these issues by exploring new electrolyte salts for lithium/ thionyl chloride cells. We have followed principles which have been successful in the past, namely, by preparing lithium salts of large anions with reduced tendency to exchange with solid lithium chloride. Unlike their predecessors, the salts to be studied required considerably less expensive starting materials, were more easily prepared, and were not subject to redox reactions in thionyl chloride.

Steps leading to the development of the voltage delay problem in lithium/ thionyl chloride cells are now well known. A thin film of lithium chloride begins to form on the surface of lithium as soon as it contacts thionyl chloride containing lithium tetrachloroaluminate. The film prevents rapid chemical reaction between the lithium and the thionyl chloride because it is nearly insoluble. Since solid lithium chloride has a conductivity of 1.2×10^{-10} S cm^{-1} at room temperature [1], due entirely to conduction by lithium ion [2], a sufficiently thin layer of lithium chloride will act as a second electrolyte in series with the liquid phase, or a solid electrolyte interphase (SEI) [3]. When corrosion of the lithium, as the result of extended storage or storage at elevated temperature, causes the film to become excesively thick, a substantial IR potential drop occurs across the SEI at the onset of discharge. The thick film is undercut by the electrolyte as discharge causes the lithium to shrink away from it. The thick film is replaced by a thin one, and discharge proceeds at a higher potential.

Proposed methods to alleviate the voltage delay problem have been previously discussed [4, 5]. The objective is to prevent the lithium chloride SEI film from becoming thicker than it must be to protect the metal from the electrolyte. While substantial improvements are possible by removing hydrolysis products and iron from the electrolyte, cleaning the electrolyte alone is insufficient to reduce the delay to an acceptable level. Exchange of the lithium chloride layer with species in solution contributes to the growth of the film, since exchange causes larger crystals in the film to grow at the expense of smaller ones. Where the salt film is thinnest, reorientation of the material in the layer allows the electrolyte access to the metal, and corrosion is encouraged. High concentrations of lithium ion increase the concentration of Li_2Cl^+, in effect, increasing the solubility of lithium chloride and disturbing the SEI [6, 7]. The electrolyte salt $LiAlCl_4$ is also in constant equilibrium with dissolved $AlCl_3$ and solid LiCl. Unfortunately, lowering the concen-

tration of $LiAlCl_4$ to decrease the voltage delay reduces the rate capability of the carbon cathode.

The use of lower concentrations of soluble lithium salts with large anions has been found effective in eliminating voltage delay without compromising rate capability. One example is that of the closoborate salts $Li_2B_{10}Cl_{10}$ and $Li_2B_{12}Cl_{12}$, which at 0.25 molar were as effective as 1.8M $LiAlCl_4$ in providing adequate rate capability in wound D cells [8]. The SEI films were equivalent to the very thin films produced in thionyl chloride without electrolyte salt. The effects were attributed to the low mobilities of the large anions, and to the effective reduction in exchange between the SEI and the solution. The salts are expensive and react when heated with thionyl chloride. A second example is $LiGaCl_4$, which markedly increases the rate capability of wound cells [9], but which is also considerably more expensive than $LiAlCl_4$.

Vallin and coworkers have suggested using $LiAl(SO_3Cl)_4$ as an additive, present at a level of only one percent in 1.35M $LiAlCl_4$/ $SOCl_2$ along with 0.6M SO_2, to reduce voltage delay [10, 11]. The solubility of the fully chlorosulfonated aluminate is limited both in liquid sulfur dioxide, from which it may be synthesized by precipitation [12], and in thionyl chloride. The same fully substituted anion was said to have formed by the reaction of sulfur trioxide or chlorosulfonic acid with $AlCl_4^-$ in $SOCl_2$, producing absorption maxima in the infrared at 660 and 1070 cm^{-1}. It is not clear whether the species which formed in thionyl chloride was the same as that which formed in sulfur dioxide, or whether it was a partially substituted anion such as $AlCl_3(SO_3Cl)^-$. Vallin's patent [10] includes only $MM'_m(SO_3X)_n$, where M is an alkali or alkaline earth metal, M' is Al, B, Ga, In, V. Sb, Nb, Si, W, or Ta; X is F, Cl, Br, or I; and m and n are unspecified. Partially substituted anions such as $AlCl_3(SO_3Cl)^-$ may exist, which might be more soluble in $SOCl_2$ and better suited for alleviation of voltage delay in Li/ $SOCl_2$ cells, and which are not covered by Vallin's patent.

Catalysts have been added to the cathodes of lithium/ thionyl chloride cells to increase the rate capability and capacity. Macrocyclic complexes of transition metals, for example cobalt dibenzotetraazaannulene [13, 14], while they do increase the capacity and rate capability, often allow the transition metal to leach partially into the electrolyte during storage. Passivation of the anode then results. The lithium salt of a large anion may make catalytic additives unnecessary, by maximizing the transferrence of lithium ions and retarding the polarization of the cathode.

The main purpose of this work has been to determine whether new lithium salt derivatives may be synthesized, and whether they are capable of improving the rate capability and startup characteristic of lithium/ thionyl chloride cells, relative to control cells containing 1M $LiAlCl_4$/ $SOCl_2$. To this end, we have investigated four major areas according to the following:

I. Partially sulfonated chloroaluminates, such as
   $AlCl_{(4-n)}(SO_3X)_n^-$, where X = F, Cl, CH_3, CF_3, $C_6H_4CH_3$
II. Partially acetated chloroaluminates, such as
   $AlCl_{(4-n)}(CO_2CX_3)_n^-$, where X = F, Cl, H
III. $AlOCl_2^-$ and "bridged" partially oxide, partially chloride aluminates
IV. Complex sulfur oxyacid salts, such as
   $S_2O_6^{2-}$ (dithionate)
   $S_4O_6^{2-}$ (tetrathionate)

CHAPTER 2

EXPERIMENTAL

The dryroom, measuring about 36 feet square, was maintained at 70°F. at a relative humidity of about 2.5%. Salts were weighed, solutions prepared, infrared samples were taken, and electrolyte solutions were refluxed in the hood inside the dryroom. In addition, the annular bobbin, case positive AA size cells were made in the dryroom.

Infrared spectra were taken using either a Perkin Elmer model 137 or 257 spectrophotometer. Measurements of hydrolysis products in thionyl chloride solution were done in a 10mm pathlength type I quartz cuvette with a Teflon stopper versus an identical empty cuvette. Spectra from 2.5 to 15 microns were taken with a demountable liquid sample cell with a 0.1 mm spacer and sodium chloride windows.

The cells were discharged at constant current using power supplies built by Starbuck Systems of Newton and controlled by an IBM compatible computer with a Starbuck interface board and protecting circuitry. The discharge and plotting programs were written by Software Tailors, Inc.

Lithium salts were prepared from methanesulfonic acid, chloroacetic acid, trifluoroacetic acid, and toluenesulfonic acid, by reaction in aqueous solution with lithium hydroxide, using bromothymol blue (pH 7) as the indicator. The water was removed first by vacuum distillation, then by heating *in vacuo* to 160°C. to constant weight. We established that the lithium salts of both methanesulfonic and chloroacetic acid could be purified by recrystallization from methanol/acetone. 97% lithium trifluoromethane sulfonate from Aldrich was used as received without further purification.

Larger quantities of methanesulfonate and chloroacetate were made by the following alternative method. A weighed amount of reagent grade lithium carbonate was suspended in methanol, and an approximately stoichiometric amount of the acid, either methanesulfonic or chloroacetic, was dissolved in methanol and added to the suspension of lithium carbonate. The acid was added until only a small portion of lithium carbonate was left suspended. The solution was then filtered, and acetonitrile was gradually added to the filtrate with rapid stirring. The lithium salts crystallized from their respective solutions.

Sulfur trioxide was distilled from oleum in batches as follows. About 200 ml of fuming sulfuric acid, containing 20% sulfur trioxide, was placed in a 500 ml round bottom flask and fitted with a sol trap, transfer tube, and an air condenser. The oleum was heated while being stirred with a magnetic bar. The sulfur trioxide was collected and stored in the dryroom in a 50 ml roundbottom, but never longer than 15 minutes before use, since unstabilized sulfur trioxide easily trimerizes to a solid.

Aluminum chloride was purified using a sublimator in the dryroom hood by distillation from molten $LiAlCl_4$ treated with calcium metal turnings. The calcium reacts quickly and smoothly with the molten salt containing extra aluminum chloride at 120 to 150°C., producing finely divided aluminum. The aluminum, present without any oxide layer, prevents iron chloride from distilling with the aluminum chloride. The molten salt allows more effective heat transfer, distillation at atmospheric pressure, and more rapid collection of purified aluminum chloride.

The characteristics of the AA case positive annular bobbin cells were as follows:

Dimensions of outer case:
1/2" O.D. x 1 7/8"; 6.03 cm^3, stainless steel case positive, hermetically sealed, TIG welded glass/ metal compression hollow feedthroughs/ fillports
Dimensions of annular bobbin:
I.D. 0.380 +/- 0.04"
O.D. 0.485 +/- 0.04"
height, 1.58 +/- 0.06"
Weight of bobbin (with binder), 0.70g
Composition of bobbin, Chevron acetylene black/ 3% Teflon
Anodes: 1.7" x 0.39" x two, located in the center of the bobbin cathodes, spring loaded against the separators/ cathodes; 0.050" thick; 8.55 cm^2; 1.09 cm^3; 2.24 Ahr
Separators: Mead Pyrex paper, 0.007"

Using infrared spectroscopy, we determined whether there were significant amounts of hydrolysis products in electrolyte samples, so that these products could be removed by refluxing. We also used infrared spectroscopy to determine whether synthetic techniques had been successful in producing derivatives soluble in thionyl chloride.

Cells were filled, sealed, and discharged, according to the following:
Electrolytes:
each of those indicated below under "Cell Tests"
Number of replicate cells for each electrolyte: 3
Discharge current:
25.6 mA (3 mA/cm^2 of anode surface area)
Discharge temperature:
ambient (19 to 31°C.)
Measurements:
Startup characteristics
Capacity to 3 volts
Capacity to 2 volts

CHAPTER 3

RESULTS AND DISCUSSION

NEW ELECTROLYTE SALTS.

We prepared 500 ml of 2M aluminum chloride in thionyl chloride, using $AlCl_3$ purified by distillation from molten lithium tetrachloroaluminate, in order to obtain a stock solution from which all experimental and control electrolytes could be made. Figure 1 shows the infrared spectrum of this solution shortly after it was prepared. Strong absorption between 3100 and 3500 cm^{-1} indicates that a considerable amount of hydrolysis products were present. Either the partially hydrolized aluminum chloride was volatile and distilled along with the aluminum chloride, or the distilled product absorbed water from the dryroom atmosphere. The solution was refluxed for about eight hours to remove the hydrolysis products. Figure 2 is a spectrum of the solution after the reflux period, although the reference port did not contain an empty quartz cell, and shows that the hydrolysis products had been removed.

This "dried" 2M $AlCl_3$/ $SOCl_2$ was used to prepare one molar solutions made by reacting portions of it with an equivalent amount of each lithium carboxylate or sulfonate, and diluting to the required volume with thionyl chloride. For solubility tests, 4 ml Savillex sample vials were used. For cell electrolytes, 100 ml volumetric flasks were used. Since the lithium salts tested did not react completely with an equivalent amount of 1 molar aluminum chloride in thionyl chloride, lithium chloride equivalent to the aluminum chloride initially present was also added to the mixtures to prevent excess aluminum chloride from corroding the sodium chloride infrared windows or the cell anodes.

One of the objects of our current study was to determine whether a partially chlorosulfonated derivative could be prepared, and if so, whether its solubility would be higher and its effect either in alleviating the voltage delay problem, or in increasing the rate capability of these cells would be enhanced.

We first attempted to prepare $Li\{AlCl_3(SO_3Cl)\}$ by way of the following reactions:

$$LiCl + SO_3 \rightarrow Li(SO_3)Cl$$

$$Li(SO_3)Cl + AlCl_3 \text{ (in } SOCl_2) \rightarrow Li\{AlCl_3(SO_3)Cl\}$$

Sulfur trioxide was found not to react with lithium chloride, since a sample of LiCl did not absorb SO_3 when treated at room temperature with an excess. Cotton and Wilkinson [15] have stated that chlorosulfonic acid forms no salts, our observation therefore confirming this admonition. Yet Vandorpe and Drache reported that SO_3 reacted with $LiAlCl_4$ dissolved in sulfur dioxide to form insoluble $LiAl(SO_3Cl)_4$ [12]. We then elected to try the following series of reactions:

$$AlCl_3 \text{ (in } SOCl_2) + SO_3 \rightarrow AlCl_2(SO_3Cl)$$

$$AlCl_2(SO_3Cl) + LiCl \text{ (in } SOCl_2) \rightarrow Li\{AlCl_3(SO_3Cl)\}$$

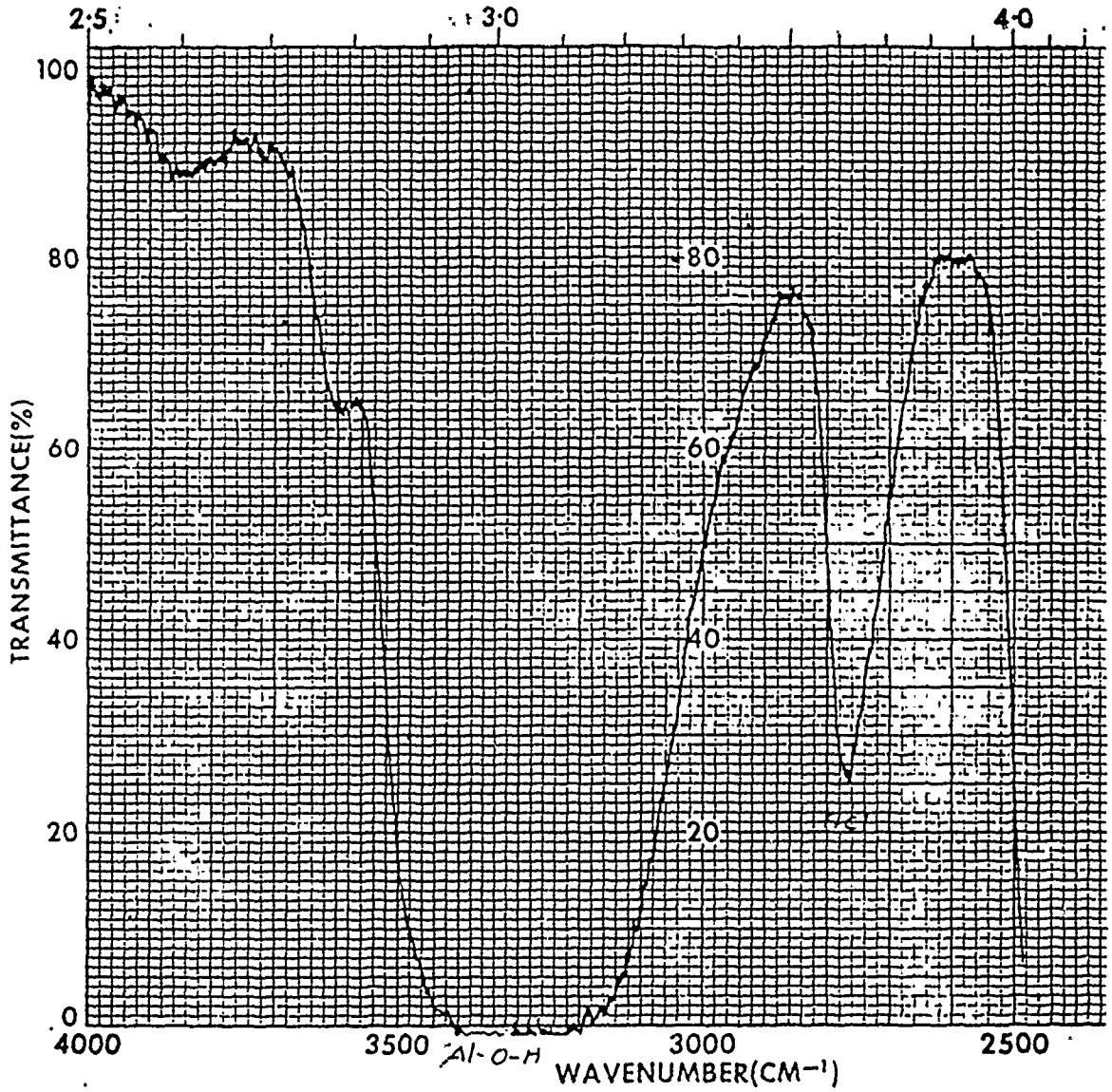

FIGURE 1. INFRARED SPECTRUM, USING THE PERKIN-ELMER 257 SPECTROPHOTOMETER AND A 10 MM PATHLENGTH TYPE I QUARTZ CELL VERSUS AN EMPTY QUARTZ CELL. 2M DISTILLED $ALCl_3$ IN THIONYL CHLORIDE, BEFORE REFLUXING.

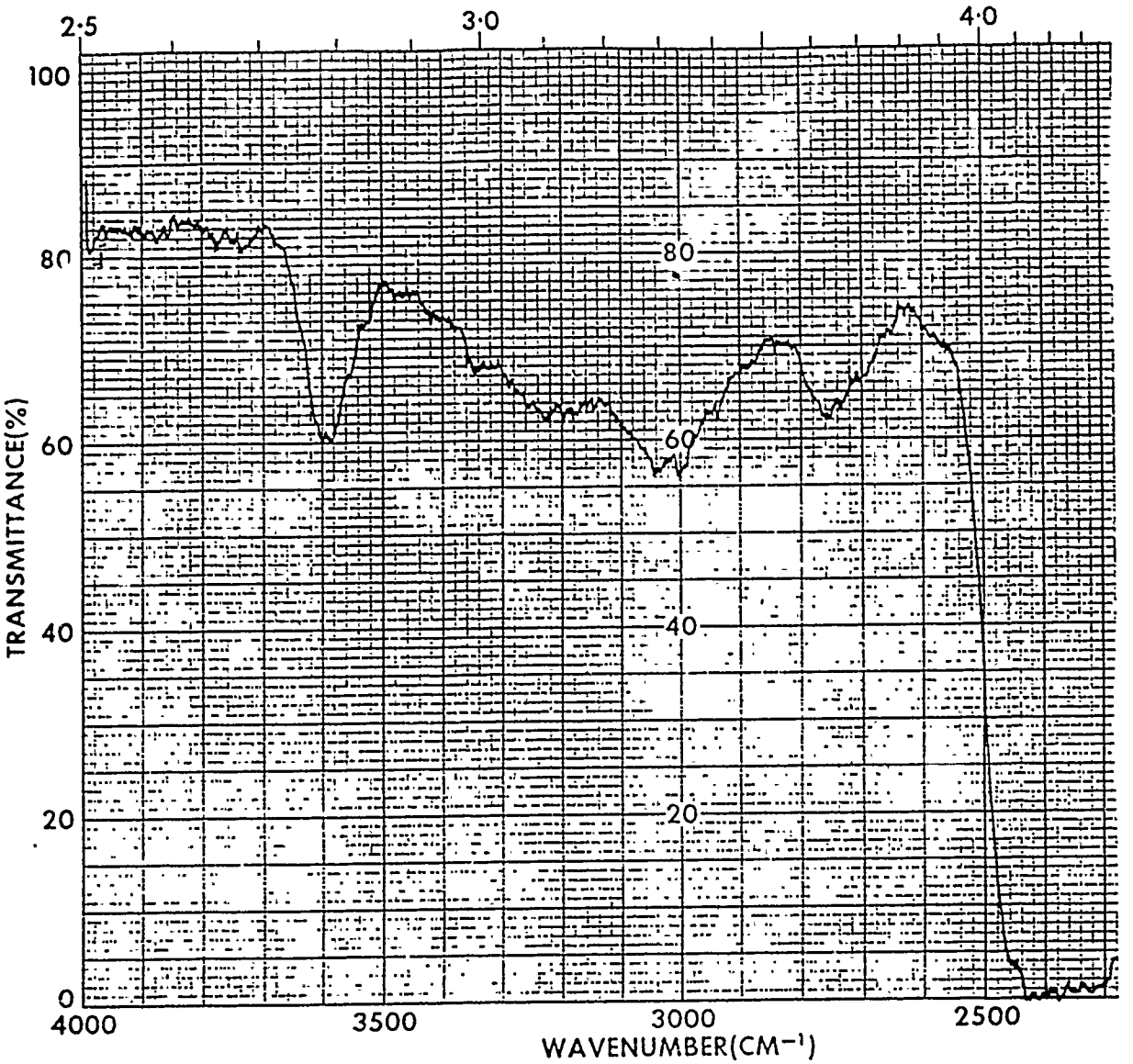

FIGURE 2. INFRARED SPECTRUM, USING THE PERKIN-ELMER 257 SPECTROPHOTOMETER AND A 10 MM PATHLENGTH TYPE I QUARTZ CELL VERSUS AN EMPTY QUARTZ CELL. 2M DISTILLED $ALCl_3$ IN THIONYL CHLORIDE, AFTER REFLUXING.

We dissolved enough purified $AlCl_3$ in thionyl chloride to prepare a 1 molar crystal clear solution. Into an aliquot of this solution was slowly pipetted one equivalent of sulfur trioxide. A precipitate appeared as soon as the sulfur trioxide contacted the solution, but with stirring, this dissolved. Near the end of this addition, a gelatinous precipitate appeared throughout the solution. Then, one equivalent of dried lithium chloride was sifted into the mixture with continued stirring. The contents reacted, forming a clear solution.

Figure 3 is an infrared spectrum of a 1M solution of $LiAlCl_4$ in thionyl chloride, showing the absorptions characteristic of thionyl chloride and $AlCl_4^-$. Figure 4 is a partial infrared spectrum of the solution described above, just after the addition of the lithium chloride. There was a very strong absorption at 1070 cm^{-1}, which is one of the frequencies assigned to tetrachlorosulfonatoaluminate [10, 11], except the concentration was much higher than that reported by Vallin and Chenebault.

By the following morning, white crystals had formed in the flask. These were filtered, washed with thionyl chloride, and dried in the dryroom atmosphere at 100°C. Three separate samples lost an average of 3.2% of what their weight had been before drying. From one of these samples, three portions of about 100 mg each were weighed carefully and the chloride content determined by potentiometric titration. The results were 133.5, 133.6, and 133.7 grams per equivalent of chloride. Calculated values for $LiAlCl_4$ and each of the possible chlorosulfonated aluminates are as follows:

	F wt. (grams/ mole)	Eq. wt. (g/ equiv. of Cl^-)
$LiAlCl_4$	175.74	43.94
$LiAlCl_3(SO_3Cl)$	255.74	63.94
$LiAlCl_2(SO_3Cl)_2$	335.74	83.94
$LiAlCl(SO_3Cl)_3$	415.74	103.94
$LiAl(SO_3Cl)_4$	495.74	123.94

We tentatively believe that we had initially formed one or more partially chlorosulfonated aluminates, but that these had disproportionated overnight to produce the less soluble, fully chlorosulfonated derivative. The extra weight could have been water absorbed from the dryroom atmosphere while the samples were being heated to remove thionyl chloride, so that what is needed is a determination of either the aluminum or the sulfate content to correlate with the chloride analyses.

Another of our objectives was to determine what other functional groups similar to chlorosulfonate could be used to replace one or more of the chlorides on tetrachloroaluminate. Our approach was to attempt the reaction of lithium salts of the candidate anions first with a solution of aluminum chloride in thionyl chloride, hoping to produce soluble derivatives according to the following general reaction:

$$LiX + AlCl_3 \text{ (in } SOCl_2) \rightarrow Li^+, AlCl_3X^-$$

An equivalent amount of each of the following salts was shaken at room temperature in a 4ml Savillex Teflon vessel with 1M purified $AlCl_3$ in thionyl chloride:

CF_3COOLi CF_3SO_3Li
CH_3SO_3Li $CH_3(C_6H_4)COOLi$
$CH_2ClCOOLi$

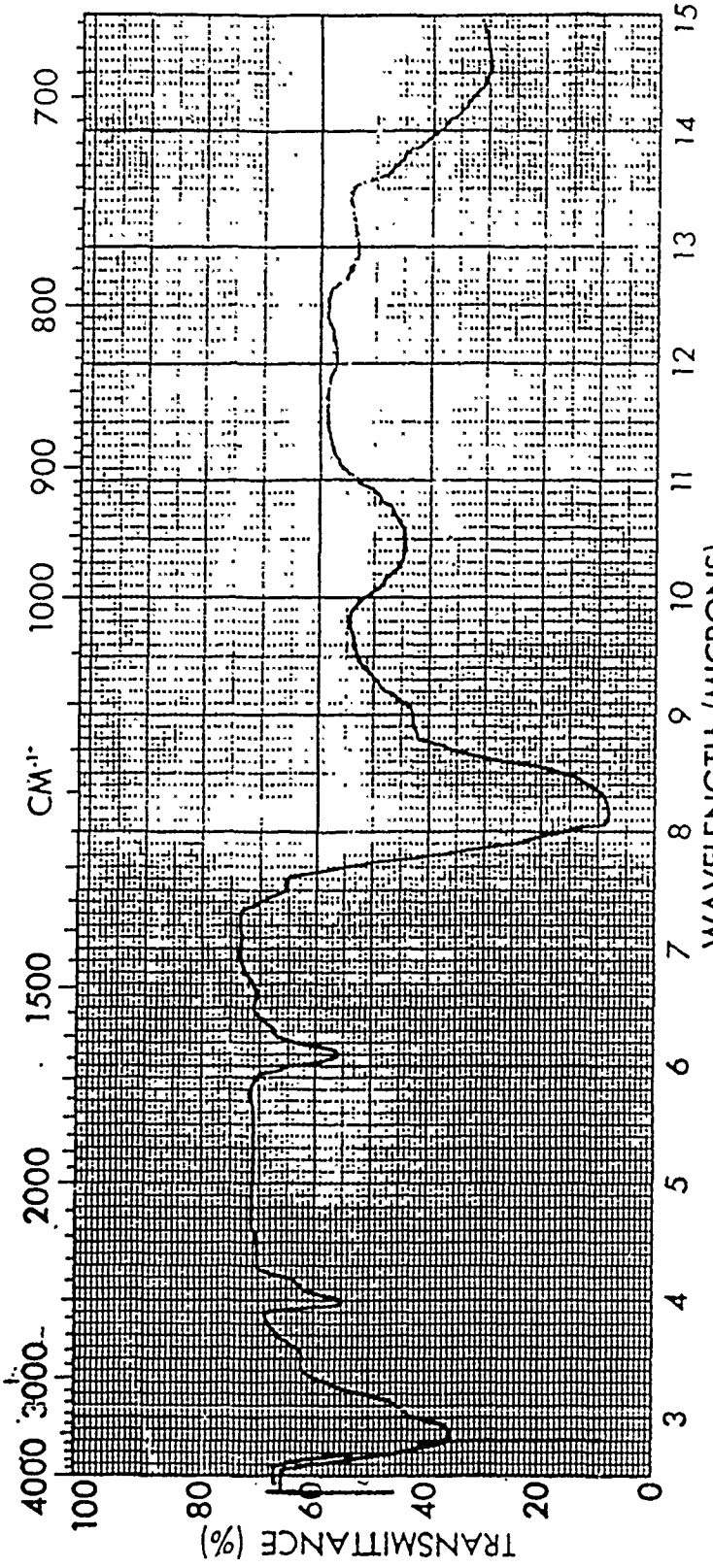

FIGURE 3. INFRARED SPECTRUM, USING THE PERKIN-ELMER 137 SPECTROPHOTOMETER, SODIUM CHLORIDE WINDOWS, AND A SPACER 0.10 MM THICK. ONE MOLAR LIAI·CL4 IN THIONYL CHLORIDE.

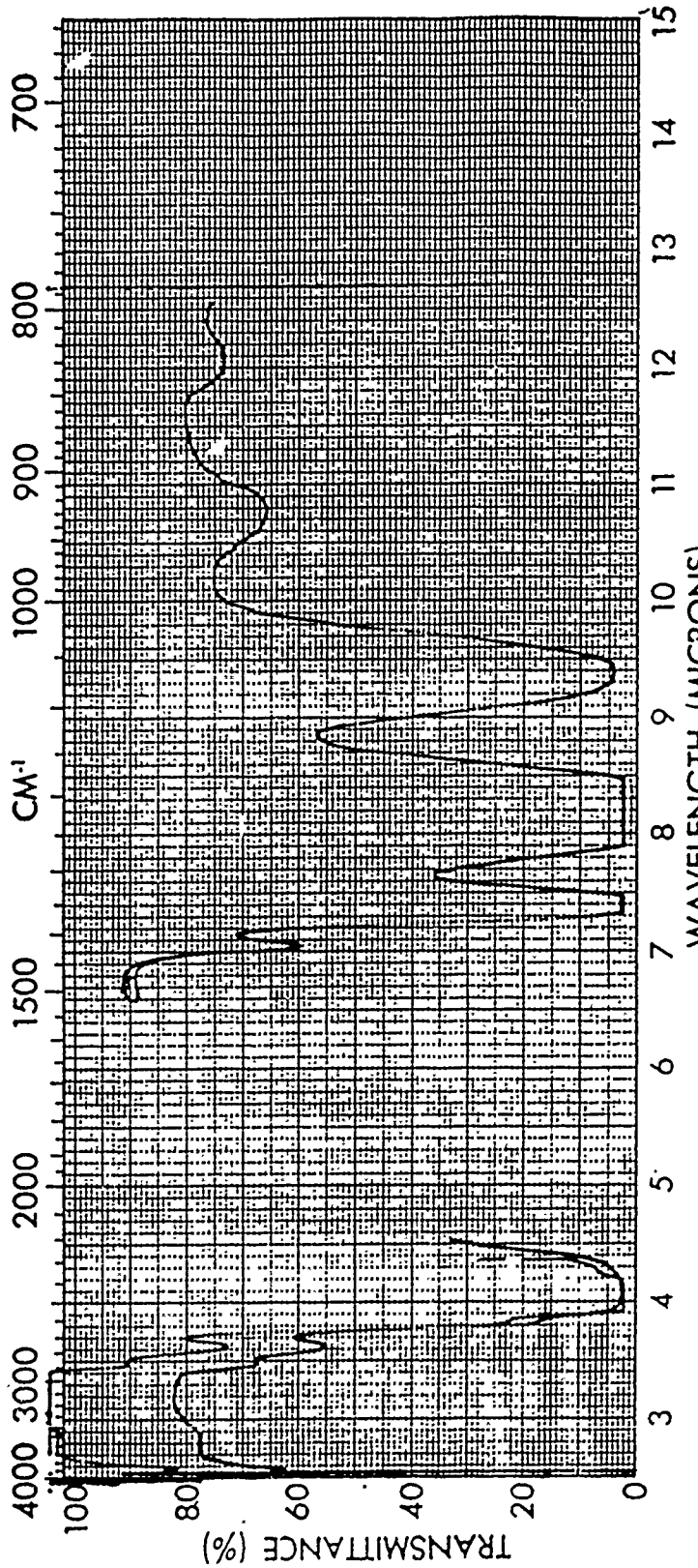

FIGURE 4. INFRARED SPECTRUM, USING THE PERKIN-ELMER 137 SPECTROPHOTOMETER, SODIUM CHLORIDE WINDOWS, AND A SPACER 0.10 MM THICK. PARTIAL SPECTRUM OF A 1 MOLAR SOLUTION OF ALUMINUM CHLORIDE IN THIONYL CHLORIDE TREATED FIRST WITH AN EQUIVALENT AMOUNT OF SULFUR TRIOXIDE, THEN AN EQUIVALENT AMOUNT OF LITHIUM CHLORIDE. THE REGION OF THE SPECTRUM BETWEEN 2.5 AND 4.5 MICRONS WAS TAKEN IN A 10 MM PATHLENGTH QUARTZ CELL VERSUS AN EMPTY QUARTZ CELL, AND SHOWS THAT THE SOLUTION WAS NEARLY FREE OF HYDROLYSIS PRODUCTS.

Of these five, only the lithium toluenesulfonate refused to react at all. The others dissolved, but only partially, the two most soluble being lithium methane sulfonate and lithium chloroacetate. Infrared spectra were taken of the first four solutions, as follows:

Figure 5	CH_3SO_3ClLi	in $SOCl_2$, 1 molar $AlCl_3$
Figure 6	$CH_2ClCOOLi$	in $SOCl_2$, 1 molar $AlCl_3$
Figure 7	CF_3COOLi	in $SOCl_2$, 1 molar $AlCl_3$
Figure 8	CF_3SO_3Li	in $SOCl_2$, 1 molar $AlCl_3$

As the spectra show, the solutions contained soluble species not present in $LiAlCl_4$/ $SOCl_2$.

To confirm that these absorptions did not come from solutions of the lithium salts by themselves in thionyl chloride, lithium trifluoromethanesulfonate was used as an example. A portion of the same Aldrich salt was used to saturate a few milliliters of thionyl chloride. A spectrum of the resulting solution (Figure 9), showed no absorption at 7.4, 9.5, or 12.9 microns. An absorption near 3.3 microns in Figure 8 may indicate that C-H stretch is present from incompletely fluorinated derivatives.

One hundred millimoles of distilled aluminum chloride were ground together in the dryroom with one hundred millimoles of sulfur and heated in a roundbottom flask to 150°C. A dark solid resulted which was freely soluble in thionyl chloride, forming a yellow solution. To the stirred mixture was added 100 mmoles of dried lithium chloride, which dissolved to form a clear solution. The mixture was transferred to a 100 ml volumetric flask and filled to the mark with thionyl chloride. An infrared spectrum (Figure 10) showed a strong, sharp absorption at about 7.55 microns (1324 cm^{-1}) with weaker absorptions at 8.72 and 9.5 microns. Hydrolysis of an aliquot in a large volume of water failed to precipitate sulfur, indicating that the electrolyte solution did not merely represent a solution either of sulfur or sulfur monochloride in thionyl chloride/ lithium tetrachloroaluminate. This mixture was used to fill three replicate test cells, as described below.

Fluka lithium acetate dihydrate, dried *in vacuo* at 160°C. overnight, lost weight corresponding to the water originally present in the hydrate. When we attempted to react a sample of the dried salt with an equivalent amount 1M aluminum chloride in thionyl chloride, the mixture evolved gas and so was discarded.

We attempted to prepare $LiOAlCl_2$ by heating $LiAlCl_4$ with Fluka chromatographic grade aluminum oxide to 400°C. for about half an hour. On treating the cooled salt mixture with clean thionyl chloride, the $LiAlCl_4$ dissolved, apparently leaving the alumina behind. An infrared spectrum (Figure 11) showed no absorption at 12.5 or 14.8 microns, where Al-O stretching or Al-O-Al bridge absorption would be expected [16, 17]. We have prepared gamma alumina, which is said to react with $AlCl_3$ while alpha alumina does not [18], but we have not yet attempted to use the gamma alumina. Lithium tetrachloroaluminate as a reagent for preparing $LiAlOCl_2$ is preferred over aluminum chloride, because the latter would be expected to produce significant pressure when heated in a sealed glass tube.

We also attempted to prepare AlOCl by refluxing approximately two molar solutions of distilled aluminum chloride in thionyl chloride to which we gradually added, with rapid stirring, water equivalent on a molar basis to the aluminum chloride originally present. The reaction of small amounts of water to solutions of aluminum

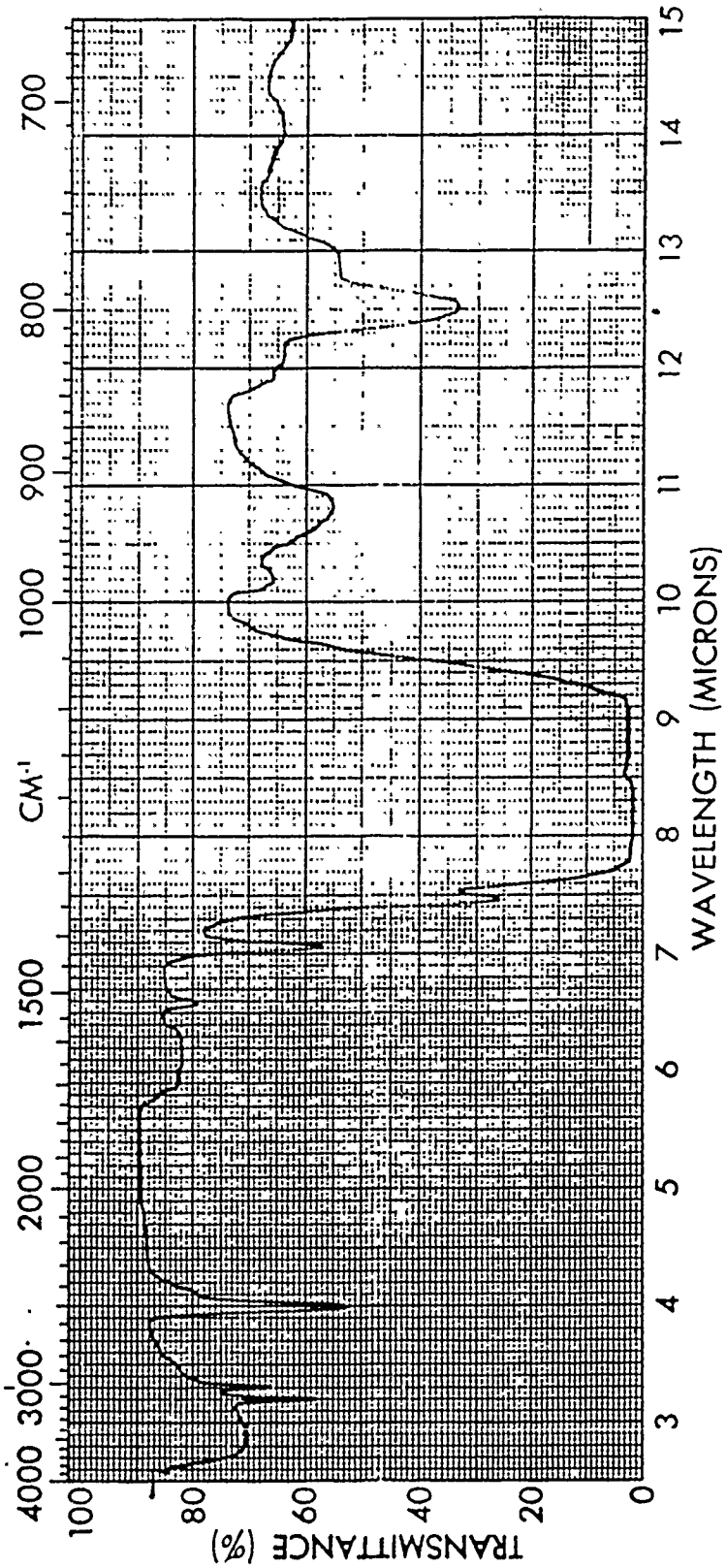

FIGURE 5. INFRARED SPECTRUM, USING THE PERKIN-ELMER 137 SPECTROPHOTOMETER, SODIUM CHLORIDE WINDOWS, AND A SPACER 0.10 MM THICK. A 1 MOLAR SOLUTION OF ALCL3 IN SOCL2 REACTED WITH AN EQUIVALENT AMOUNT OF DRIED LITHIUM METHANESULFONATE.

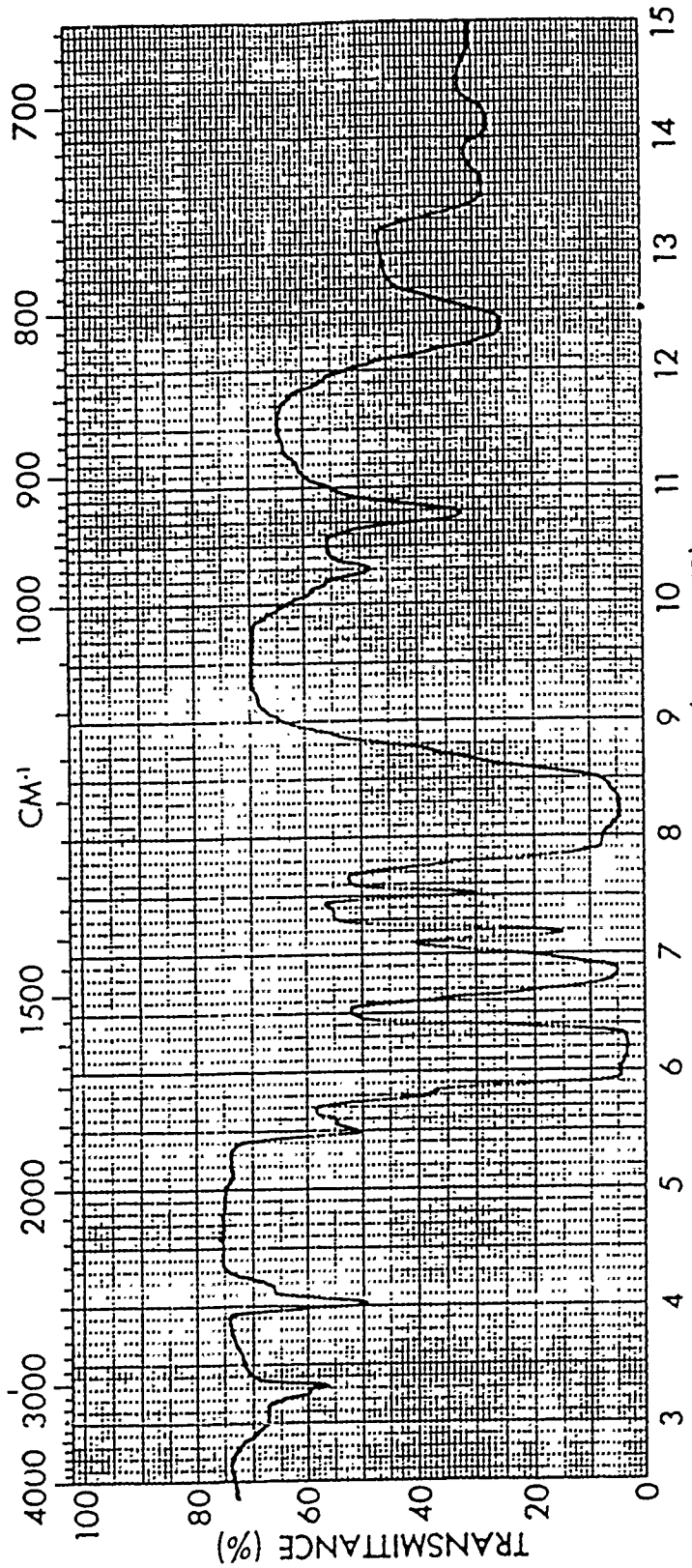

FIGURE 6. INFRARED SPECTRUM, USING THE PERKIN-ELMER 137 SPECTROPHOTOMETER, SODIUM CHLORIDE WINDOWS, AND A SPACER 0.10 MM THICK. A 1 MOLAR SOLUTION OF ALCL3 IN SOCL2 REACTED WITH AN EQUIVALENT AMOUNT OF DRIED LITHIUM CHLOROACETATE.

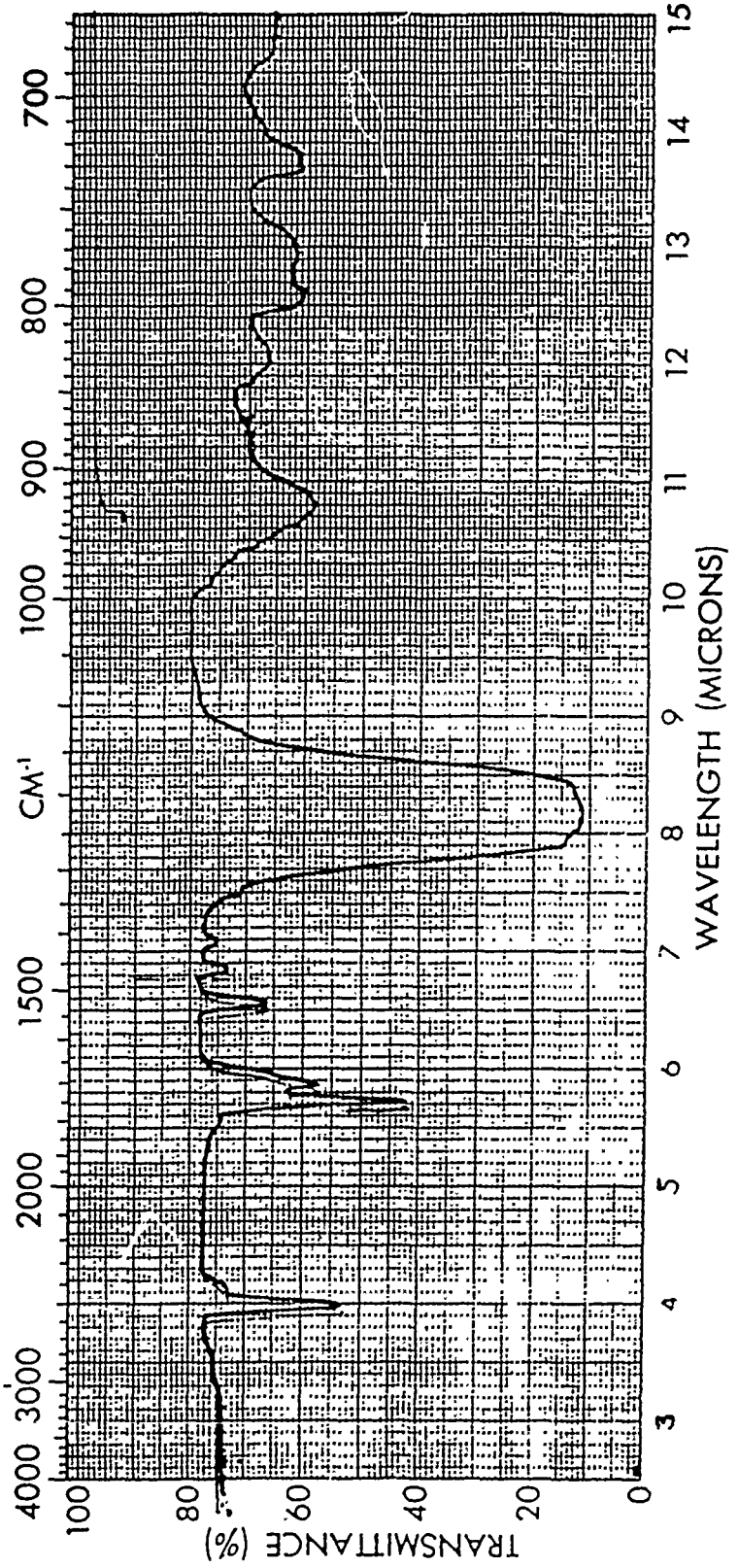

FIGURE 7. INFRARED SPECTRUM, USING THE PERKIN-ELMER 137 SPECTROPHOTOMETER, SODIUM CHLORIDE WINDOWS, AND A SPACER 0.10 MM THICK. A 1 MOLAR SOLUTION OF ALCL3 IN SOCL2 REACTED WITH AN EQUIVALENT AMOUNT OF DRIED LITHIUM TRIFLUOROACETATE.

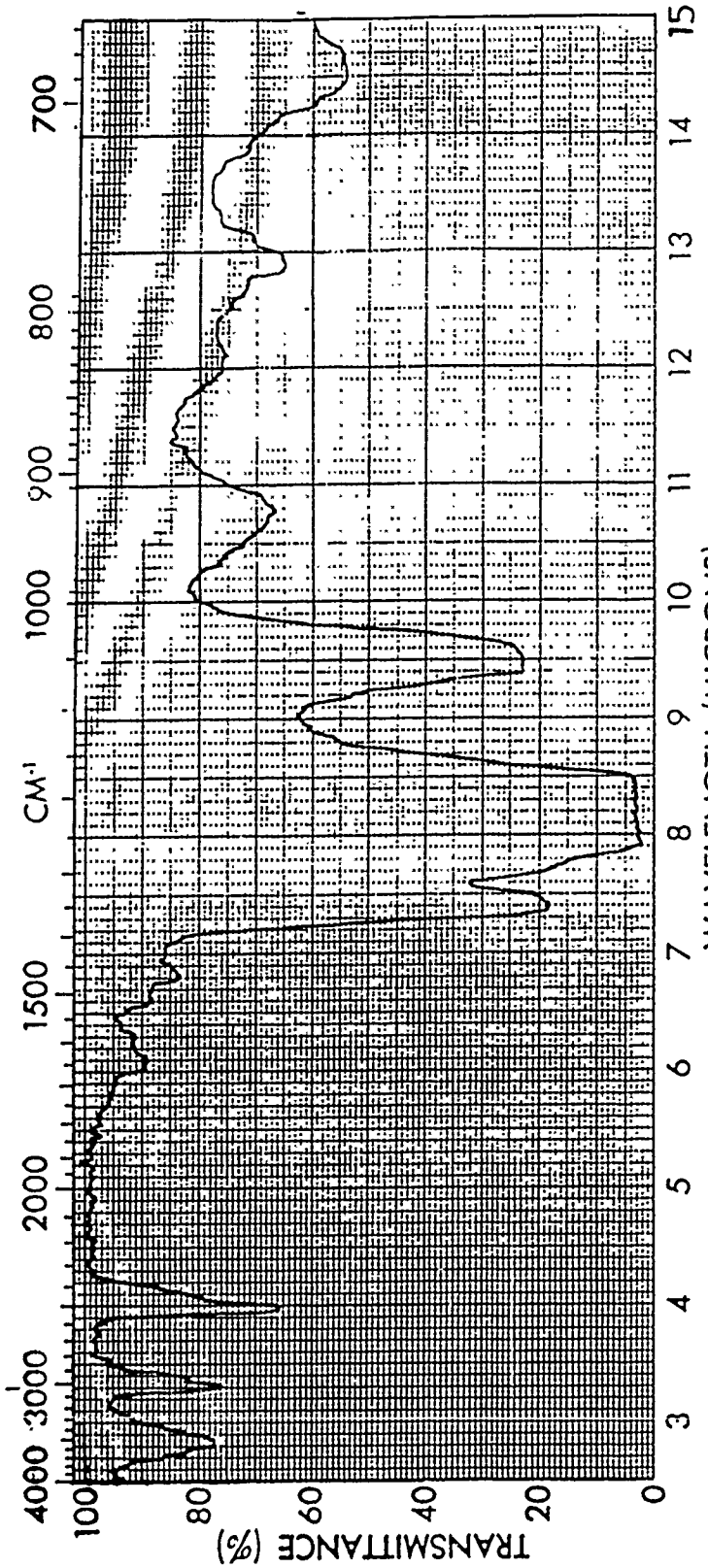

FIGURE 8. INFRARED SPECTRUM, USING THE PERKIN-ELMER 137 SPECTROPHOTOMETER WITH A DEMOUNTABLE CELL, SODIUM CHLORIDE WINDOWS, AND A SPACER 0.10 MM THICK. ONE MOLAR $ALCl_3$ IN THIONYL CHLORIDE TREATED FIRST WITH AN EQUIVALENT AMOUNT OF 97% LITHIUM TRIFLUOROMETHANE SULFONATE AND THEN AN EQUIVALENT AMOUNT OF LITHIUM CHLORIDE.

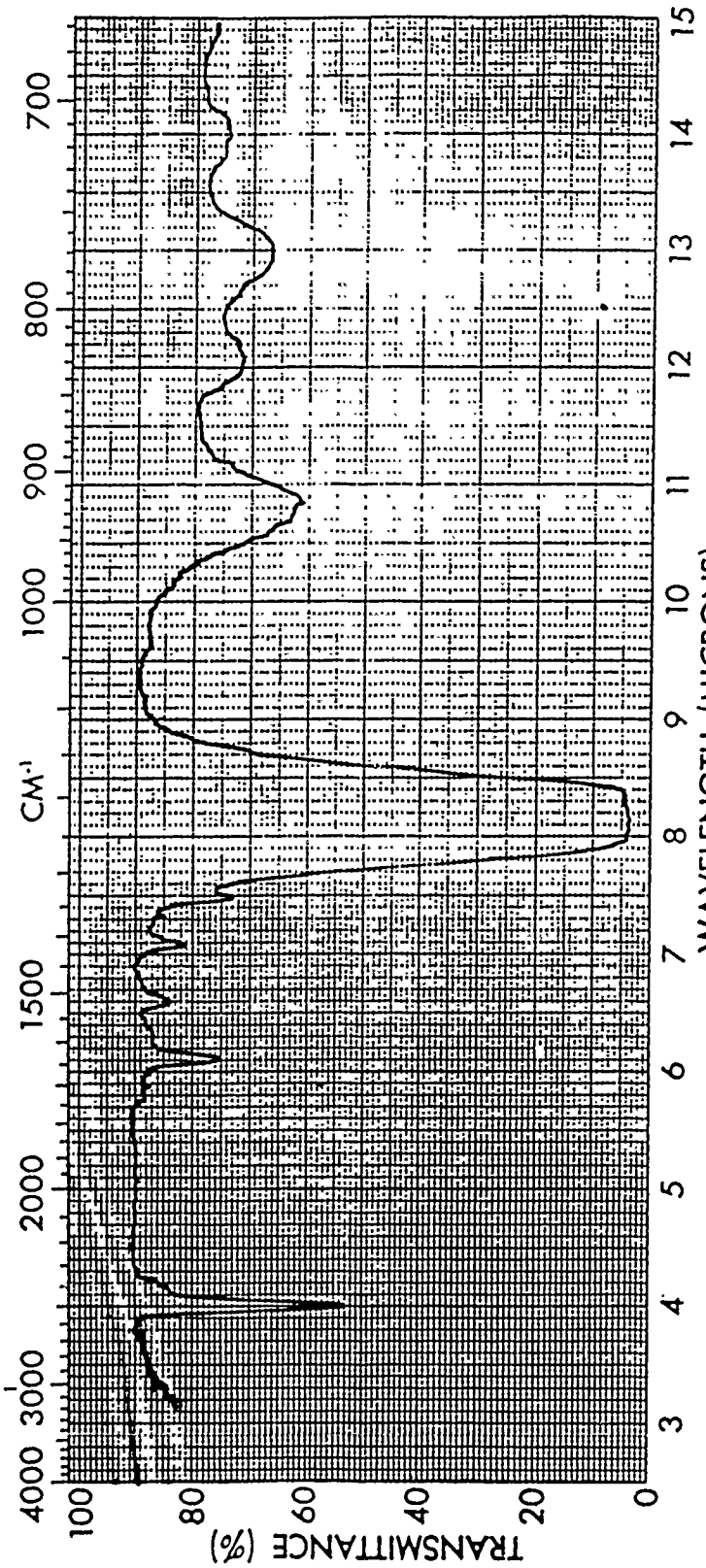

FIGURE 9. INFRARED SPECTRUM, USING THE PERKIN-ELMER 137 SPECTROPHOTOMETER WITH A DEMOUNTABLE CELL, SODIUM CHLORIDE WINDOWS, AND A SPACER 0.10 MM THICK. THIONYL CHLORIDE SATURATED WITH 97% LITHIUM TRIFLUOROMETHANE SULFONATE.

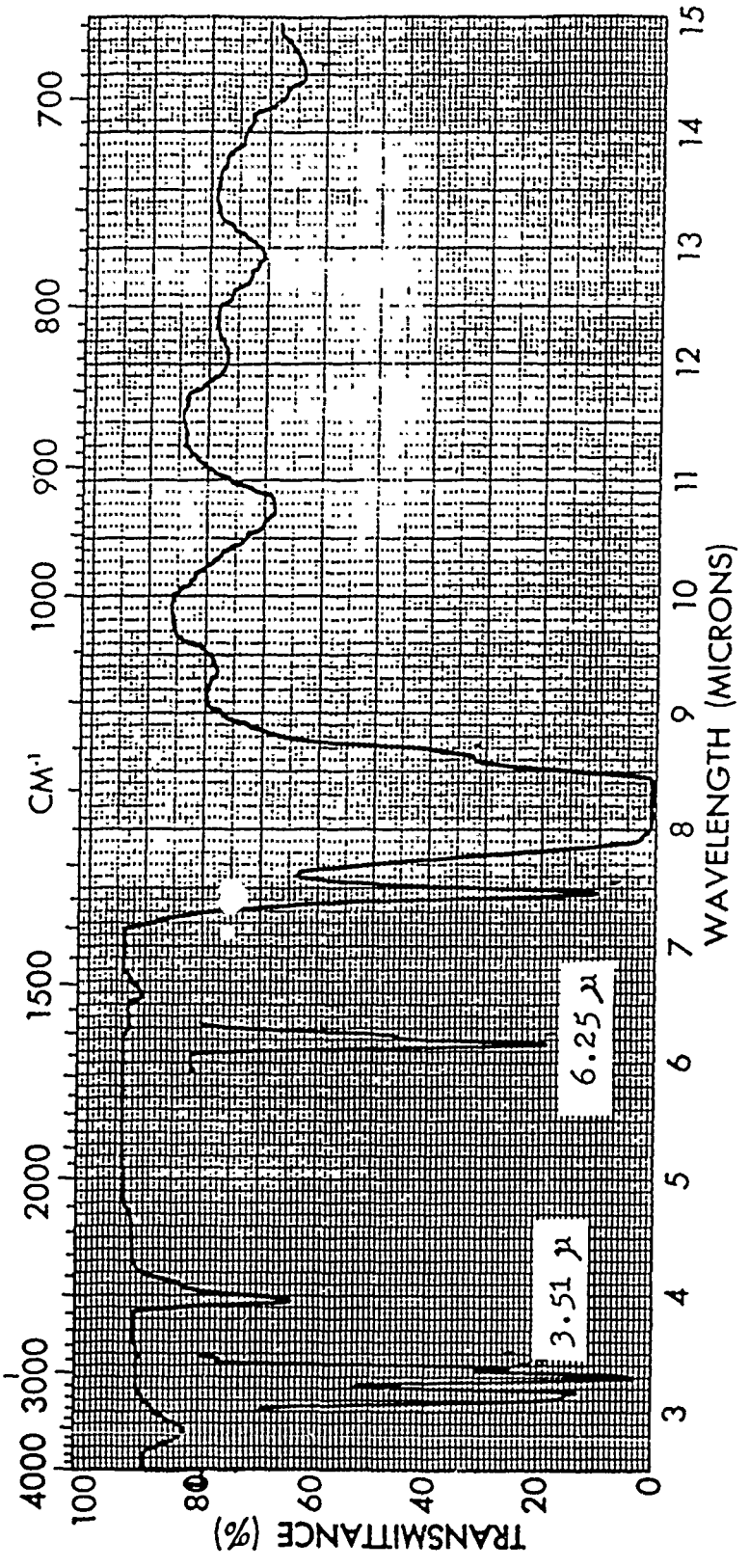

FIGURE 10. INFRARED SPECTRUM, USING THE PERKIN-ELMER 137 SPECTROPHOTOMETER WITH A DEMOUNTABLE CELL, SODIUM CHLORIDE WINDOWS, AND A SPACER 0.10 MM THICK. THIONYL CHLORIDE WITH 1 M ALUMINUM (III). A MOLAR EQUIVALENT AMOUNT OF $AlCl_3$ HAD BEEN MELTED WITH SULFUR, DISSOLVED IN $SOCl_2$, AND THEN TREATED WITH AN EQUIVALENT AMOUNT OF LiCl.

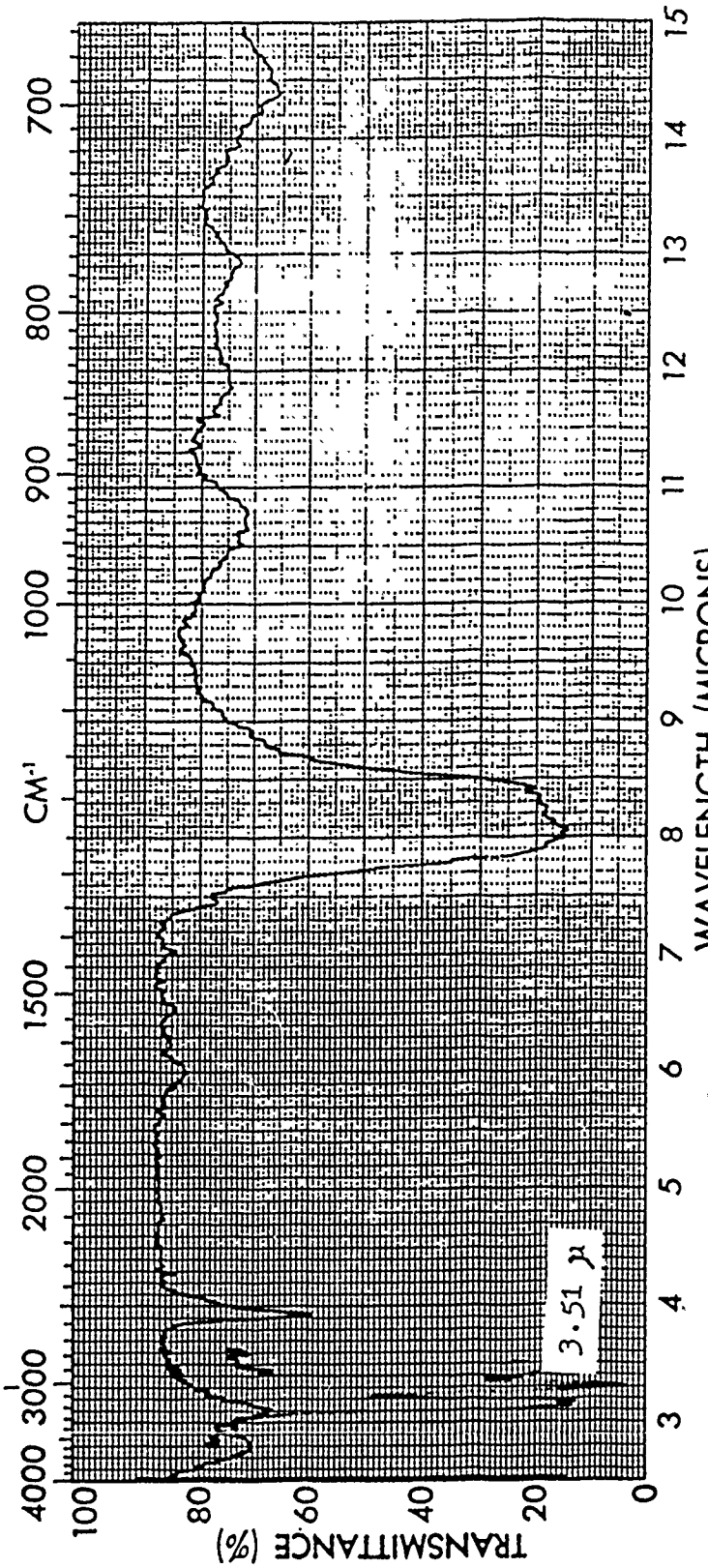

FIGURE 11. INFRARED SPECTRUM OF 1M $LiAlCl_4/SOCl_2$, THE SALT HAVING FIRST BEEN HEATED TO 400°C. AND THE MELT SATURATED WITH CHROMATOGRAPHIC GRADE ALPHA ALUMINA, THE MIXTURE THEN DISSOLVED IN $SOCl_2$. DEMOUNTABLE CELL WITH 0.1MM PATHLENGTH SPACER, SODIUM CHLORIDE WINDOWS. SPECTRUM INCLUDES POLYSTYRENE REFERENCE PEAKS.

chloride in thionyl or sulfuryl chloride was reported to produce soluble materials [19]. All the precipitate which formed as the entire amount of water was added eventually dissolved again during the stirring. We had hoped that on continued refluxing, either AlOCl or a bridged aluminum oxychloride would form, as HCl was expelled from the solution [16].

As infrared spectra in 10 mm pathlength quartz cells showed, the refluxing failed to clear all of the protons, present apparently on the aluminum as Al-OH groups, from the solution. Refluxing for about 16 hours did manage to remove the bulk of the OH groups, since infrared absorption between 2.6 and 3.2 microns diminished. We then tried again, using an amount of water equivalent to just 80 mole percent of the aluminum chloride present. Ironically, removing the OH infrared absorption proved even more difficult. Absorptions at 7.5 microns were prominent in both solutions, and at 9.35 microns in the first solution. Very broad, weak absorptions were present between 11 and 15 microns.

When the second solution (to which had been added water equivalent to 80% of the $AlCl_3$) was diluted to one molar, the absorptions at 7.5 and 9.35 microns disappeared. Then, a 1 molar solution of $LiAlCl_4$ prepared with purified salts but which had not been refluxed showed weak absorptions at 7.5 and 9 microns (these likely caused by sulfur dioxide in this case), plus a distinct absorption at 14.5 microns. Absorption at 7.5 and 9.35 microns might therefore be caused by either SO_2, chlorosulfonato groups, or by $SOCl_2$ complexed with more than one equivalent of $LiAlCl_4$. The only spectrum which contained absorption at either 12.5 or 14.8 microns, attributed to Al-O stretching by Bailey and Blomgren [16], was the one which had not been refluxed at all.

The infrared spectra, taken with both the 10mm pathlength quartz cells and the 0.1 mm sodium chloride demountable cells, are summarized below:

Figure #	Data (infrared spectra of the following solutions):
12	2M $AlCl_3$/ 1 equiv. H_2O/ 16 hr. reflux/ 1 equiv. LiCl
13	2M $AlCl_3$/ 0.8 equiv. H_2O/ 16 hr. reflux/ 1 equiv. LiCl
14	Same as Figure 13, diluted to 1 molar
15	1M $AlCl_3$/ 1 equiv. LiCl/ no refluxing

The solution represented by Figure 14 was used to fill three replicate test cells, even though the infrared spectrum was not able to distinguish it from the control electrolyte.

We attempted to prepare $LiSO_3F$ by reacting LiF with an excess of sulfur trioxide. Although lithium fluoride does absorb SO_3, we were not been able to obtain a satisfactory product.

Samples of the the following sodium sulfur oxyacid salts were equilibrated with Mobay thionyl chloride, used as received, in order to determine qualitatively whether any were substantially soluble. Sodium salts were used because the lithium salts were not immediately available. Those tested included the following:

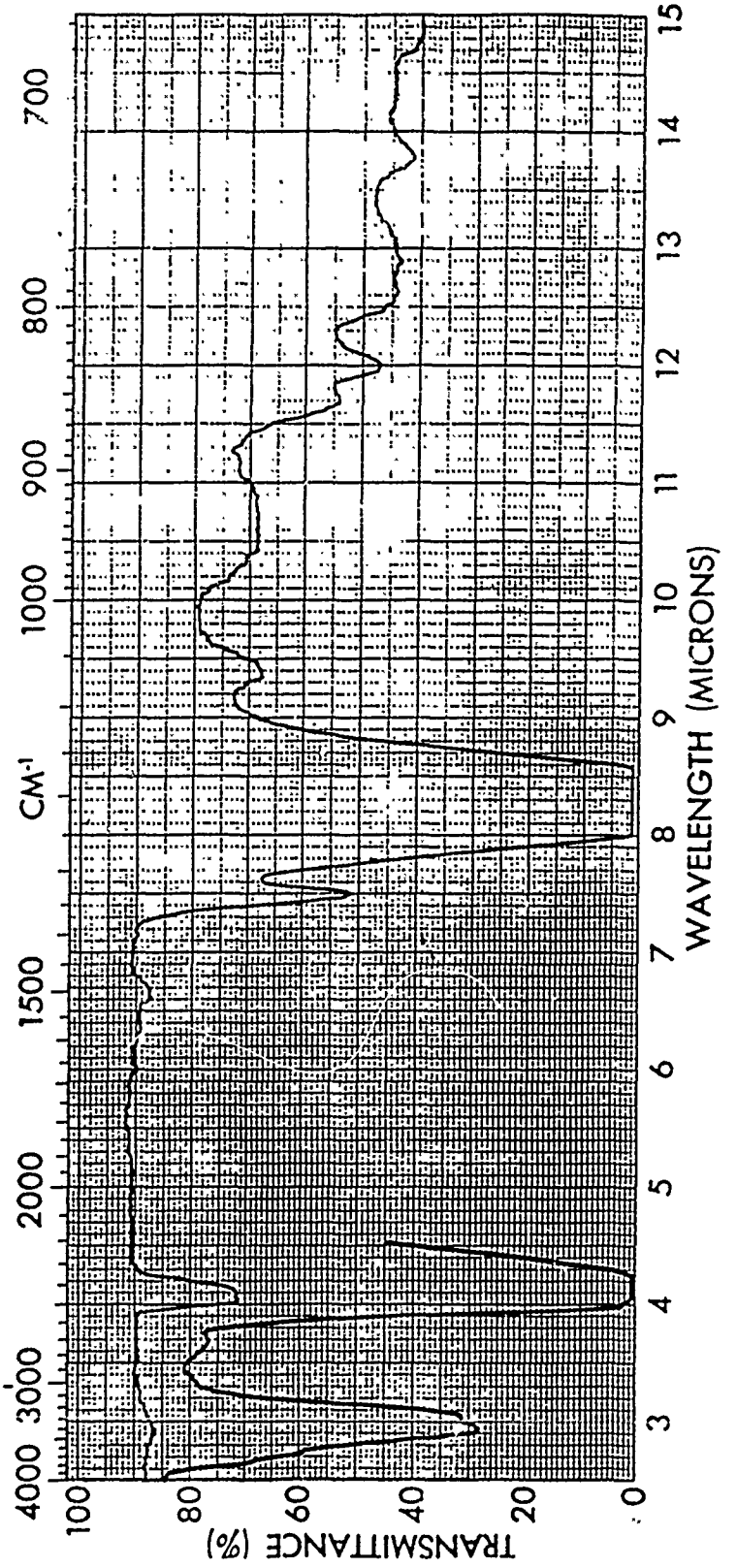

FIGURE 12. INFRARED SPECTRUM, USING THE PERKIN-ELMER 137 SPECTROPHOTOMETER WITH A DEMOUNTABLE CELL, SODIUM CHLORIDE WINDOWS, AND A SPACER 0.10 MM THICK. ALSO WITH A 10 MM PATHLENGTH QUARTZ CELL VERSUS AN EMPTY CELL (2.5 TO 4.5 MICRONS ONLY). THIONYL CHLORIDE WITH ABOUT 2M ALUMINUM (III). $ALCl_3$ DISSOLVED IN THIONYL CHLORIDE HAD BEEN REACTED WITH A MOLAR EQUIVALENT AMOUNT OF WATER, REFLUXED 16 HOURS, AND THEN TREATED WITH AN EQUIVALENT AMOUNT OF LICL.

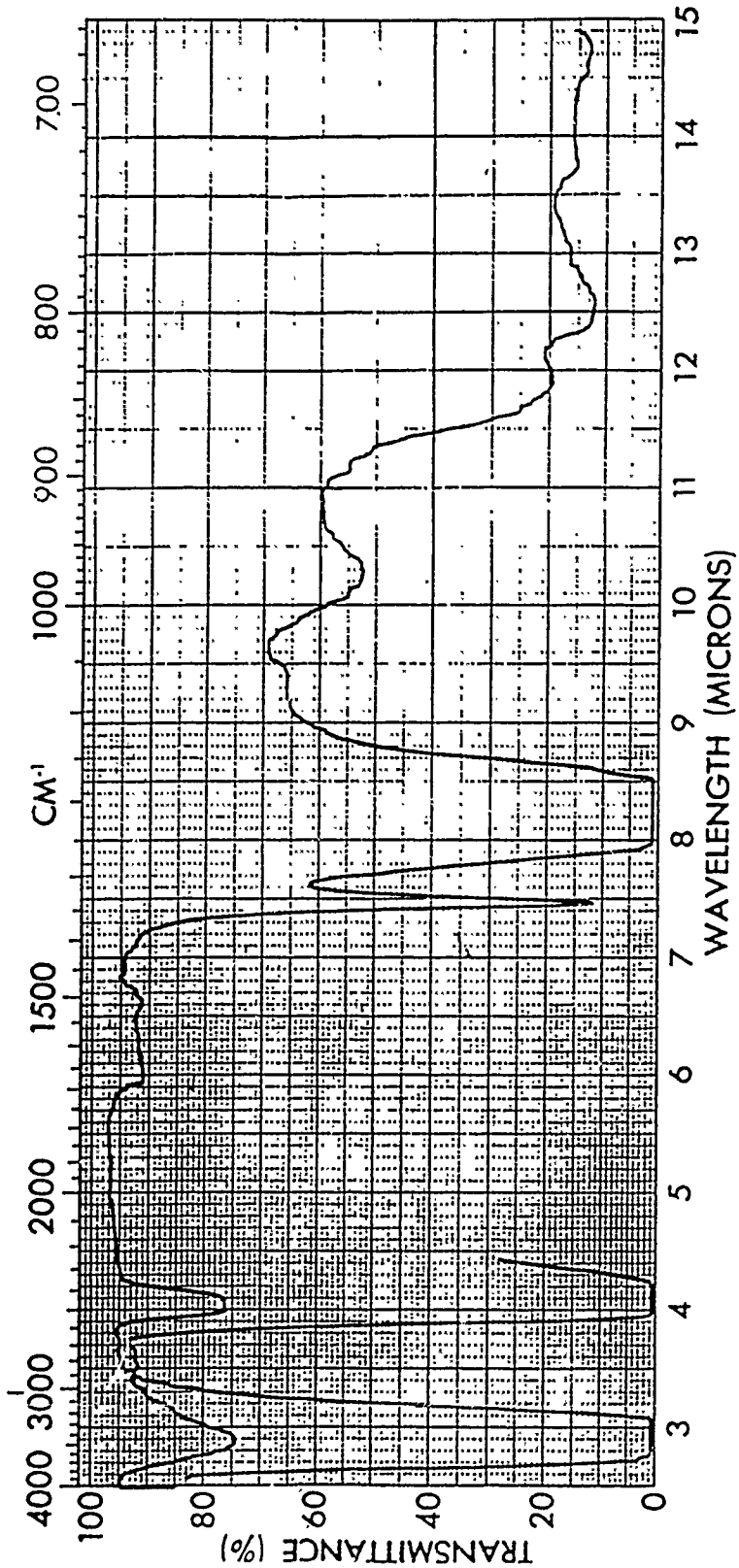

FIGURE 13. INFRARED SPECTRUM, USING THE PERKIN-ELMER 137 SPECTROPHOTOMETER WITH A DEMOUNTABLE CELL, SODIUM CHLORIDE WINDOWS, AND A SPACER 0.10 MM THICK. ALSO WITH A 10 MM PATHLENGTH QUARTZ CELL VERSUS AN EMPTY CELL (2.5 TO 4.5 MICRONS ONLY). THIONYL CHLORIDE WITH ABOUT 2M ALUMINUM (III). $ALCL_3$ DISSOLVED IN THIONYL CHLORIDE HAD BEEN REACTED WITH AN 80% MOLAR EQUIVALENT AMOUNT OF WATER, REFLUXED 16 HOURS, AND THEN TREATED WITH AN EQUIVALENT AMOUNT OF LICL.

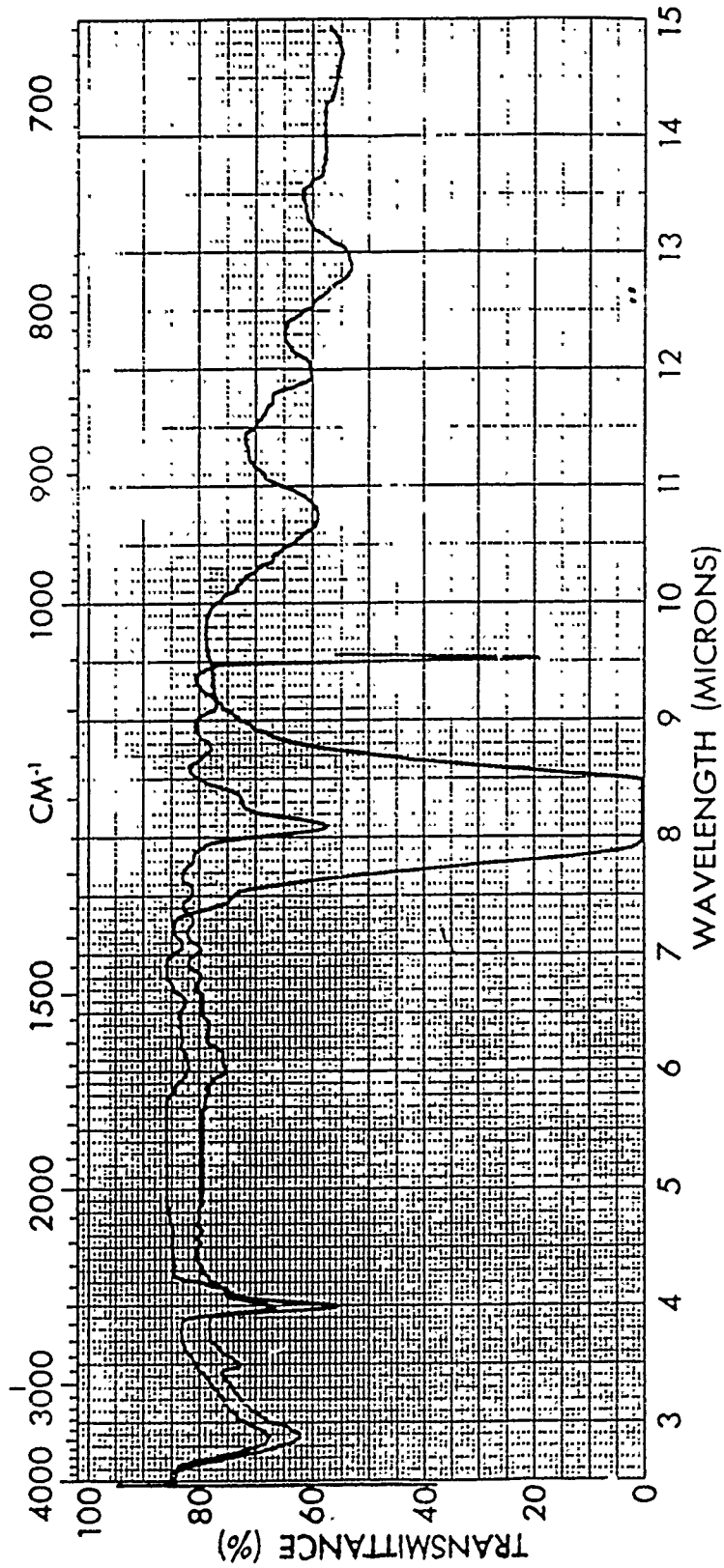

FIGURE 14. INFRARED SPECTRUM, USING THE PERKIN-ELMER 137 SPECTROPHOTOMETER WITH A DEMOUNTABLE CELL, SODIUM CHLORIDE WINDOWS, AND A SPACER 0.10 MM THICK. $ALCl_3$ DISSOLVED IN THIONYL CHLORIDE HAD BEEN REACTED WITH AN 80% MOLAR EQUIVALENT AMOUNT OF WATER, REFLUXED 16 HOURS, AND THEN TREATED WITH AN EQUIVALENT AMOUNT OF LICL. THIS SOLUTION WAS THE SAME AS IN FIGURE 13, BUT DILUTED TO 1 MOLAR.

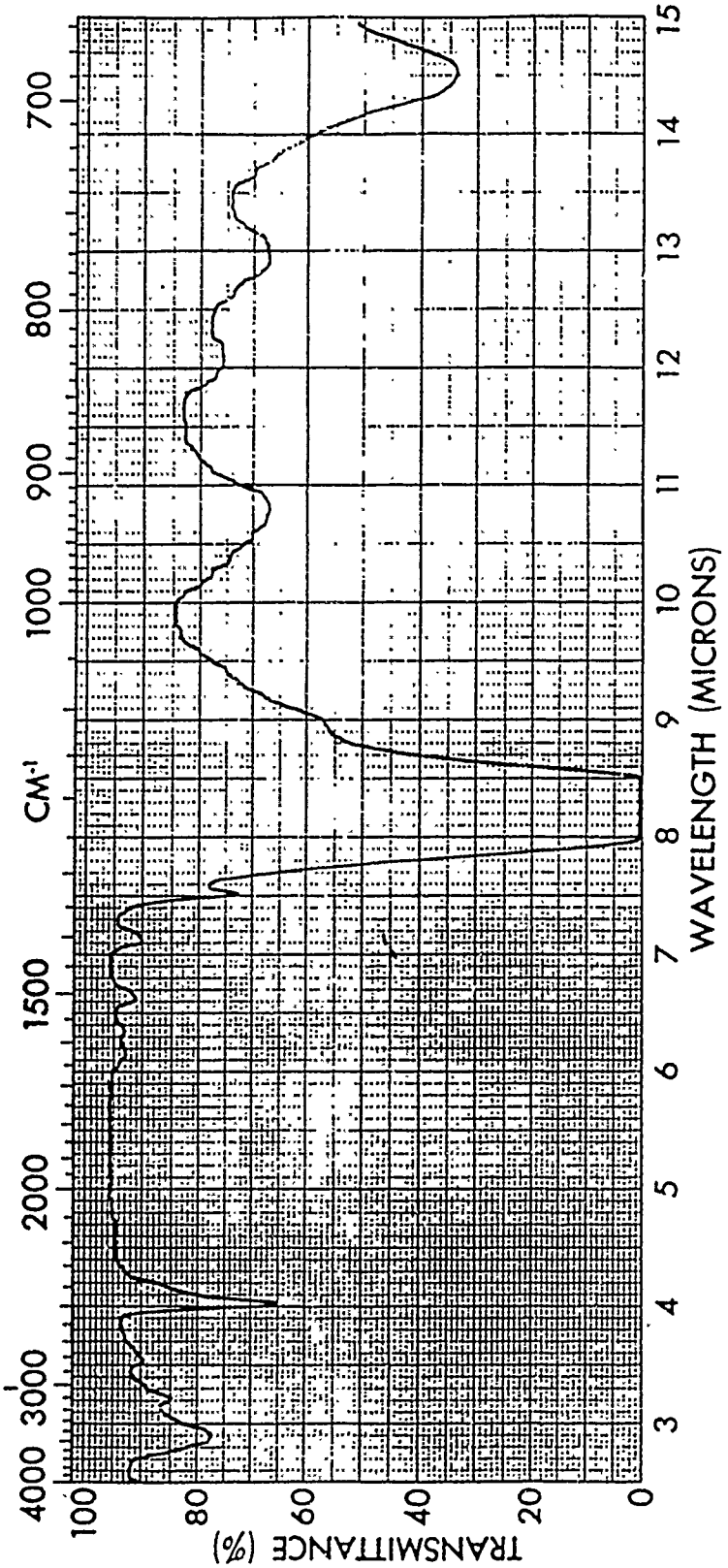

FIGURE 15. INFRARED SPECTRUM, USING THE PERKIN-ELMER 137 SPECTROPHOTOMETER WITH A DEMOUNTABLE CELL, SODIUM CHLORIDE WINDOWS, AND A SPACER 0.10 MM THICK. THIONYL CHLORIDE WITH 1 M ALUMINUM (III). A MOLAR EQUIVALENT AMOUNT OF DISTILLED $ALCL_3$ HAD BEEN TREATED WITH AN EQUIVALENT AMOUNT OF DRIED LICL WITHOUT REFLUXING.

Salt	Source
$Na_2S_4O_6$ (tetrathionate)	Pfaltz and Bauer
$Na_2S_2O_6$ (dithionate)	Pfaltz and Bauer
$Na_2S_2O_5$ (metabisulfite)	EM Science
$Na_2S_2O_3$ (thiosulfate)	EM Science
$Na_2Cr_2O_7$ (dichromate)	EM Science

Sodium dichromate was tested because lithium dichromate is known to be highly soluble in thionyl chloride. It was hoped that sodium dichromate could be used as a rough analogy to determine the validity of substituting other sodium salts where the lithium salts were not available. Sodium dichromate gave a distinctly orange color to the solvent, but did not appear to be substantially soluble. None of the other salts listed appeared to be substantially soluble either, but no infrared spectra have yet been taken to establish whether any of the colorless sodium salts were partially soluble. Tests with the above listed sodium salts may not indicate definitively whether any of the corresponding lithium salts would be sufficiently soluble to be useful as electrolytes for lithium/ thionyl chloride cells. Small quantities of the corresponding lithium salts could likely be obtained by ion exchange, using a column loaded with resin substituted with lithium ion.

CELL TESTS

The following electrolytes were prepared:

- 100 ml 1M $AlCl_3$ in $SOCl_2$, treated with an equivalent amount of lithium chloride (control electrolyte).
- 100 ml 1M $AlCl_3$ in $SOCl_2$, saturated with lithium chloroacetate, then treated with an equivalent amount of lithium chloride.
- 100 ml 1M $AlCl_3$ in $SOCl_2$, saturatred with lithium methane sulfonate, then treated with an equivalent amount of lithium chloride.
- 100 ml 1M $AlCl_3$ in $SOCl_2$, saturated with lithium trifluoromethanesulfonate, then treated with an equivalent amount of lithium chloride.
- 100 ml 1M $AlCl_3$ in $SOCl_2$, treated with 50 mm of sulfur trioxide, left to stir 4.5 hours, then treated with an excess of lithium chloride and allowed to equilibrate overnight.
- 100 ml 1M $AlCl_3$ in $SOCl_2$, in which 100 mm of $AlCl_3$ had been melted with 100 mm of sulfur, dissolved, treated with 100 mm of LiCl, and diluted.
- 100 mmoles of $AlCl_3$ in $SOCl_2$, to which 80 mmoles of water had been added while the $AlCl_3$ concentration was about 2 molar, the solution refluxed for 16 hours, 200 mmoles of lithium chloride then added, and the solution diluted to 1 molar.

The startup characteristics for each of three groups of cells are shown in Figures 16 to 18, as follows:

Saturated with LiCl (control)	Figure 16
Saturated with $Li(CH_2ClCOO)$	Figure 17
Saturated with $Li(CH_3SO_3)$	Figure 18

Discharge began after the cells had spent only a few hours at ambient temperature on open circuit. While the amount of delay was negligible, differences between the electrolytes still appeared. Cells saturated with lithium methane sulfonate showed the least delay.

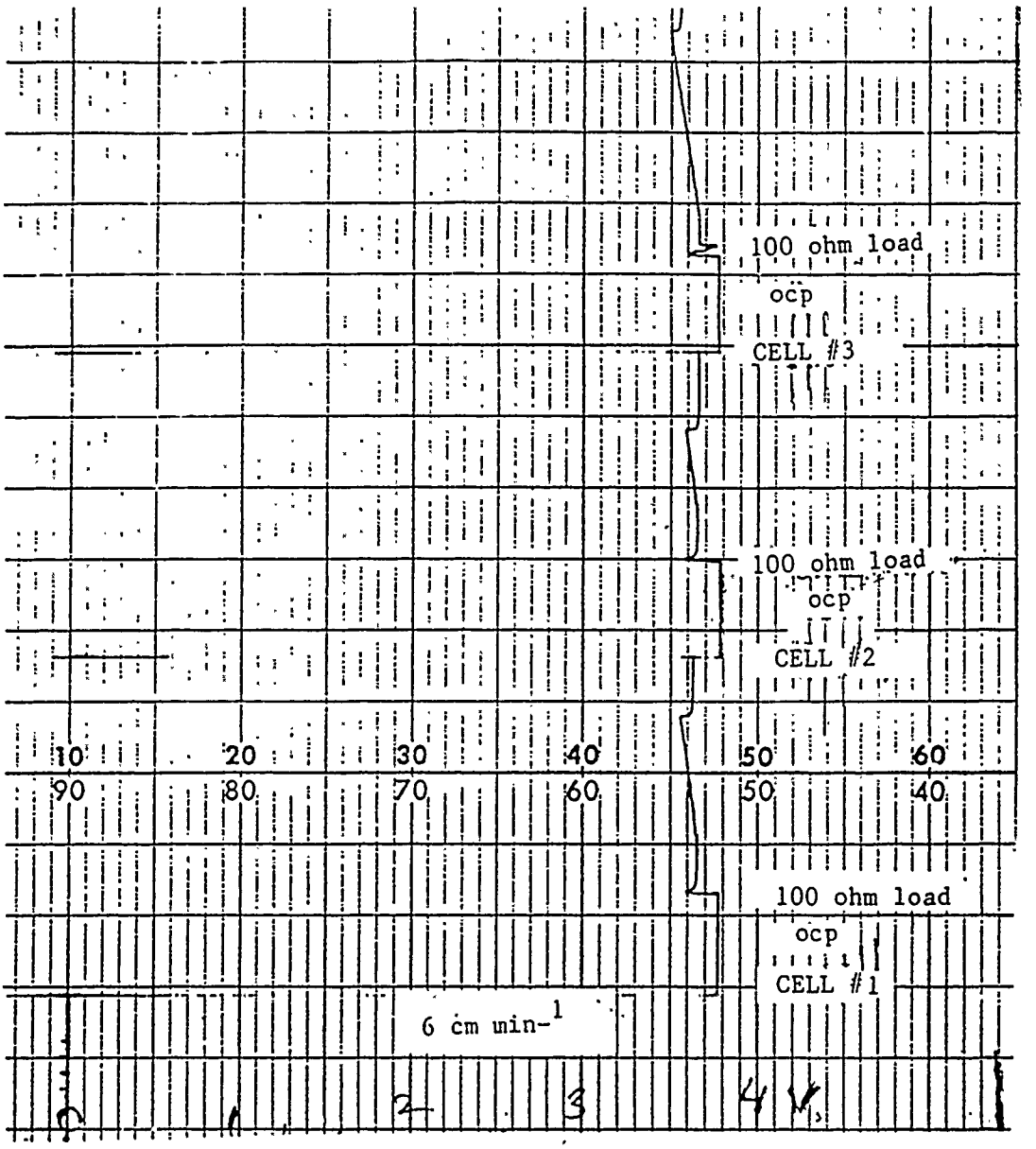

FIGURE 16. RECORDER PLOTTED STARTUP PROFILES FOR CONTROL CELLS. LOAD, 100 OHMS (ABOUT 36 MILLIAMPS OR 4.2 MA/CM^2). 6 CM/MIN; 10 = ZERO VOLTS, 50 = 4 VOLTS

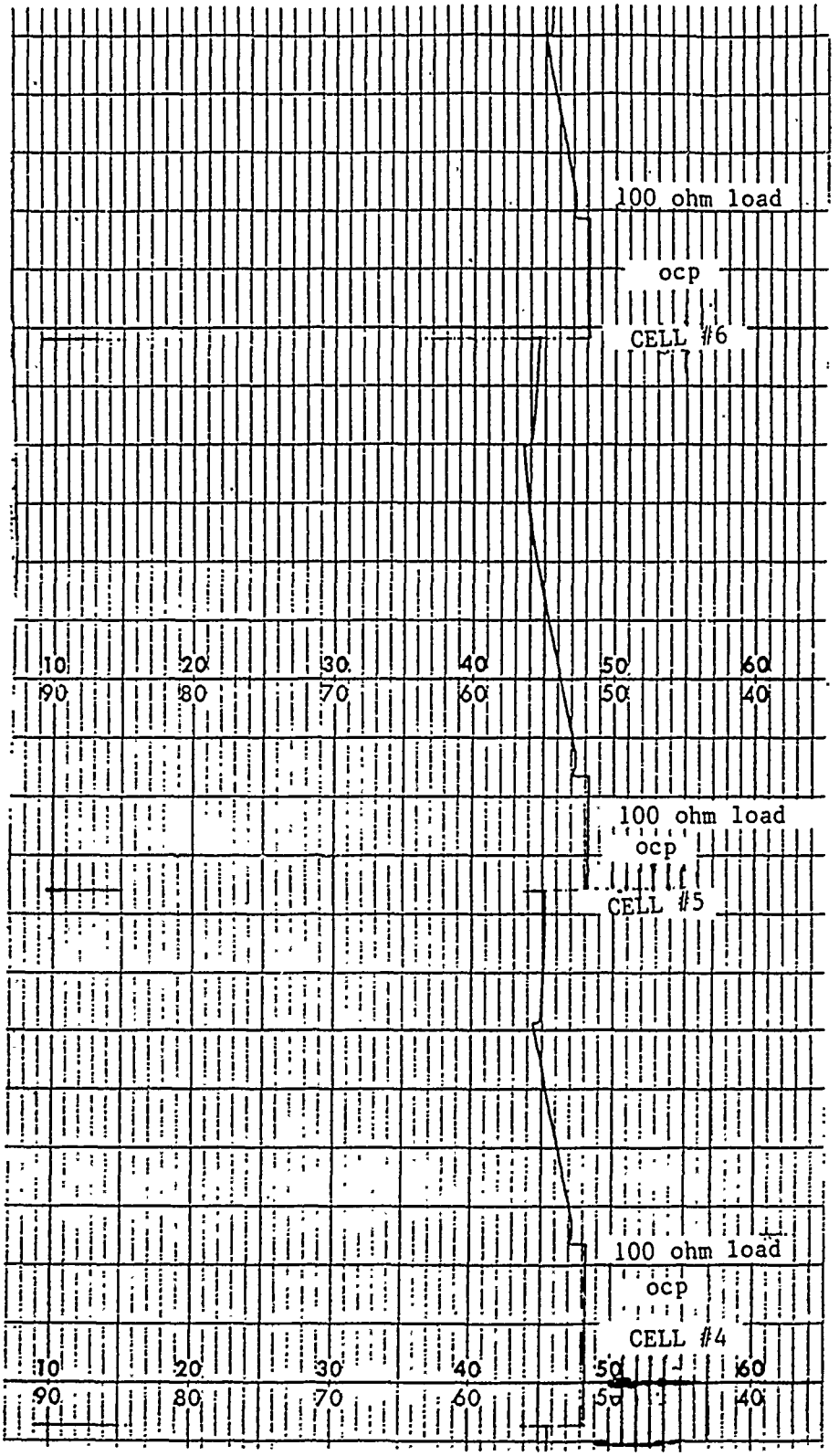

FIGURE 17. RECORDER PLOTTED STARTUP PROFILES FOR CELLS CONTAINING ELECTROLYTE SATURATED WITH LITHIUM CHLOROACETATE. LOAD, 100 OHMS (ABOUT 36 MILLIAMPS OR 4.2 MA/CM²). 6 CM/MIN; 10 = ZERO VOLTS, 50 = 4 VOLTS.

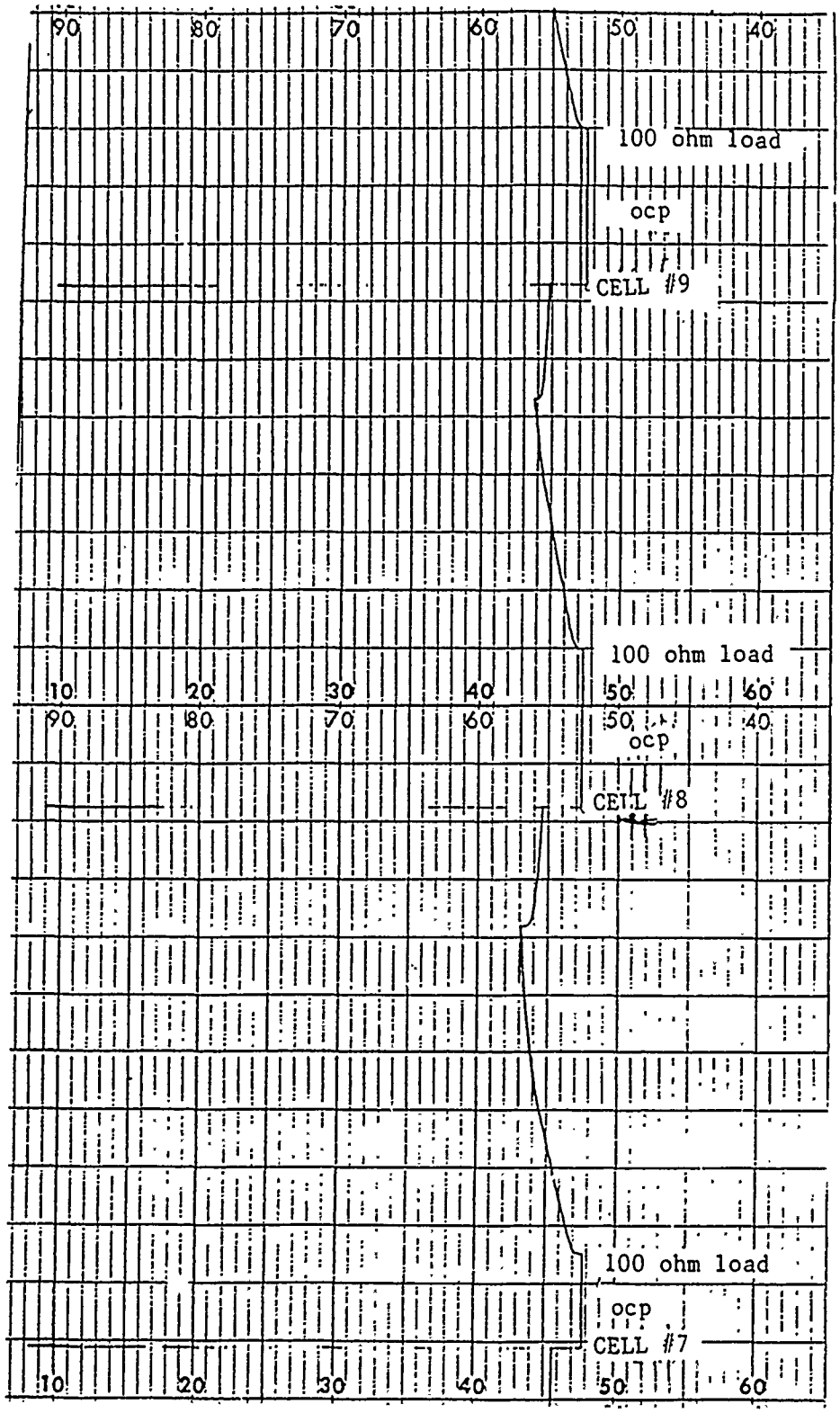

FIGURE 18. RECORDER PLOTTED STARTUP PROFILES FOR CELLS CONTAINING ELECTROLYTE SATURATED WITH LITHIUM METHANE SULFONATE. LOAD, 100 OHMS (ABOUT 36 MILLIAMPS OR 4.2 MA/CM²). 6 CM/MIN; 10 = ZERO VOLTS, 50 = 4 VOLTS

Figure 19 shows the discharge profile for cell 33-37-1, omitting the first 16 hours and 16 minutes. The plotter program as it is now written does not allow plots which contain more than two data files. Figure 20 shows the entire discharge profile for cell 33-37-5, and Figure 21, the profile for cell 33-37-7. Except for variations caused by changes in temperature, the discharge profiles were flat and approached the end of discharge abruptly. Figure 22 is a plot of the last two data files for the discharge profile of cell 26-84-2, containing lithium trifluoromethanesulfonate, and Figure 23 shows the last two files for cell 26-84- 5, containing partially chlorosulfonated aluminate. Likewise, Figure 24 shows cell 37-12-1, and Figure 25, cell 37-12-6. Each was typical for the cells of its respective group, and all showed steady discharge potentials rapidly decaying at the end of discharge with no intermittent behavior.

The capacities in milliamp hours for each cell are given in Table 1. The cathode current density was evidently high enough to stress the cathodes and cause differences in capacity with differences in the electrolyte composition. The amount of lithium present was equivalent to 2.24 amp hours, and the carbon at 700 mg equivalent to 1.4 to 2.1 amp hours. Cells containing the partially chlorosulfonated aluminate unexpectedly showed lower capacities than the control cells, and cells with the trifluoromethane sulfonate electrolyte unexpectedly gave capacities near those observed for the control cells. Cells containing electrolyte prepared from hydrolyzed $AlCl_3$, followed by refluxing for 16 hours, followed by reaction with an equivalent amount of LiCl, on average gave the highest capacity, exceeding that of the control group by about 9%.

Table 1. Capacities of Case Positive Annular Bobbin AA Cells Discharged at 25.6 mA (3 mA/cm^2 of anode surface area)

Cell #	Li salt	Capacity (mAh) to 3V	2V
33-37-1	LiCl (control)	1,414	1,449
33-37-2	LiCl (control)	1,406	1,437
33-37-3	LiCl (control)	1,164	1,191
33-37-4	$Li(CH_2ClCOO)$	1,071	1,097
33-37-5	$Li(CH_2ClCOO)$	990	1,014
33-37-6	$Li(CH_2ClCOO)$	1,076	1,098
33-37-7	$Li(CH_3SO_3)$	454	475
33-37-8	$Li(CH_3SO_3)$	787	805
33-37-9	$Li(CH_3SO_3)$	613	631
26-84-1	$AlCl_3/Li(CF_3SO_3)$	1,453	1,471
26-84-2	$AlCl_3/Li(CF_3SO_3)$	1,396	1,417
26-84-3	$AlCl_3/Li(CF_3SO_3)$	1,317	1,333
26-84-4	$AlCl_3/SO_3/LiCl$	832	857
26-84-5	$AlCl_3/SO_3/LiCl$	975	998
26-84-6	$AlCl_3/SO_3/LiCl$	992	1,015
37-12-1	$AlCl_3/S/LiCl$	992	1,011
37-12-2	$AlCl_3/S/LiCl$	1,418	1,437
37-12-3	$AlCl_3/S/LiCl$	1,470	1,512
37-12-4	$AlCl_3/H_2O/LiCl$	1,313	1,344
37-12-5	$AlCl_3/H_2O/LiCl$	1,507	1,539
37-12-6	$AlCl_3/H_2O/LiCl$	1,531	1,571

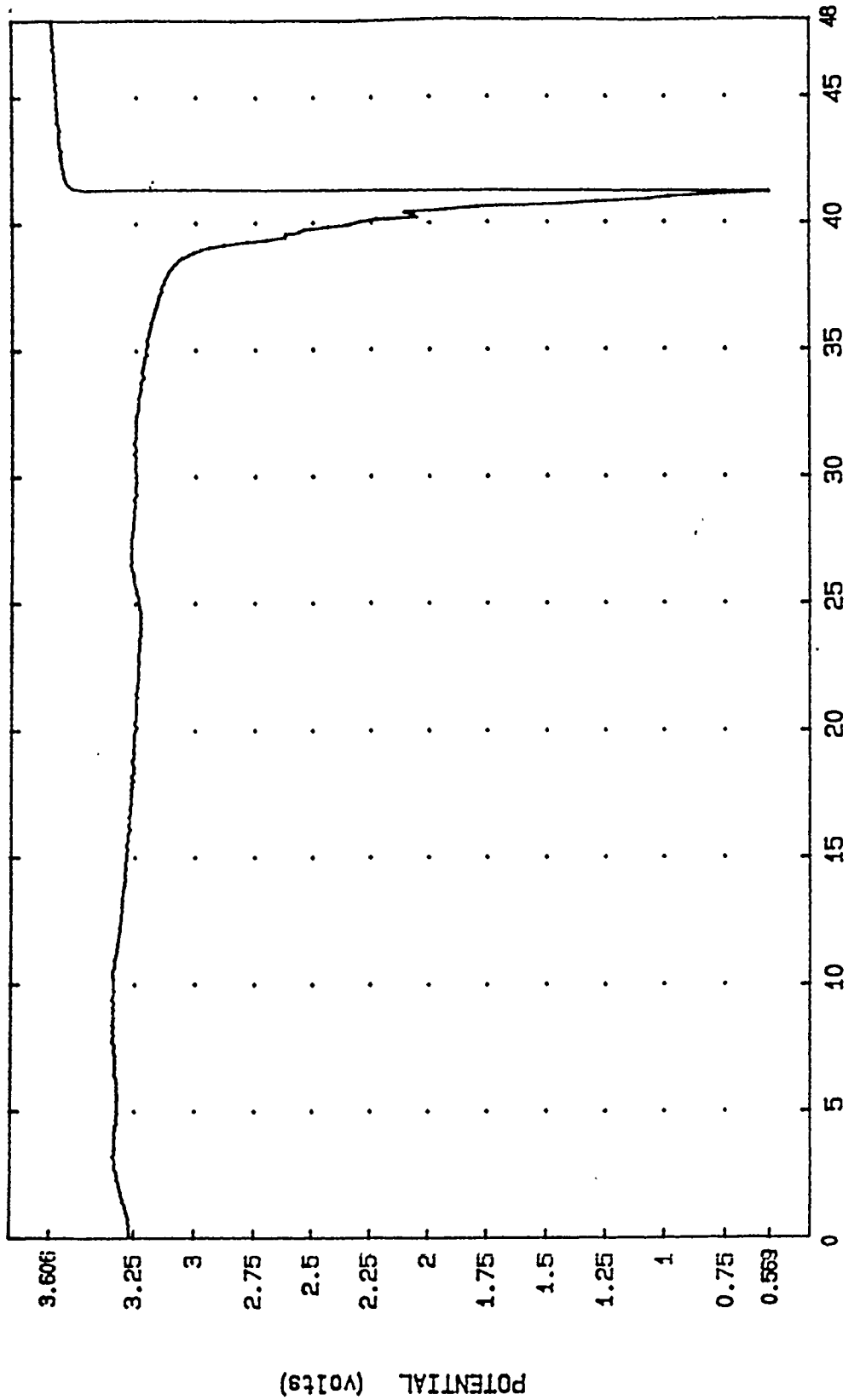

FIGURE 19. DISCHARGE PROFILE FOR CELL 33-37-1, OMITTING THE FIRST 16 HOURS, 16 MINUTES.

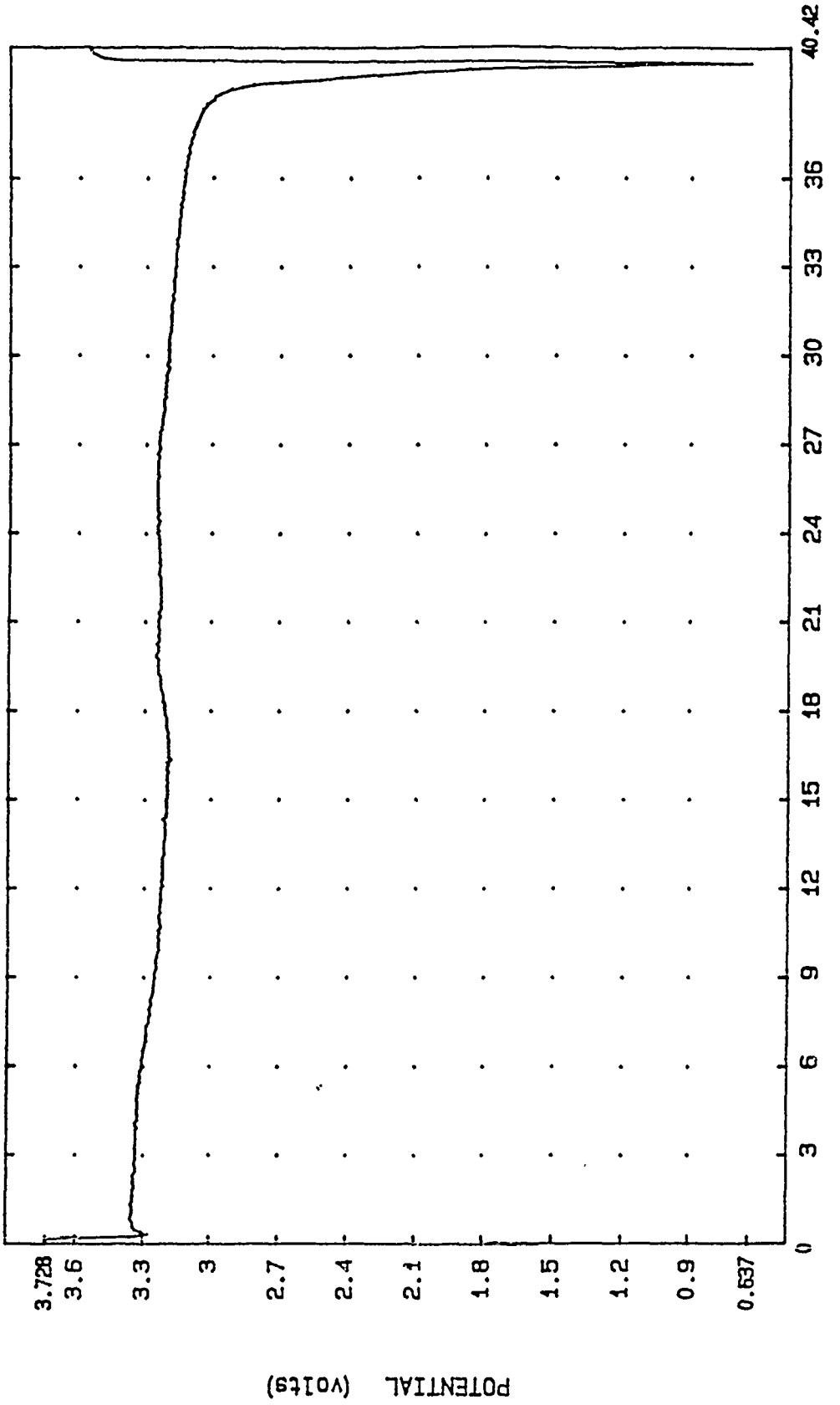

FIGURE 20. DISCHARGE PROFILE FOR CELL 33-37-5.

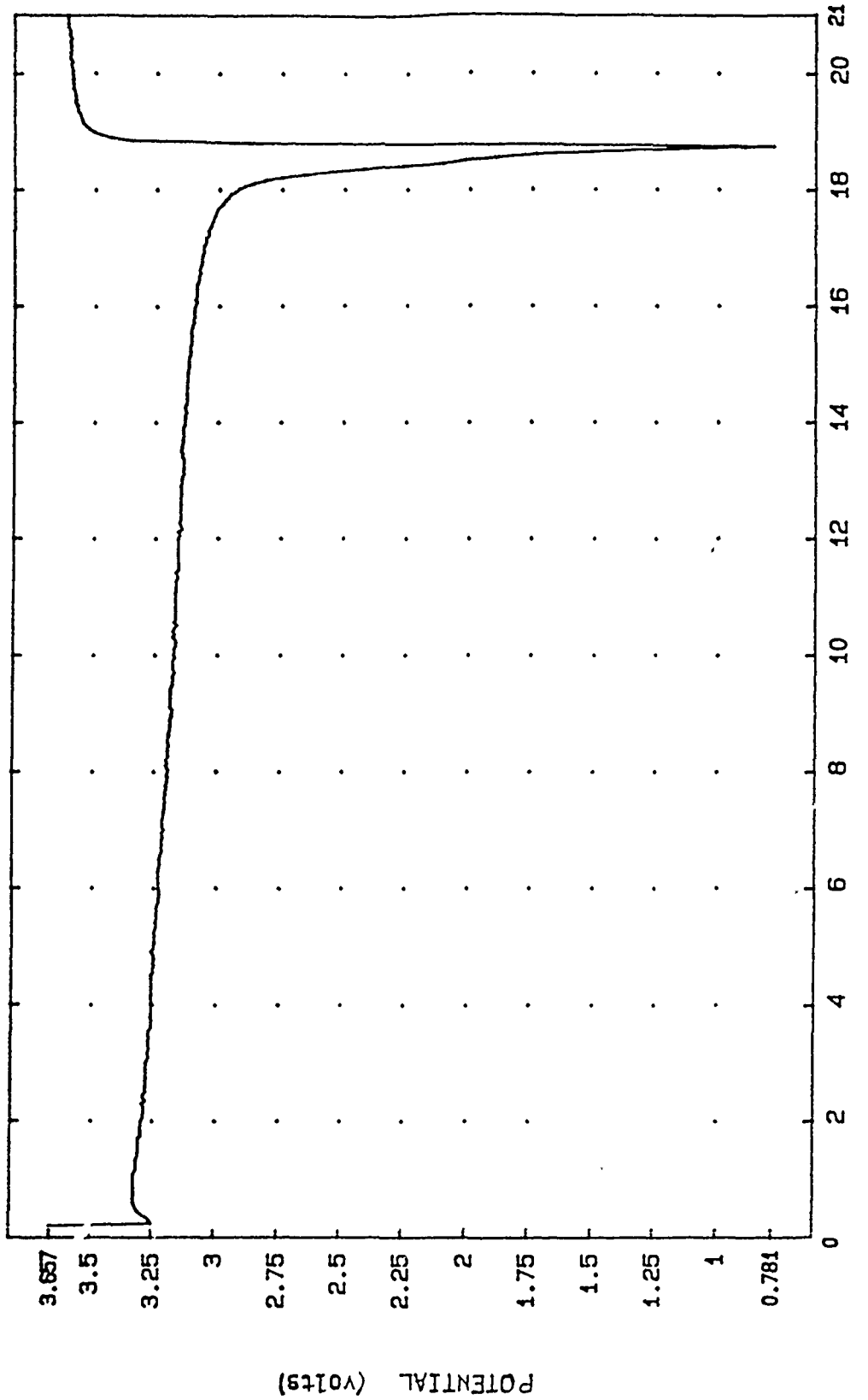

FIGURE 21. DISCHARGE PROFILE FOR CELL 33-37-7.

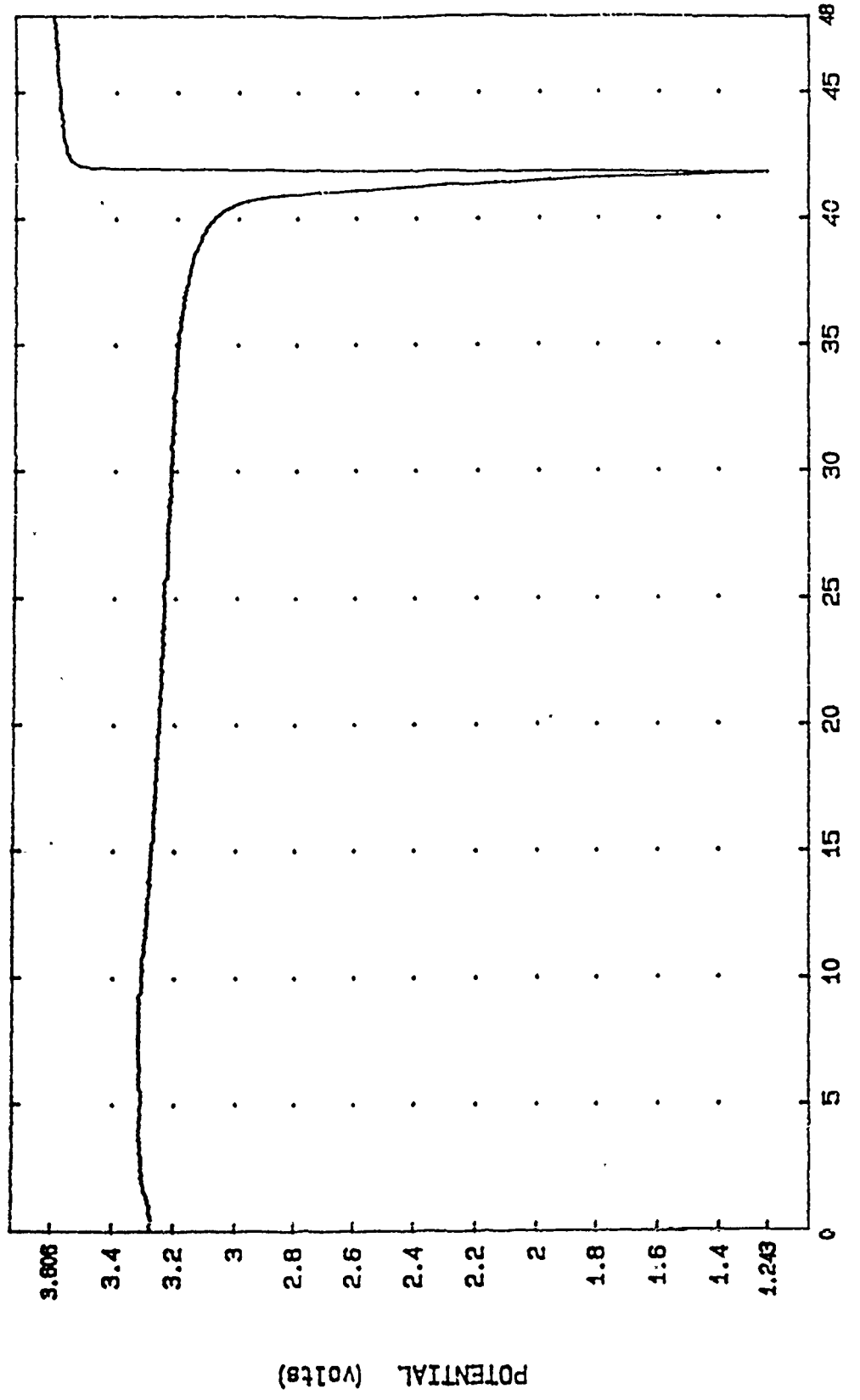

FIGURE 22. DISCHARGE PROFILE FOR CELL 26-84-2, USING THE LAST TWO DATA FILES. AMBIENT TEMPERATURE, 25.65 MA (3 MA/CM² OF ANODE SURFACE AREA). ELECTROLYTE, 1M $ALCl_3/SOCl_2$, SATURATED FIRST WITH $LI(CF_3SO_3)$, THEN LICL.

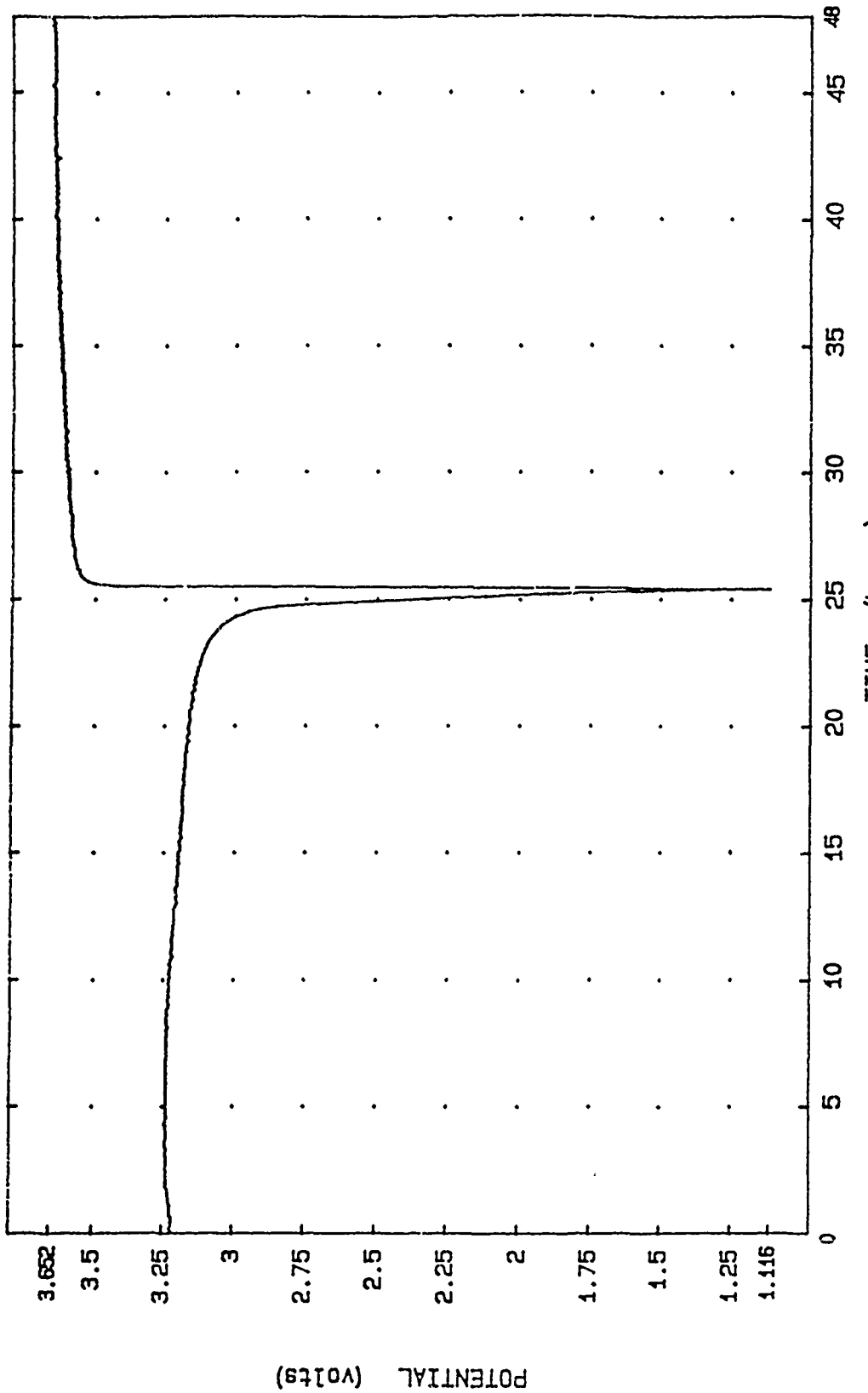

FIGURE 23. DISCHARGE PROFILE FOR CELL 26-84-5, USING THE LAST TWO DATA FILES. AMBIENT TEMPERATURE, 25.65 MA (3 MA/CM² OF ANODE SURFACE AREA). ELECTROLYTE, 1M $ALCl_3/SOCl_2$, TREATED FIRST WITH 50 MM OF SO_3, THEN SATURATED WITH LICL.

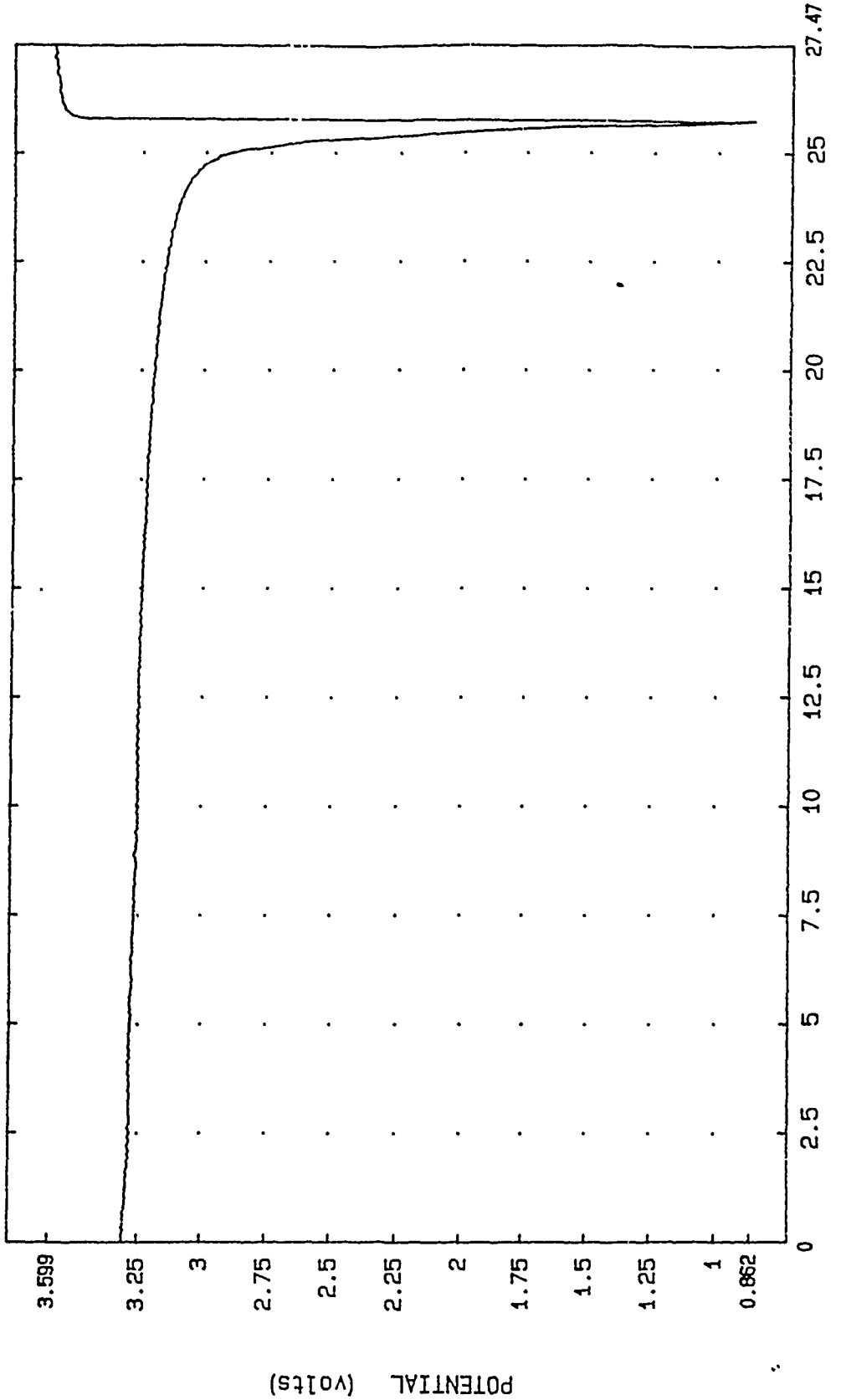

FIGURE 24. DISCHARGE PROFILE FOR CELL 37-12-1, USING THE LAST TWO DATA FILES. AMBIENT TEMPERATURE, 25.65 MA (3 MA/CM² OF ANODE SURFACE AREA). ELECTROLYTE, 1M ALUMINUM (III), IN WHICH $ALCl_3$ WAS FIRST MELTED WITH A MOLAR EQUIVALENT AMOUNT OF SULFUR, DISSOLVED IN THIONYL CHLORIDE, THEN SATURATED WITH LICL.

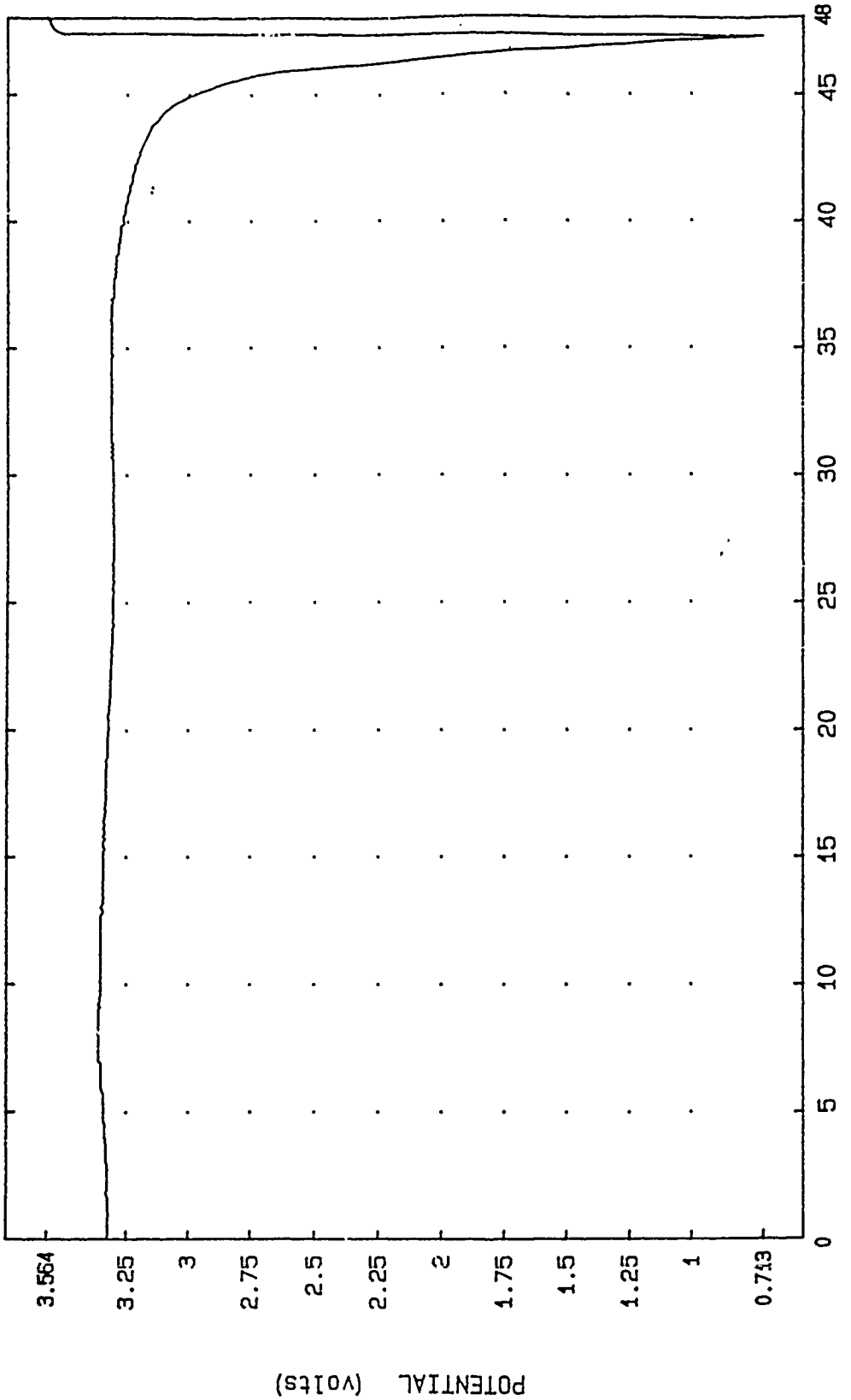

FIGURE 25. DISCHARGE PROFILE FOR CELL 37-12-6, USING THE LAST TWO DATA FILES. AMBIENT TEMPERATURE, 25.65 MA (3 MA/CM² OF ANODE SURFACE AREA). ELECTROLYTE, 1M ALUMINUM (III), IN WHICH $ALCl_3$ WAS FIRST DISSOLVED IN THIONYL CHLORIDE, REACTED WITH AN 80 MOLE PERCENT OF WATER, REFLUXED 16 HOURS, THEN SATURATED WITH LICL.

Infrared spectra of the electrolytes used to fill the test cells 26-84-1 through -6 were taken. Figure 26 shows two separate runs using pure thionyl chloride. Figure 27 shows the 1M $AlCl_3$ saturated first with lithium trifluoromethane sulfonate, then with lithium chloride, and Figure 28 the partially chlorosulfonated tetrachloroaluminate. The reaction which originally produced a trifluoromethane sulfonate derivative did not occur as it had before (see Figure 18), and the concentration of the substituted derivative was considerably lower. The reasons for this difference are not yet clear, but the derivative present at this level evidently did not adversely affect the capacity with respect to that observed for the control cells.

The spectrum of the chlorosulfonated aluminate electrolyte used to fill cells 26-84-4 through -6 (Figure 28) indicates that a derivative or derivatives were present in high concentration. Open circuit potentials near 3.9 volts and infrared absorption near 7 microns may also indicate that some of the sulfur trioxide reacted with the thionyl chloride to produce sulfuryl chloride.

In order to determine whether electrolytes used in the earlier test cells contained derivatives at the same concentration as first observed in infrared spectra, spectra were run on the electrolytes used to fill cells 33-37-4 through 33-37-9. Figure 29 shows 1M $AlCl_3$ saturated with $Li(CH_3SO_3)$, and Figure 30 shows the electrolyte saturated with $Li(CH_2ClCOO)$. Again, we found that the concentrations were substantially lower than we had first observed. The concentrations of the derivatives may have been affected by storage, or through contamination of the starting materials by water.

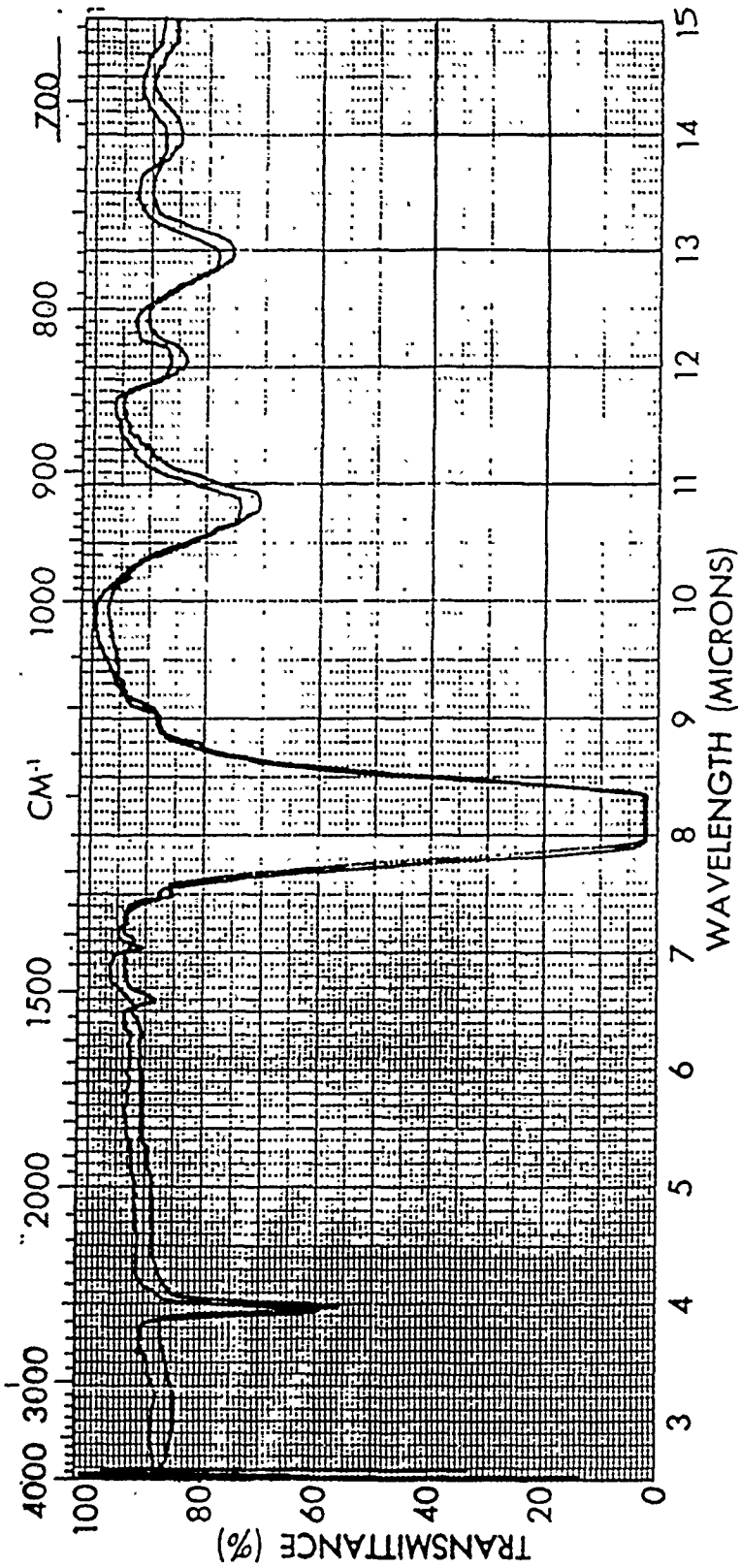

FIGURE 26. INFRARED SPECTRUM OF PURE THIONYL CHLORIDE, USING TWO SEPARATE RUNS. DEMOUNTABLE CELL WITH 0.1MM PATHLENGTH SPACER, SODIUM CHLORIDE WINDOWS.

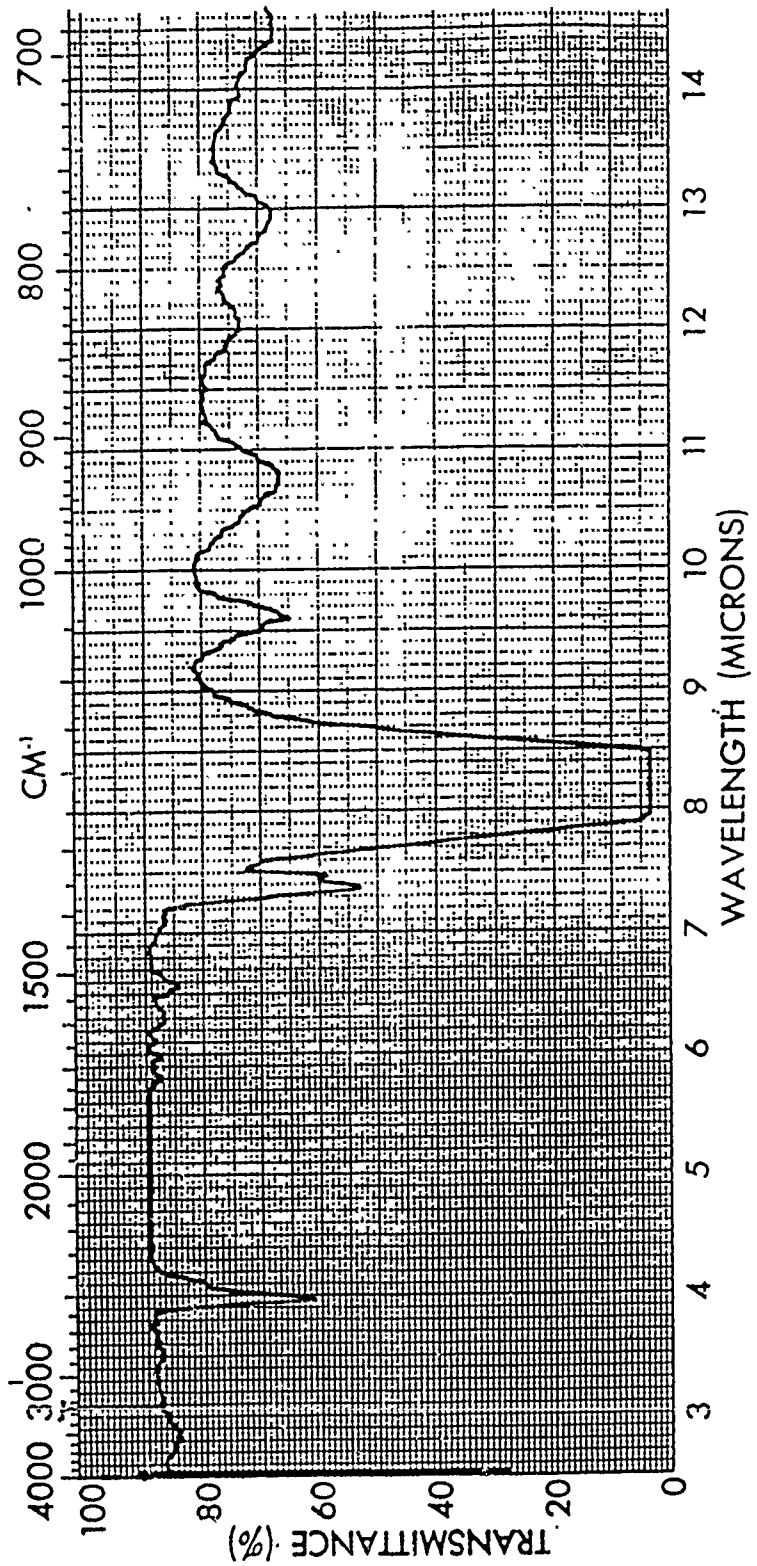

FIGURE 27. INFRARED SPECTRUM OF 1M $ALCl_3$/ $SOCl_2$, SATURATED FIRST WITH LI(CF_3SO_3), THEN LICL, USED TO FILL CELLS 26-84-1 THROUGH -3. DEMOUNTABLE CELL WITH 0.1MM PATHLENGTH SPACER, SODIUM CHLORIDE WINDOWS.

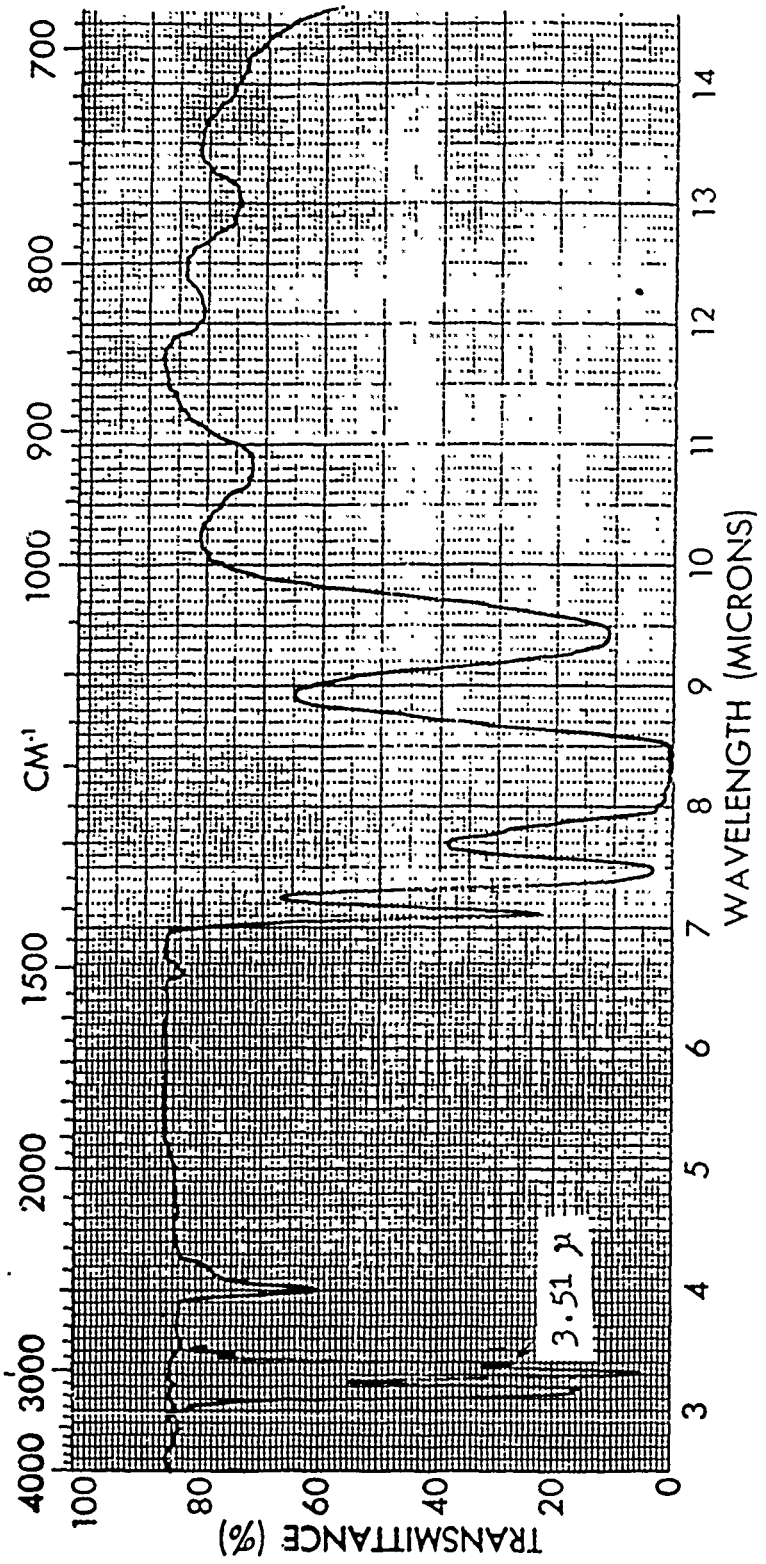

FIGURE 28. INFRARED SPECTRUM OF 1M $ALCL_3$/ $SOCL_2$, TREATED FIRST WITH 50 MM OF SO_3, THEN SATURATED WITH LICL, USED TO FILL CELLS 26-84-4 THROUGH -6. DEMOUNTABLE CELL WITH 0.1MM PATHLENGTH SPACER, SODIUM CHLORIDE WINDOWS. SPECTRUM INCLUDES POLYSTYRENE REFERENCE PEAKS.

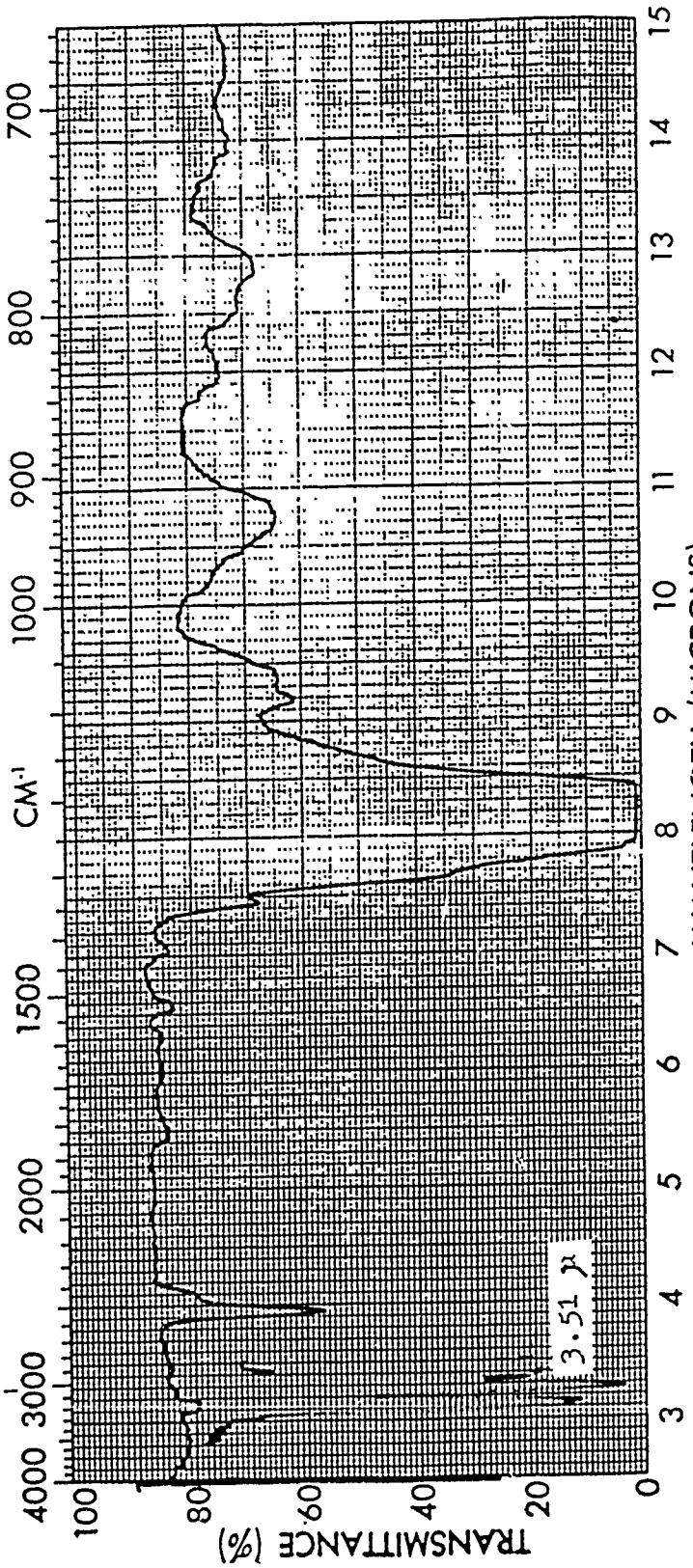

FIGURE 29. INFRARED SPECTRUM OF 1M $ALCL_3$/ $SOCL_2$, SATURATED FIRST WITH LI(CH_3SO_3), THEN LICL, USED TO FILL CELLS 33-37-7 THROUGH -9. DEMOUNTABLE CELL WITH 0.1MM PATHLENGTH SPACER, SODIUM CHLORIDE WINDOWS. SPECTRUM INCLUDES POLYSTYRENE REFERENCE PEAKS.

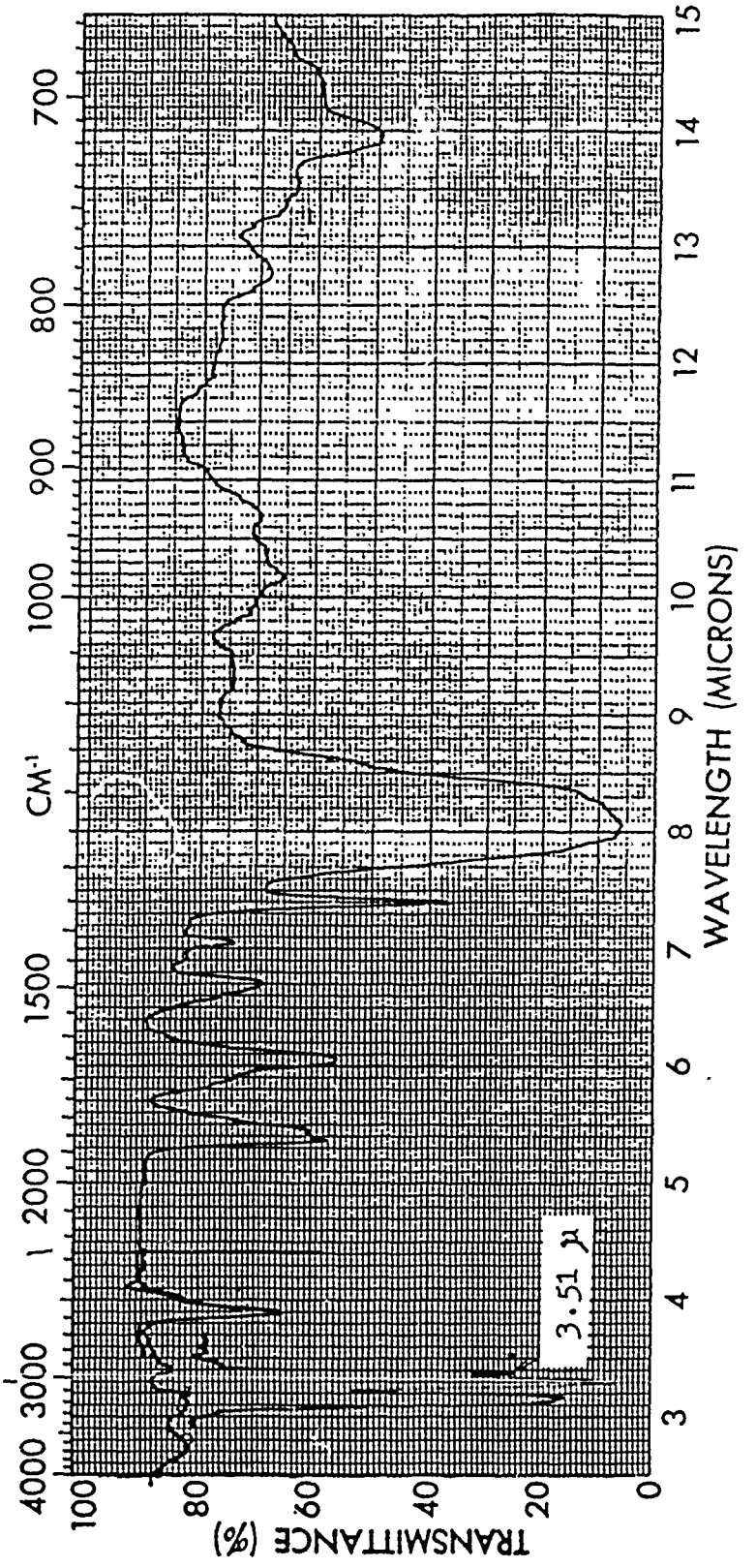

FIGURE 30. INFRARED SPECTRUM OF 1M $ALCL_3$/ $SOCL_2$, SATURATED FIRST WITH LI(CH_2CLCOO), THEN LICL, USED TO FILL CELLS 33-37-4 THROUGH -6. DEMOUNTABLE CELL WITH 0.1MM PATHLENGTH SPACER, SODIUM CHLORIDE WINDOWS. SPECTRUM INCLUDES POLYSTYRENE REFERENCE PEAKS.

CHAPTER 4

CONCLUSIONS AND RECOMMENDATIONS

It appears that of all the experimental electrolytes, the cells with lithium trifluoromethanesulfonate or $AlCl_3$ melted with sulfur matched the capacity obtained from cells with the control electrolyte under the conditions of these tests, while the capacity of the cells containing hydrolyzed/ refluxed electrolyte modestly exceeded that of the control cells.

We have arbitrarily made the assumption that if a derivative such as partially or totally chlorosulfonated aluminate present at low concentration is beneficial, then the same or similar derivatives present at a higher concentration should be even more beneficial. If a derivative at low concentration such as Vallin's $LiAl(SO_3Cl)_4$ is capable of alleviating the voltage delay without adversely affecting the capacity, then its presence is clearly beneficial, whether or not it increases the capacity. By the same token, the new derivatives may be valuable alternatives for reducing voltage delay when present at the right level of concentration.

The data we have collected to date demonstrate only that substituted chloroaluminates may be prepared by the techniques which we have outlined. Variations in the concentrations of the partially substituted chloroaluminate derivatives which we observed during synthesis indicates that more needs to be known about their stability and how their formation is affected by the concentration of reactants and the presence of moisture. At that point, their potential usefulness in increasing the capacity may be fairly evaluated. We currently have little information as to how the concentrations may be maximized, or how they may affect performance. We would recommend that further studies be carried out to resolve these questions, particularly since we have observed some modest inprovement in the capacity with hydrolyzed/ refluxed electrolyte.

Below is a brief outline of the tasks suggested by the results of this effort:

1. Determine by difference in weight what the maximum solubility in 1M $AlCl_3$/ $SOCl_2$, refluxed until "dry", is for each of the following:
   a. CH_3SO_3ClLi
   b. $CH_2ClCOOLi$
   c. CF_3COOLi
   d. CF_3SO_3Li

   In each case, the salts should be dried at 150°C. for a minimum of 16 hours, and tested immediately after drying. Repeat for 2M $AlCl_3$/ $SOCl_2$.

2. For each of the saturated solutions from (1), treat with an excess of lithium chloride. Using infrared spectroscopy with a 0.1 mm pathlength cell, determine whether the absorption maxima change in intensity with time during storage at ambient temperature over a period of two months.

3. Determine the startup and capacity to 3 and to 2 volts for AA annular bobbin

cells discharged at 3 mA/cm² of anode surface area, using each of the saturated solutions from (2) containing 1 M aluminum. Repeat for electrolytes containing 5% and 1% substituted aluminate, the balance up to 1 M aluminum made up by $LiAlCl_4$. If the capacities and/ or startup characteristics are better than those of control cells (1 M $LiAlCl)_4$, repeat the tests at reduced temperature and after storage at elevated temperature.

REFERENCES

1. D. C. Ginnings and T. E. Phipps, *J. Am. Chem. Soc.* 52 (1930) 1340.

2a. A. J. Dekker, "Solid State Physics", Prentice Hall, Inc. (1957), p. 145.

2b. L. Heyne, *Electrochem. Acta*, 15 (1970) 1251.

3. E. Peled, in J. P. Gabano (ed.), "Lithium Batteries", Academic Press, London, (1983), pp. 43-69.

4. C. R. Schlaikjer, *Progress in Batteries and Solar Cells 4* (1982) 40.

5. C. R. Schlaikjer, in J. P. Gabano (ed.), "Lithium Batteries", Academic Press, London, (1983), pp 333-338.

6. M. Salomon, *J. Electrochem. Soc., 128* (1981) 233.

7. W. P. Hagan and N. A. Hampson, *Electrochimica Acta 32* (1987) 1787.

8. C. Schlaikjer, C. A. Young, and M. Dobrusin, ERADCOM Report No. DELET-TR-78-0558.1F (May, 1980), G.T.E. Labs., Inc.

9. A. N. Dey, J. S. Miller, and W. L. Bowden, U. S. Patents 4,177,329 (December 4, 1979); 4,238,552 (December 9, 1980).

10. D. Vallin, J. Y. Grassien, P. Chenebault, and A. Keroutanon, U. S. Patent 4,547,441 (October 15, 1985).

11. D. Vallin and P. Chenebault, *Power Sources Symposium*, Cherry Hill, N.J., 1986.

12. B. Vandorpe, M. Drache, *Bull. Soc. Chim. France*, 2878, (1986).

13. F. Walsh and R. S. Morris, U. S. Patent 4,469,763 (Sept. 4, 1984).

14. F. Walsh and M. Yaniv, in A. N. Dey (ed.), *Proceedings, Vol. 84-1*, The Electrochemical Society, Pennington, New Jersey (1984), pp. 103-110.

15. F.A. Cotton and G. Wilkinson, "Advanced Inorganic Chemistry", Interscience (John Wiley), 1962, page 436.

16. J.C. Bailey and G.E. Blomgren, *Electrochem. Soc. Fall Meeting*, 1987, Abstract 76.

17. P.A. Flowers, T.M. Laher, and G. Mamantov, *Electrochem. Soc. Fall Meeting*, 1986, Abstract 659.

18. H. Schaefer, C. Goeser, and L. Bayer, *Z. anorg. allgem. Chem. 263*, 87 (1950).

19. K. French, P. Cukor, C. Persiani, and J. Auborn, *J. Electrochem. Soc. 126*, 1045 (1974).

APPENDIX D

DEVELOPMENT OF CALCIUM PRIMARY CELLS WITH IMPROVED ANODE STABILITY AND ENERGY DENSITY

FINAL REPORT
December 1987 - May 1988

Prepared for:

Naval Surface Warfare Center
Silver Spring, MD 20903-5000

Under Contract No. N60921-88-C-0058

Battery Engineering, Inc.
1636 Hyde Park Avenue
Hyde Park, MA 02136

C. R. Schlaikjer
Principal Investigator

W. Kilroy
Project Manager

TABLE OF CONTENTS

FIGURES

TABLES

CHAPTER 1

INTRODUCTION

Lithium/ thionyl chloride cells have been of particular interest to the military agencies for a wide range of electronic devices because of their high energy and power density. However, if heating from external or internal sources causes the temperature of part or all of the anode to rise to the melting point of lithium at 180°C., the lithium chloride layer on the surface of the metal protecting it from the electrolyte will be breached, and the cell can be subject to rapid redox reactions leading to explosion and fire. Internal heating can occur generally as the result of a short circuit, or over a concentrated area because of rapid chemical reactions [1].

Calcium/ thionyl chloride and calcium/ sulfuryl chloride cells have promised greater safety, principally because the melting point of calcium, at 838°C., is so much higher than that of lithium. For lithium anodes, the ionically conductive, nearly insoluble lithium chloride film on the surface of the metal is exclusively permeable to lithium ions. For calcium anodes, the calcium chloride salt film is permeable almost exclusively to chloride ions, which has been blamed for both the observed high overpotential during discharge and significant calcium corrosion [2]. As a result, calcium/ thionyl chloride cells have about the same energy density as lithium/ sulfur dioxide cells, when they should have nearly the same as lithium/ thionyl chloride cells [3].

We had discovered that the reduction of sulfur dioxide in the presence of dissolved calcium bromide with acetonitrile and propylene carbonate produced not dithionite, as is the case in the similar lithium/ sulfur dioxide primary system, but sulfide. Electrical conduction in solid calcium sulfide occurs exclusively through cation transport [4]. If calcium sulfide were the predominant species in the solid electrolyte interphase on the calcium anodes, the possibility existed that calcium anodes would discharge without the significant overpotential or corrosion which had been observed in the calcium/ thionyl chloride cells.

In addition, the reduction of sulfur dioxide to sulfide signifies that the discharge realizes at least two equivalents of charge per mole of sulfur dioxide:

$$3Ca + 3SO_2 \text{ ---> } CaS + 2CaSO_3 \qquad (1a)$$

$$2Ca + 2SO_2 \text{ ---> } CaS + CaSO_4 \qquad (1b)$$

The identities of the other products were not known. The formation of other reduced products such as sulfur, thiosulfate, or trithionate would yield more than two equivalents per mole of sulfur dioxide. The theoretical energy densities of the calcium/ sulfur dioxide system were compared with those of other relevant systems:

Couple	Number of equivalents per mole of cathode	Assumed average potential (V)	Whr / cm^3	Whr / Kg
Ca/SO_2	2	2.80	2.07	1,440
Li/SO_2	1	2.85	1.28	1,076
$Li/SOCl_2$	2	3.30	1.81	1,332
$Ca/SOCl_2$	2	2.80	1.54	944

Our overall objective was to determine whether the acetonitrile/ propylene carbonate or other nonaqueous system containing sulfur dioxide with a calcium salt and a calcium metal anode could provide a superior power source combining the performance and storage capability of lithium cells with the safety of the calcium cells. We were particularly interested in inorganic electrolytes such as $Ca(AlCl_4)_2*6SO_2$, because of the higher conductivity, lower cost, and nonflammability of the mixture. If we were able to obtain adequate performance using wound D size prototype cells containing a number of different carbon cathodes, we intended to extend the testing, varying the current density and the discharge temperature to characterize the system more fully, and to measure the extent of calcium corrosion during discharge and storage.

CHAPTER 2

EXPERIMENTAL

The dryroom, measuring about 36 feet square, was maintained at 70°F. at a relative humidity of about 2.5%. Salts were weighed, solvents fractionally distilled, solutions prepared, and infrared samples taken in the hood inside the dryroom. In addition, the wound D size, case negative cells were made in the dryroom.

Standard laboratory glassware was used fractionally to distil solvents and prepare calcium salts. A 0.6 cu. ft. vacuum oven capable of heating samples to 200°C., located in the laboratory, was used to dry calcium chloride and bromide. To unload the oven, it was disconnected and moved to the dryroom hood, backfilled, opened, and unloaded while hot. A Pyrex sublimator with a 7" diameter inner condensing cylinder was used in the dryroom hood to purify the aluminum chloride. Halide analysis was carried out using a Sartorius analytical balance in the dryroom. Potentiometric titrations were performed with a silver/ silver iodide reference electrode against a similar working electrode.

Infrared spectra were taken using either a Perkin Elmer model 137 or 257 spectrophotometer. Measurements of hydrolysis products in sulfur dioxide solution were done in a 10mm pathlength type I quartz cuvette with a Teflon stopper versus an identical empty cuvette. Spectra of organic solvents from 2.5 to 15 microns were taken with a demountable liquid sample cell with a 0.1 mm spacer and sodium chloride windows.

A press and a rolling mill, located in the dryroom, were used to prepare calcium foil from cut billets. A Pyrex furnace tube 3" in diameter x 48" long, with a glass flange on one end and sealed at the other, was used to anneal the calcium foil. The tube had a removable Pyrex cap with a matching flange and a Pyrex/ Teflon needle valve through which the furnace tube could be evacuated. The flanges were sealed with an O ring and held by aluminum collars bolted together. The loaded furnace tube was carried to the laboratory, placed in the tube furnace, and evacuated with a pump placed near the furnace.

The cells were filled to capacity using a frame which held the Savillex vessel, a Hamilton gas tight syringe to measure electrolyte volume, a Hamilton four-way Teflon valve, and Teflon connectors and tubing. The cells were discharged at constant current using power supplies built by Starbuck Systems of Newton and controlled by an IBM compatible computer with a Starbuck interface board and protecting circuitry. The discharge and plotting programs were written by Software Tailors, Inc.

We obtained acetonitrile and propylene carbonate from Aldrich Chemical. Calcium bromide was synthesized from Fisher chelometric grade calcium carbonate and Fisher reagent grade hydrobromic acid in aqueous suspension. After the addition of a slight excess of acid, the water was removed by vacuum distillation and heating *in vacuo* overnight at 200°C. Potentiometric titration with standard silver nitrate showed that the salt had been thoroughly dried. The acetonitrile was fractionally distilled at atmospheric pressure and the propylene carbonate vacuum distilled until the infrared absorption near 3600 cm(-1) in each case was reduced to a minimum.

We developed a method for the purification of aluminum chloride by distillation from melted lithium or sodium tetrachloroaluminate in the presence of calcium foil cuttings at atmospheric pressure. The method delivers product rapidly, removes all or-

ganic impurities and iron, and provides a completely white crystalline product with low surface area.

Calcium metal in the form of 1 pound "coupons" was received from Pfizer. The coupons were cut from a "crown" of redistilled metal, which was said to be better than 99.5% pure, with less than 1,000 ppm magnesium and 50 ppm iron. Each measured about 12.5" by 2.5" by 0.5". Each was cut into 25 billets 2.5" x 0.5" x 0.5", pressed and rolled in mineral oil to approximate dimensions of 14" x 2" x 0.020", then cut to 1 7/8" wide up to about 12-13" long to remove uneaven ends. The foil was kept under mineral oil in the dryroom until it was needed for cells. Ten calcium strips, 14" by 2", could be placed in the furnace tube at once. These were cleaned in hexane, separated from each other by pieces of stainless steel foil, and heated *in vacuo* at 400°C. for 1 hour. The furnace tube was brought back to the dryroom, allowed to cool, backfilled with dryroom air, and opened.

The resulting foil strips were completely softened, but the mineral oil had not been entirely removed during the hexane washing before the first try. The calcium surface had been darkened. Before the calcium was used to make cells, it was wire brushed to remove all tarnish, cut to the desired width (about 1 $^{7}/_{8}$"), spliced if necessary, and cut to the desired length. Tests showed that annealing the calcium in the presence of small amounts of oil lowered the open circuit potential of organic electrolyte cells, but did not significantly affect the performance of any cells. Heating *in vacuo* completely removed the mineral oil, which then condensed on cooler parts of the tube.

We prepared 100 ml batches of a sulfur dioxide/calcium bromide electrolyte with the purified materials, using the following composition:

8.0 M SO_2
0.85 M $CaBr_2$
propylene carbonate/ acetonitrile =
3/ 10 by volume

The calcium bromide and solvents were added to a 100 ml. Savillex vessel, and liquified sulfur dioxide just below its boiling point was carefully poured into the vessel. The cap on the vessel was tightened and the mixture allowed to warm back to ambient temperature. While the calcium bromide dissolved completely, releasing the pressure by opening a valve at the top of the vessel caused the solution to boil. An electrolyte made with 1.7 molar lithium bromide in place of the calcium bromide had been observed to have a boiling point near room temperature.

Inorganic electrolyte of the stoichiometric composition $CaCl_2*2AlCl_3*6SO_2$ was prepared in a 100 ml Savillex Teflon vessel, using distilled aluminum chloride, reagent grade calcium chloride dried overnight at 200°C. *in vacuo*, and reagent grade Matheson sulfur dioxide, added to the Savillex vessel as a vapor at atmospheric pressure, monitored with a bubbler to avoid adding the gas faster than it could be absorbed. When the salt mixture no longer rapidly absorbed the gas, the mixture was allowed to cool back to room temperature, and the remainder of the sulfur dioxide was added as a liquid, having been prepared by condensing the gas from the main tank at reduced temperature and atmospheric pressure.

All cells had the following characteristics:

Case:
- stainless steel; TIG welded cover
- glass/ metal compression electrical feedthrough/ fill tube, TIG welded after filling
- D size, wound electrodes, case negative

Anodes:
- width, 1 7/8"
- thickness, 0.020"

Cathodes:
- width, 1 7/8"
- binder: 10% Teflon

Separators:
- Craneglass nonwoven Pyrex fabric, 0.005" to 0.007" thick

The length, thickness, and composition of the cathode were varied, and the length of the calcium anode varied accordingly. The carbon material was either 100% Chevron acetylene black, or 75% acetylene black with 25% Ketjenblack, recommended by Walker *et al.* as more effective in calcium/ thionyl chloride cells than acetylene black alone [5]. Cells with "rolled" cathodes were prepared by spreading a thick mixture of carbon and Teflon in an isopropanol/ water mixture on the cathode support, a 12" x 14" aluminum or nickel screen, using a dough sheeter. Cells with "pressed" cathodes were made by first preparing the mix, curing it separately, chopping it in a blender, spreading a weighed amount of mixture evenly and one side at a time, and finally pressing it with the dough sheeter roller onto the screen using a thin die with a 360 mm x 47 mm cavity.

The cells were filled to capacity with electrolyte, which amounted to about 25 ml. At two electrical equivalents per mole of sulfur dioxide, the 8M SO_2 in the organic electrolyte represented 10.7 amp hours, and in the inorganic electrolyte $Ca(AlCl_4)_2 * 6SO_2$, 17.6 amp hours.

Infrared spectra were used to estimate when fractionation of the solvents had succeded in removing water, and to detect the presence of hydrolysis products in $Ca(AlCl_4)_2 * 6SO_2$. A chart recorder plotted the cell terminal potentials as a function of time during cell startup. The computer was used to record cell potentials as a function of time during constant current discharge at ambient temperature, to a cutoff near 0.65 volts. Data presented include copies of infrared charts, recorder traces, discharge profiles, and a table of cell parameters and capacities.

CHAPTER 3

RESULTS AND DISCUSSION

The infrared spectrum of $Ca(AlCl4)2*6SO_2$ prepared as described above absorbed strongly between 3100 and 3500 cm^{-1} in a 10 mm pathlength type I quartz cuvette, the spectrum taken versus an empty cuvette. We attempted to "dry" this mixture by adding sulfur trioxide, distilled from reagent grade oleum, but addition of the pure SO_3 to the mixture caused a precipitate which stirring would not dissolve. We tried again with SO_3 dissolved in SO_2 and were successful in adding about 1.5g of SO_3, an amout equivalent to about 4 mole percent of the aluminum chloride originally added, without causing precipitation. However, no crystalline product separated on standing, and as shown in Figure 1, the solution still absorbed strongly between 3100 and 3500 cm^{-1}.

We then attempted to "dry" a mixture of distilled aluminum chloride (as opposed to $Ca(AlCl_4)_2$) and sulfur dioxide in the molar ratio Al : S = 1 to 3 by adding sulfur trioxide, similar to the procedure which had worked for drying electrolyte solutions in thionyl chloride (compare Contract N-60921-88-C-0057). We found not only that a 1 to 3 mixture of $AlCl_3$ to SO_2 was highly viscous at room temperature, it foamed when the pressure was released at ambient temperature by opening the valve in the Teflon vessel. The electrolyte solution used to fill cells 33-30-3 and 33-30-4 was therefore the one which had been treated with sulfur trioxide <u>after</u> the addition of both the aluminum chloride and the calcium chloride to the sulfur dioxide.

Two separate attempts were then made to "dry" $Ca(AlCl_4)_2*6SO_2$, by melting calcium tetrachloroaluminate in the presence of calcium metal. Calcium had been found effective in removing iron from molten $LiAlCl_4/AlCl_3$ during the purification of aluminum chloride by distillation. Since the calculated free energy change for the reduction of aluminum chloride by calcium is negative, the calcium likely formed finely divided aluminum, which without any oxide layer was able to reduce the iron in the melt. We had hoped that the aluminum would reduce the hydrolysis products and maintain a chemically active surface in the molten calcium tetrachloroaluminate. We melted the calcium chloride with a stoichiometric amount of purified aluminum chloride, added calcium chips, and stirred for about an hour. The molten salt mixture was then cast into a clean stainless steel pan, broken into fragments, added to a 100 ml Savillex Teflon vessel, and dissolved in the appropriate amount of liquid sulfur dioxide. Infrared spectra of the solutions showed them still to contain hydrolysis products, and to be qualitatively the same as $Ca(AlCl_4)_2*6SO_2$ which had been treated with SO_3 dissolved in SO_2. Cells 37-4-4 and 37-4-5 were filled with $Ca(AlCl_4)_2*6SO_2$ prepared by melting the salt in the presence of calcium foil cuttings.

Table 1 summarizes the results of the discharge tests, showing anode lengths and capacities; cathode lengths, thicknesses, loadings, and type of screen; the electrolyte; current density, capacity in amp hours to 0.65 volts; and the figures corresponding to each cell.

The open circuit potentials of 33-30-1 and 33-30-2, its duplicate cell, were considerably lower than expected, each measuring about 1.95 volts. When briefly loaded with 100 ohm resistors, cell 33-30-1 dropped to about 1.1 volts, then recovered to 1.9 volts during a seven minute interval. On returning to open circuit, the potential rose to about 2.2 volts, then began falling off to the original 1.9 volts again (Figure 2). This behavior is similar to that observed in calcium/ thionyl chloride

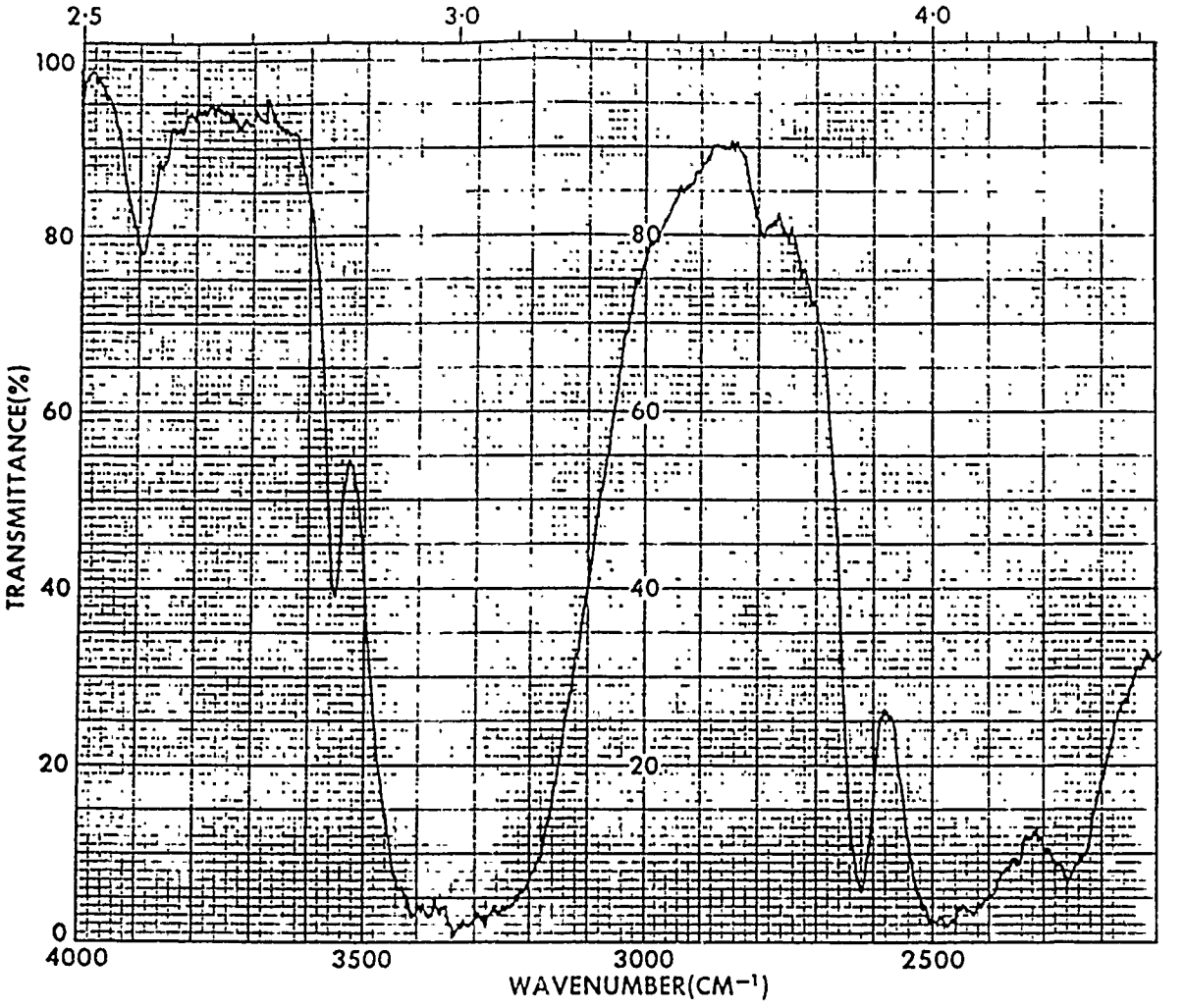

FIGURE 1. INFRARED SPECTRUM OF $CA(ALCL_4)_2*6SO_2$ AFTER TREATMENT WITH A SOLUTION OF SO_3 IN SO_2 EQUIVALENT TO 4 MOLE PERCENT OF THE ALUMINUM PRESENT FOLLOWED BY AN OVERNIGHT STAND. PATHLENGTH, 10 MM, IN A TYPE I QUARTZ CELL VERSUS AN EMPTY QUARTZ CELL.

TABLE 1. CELL CHARACTERISTICS AND DISCHARGE CAPACITIES

Cell #	Anode[1]		Cathode[2]					Elect.[3]	Discharge[4]		Fig. / #
	length	Ah	l	t	mat'l	wt(g)	scr		mA/ cm²	capac. (0.65V)	
33-30-1	12	15	13	32	25/75(r)	3.5	Al	organic	1; 0.5	1.75	2,3
33-30-3	12.1	15	13	32	25/75(r)	3.5	Al	inorg.	1	1.24	4
33-30-4	12.9	16	13	32	a.b.(r)	3.5	Al	inorg.	1	1.06	5
26-91-1	12.7	15.8	14.1	32	a.b.(r)	3.8	Al	organic	0.96	2.01	6,7
26-96-1	12-13	16	11.75	39	a.b.(p)	3.93	Al	organic	1.04	1.55	8
26-96-2	12-13	16	11.75	39	a.b.(p)	3.93	Al	organic	1.04	1.98	9
37-4-1	17.75	23	17	20	25/75(r)	2.57	Ni	inorg.	1	2.31	10,11
37-4-2	17.75	23	17	20	25/75(r)	2.57	Ni	inorg.	1	2.35	10,12
37-4-4	17.75	23	17	20	25/75(r)	2.57	Ni	organic	1	1.3	13
37-4-5	17.75	23	17	20	25/75(r)	2.57	Ni	organic	1	1.25	14
37-11-1	14	17.5	13	40	50/50(r)	2.43	Ni	inorg.	1	2.63	15
37-11-2	14	17.5	13	40	50/50(r)	2.43	Ni	inorg.	1	2.84	16

[1] Anode length in inches
Capacity in Amp Hours

[2] Cathode length (l) in inches
Cathode thickness (t) in 0.001"
Cathode material:
25/75 = 25% Ketjenblack/ 75% acetylene black
a.b. = acetylene black
(r) = rolled; (p) = pressed
weight in grams of mixture
Screen:
aluminum or nickel

[3] Electrolyte:
organic = 8.0 M SO_2; 0.85 M $CaBr_2$; Propylene carbonate: acetonitrile = 3:10
inorganic = $Ca(AlCl_4)_2*6SO_2$

[4] Discharge at ambient temp.; mA/cm² of common electrode area
Capacity in Ahr to a 0.56 volt cutoff

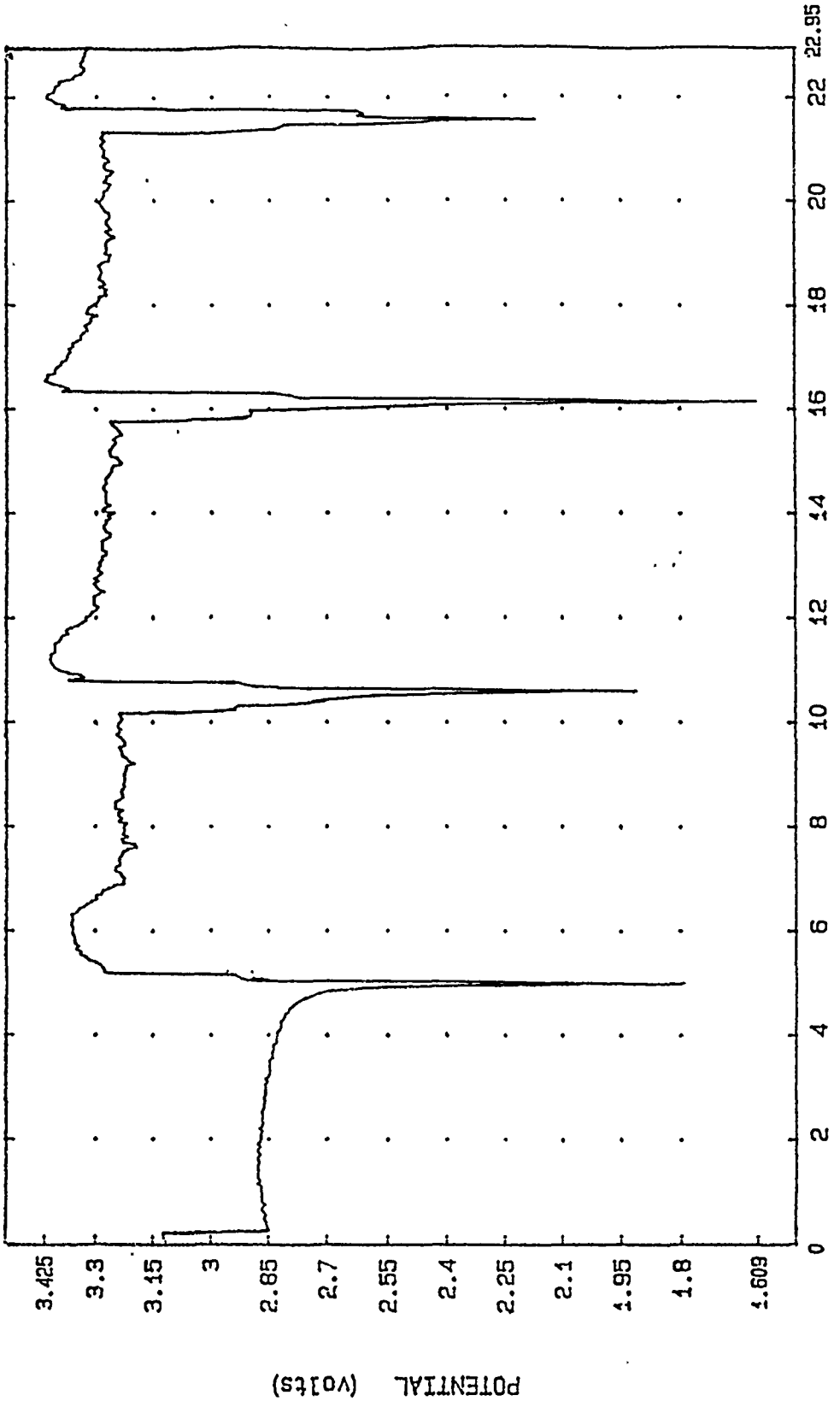

FIGURE 2. Cycle profile, cell #37-53-3, first four cycles
separator: Craneglass
pos. screen/contact: Al/Ni
electrolyte: 2M NH_4SCN / 0.25M LiSCN

cells, and has been explained as the result of anionic conduction in the solid electrolyte interphase. The low open circuit and running potentials were originally thought to have resulted from mineral oil which was inadvertently left on the rolled foil before annealing, but as discussed below, cells made from carefully cleaned foil behaved in a similar fashion. Cell 33-30-2 would not function, evidently because an internal tab became disconnected.

Cell 33-30-1 was placed on the computer at a constant current discharge of 1 mA/cm^2, where it ran for only about five hours between 1 and 0.75 volts. It was then restarted at 0.5 mA/cm^2, but ran for only about two hours, giving a total capacity of about 1.75 amp hours (Figure 3).

The discharge profiles for cells 33-30-3 and 33-30-4 are shown in Figures 4 and 5, respectively. Each cell was discharged at a constant current equivalent to about 1 mA/cm^2 of common electrode surface area. The potential drop in the leads from the computer to the cells amounted to about 80 mV. The cells therefore ran above two volts, but only just barely. Cell 33-30-3 gave a total capacity of 1.24 Ah, and 33-30-4, 1.06 Ah.

The cathodes of cells 26-91-1, 26-96-1, and 26-96-2 contained 100% Chevron acetylene black/ 10% Teflon on aluminum screens. The cathode of cell 26-91-1 was prepared by rolling a slurry of the cathode mixture in water/ isopropanol onto the screen. For cells 26-96-1 and 26-96-2, the cathode mixture was made and cured separately, then chopped in a blender and pressed on the aluminum screens, using a thin die with a 360 mm x 47 mm cavity and a mechanical roller. Cells 26-91-1, 26-96-1, and 26-96-2 contained the organic electrolyte 0.85M $CaBr_2$/ 8.0M SO_2/ propylene carbonate: acetonitrile = 3/10 by volume (Figures 6 through 9).

The capacities and running potentials of cells 26-91-1, 26- 96-1, and 26-96-2 were dissapointingly lov. Lithium/ sulfur dioxide primary cells typically realize between 7 and 9 amp hours. At 3.9 grams of cathode material, the capacity of these calcium cells represents only about 0.46 amp hours per gram. While the open circuit potential was improved, the capacity was not dramatically affected by the absence of mineral oil during the annealing of calcium foil anodes, nor by whether the cathodes had been pressed or rolled.

A nev set of cells was prepared with thinner, longer cathodes using stronger, nickel screens. Cells 37-4-1, -2, -4, and -5 contained 17" cathodes, only 20 mils thick. The carbon was 25% Ketjenblack/ 75% acetylene black, washed with acetone as recommended by Walker *et al.* [5], and the loading considerably lower at 2.57 grams of cathode mixture per cell. The spliced anodes were still 20 mils thick as well, and at $17^3/_4$" long, were in great excess at 23 amp hours of calcium.

Cells 37-4-1 and 37-4-2, duplicates with inorganic electrolyte, were started on the recorder, the first at 1 Kohm and at 1.5 ohm, the second at 1.5 ohm. As shown in Figure 10, brief discharge caused the open circuit potentials to increase, as was previously observed for cell 33-30-1 containing the organic electrolyte. Cells 37-4-1 and 37-4-2 were each able to sustain a current of about 1.4 amps at 2.1 volts for 1 minute. The discharge profiles for the four cells are shown in Figures 11 through 14, respectively. While the total current was increased about 45% to 398 mA, the current density was maintained at 1 mA/cm^2. The capacities to cutoff for the inorganic electrolyte cells were the highest yet recorded for any cells during this project, but for the organic electrolyte cells, the lovest. Again, the inorganic

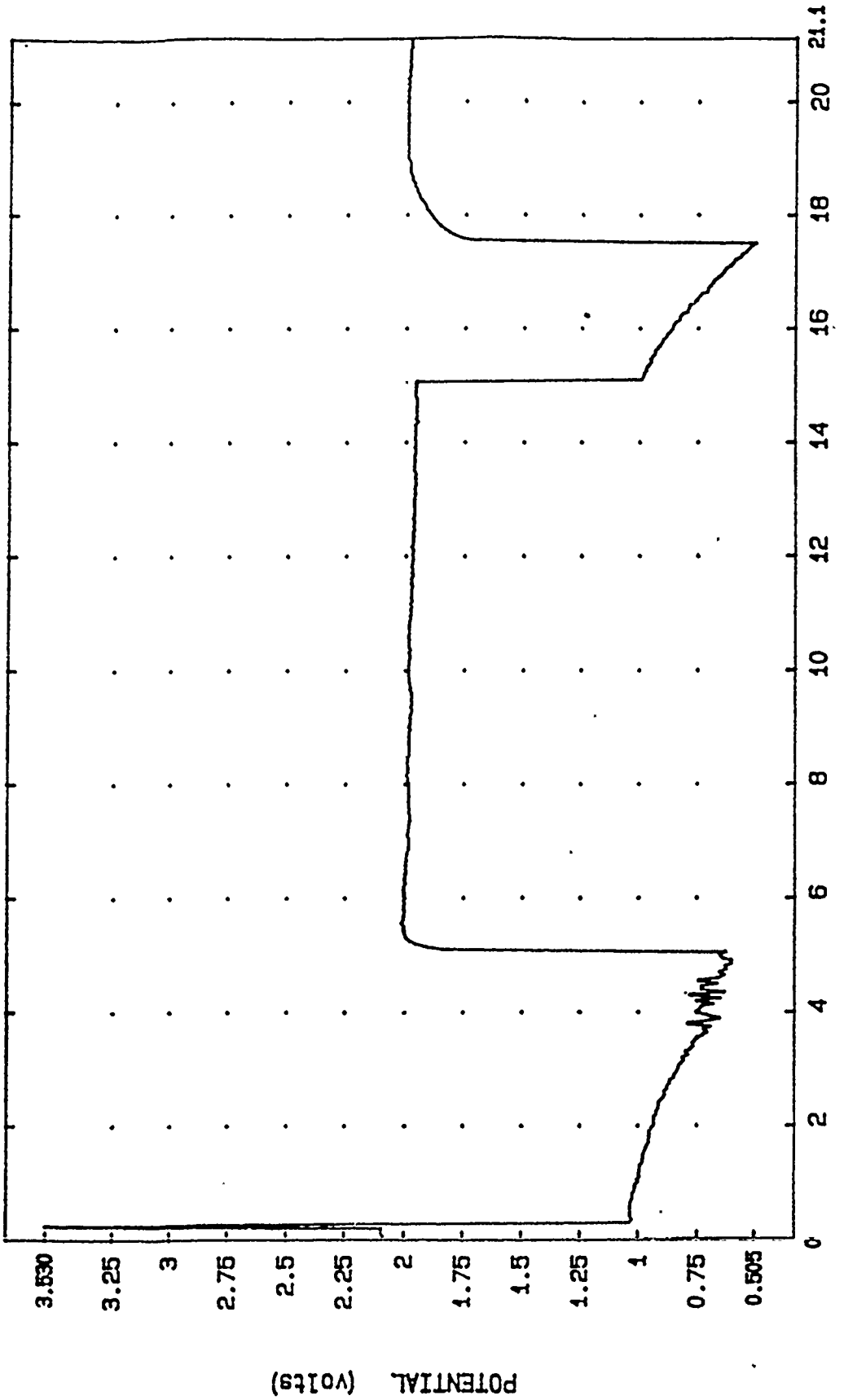

FIGURE 3. DISCHARGE PROFILE OF CELL 33-30-1, FIRST AT 1 MA/CM², THEN AT 0.5 MA/CM². ORGANIC ELECTROLYTE CONTAINING CALCIUM BROMIDE, ACETONITRILE, AND PROPYLENE CARBONATE; ROLLED CATHODE, 25/ 75 KETJENBLACK/ ACETYLENE BLACK.

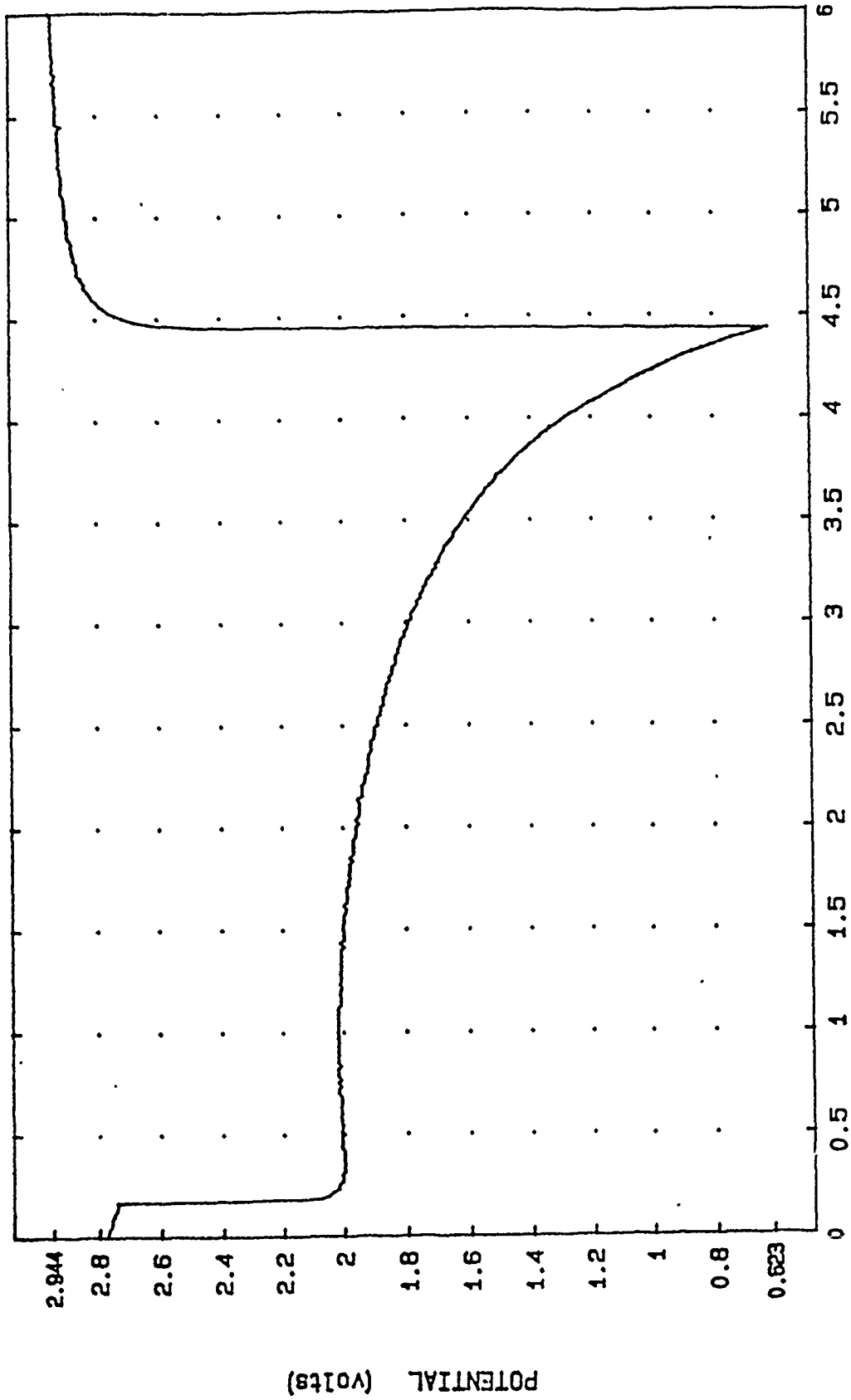

FIGURE 4. DISCHARGE PROFILE OF CELL 33-30-3 AT 1 MA/CM². INORGANIC ELECTROLYTE CONSISTING OF $CA(ALCL_4)_2*6SO_2$; ROLLED CATHODE, 25/ 75 KETJENBLACK/ ACETYLENE BLACK.

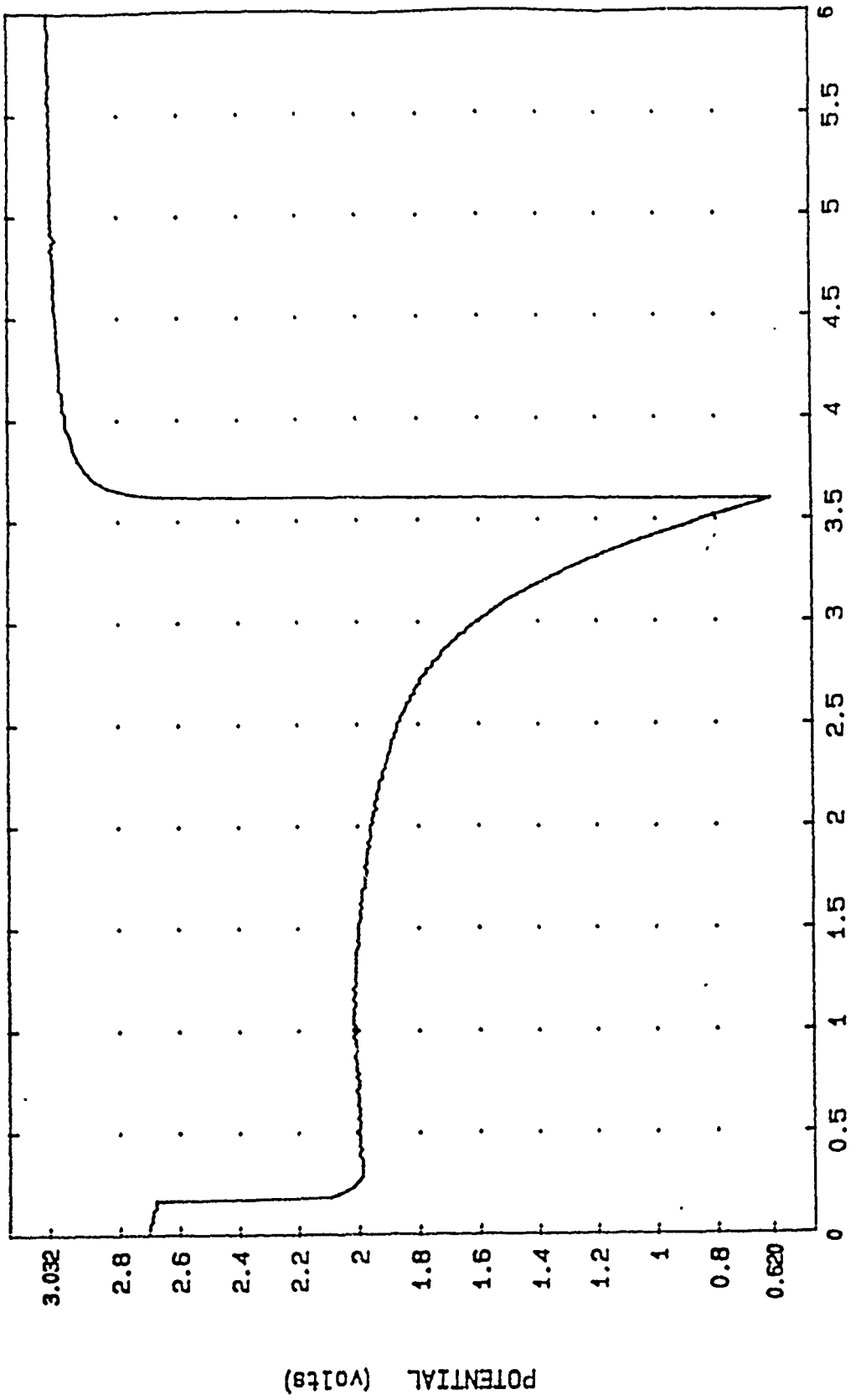

FIGJRE 5. DISCHARGE PROFILE OF CELL 33-30-4 AT 1 MA/CM². INORGANIC ELECTROLYTE CONSISTING OF $CA(ALCL_4)_2*6SO_2$. ACETYLENE BLACK ONLY, ROLLED CATHODE.

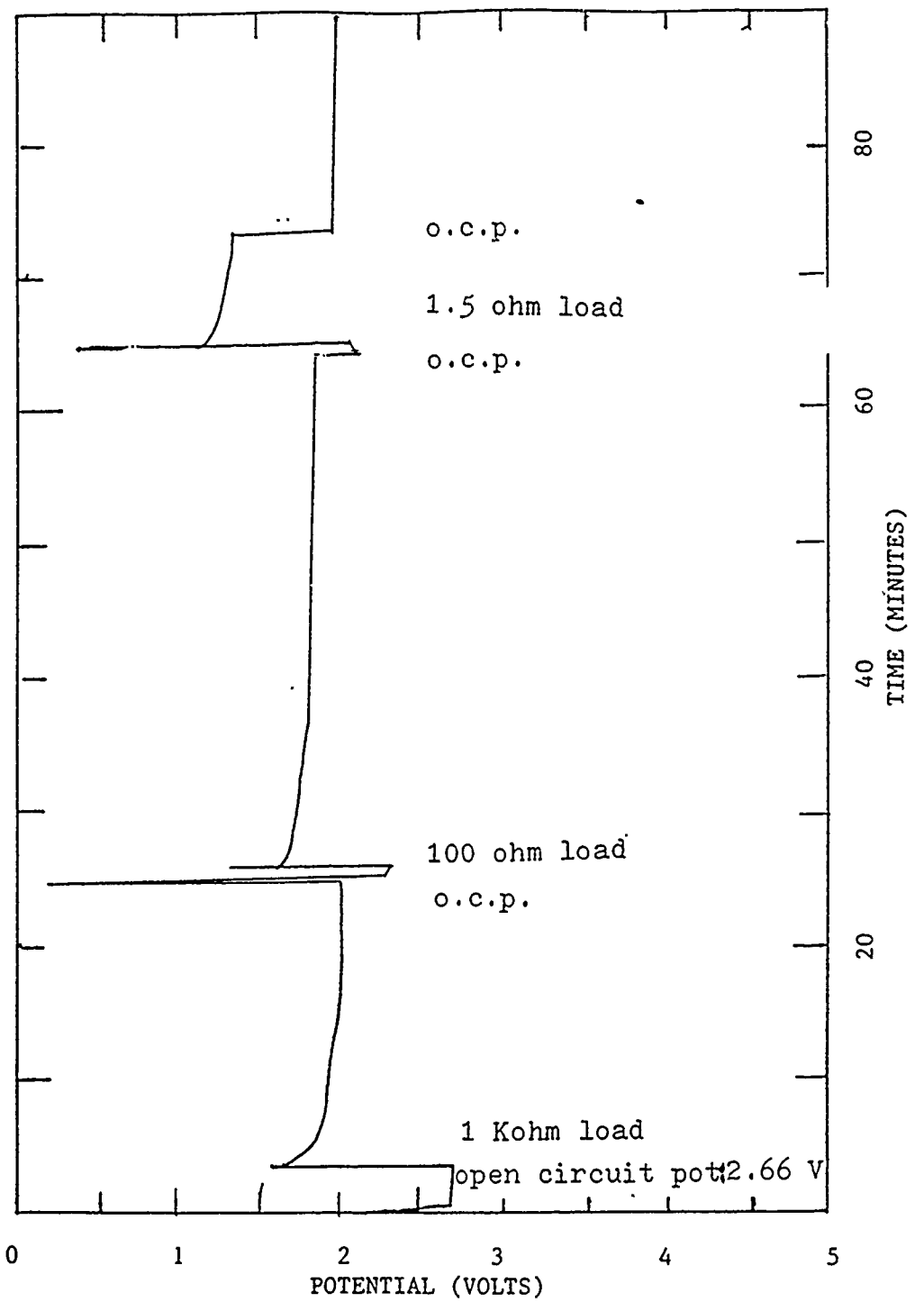

FIGURE 6. OPEN CIRCUIT POTENTIAL AND STARTUP PROFILES FOR CELL 26-91-1 AT 1 KOHM, 100 OHM, AND 1.5 OHM LOADS. COPY OF RECORDER TRACE. ONE VOLT/ INCH; 5 MIN./ CM.

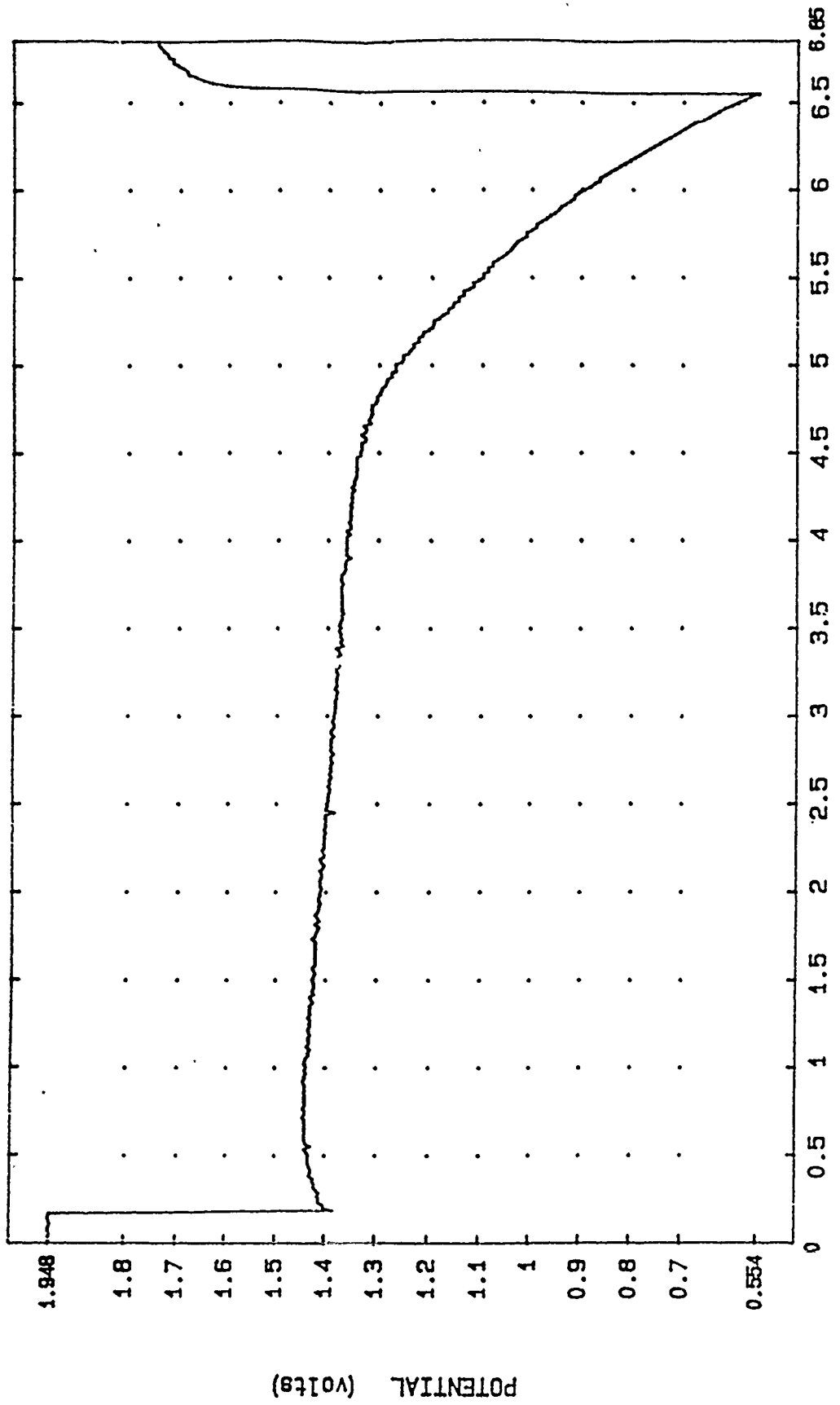

FIGURE 7. DISCHARGE PROFILE FOR CELL 26-91-1. 0.85M $CABr_2$/ 8.0M SO_2/ PROPYLENE CARBONATE: ACETONITRILE = 3:10 BY VOLUME. ROLLED CATHODE, ACETYLENE BLACK ONLY, 295 MA.

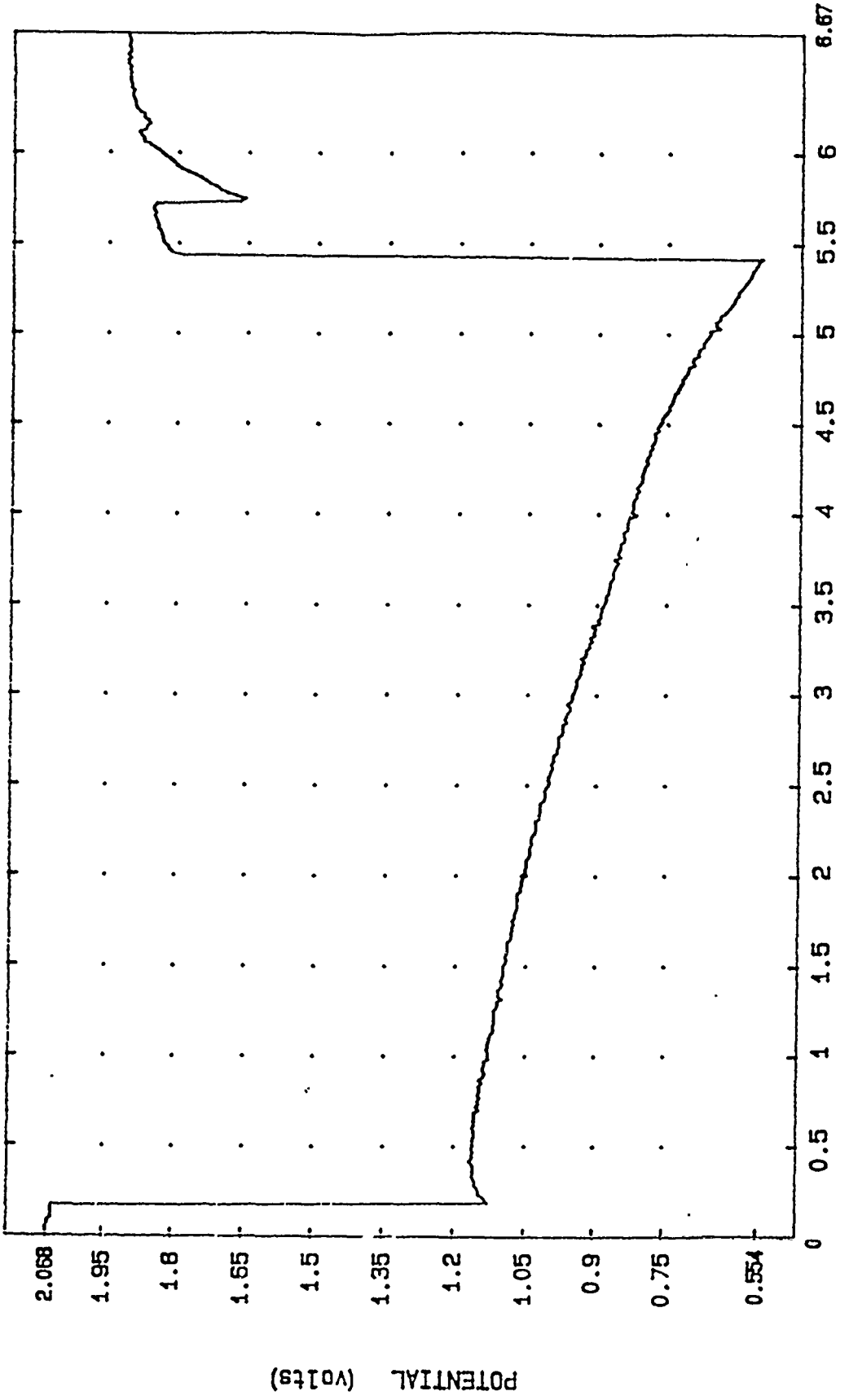

FIGURE 8. DISCHARGE PROFILE FOR CELL 26-96-1. 0.85M $CABR_2$/ 8.0M SO_2/ PROPYLENE CARBONATE: ACETONITRILE = 3:10 BY VOLUME. PRESSED CATHODE, ACETYLENE BLACK ONLY, 295 MA.

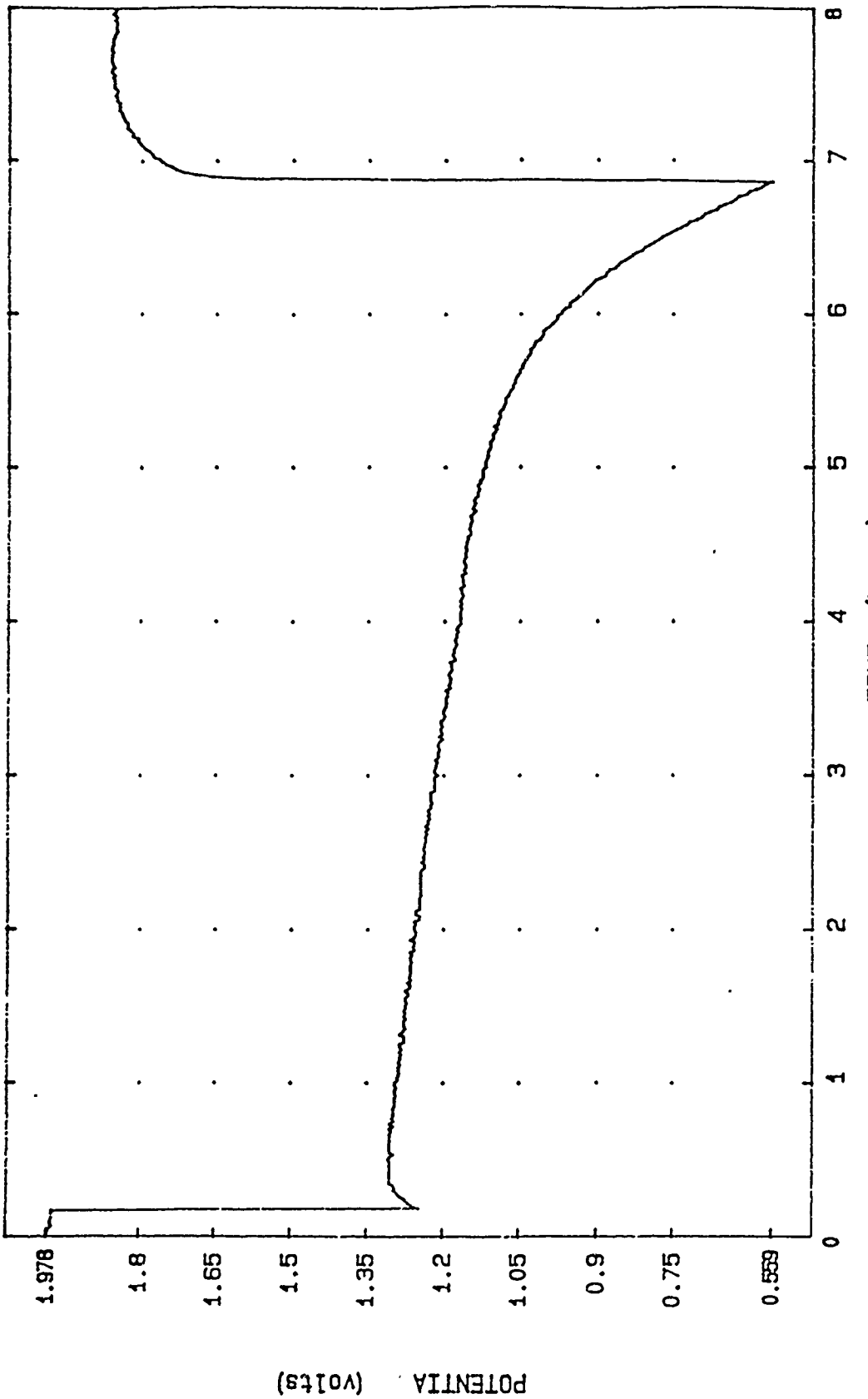

FIGURE 9. DISCHARGE PROFILE FOR CELL 26-96-2. 0.85M $CABR_2$/ 8.0M SO_2/ PROPYLENE CARBONATE: ACETONITRILE = 3:10 BY VOLUME. PRESSED CATHODE, ACETYLENE BLACK ONLY, 295 MA (1 MA/CM^2).

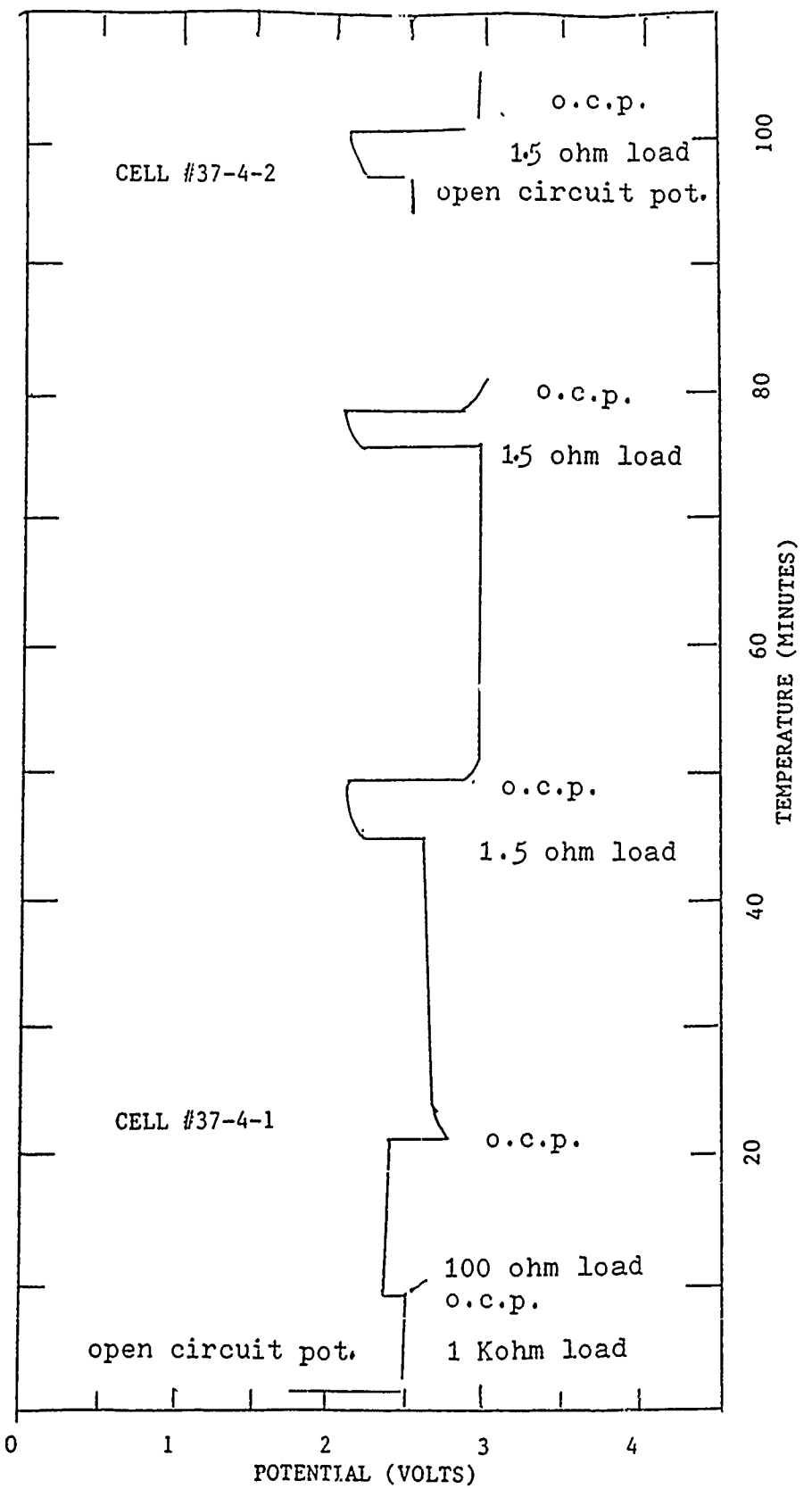

FIGURE 10. OPEN CIRCUIT POTENTIAL AND STARTUP PROFILES FOR CELLS 37-4-1 AND 37-4-2 AT A 1.5 OHM LOAD. COPY OF RECORDER TRACE. ONE VOLT/ INCH; 5 MIN./ CM.

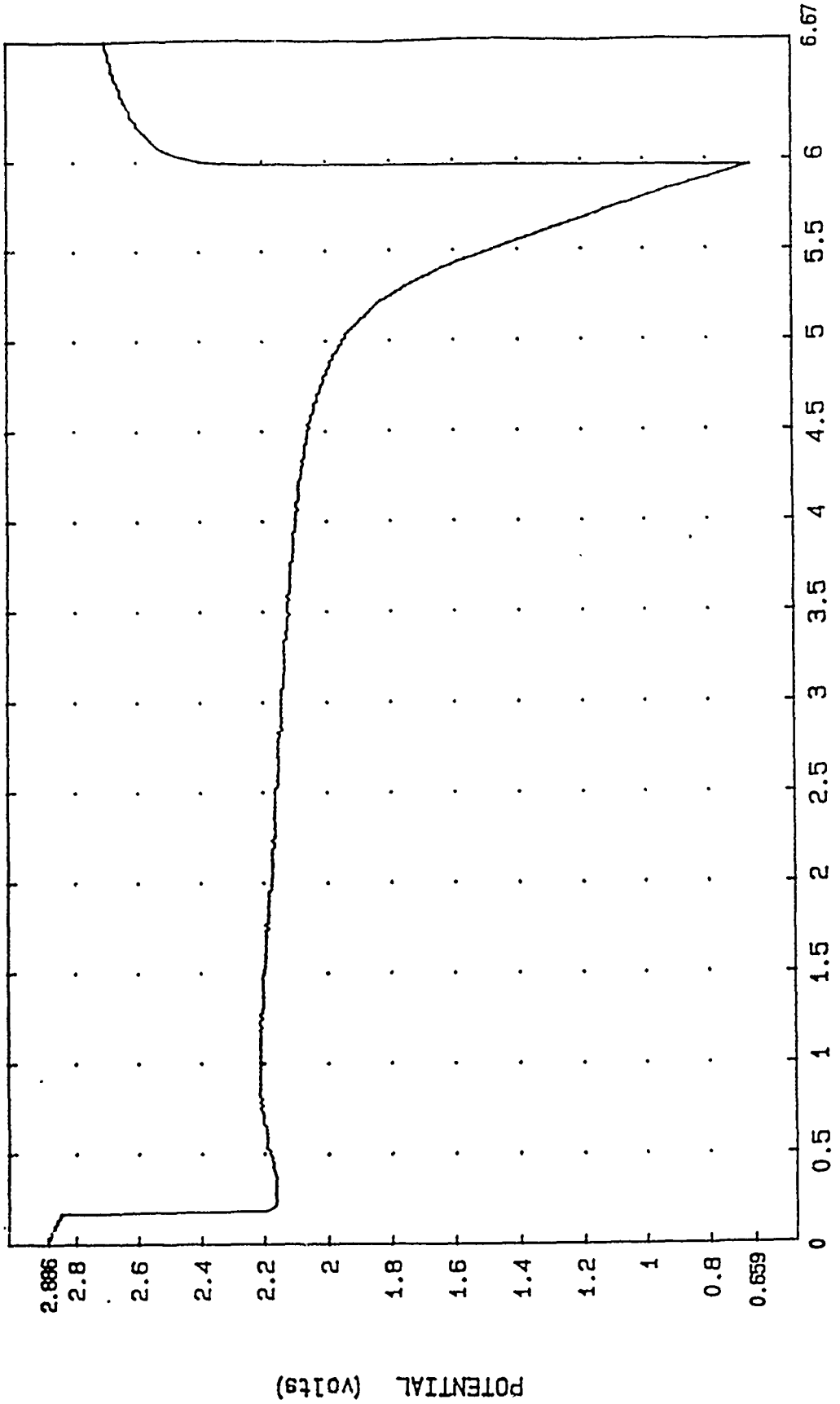

FIGURE 11. DISCHARGE PROFILE OF CELL 37-4-1 AT 1 MA/CM². INORGANIC ELECTROLYTE CONSISTING OF $CA(ALCL_4)_2*6SO_2$. ROLLED CATHODE, NICKEL SCREEN. 25/ 75 KETJENBLACK/ ACETYLENE BLACK.

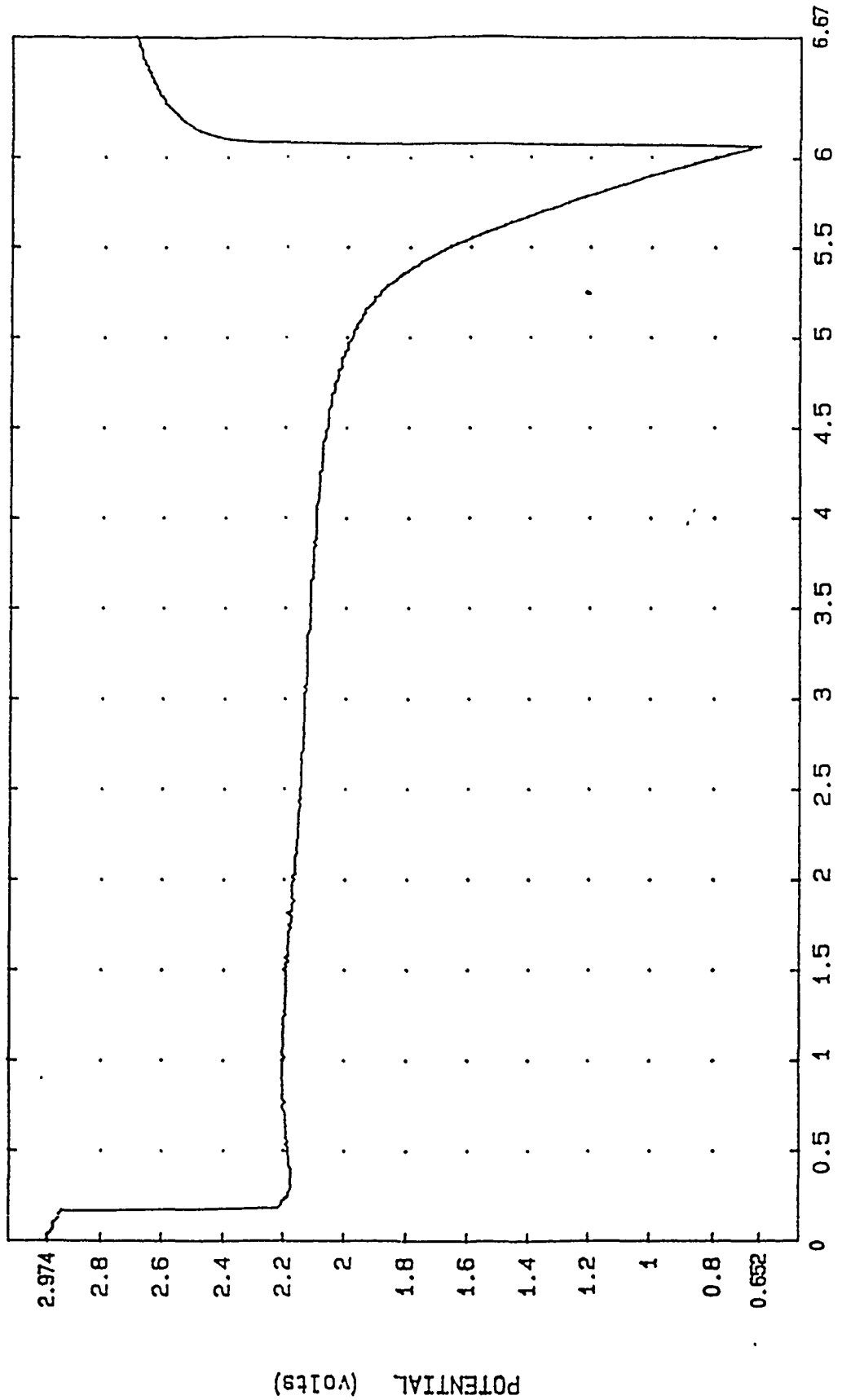

FIGURE 12. DISCHARGE PROFILE OF CELL 37-4-2 AT 1 MA/CM². INORGANIC ELECTROLYTE CONSISTING OF $CA(ALCL_4)_2*6SO_2$. ROLLED CATHODE, NICKEL SCREEN. 25/ 75 KETJENBLACK/ ACETYLENE BLACK.

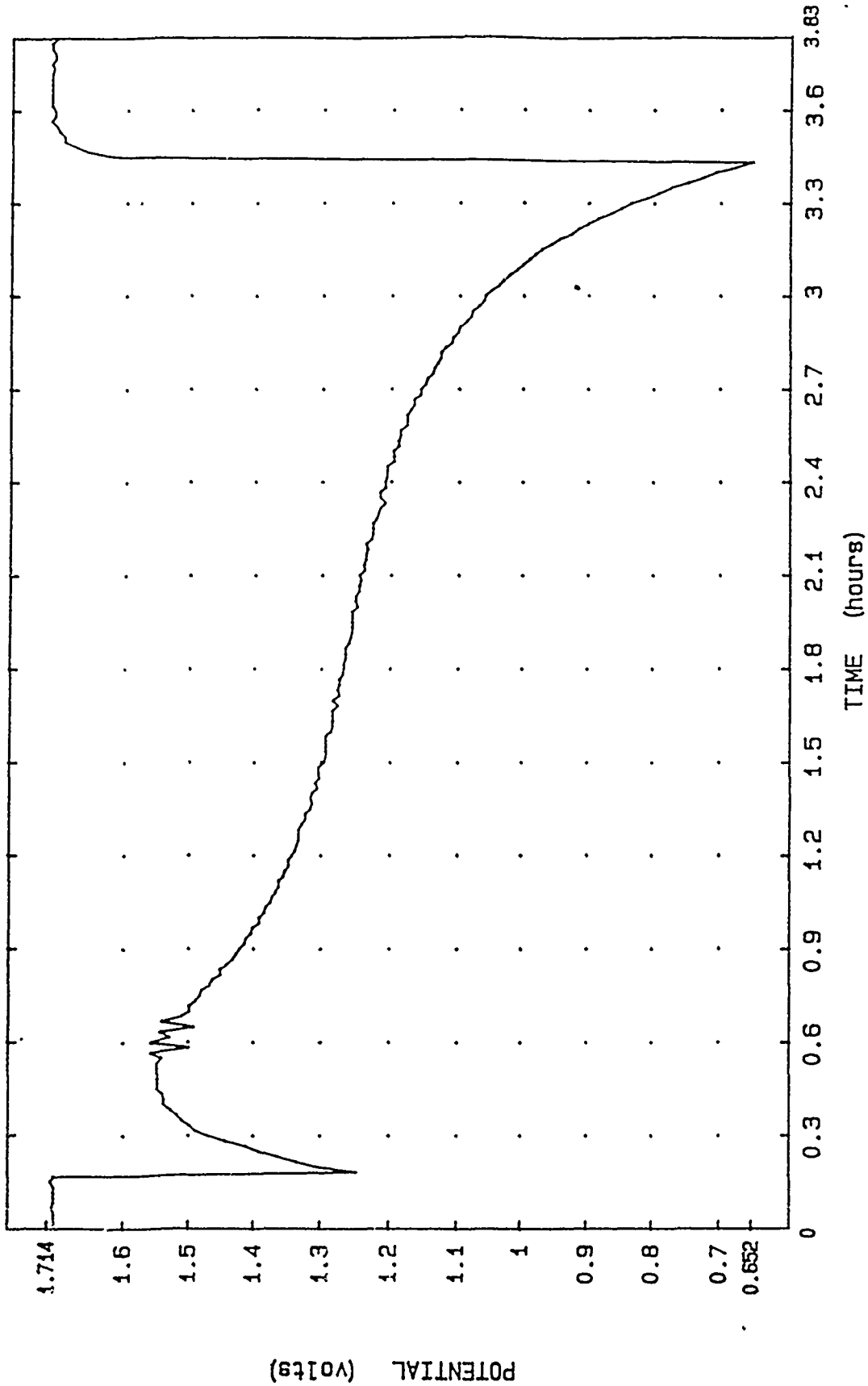

FIGURE 13. DISCHARGE PROFILE FOR CELL 37-4-4. 0.85M $CaBr_2$/ 8.0M SO_2/ PROPYLENE CARBONATE: ACETONITRILE = 3:10 BY VOLUME. ROLLED CATHODE, 1 MA/CM^2. 25/ 75 KETJENBLACK/ ACETYLENE BLACK.

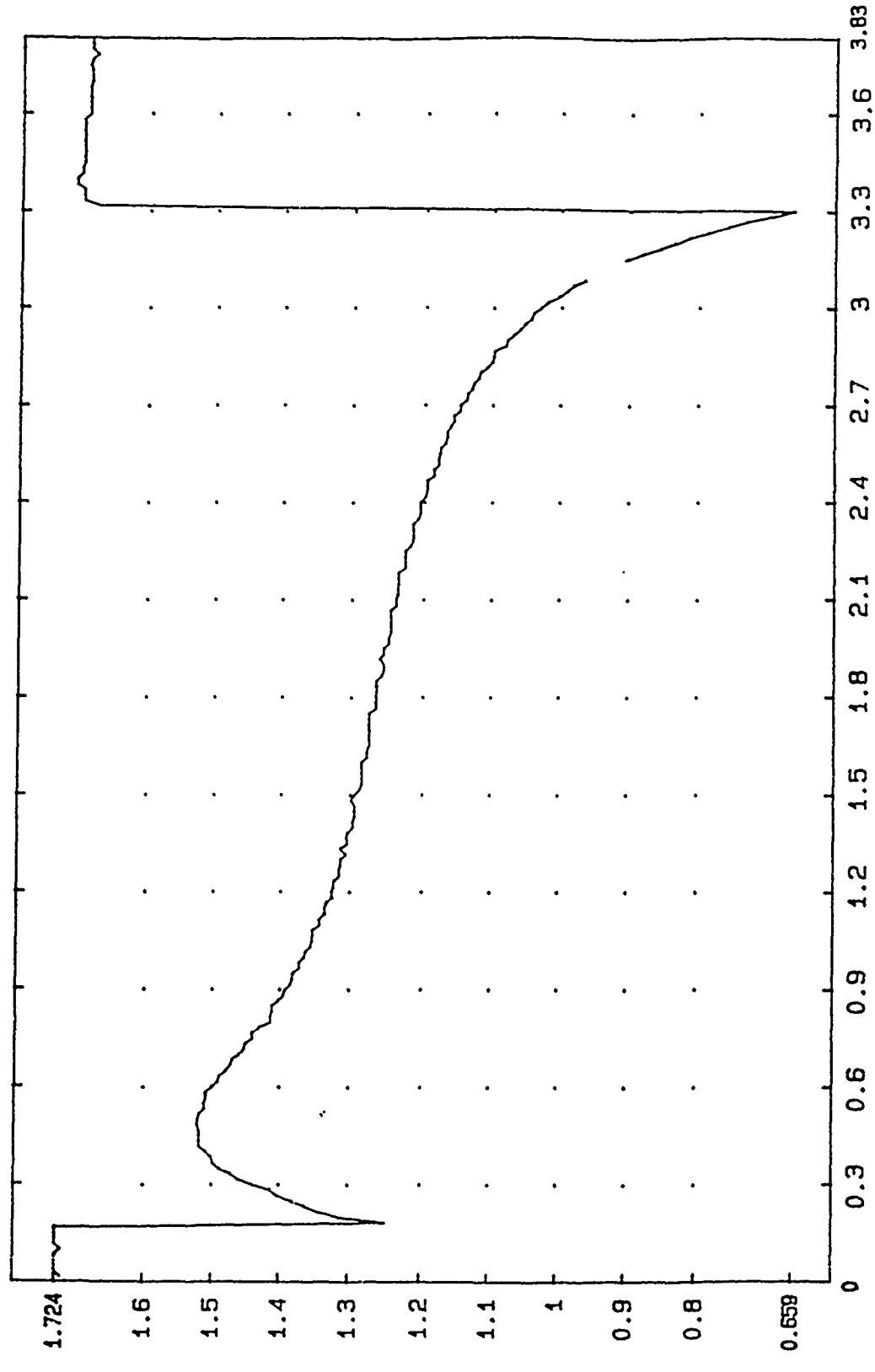

FIGURE 14. DISCHARGE PROFILE FOR CELL 37-4-5. 0.85M $CABR_2$/ 8.0M SO_2/ PROPYLENE CARBONATE: ACETONITRILE = 3:10 BY VOLUME. ROLLED CATHODE, 1 MA/CM^2. 25/ 75 KETJENBLACK/ ACETYLENE BLACK.

electrolyte cells ran above two volts while the organic electrolyte cells ran on an average of about 1.3 volts, showed a protracted startup delay, and a sloping profile. The inorganic electrolyte cells ran steadily at about 2.2 volts.

Cells 37-11-1 and 37-11-2 were duplicates run with the inorganic electrolyte, but the cathodes were 50% Ketjenblack/ 50% acetylene black/ 9% binder (Figures 15 and 16). Each carbon had been individually washed first with acetone, then with water before they were fabricated into cathodes. At 1 mA/cm^2, these showed the highest capacity of all the tests performed. We did notice, however, that the cells were warm to the touch during discharge. When cell #37-11-1 was cut open, the remaining part of the calcium anode facing discharged, that is, hard and brittle cathode material, was very brittle, tore easily, and appeared to be porous under the optical microscope. Calcium in the very center of the wound structure, where the cathode was not brittle, had retained its mechanical strength and shiny appearance.

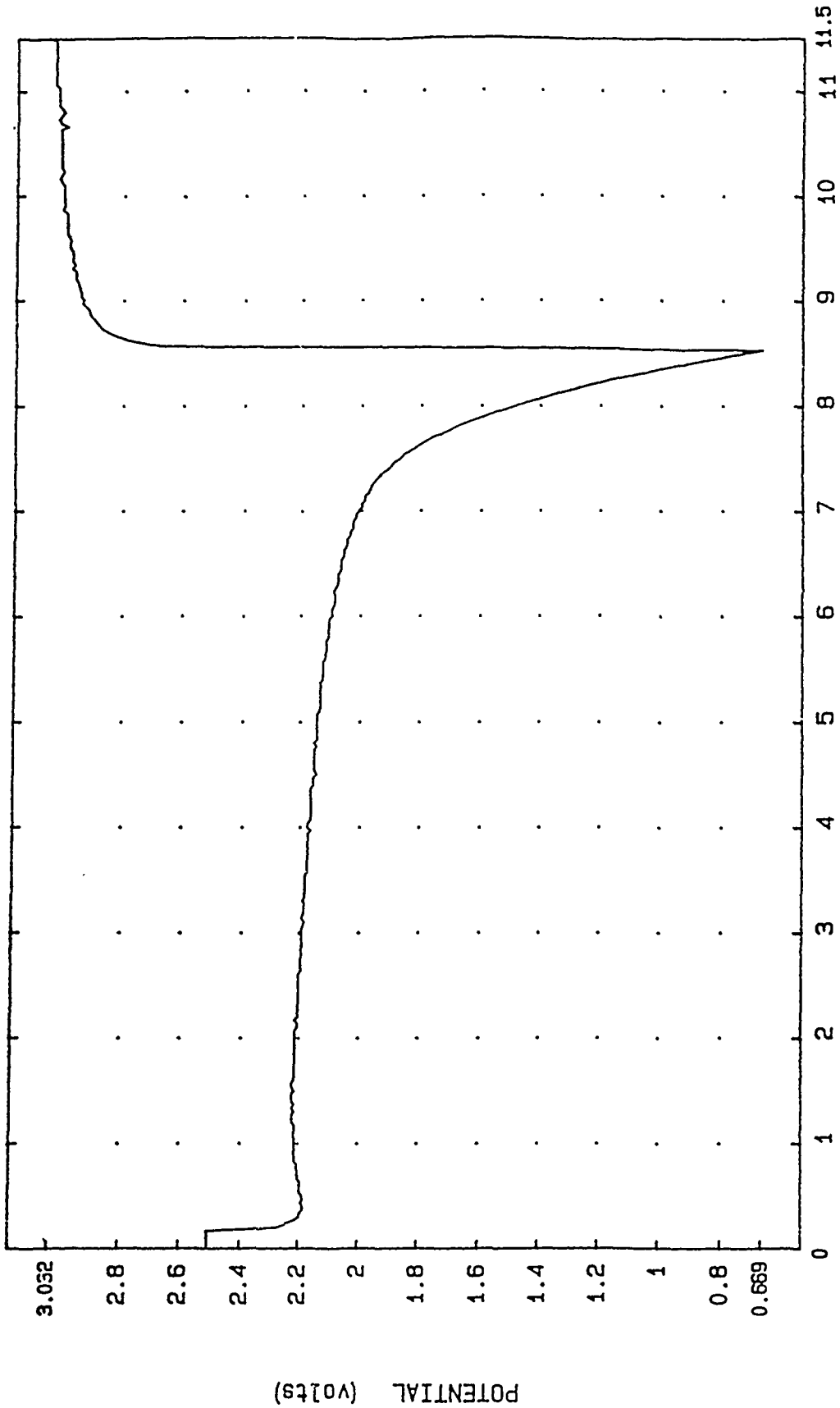

FIGURE 15. DISCHARGE PROFILE OF CELL 37-11-1 AT 1 MA/CM². INORGANIC ELECTROLYTE CONSISTING OF $CA(ALCL_4)_2*6SO_2$. ROLLED CATHODE, NICKEL SCREEN. 50/ 50 KETJENBLACK/ ACETYLENE BLACK; BOTH CARBONS WASHED WITH ACETONE, THEN WATER BEFORE CATHODE PREPARATION.

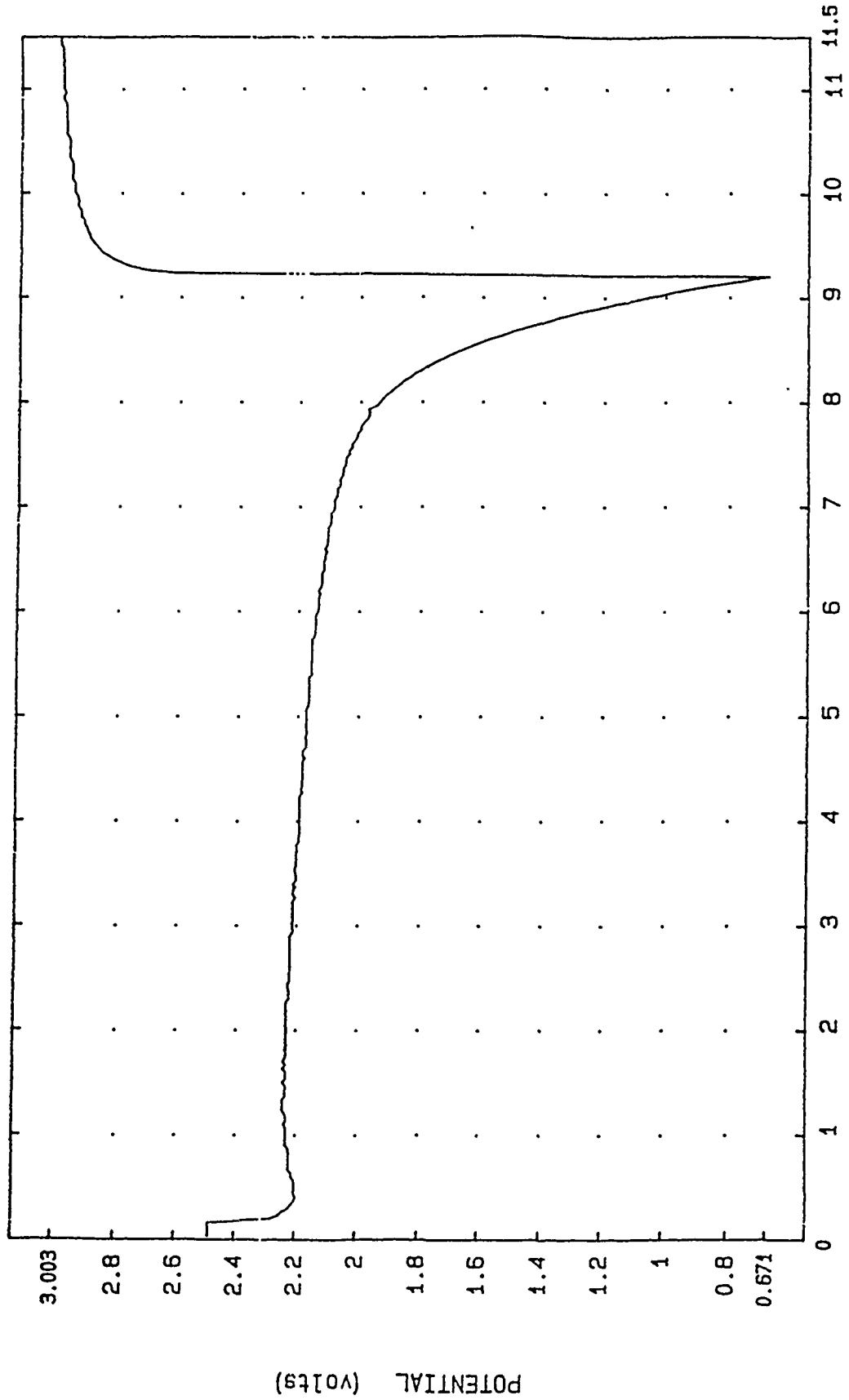

FIGURE 16. DISCHARGE PROFILE OF CELL 37-11-2 AT 1 MA/CM². INORGANIC ELECTROLYTE CONSISTING OF $CA(ALCL_4)_2*6SO_2$. ROLLED CATHODE, NICKEL SCREEN. 50/ 50 KETJENBLACK/ ACETYLENE BLACK; BOTH CARBONS WASHED WITH ACETONE, THEN WATER BEFORE CATHODE PREPARATION.

CHAPTER 4

CONCLUSIONS

The most important goals of this work have been to establish whether calcium anode primary cells in which sulfur dioxide replaces thionyl chloride as the sole electrolyte solvent can be made to discharge with equal or superior energy density, and whether a sulfur dioxide based electrolyte is able to prevent the calcium from corroding during discharge. If the practical energy density of Ca/ SO_2 cells is substantially below that of the competing Li/ SO_2, Li/ $SOCl_2$, or the Ca/ $SOCl_2$ systems, or the cells run at less than two volts, then corrosion of the anode is not an issue. The organic electrolyte cells have shown startup delays and have consistently discharged below two volts with low capacities. Open circuit potentials above two volts were observed only with carefully cleaned calcium anodes, and partial discharge lowered the subsequent open circuit potential below 2 volts.

While the inorganic electrolyte cells we have studied thus far have not given adequate capacities, cells with $Ca(AlCl_4)_2*6SO_2$ delivered about 2 amp hours above 2 volts. Thin electrodes with high surface area carbon appear to favor cells with the inorganic electrolyte. Fresh cells, at least, started without delay and ran at a flat potential above two volts. There may be, however, anionic charge transport in the solid electrolyte interphase and significant anode corrosion during discharge, problems in common with the calcium/ thionyl chloride system. We observed significant cell warming during discharge, and an anode from a cell disassembled immediately after discharge was found to be brittle and porous.

While we have established the feasability of a calcium/ sulfur dioxide inorganic electrolyte primary cell, substantial improvement in the capacity will be required before the system becomes a practical one. During Phase I, we studied cells only at 1 mA/cm^2 and at ambient temperature, attempting to obtain satisfactory capacity by varying the cell design. The discharge products formed on the carbon electrode in the inorganic electrolyte cells are not known, but may resemble the product formed during the discharge of lithium/ sulfur dioxide inorganic electrolyte rechargeable cells which also contain a tetrachloroaluminate in liquid sulfur dioxide [6]. The aluminum takes part with the sulfur dioxide during the discharge to produce a sulfur (III) complex, at one equivalent per mole of sulfur dioxide. If the discharge reaction in the calcium cells realizes only one electrical equivalent per mole of sulfur dioxide, then the maximum theoretical capacity would be only about 8.8 amp hours.

We should therefore attempt to improve the capacity by learning more about the reactions which occur in the cathode during discharge as well as the corrosion reaction at the anode. This should be done by varying both the compositions of the cathode and of the electrolyte.

Below is a brief outline of the tasks suggested by the results of this effort.

1. Optimize the capacity of Ca/ SO_2 cells containing $Ca(AlCl_4)_2*6SO_2$ by varying the ratio between the Ketjenblack and the acetylene black from 10% to 100%, in 10 %. intrervals, keeping the Teflon content at 10 %.

2. Determine whether sulfide is one of the discharge products in the calcium/ inorganic electrolyte cells. If the discharge instead produces an aluminum complex similar to that produced in the lithium/ inorganic electrolyte

rechargeable cells [6], determine whether the presence of lithium ion will increase the capacity of the primary calcium cells.

3. Attempt to determine why the potential of the calcium/ organic electrolyte cells during discharge is lover than expected, first by building in reference electrodes using cell tops on either end of stainless steel tubes cut to the length of the D size cells. Determine whether a lithium- based electrolyte with a calcium anode will show plateaus in the discharge profiles as the lithium in the electrolyte migrates to the cathode, or whether the running potential and the capacity may be improved.

4. If cells with adequate capacity can be built, measure calcium corrosion during discharge and storage, by weighing anodes before cell assembly, recovering the remaining calcium from stored/ discharged cells, hydrolysis, adding excess aqueous standardized acid, and back titration of the excess acid.

REFERENCES

1. C. R. Schlaikjer, in J. P. Gabano (ed.) "Lithium Batteries", Academic Press, London (1973), Chapter 13.

2. R. Staniewicz, *J. Electrochem. Soc.*, *127* (1980) 782.

3. E. Peled, R. Tulman, and E. Elster, *Progress in Batteries and Solar Cells*, *5* (1984) 299.

4a. T. L. Wen, W. Weppner, and A. Rabenau, *Electrochem. Soc. Spring Meeting*, (1982), Abstract #706.

4b. T. L. Wen, W. Weppner, and A. Rabenau, *Z. anorg. allgem Chem.*, *93* (1983) 497.

4c. T. L. Wen, W. Weppner, and A. Rabenau, *Stud. Inorg. Chem. (Solid State Chem.)*, *3* (1983) 343.

5. C. W. Walker, Jr., W. L. Wade, Jr., M. Binder, and S. Gilman, *J. Electrochem. Soc.*, *133* (1986) 1555.

6. A. N. Dey, H. C. Kuo, D. Foster, C. R. Schlaikjer, and M. Kallianidis, in *Power Sources Symposium (1986)*, Cherry Hill, New Jersey. The Electrochemical Society, Pennington, New Jersey.

DISTRIBUTION

	Copies
Defense Technical Information Center Cameron Station Alexandria, VA 22304-6145	12
Library of Congress Attn: Gift and Exchange Div. Washington, DC 20540	4
Office of Naval Research Attn: Code ONR1113ES (R. Nowak) 800 North Quincy Street Arlington, VA 22217	1
Naval Ocean Systems Center Attn: Code 6343 (Dr. S. Szpak) San Diego, CA 92152	1
Naval Weapons Center Attn: Dr. M. Miles China Lake, CA 93555	1
Naval Weapons Support Center Attn: Code 3054 (S. Shuler) Electrochemical Power Sources Div. Crane, IN 47522	1
Air Force Wright Aeronautical Labs Aero Propulsion Lab., P00C Attn: Code AFWAL-P00S-2 (R. Marsh) Wright-Patterson AFB OH 45433	1
Center for Naval Analyses 4401 Fort Avenue P.O. Box 16268 Alexandria, VA 22302-0258	2
U.S. Army Electronics Command Attn: Code DRSEL-TL-PD (Dr. W. K. Behl) Code DELET-BR (Mr. Sol Gilman) (M. Salomon) Fort Monmouth, NJ 07703	1 1 1
Air Force of Scientific Research Attn: Dir. of Chemical Science 1400 Wilson Boulevard Arlington, VA 22209	1
Department of National Defense Attn: G. Donaldson Defense Rsch Establishment Ottawa Ottawa, Ontario K1A 0Z4 Canada	1
Office of Naval Technology Attn: Code 23 (A. J. Faulstich) 800 North Quincy Street Arlington, VA 22217	1
Central Intelligence Agency Attn: T. Mahy Washington, DC 20505	1
California Institute of Technology Attn: G. Halpert A. Attia Jet Propulsion Laboratory 4800 Oak Grove Drive Pasadena, CA 91109	1 1

DISTRIBUTION (Cont.)

	Copies
Johns Hopkins Applied Research Laboratory Attn: Library Johns Hopkins Road Laurel, MD 20707	1
Tel-Aviv University Attn: E. Peled Department of Chemistry Tel Aviv, Israel 69978	1
University of California Attn: Dr. R. A.Huggins Dept. Material Science & Engr. Stanford, CA 94305	1
University of Rome Attn: Dr. . Scrosati Istituto di Chimica Fisica P. le A. Moro 5, 00185 Rome, Italy	1
Argonne National Laboratory Attn: Dr. D. Vissars 9700 South Cass Avenue Argonne, IL 60439	1
Sandia Laboratories Attn: Mail Services Sect. 3154-3 (Sam Levy) P.O. Box 5800 Albuquerque, NM 87715	1
Nippon Telegraph and Telephone Corporation Attn: Dr. J. Yamaki NTT Applied Electronics Laboratories Tokai-Mura, Naka-Gun Ibaraki-Ken, 319-11 Japan	1
Chemtech Systems, Inc. Attn: Dr. M. L. Gopikanth P.O. Box 1067 Burlington, MA 01803	1
Union Carbide Corporation Battery Products Division Attn: G. E. Bloomgren P.O. Box 45035 Westlake, OH 44145	1
Wilson Greatbatch Ltd. Attn: Dr. W. Clark 1000 Wehrle Drive Clarence, NY 14030	1
Yardney Electric Corporation Attn: Library 82 Mechanic Street Pawcatuck, CT 02891	1
Honeywell Corporate Technology Center Attn: H. V. Venkatasetty 10701 Lyndale Avenue, South Bloomington, MN 55420	1
The Aerospace Corporation Attn: H. Bittner P.O. Box 92957 Los Angeles, CA 90009	1
Honeywell Power Sources Corporation Attn: Dr. D. L. Chua 104 Rock Road Horsham, PA 19044	1
Bell Laboratories Attn: Dr. J. J. Auborn 600 Mountain Avenue Murray Hill, NJ 07974	1
Battery Engineering, Inc. Attn: Dr. N. Marincic C. Schlaikjer 1636 Hyde Park Avenue Hyde Park, MA 02136	1 1

DISTRIBUTION (Cont.)

	Copies
RAY-O-VAC Attn: F. Fleischer 630 Forward Drive Madison, WI 53711	1
TRW Systems Attn: G. L. Juvinal One Space Park Redondo Beach, CA 90278	1
Altus Corporation Attn: Dr. Jeffrey Phillips 1610 Crane Court San Jose, CA 95112	1
Hyde Park Estates Attn: Dr. P. Bro Santa Fe, NM 87501	1
Catalyst Research Corporation Attn: J. Joelson 1421 Clarkview Road Baltimore, MD 21209	1
ESB Research Center Attn: Library 19 West College Avenue Yardley, PA 19067	1
EIC Laboratories, Inc. Attn: K. M. Abrahem 111 Downey Street Norwood, MA 02062	1
Eagle-Picher Industries, Inc. Attn: R. L. Higgins Electronics Division P.O. Box 47 Joplin, MO 64802	1
Whittaker Yardney Attn: R. McDonald 40 Sylvan Road Waltham, MA 02254	1

	Copies
Lockheed Missiles & Space Co., Inc. Attn: Library Lockheed Palo Alto Rsch Lab 3251 Hanover Street Palo Alto, CA 04304	1
Duracell International, Inc. Attn: W. Bowden A. N. Dey Duracell Research Center 37 A Street Needham, MA 02194	1 1
Boeing Aerospace Company Attn: C. Johnson P.O. Box 3999 Seattle, WA 98124	1
Electrochimica Corporation Attn: M. Eisenberg 2485 Charleston Road Mt. View, CA 94040	1
Saft America, Inc. Attn: Dr. R. J. Staniewicz 107 Beaver Court Cockeysville, MD 21030	1
Tadiran Attn: M. Babai P.O. Box 75 Rehovot, Isreal	1
Power Conversion, Inc. Attn: Dr. T. Reddy 495 Boulevard Elmwood Park, NJ 07407	1
ECO Energy Conversion Attn:Dr. F. M. Walsh 225 Needham Street Newton, MA 02164	1

DISTRIBUTION (Cont.)

	Copies
Medtronics, Inc. Attn: Dr. D. Untereker 6700 Shingle Creek Parkway Brooklyn Center, MN 55430	1
ELTECH Systems Corporation Attn: D. E. Harney Research & Development Center 625 East Street Fairport Harbor, OH 44077	1
Harkness Consultants, Inc. Attn: Dr. A. C. Harkness Suite 1601 150 - 24th Street West Vancouver, BC V7V 4G8 Canada	1
Dr. Boone B. Owens P.O. Box 8205 St. Paul, MN 55108	1
Ultra Technologies - Kodak Attn: P. F. Dickinson P.O. Box 267 Rt. 88 South Newark, NY 14513	1
Power Information Center CSR, Inc. 1400 Eye Street, NW Suite 600 Washington, DC 20005	1
Internal Distribution	
E231	2
E232	3
E342 (GIDEP)	1
R05 (D. Wilson)	2
R33 (W. P. Kilroy)	5

REPORT DOCUMENTATION PAGE

Form Approved
OMB No. 0704-0188

1. AGENCY USE ONLY (Leave blank)	2. REPORT DATE	3. REPORT TYPE AND DATES COVERED
	November 1989	

4. TITLE AND SUBTITLE
SBIR REPORTS ON THE CHEMISTRY OF LITHIUM BATTERY TECHNOLOGY

5. FUNDING NUMBERS

6. AUTHOR(S)
W. P. Kilroy, Editor

7. PERFORMING ORGANIZATION NAME(S) AND ADDRESS(ES)
Naval Surface Warfare Center (R33)
10901 New Hampshire Avenue
Silver Spring, MD 20903-5000

8. PERFORMING ORGANIZATION REPORT NUMBER
NSWC MP 89-242

9. SPONSORING/MONITORING AGENCY NAME(S) AND ADDRESS(ES)

10. SPONSORING/MONITORING AGENCY REPORT NUMBER

11. SUPPLEMENTARY NOTES

12a. DISTRIBUTION/AVAILABILITY STATEMENT
Approved for public release; distribution is unlimited.

12b. DISTRIBUTION CODE

13. ABSTRACT (Maximum 200 words)

This report is a composite collection of four Phase I Small Business Innovative Research final reports. The work was conducted under contracts N60921 86-C-A457, N60921-88-C-0058, N60921-86-C-0274, and N60921-88-C-0057.

14. SUBJECT TERMS
Lithium Battery Technology

15. NUMBER OF PAGES
184

16. PRICE CODE

17. SECURITY CLASSIFICATION OF REPORT	18. SECURITY CLASSIFICATION OF THIS PAGE	19. SECURITY CLASSIFICATION OF ABSTRACT	20. LIMITATION OF ABSTRACT
UNCLASSIFIED	UNCLASSIFIED	UNCLASSIFIED	

GENERAL INSTRUCTIONS FOR COMPLETING SF 298

The Report Documentation Page (RDP) is used in announcing and cataloging reports. It is important that this information be consistent with the rest of the report, particularly the cover and its title page. Instructions for filling in each block of the form follow. It is important to ***stay within the lines*** to meet ***optical scanning requirements***.

Block 1. Agency Use Only *(Leave blank)*.

Block 2. Report Date. Full publication date including day, month, and year, if available (e.g. 1 Jan 88). Must cite at least the year.

Block 3. Type of Report and Dates Covered. State whether report is interim, final, etc. If applicable, enter inclusive report dates (e.g. 10 Jun 87 - 30 Jun 88).

Block 4. Title and Subtitle. A title is taken from the part of the report that provides the most meaningful and complete information. When a report is prepared in more than one volume, repeat the primary title, add volume number, and include subtitle for the specific volume. On classified documents enter the title classification in parentheses.

Block 5. Funding Numbers. To include contract and grant numbers; may include program element number(s), project number(s), task number(s), and work unit number(s). Use the following labels:

C -	Contract	**PR** -	Project
G -	Grant	**TA** -	Task
PE -	Program Element	**WU** -	Work Unit Accession No.

BLOCK 6. Author(s). Name(s) of person(s) responsible for writing the report, performing the research, or credited with the content of the report. If editor or compiler, this should follow the name(s).

Block 7. Performing Organization Name(s) and Address(es). Self-explanatory.

Block 8. Performing Organization Report Number. Enter the unique alphanumeric report number(s) assigned by the organization performing the report.

Block 9. Sponsoring/Monitoring Agency Name(s) and Address(es). Self-explanatory.

Block 10. Sponsoring/Monitoring Agency Report Number. *(If Known)*

Block 11. Supplementary Notes Enter information not included elsewhere such as: Prepared in cooperation with...; Trans of...; To be published in.... When a report is revised, include a statement whether the new report supersedes or supplements the older report.

Block 12a. Distribution/Availability Statement. Denotes public availability or limitations. Cite any availability to the public. Enter additional limitations or special markings in all capitals (e.g. NOFORN, REL, ITAR).

DOD -	See DoDD 5230.24, "Distribution Statements on Technical Documents."
DOE -	See authorities.
NASA -	See Handbook NHB 2200.2
NTIS -	Leave blank.

Block 12b. Distribution Code.

DOD -	Leave blank.
DOE -	Enter DOE distribution categories from the Standard Distribution for Unclassified Scientific and Technical Reports.
NASA -	Leave blank.
NTIS -	Leave blank.

Block 13. Abstract. Include a brief ***(Maximum 200 words)*** factual summary of the most significant information contained in the report.

Block 14. Subject Terms. Keywords or phrases identifying major subjects in the report.

Block 15. Number of Pages. Enter the total number of pages.

Block 16. Price Code. Enter appropriate price code ***(NTIS only)***

Blocks 17.-19. Security Classifications. Self-explanatory. Enter U.S. Security Classification in accordance with U.S. Security Regulations (i.e., UNCLASSIFIED). If form contains classified information, stamp classification on the top and bottom of the page.

Block 20. Limitation of Abstract. This block must be completed to assign a limitation to the abstract. Enter either UL (unlimited) or SAR (same as report). An entry in this block is necessary if the abstract is to be limited. If blank, the abstract is assumed to be unlimited.


UNITED STATES NAVY
SURFACE WARFARE CENTER